UNIVERSITY OF HULL

The Role of Environmentally Relevant Concentrations of SSRIs in Human Wound Healing

Thesis submitted for the degree of Doctor of Philosophy (PhD)

The University of Hull

by

Quentin Rodriguez-Barucg

BSc., University of Paris XI Orsay

MSc. (Hons), University of Montpellier

April 2025

Abstract

This thesis investigates the role of environmentally relevant concentrations of fluoxetine, a commonly prescribed selective serotonin reuptake inhibitor (SSRI), in wound healing. While SSRIs are effective in treating psychiatric conditions, their increasing presence in aquatic environments has raised concerns about unintended biological impacts. SSRI are widely-used antidepressants, and in the UK, antidepressant prescriptions have almost doubled in the past decade (Heald et al., 2021). After ingestion, SSRI are excreted via urine. Wastewater treatment does not remove SSRI effectively, leading to accumulation in freshwater courses (to 0.4-3,645 ng/l), making SSRI priority contaminants in ecotoxicology. Average fluoxetine and sertraline concentrations in England rivers across 2016-2024 were 218 and 15 ng/l, respectively, and up to 2,560 ng/l fluoxetine in post-treatment effluents. Population growth, urbanisation, and regional climate change-induced water scarcity can increase these concentrations. While exposure to environmental SSRI affects the physiology and behaviour of freshwater species, little is known about effects of exposure on human health. My hypothesis was that SSRIs, particularly fluoxetine, at environmentally relevant concentrations promote wound healing through serotonin signalling. To test this hypothesis, here, I investigate the influence of fluoxetine on wound healing models using human keratinocytes and *ex-vivo* human skin biopsies, assessing its effects on serotonin signalling pathways and cell proliferation.

Using a combination of molecular and cell biology techniques, including scratch assays, RNA sequencing (RNAseq), protein microarrays and phosphoproteomics, alongside using an ex-vivo human skin model, I investigated the impact of fluoxetine at environmentally relevant concentrations (62.5-5400 ng/l) on wound closure, cell proliferation, and key signalling pathways. Results showed that fluoxetine increased scratch closure in a dose-dependent manner (by 5% and 20% at 125 and 5400 ng/l of fluoxetine) in keratinocyte models by promoting cell proliferation through serotonin receptor-mediated pathways. RNAseq revealed differential expression of exactly 100 upregulated and 250 downregulated genes involved in cell cycle progression, energy metabolism, cell proliferation, and cellular resilience. Protein microarrays and phosphoproteomics indicated dynamic changes in phosphorylation among key kinases, including GSK3β, MSK1/2, and p70 S6K, with 190 upregulated and 45 downregulated phosphorylated proteins. These proteins showed enrichment in GO terms and KEGG pathways related to cellular structure, stress response, and kinase signalling pathways, particularly in HIPPO and PI3K/AKT signalling. *Ex-vivo* experiments with human skin validated these findings in a physiologically-relevant model that maintains the wound microenvironment. I

observed an increase in wound healing of 30% at 5400 ng/l compared to control biopsies, demonstrating enhanced wound closure upon exposure to environmentally relevant fluoxetine associated with serotonin pathway activation.

Human wounds cost the NHS >£8.3 billion/year and new treatments are direly needed. This research underscores both the potential therapeutic applications of low-dose fluoxetine in wound care, and the importance of understanding its effects on healthy skin as an environmental pollutant. Together, these findings contribute to a deeper insight into the molecular and phenotypical impact of fluoxetine on human skin, with implications for both clinical and environmental health. My results justify a transition from the study of behavioural effects of environmental fluoxetine in aquatic animals to the investigation of effects of exposure on wound healing in aquatic and terrestrial animals, including direct impacts on human health. I also open avenues to investigate low-dose SSRI as new treatments to promote wound healing.

Acknowledgements

First, I would like to express my sincere gratitude to my main supervisor, Dr. Pedro Beltran-Alvarez, for his constant support and guidance throughout my PhD journey. Your encouragement and insight have been invaluable to my research. I also wish to thank my secondary supervisors, Prof. Matt Hardman and Dr. Holly Wilkinson, for their expertise and mentorship, which have greatly enriched my experience.

I extend my appreciation to the examiners of my thesis: Dr. Jacobo Elies-Gomez, my external examiner, and Dr. Paul Hiebert, my internal examiner, for their constructive feedback and support. I am grateful for the financial support provided by the University of Hull, which also funded the Happy Chemical Cluster. This collaborative environment, including Dr. Domino Joyce, Dr. Thomas Breithaupt, Paige Lee, and Areeba Khan, has been essential for my research development.

I would like to acknowledge my colleagues from the team based at Castle Hill Hospital, particularly Amber Stafford, Alexander Johns, Laden Fenercioglu, Paisleigh Smythe, and Xuanyuan Zhang, for their training and collaboration. I also wish to thank Belen Garcia-Merino and Tomilayo Akinmola for their contributions to my research.

Additionally, I am thankful for my fellow lab members (and friends), Sabrina Samuel, Antonia Barry, Thomas Francis, Lucie Bilton, and Danielle Marsh, who made this journey enjoyable and memorable. Your support during both challenging and rewarding times has been greatly appreciated.

Finally, I would like to express my deepest gratitude to my family, my parents and sister, for their unconditional love and encouragement. Your belief in me has been a constant source of motivation, and I couldn’t have reached this milestone without you.

Publications and Conferences

Related Peer Reviewed Publications:

Rodriguez-Barucg, Q., Garcia, A.A., Garcia-merino, B., Akinmola, T., Okotie-eboh, T., Francis, T., Bringas, E., Ortiz, I., Wade, M.A., Dowle, A., Joyce, D.A., Hardman, M.J., Wilkinson, H.N., Beltran-Alvarez, P., 2024. Environmental fluoxetine promotes skin cell proliferation and wound healing. Environ. Pollution. 362, 124952. https://doi.org/10.1016/j.envpol.2024.124952

Conferences:

- September 2023, Poster presentation at the North of England Cell Biology (NECB) forum (University of Sheffield).
- May 2023, Poster presentation at the Allam Lecture (University of Hull).
- June 2022, 5-minute talk at Sustainable Development Goals Conference (University of Hull).
- May 2022, Poster presentation at the Research Celebration Event conference (University of Hull).
- September 2021, Poster presentation at the Allam Lecture (University of Hull).

Declaration

I declare that this thesis is original and is my own work. All experimental data, unless otherwise stated, have been generated by me. Data analysis, including statistical methods, has been conducted by me. I have written the initial drafts of each chapter, which have been reviewed and received feedback from my supervisor Dr Pedro Beltran-Alvarez. All contributions from collaborators have been acknowledged in the relevant chapters. I confirm that any material sourced from academic papers, books, the internet, or other sources has been clearly cited, following the guidelines of the University of Hull, the University of York, and HYMS regarding plagiarism and academic integrity. I have adhered to the HYMS Code of Practice on Academic Misconduct throughout this work

Table of Contents

List of Figures

List of Tables

List of abbreviations

2D/3D PCA	2D/3D Principal Component Analysis
5-HT	5-Hydroxytryptamine (serotonin)
5-HTP	5-hydroxytryptamine
5-HTR	5-Hydroxytryptamine Receptor (serotonin receptor)
AADC	Aromatic Amino Acid Decarboxylase
AC	Adenylyl Cyclase
ADP	Adenosine Diphosphate
Akt	Protein Kinase B
ANAPC10	Anaphase-Promoting Complex Subunit 10
ANAPC11	Anaphase-Promoting Complex Subunit 11
ANOVA	Analysis of variance
APC/C	Anaphase-Promoting Complex
APS	Ammonium Persulfate
ATP	Adenosine Triphosphate
ATP5PO	ATP Synthase Peripheral Stalk Subunit OSCP (Oligomycin Sensitivity-Conferring Protein)
BRAF	B-Rapidly Accelerated Fibrosarcoma
cAMP	Cyclic Adenosine Monophosphate
CDK4/6	Cyclin-Dependent Kinases 4 and 6
CNS	Central Nervous System
COX5B	Cytochrome C Oxidase Subunit 5B
COX6C	Cytochrome C Oxidase Subunit 6C
CRH	Corticotropin-releasing Hormone
CRMP2	Collapsin Response Mediator Protein 2
DAG	Diacylglycerol
DAPI	4',6-Diamidino-2-Phenylindole
DDA	Data-Dependent Acquisition
DEGs	Differentially Expressed Genes
DMEM	Dulbecco's Modified Eagle Medium
DNA	Deoxyribonucleic Acid
DPBS	Dulbecco's Phosphate-Buffered Saline
DTT	Dithiothreitol
E2F	E2 Transcription Factor
ECAR	Extracellular Acidification Rate
ECM	Extracellular Matrix
EDTA	Ethylenediaminetetraacetic Acid
EdU	5-Ethynyl-2'-deoxyuridine
eNOS	Endothelial Nitric Oxide Synthase
FBS	Foetal Bovine Serum
FGF-2	Fibroblast Growth Factor-2
FGFRs	Fibroblast Growth Factor Receptors
FLX	Fluoxetine
GO	Gene Ontology
H_20	Water

H4C6	Histone H4 Cluster 6
HaCaT	Human Adult Low Calcium Temperature
HATs	Histone Acetyltransferases
HBSS	Hank's Balanced Salt Solution
HCL	Hydrochloride
HEPES	4-(2-Hydroxyethyl)-1-Piperazineethanesulfonic Acid
HRP	Horseradish Peroxidase
HSD	Honestly Significant Difference
IL	Interleukin
IP3	Inositol Trisphosphate
JAK	Janus Kinase
KEGG	Kyoto Encyclopaedia of Genes and Genomes
KRAS	Kirsten Rat Sarcoma Viral Oncogene
LATS1/2	Large Tumour Suppressor Kinase 1 and 2
LF	Low Fluoxetine (540 ng/l)
MAOI	Monoamine Oxidase Inhibitor
MEK/MAPK	Mitogen-activated Protein Kinase
MMPs	Matrix Metalloproteinases
MRPL11	Mitochondrial Ribosomal Protein L11
MSK1/2	Mitogen- and Stress-Activated Protein Kinases 1 and 2
MST1/2	Mammalian Sterile 20-like Kinase 1 and 2
NADH	Nicotinamide Adenine Dinucleotide (reduced)
NDUFA2	NADH: Ubiquinone Oxidoreductase Subunit A2
NDUFB10	NADH: Ubiquinone Oxidoreductase Subunit B10
NO	Nitric Oxide
OCD	Obsessive-Compulsive Disorder
p70 S6K	p70 Ribosomal S6 Kinase
PBS	Phosphate-Buffered Saline
PDGF	Platelet-Derived Growth Factor
PERMANOVA	Permutational Multivariate Analysis of Variance
PI3K	Phosphoinositide 3-Kinase
PIAS	Protein Inhibitors of Activated STATs
PKA	Protein Kinase A
PKC	Protein Kinase C
PLC	Phospholipase C
POLR2J	RNA Polymerase II Subunit J
PPI	Protein-Protein Interaction
PRP	Platelet-rich Plasma
PTMs	Post-translational Modifications
PTSD	Post-Traumatic Stress Disorder
p-value	Probability value
Rb	Retinoblastoma Protein
RBX1	Ring-Box 1 (a component of the E3 ubiquitin ligase complex)

RNA	Ribonucleic acid
RNAseq	RNA sequencing
ROS	Reactive Oxygen Species
RPL35	Ribosomal Protein L35
RPL39	Ribosomal Protein L39
RPS9	Ribosomal Protein S9
SDS	Sodium Dodecyl Sulfate
SERT	Serotonin/5-HT Transporters
SNRI	Serotonin-Norepinephrine reuptake inhibitor
SOCS	Suppressors of Cytokine Signalling
Src	Proto-Oncogene Tyrosine-Protein Kinase Src
SSRIs	Selective Serotonin Reuptake Inhibitors
STAT	Signal Transducer and Activator of Transcription
TAZ	Transcriptional Coactivator with PDZ-Binding Motif
TCA	Tricyclic Antidepressant
TEMED	N,N,N',N'-Tetramethylethylenediamine
TFA	Trifluoroacetic Acid
TGF	Transforming Growth Factor
TPH	Tryptophan Hydroxylase
UBE2S	Ubiquitin-Conjugating Enzyme E2 S
UPS	Ubiquitin-proteasome system
VEGF	Vascular Endothelial Growth Factor
YAP	Yes-Associated Protein
α-SMA	Alpha-smooth Muscle Actin

Chapter 1: General Introduction

1.1 SSRIs: development, how they work, and public perception

1.1.1 The development of SSRIs: a milestone in psychiatric medicine

The history and advancements in Serotonin Reuptake Inhibitors (SSRIs) represent a crucial progression in the treatment of depression and other psychiatric disorders. This journey commenced in the 1970s, a period when the psychiatric community was fervently searching for newer, safer and more tolerable antidepressants than tricyclic antidepressants (TCAs) and monoamine oxidase inhibitors (MAOIs) used at that time (Gillman, 2007). The introduction of SSRIs on the market marked a significant advancement in the way depression and other psychiatric disorders were treated. They work by inhibiting the reuptake of serotonin (5-hydroxytryptamine, 5-HT) into presynaptic neurons (Figure 1.1), consequently increasing the concentration of serotonin in the central nervous system and making them effective for treating mood disorders (Albert and Lemonde, 2004; Kreke and Dietrich, 2008; Lattimore et al., 2005).

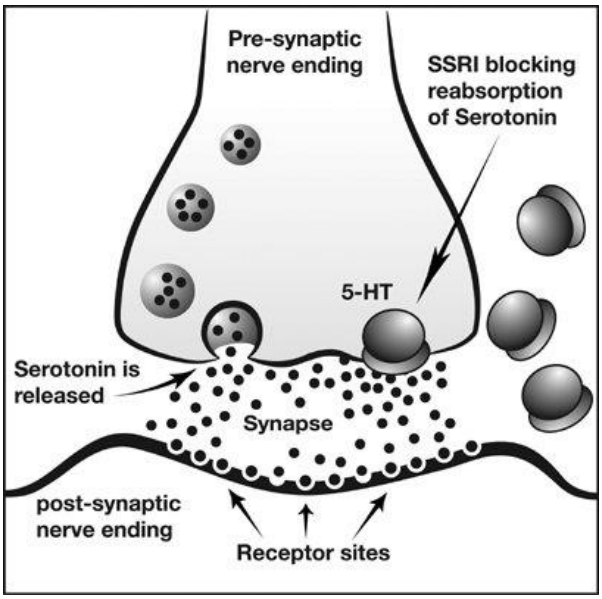

Figure 1.1: Schematic diagram showing the mechanism of action of SSRIs. *These agents block serotonin reuptake at the presynaptic membrane, thus increasing its concentration at the postsynaptic nerve terminal membrane. From Lattimore et al.2005*

When the first SSRI, fluoxetine (Prozac), was discovered by scientists at Eli Lilly in the late 1970s, it was considered a revolutionary event. Fluoxetine was developed on the hypothesis that by strengthening serotonergic transmission, it was possible to treat depression very effectively, and this hypothesis turned out to be successful (Campos et al., 2012; Sommi et al., 1987). Soon after the initial triumph of fluoxetine, other SSRIs were developed (Figure 1.2),

such as sertraline (Zoloft), paroxetine (Paxil), citalopram (Celexa) and escitalopram (Lexapro). Each of these SSRIs had a similar mode of action, they selectively inhibited serotonin reuptake by neurons but with different profiles that made them suitable for various patients and conditions. For example, escitalopram dual binding to orthosteric sites (primary functional sites) and allosteric sites (secondary functional sites) on 5-HT transporters (SERT) is highlighted as a possible mechanism for its high efficacy and rapid onset of action when compared to sertraline and paroxetine (Sanchez et al., 2014).

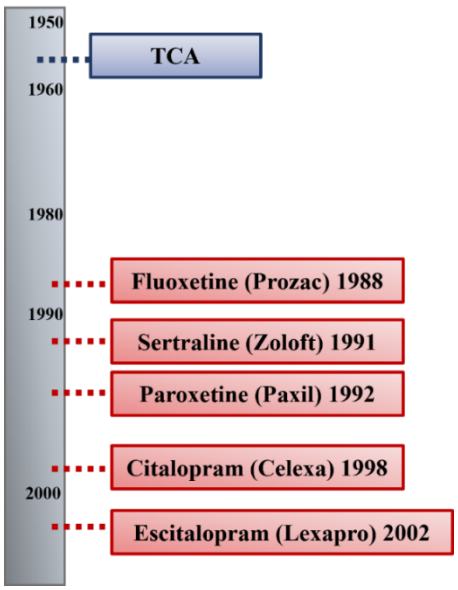

Figure 1.2: Milestones in antidepressant therapy: a timeline of SSRIs development. *Created by Rodriguez-Barucg, 2023*

Prozac and its subsequent products have revolutionised the concept of depression and its therapy. SSRIs were seen as drugs that could bring relief to millions of people who suffered from depression and other major mental disorders. With time, the usage of SSRIs was broadened not only for depression but also for the therapy of various psychiatric conditions like anxiety disorders, obsessive-compulsive disorder (OCD), post-traumatic stress disorder (PTSD), by reducing symptoms such as obsessions and compulsions (Bokor and Anderson, 2014; Diniz et al., 2011; Gosmann et al., 2021). SSRIs do not affect other neuroreceptors and adrenergic receptors, this allows for fewer side effects than TCAs (Peretti et al., 2000; Wilson and Mottram, 2004). By being safer and better tolerated, SSRIs eventually replaced TCAs as the most prescribed type of antidepressant, (Figure 1.3) (Bogowicz et al., 2021; Hillhouse and Porter, 2015; Lattimore et al., 2005; Von Wolff et al., 2013).

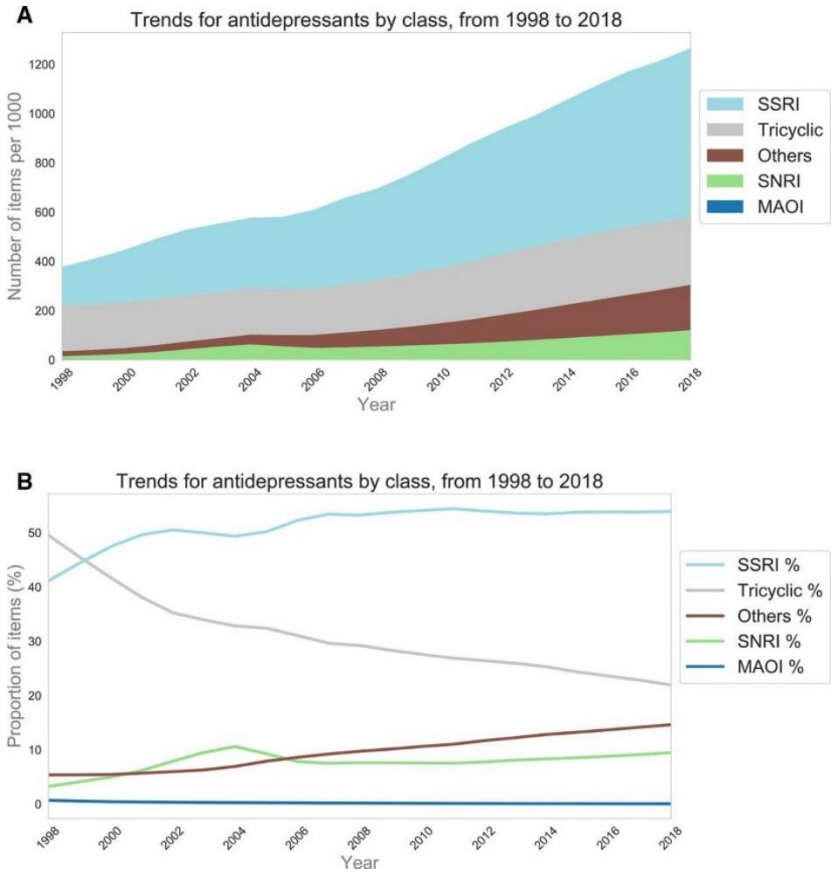

Figure 1.3: Two-decade trends in antidepressant prescribing: The rise of SSRIs and the decline of TCAs. *The population standardised numbers (A) and proportions (B) of prescribed antidepressant items by class from 1998–2018. MAOI = monoamine oxidase inhibitor. SNRI = serotonin-norepinephrine reuptake inhibitor. SSRI = selective-serotonin reuptake inhibitor. From Bogowicz et al., 2021.*

1.1.2 Comprehensive mechanisms and clinical implications of SSRIs

Building on the basic understanding of SSRIs introduced earlier, this section delves into the detailed pharmacological mechanisms that explain how these drugs affect serotonin levels and the broader nervous system. By exploring these processes further, we can gain a clearer view of their role in treating psychiatric disorders and the factors influencing their effectiveness.

SSRIs selectively block serotonin reuptake, which occurs in the synaptic cleft, a small gap between neurons where neurotransmitters are released and then bind to receptors on receiving neurons (Figure 1.1) (Kreke and Dietrich, 2008; Lattimore et al., 2005). Usually, serotonin released into the synaptic cleft is sucked back into pre-synaptic neurons through SERT. The reuptake process is blocked by SSRIs, which elevates the levels of serotonin in the synaptic cleft and improves serotonergic neurotransmission (Tate et al., 2021). This increase in serotonin availability is what made SSRIs so effective as antidepressants. Nevertheless, the exact mode

of action SSRIs is challenging to understand, and there is also a downstream modulation of neural circuits and neurotransmitter systems that happens, rather than just the increase in synaptic serotonin. An essential part of the effectiveness and safety of SSRIs is their pharmacokinetics (absorption, distribution, metabolism, and excretion). While SSRIs usually have a high oral bioavailability and can be taken in tablet form, food intake can highly influence their efficiency (van Harten, 1993). Once consumed, they are distributed widely throughout the body and brain. With their capacity to cross the blood-brain barrier, SSRIs affect the central nervous system. (Rochat et al., 1999). SSRIs are metabolised mainly in the liver into active metabolites or inactive compounds (Silva et al., 2012). Most of those compounds are excreted in urine (Edinoff et al., 2021; Vaswani et al., 2003). For example, fluoxetine is metabolised into norfluoxetine mainly through demethylation (Figure 1.4) by an enzyme of the cytochrome P450 family (CYP2D6) before being excreted (Dubovsky, 2015; Smith et al., 2010). Genetic variations in these enzymes can influence the efficacy of SSRIs and their potential drug-drug interactions (Dubovsky, 2015).

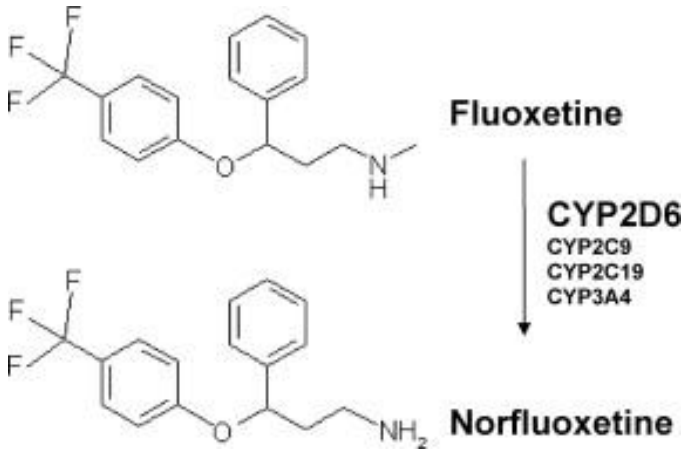

Figure 1.4: The chemical structure of fluoxetine and its active demethylated metabolite, norfluoxetine. *CYP2D6 is the dominant human CYP responsible for this metabolism. From Silva et al., 2012*

Although SSRIs are generally considered more benign than older antidepressants, they still come with a range of side effects that need careful management in clinical practice. Common adverse effects include nausea, headache, sexual dysfunction, and sleep disturbances (Clevenger et al., 2018; Strawn et al., 2015). The pharmacological basis of these side effects must be understood to manage them effectively (Wood and Hashemi, 2013). Beyond these, SSRIs have been linked to other symptoms such as drowsiness, weight gain, dry mouth, and fatigue (Atmaca, 2020; Ferguson, 2001; Jing and Straw-Wilson, 2016). In some cases,

movement-related concerns, including tremors or involuntary physical movements, have been reported (Zahra et al., 2022).

The widespread use of SSRIs has also sparked debates over their long-term efficacy and safety, particularly concerning vulnerable populations like pregnant women and neonates (Domingues et al., 2022; Kaihola et al., 2015). Early treatment phases can exacerbate symptoms like anxiety, sleep disturbances, and sexual dysfunction (Björkenstam et al., 2013), with an increased risk of suicidal ideation in children, adolescents, and young adults requiring close monitoring during the initial stages of treatment or dosage adjustments (K. Li et al., 2022). Genetic variability and underlying medical conditions further complicate patient responses, highlighting the importance of individualised treatment approaches that consider pharmacogenomic testing and patient history (Barbui et al., 2009; Hedna et al., 2021; van Westrhenen et al., 2020).

SSRIs are not considered addictive, but sudden cessation can lead to withdrawal-like symptoms known as discontinuation syndrome (Fava et al., 2015; Roose and Rutherford, 2016). This condition emphasises the need for a medically supervised discontinuation process to prevent complications (Marchocki et al., 2013). As SSRIs remain a cornerstone in psychiatric treatment, balancing their therapeutic benefits with the management of potential side effects is critical to their continued success.

1.1.3 SSRIs in the public and medical discourse

The public and medical opinion on SSRIs is complex. Their discovery revolutionised the way depression and other major psychiatric disorders were treated, but such a quick change of paradigm brought controversies. While being considered safer than already existing antidepressants (TCAs, MAOIs) due to their low risk of overdose (Jung et al., 1997), their mild side-effect profile (Bayes and Parker, 2019), their lower suicidal risk when compared to TCAs (Gibbons et al., 2005), SSRIs also face controversies regarding their effectiveness. For example, a meta-analysis comparing antidepressants and placebos in the treatment of mild depression in Parkinson's disease found that there was insufficient evidence to reject the null hypothesis of no differences in efficacy between SSRIs and placebo (Skapinakis et al., 2010). But on the other end, another study found that all antidepressants were more effective than

placebo in adults with major depressive disorder (Cipriani et al., 2018). This is a prime display of the constant controversies regarding the effectiveness of SSRIs.

Another main controversy is the risk of withdrawal symptoms. As mentioned previously, those symptoms are variable, usually occur within a few days of discontinuation, and can last up to a few weeks (Fava et al., 2015). They range from flu-like symptoms and tremors to mood swings or hallucinations, among others, Table 1.1 is a list of signs and symptoms of withdrawal from SSRIs. The primary debate among clinicians arising from the presence of withdrawal symptoms is whether or not to add SSRIs to the list of drugs potentially inducing withdrawal symptoms upon discontinuation. The term 'discontinuation syndrome' currently used being considered to minimise vulnerabilities induced by SSRIs and should be replaced by 'withdrawal syndrome' (Fava et al., 2015).

System involved	Symptoms
General	Flu-like symptoms, fatigue, weakness, tiredness, headache, tachycardia, dyspnea
Balance	Gait instability, ataxia, dizziness, light-headedness, vertigo
Sensory	Paresthesias, electric-shock sensations, myalgias, neuralgias, tinnitus, altered taste, pruritus
Visual	Visual changes, blurred vision
Neuromotor	Tremor, myoclonus, ataxia, muscle rigidity, jerkiness, muscle aches, facial numbness
Vasomotor	Sweating, flushing, chills
Sleep	Insomnia, vivid dreams, nightmares, hypersomnia, lethargy
Gastrointestinal	Nausea, vomiting, diarrhea, anorexia, abdominal pain
Affective	Anxiety, agitation, tension, panic, depression, intensification of suicidal ideation, irritability, impulsiveness, aggression, anger, bouts of crying, mood swings, derealization and depersonalization
Psychotic	Visual and auditory hallucinations
Cognitive	Confusion, decreased concentration, amnesia
Sexual	Genital hypersensitivity, premature ejaculation

Table 1.1: Signs and symptoms of withdrawal from SSRIs *From Fava et al. 2015*

The general public view on SSRIs is also highly variable; on the one hand, there is a growing awareness and acceptance of mental health issues in our society, but for some, there is an over-consumption of antidepressants (Bouckaert, 2021; Katolik and Oswald, 2017). The broad availability of SSRIs highly participated in the promotion of mental well-being and a better consideration for people suffering from mental illnesses (Bülow, 2022). However, part of the population criticises how appropriate it is to prescribe SSRIs as the treatment for major mental disorders. It considers that SSRIs are used as "quick fixes" for more complex issues (Golder et al., 2023).

In conclusion, the dichotomy in the public perception of SSRIs highlights two significant trends in mental health treatment, one advocating for a medicalised treatment using SSRIs as the primary described drug, and one that, while acknowledging the positive impact of SSRIs

advocates for a more appropriate use of SSRIs in consideration of their potential side effects and withdrawal symptoms.

1.1.4 Future directions in SSRIs research and development

As SSRIs continue to represent the most prescribed antidepressants to treat depression and other major psychiatric disorders, research tends to focus on resolving current limitations and finding new uses for SSRIs. One of the limitations of SSRIs is their excellent efficacy in favourable conditions but their limited efficacy in stressful situations. In order to increase the efficacy of SSRI in stressful conditions, the new approach is to have a polypharmacological strategy (Fineberg et al., 2018; Hjorth et al., 2022; Mayo-Wilson et al., 2014). By using a combination of SSRIs and other drugs, the efficacy of SSRIs could be increased. This has been tested in mice suffering from depression by using a combination of fluoxetine and metformin, a drug that improves the metabolic profile. The results were that the combined treatments were more effective than fluoxetine alone in ameliorating depression symptoms after just a week of treatment (Poggini et al., 2019).

Another research focus is the way SSRIs are delivered; some new delivery systems are being thought of as a way to increase bioavailability while reducing side effects. A novel way to deliver SSRIs is Fast Dissolving Tablets (FDT), which allow more than 95% of the drugs to be available within 10 minutes (Bhatia et al., 2022). This fast delivery allows for the initial increase in plasma concentration, which is mandatory in an acute depression attack. Another promising delivery system is transdermal patches. Drugs like sertraline, paroxetine, and escitalopram have been investigated using various transdermal strategies, and with further development, these products show significant potential for reaching the market. For these drugs, advantages, including the suppression of side effects and improved tolerance, are predicted (Tijani et al., 2021).

By improving the efficacy of SSRIs and bioavailability, there is hope for greater flexibility and individualised patient care. With advances such as Fast Dissolving Tablets and transdermal patches, these new methods offer the potential to optimise treatment outcomes by addressing the varied needs of patients, particularly in cases requiring rapid relief or tailored therapeutic regimens. As research in this area continues, these innovations may help enhance both the therapeutic effectiveness and the tolerability of SSRIs, ultimately improving patient experiences.

1.2 Environmental impact of SSRIs

1.2.1 Environmental presence of SSRIs

The presence of SSRIs in freshwater ecosystems has become a growing concern, combining pharmacological insights with ecological considerations. Once prescribed for psychiatric conditions and consumed by patients, a significant portion of these drugs, along with their metabolites, are excreted unchanged into wastewater as illustrated in Figure 1.5 (Silva et al., 2012). Wastewater treatment plants are often unable to fully eliminate these compounds, leading to their release into surface water bodies such as lakes and rivers, as well as into human water supplies (Bossus et al., 2014; Brooks et al., 2005; Christensen et al., 2007; Henry et al., 2004). Many SSRI metabolites retain some pharmacological activity such as norfluoxetine, although typically less potent than the parent compound, with the notable exception of norfluoxetine, which remains significantly active (Silva et al., 2012).

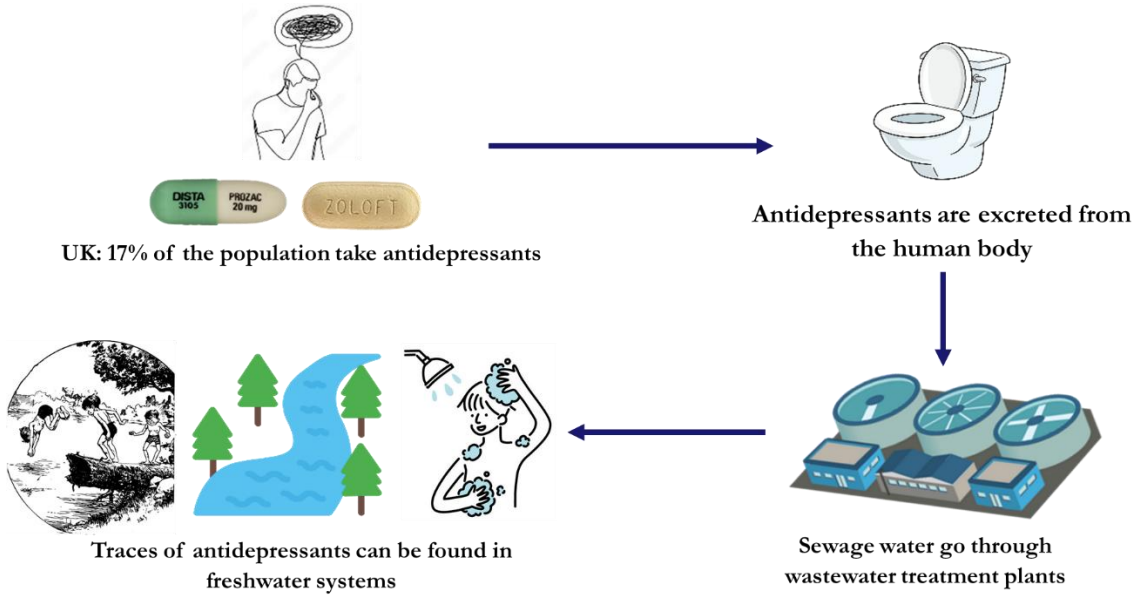

Figure 1.5: Pathway of Selective Serotonin Reuptake Inhibitors (SSRIs) from Clinical Use to Aquatic Environmental Contamination. *Created by Rodriguez-Barucg, 2023.*

Studies have detected SSRIs in various freshwater sources across Europe and North America. In Poland, for example, in the Warsaw region (Poland), traces of various antidepressants have been found in rivers and even in tap water in concentrations up to 3 ng/l (for sertraline) (Giebułtowicz and Nałecz-Jawecki, 2014). Those results are similar to those found in other European countries; for instance, in Spain, the presence of fluoxetine has been recorded at concentrations of up to 44 ng/l in 80% of the sampling sites from the main rivers of the Madrid metropolitan area: Jarama, Manzanares, Guadarrama, Henares and Tajo. Other several

antidepressants were present in the surface water of that region, including venlafaxine, at concentrations of up to 387 ng/l and found in 100% of the sampling sites (González Alonso et al., 2010). The presence of fluoxetine and venlafaxine in surface water can be explained by the fact that wastewater treatment processes do not completely remove those drugs from the water. Different studies have shown that water released from wastewater treatment plants still has presence of those drugs, as shown in the Rhine river (fluoxetine 24 ng/l, norfluoxetine 13 ng/l) (Schlüsener et al., 2015). The water coming out of those wastewater treatment plants is considered the main source of SSRIs in surface water (Writer et al., 2013). In the U.S., antidepressants (such as fluoxetine, citalopram, etc.…) were present up to 8.4km downstream of the outfalls of two effluent-impacted streams, Boulder Creek (Colorado) and Fourmile Creek (Iowa) at concentrations of up to 12.1 ng/l and 11.1 ng/l, respectively (Schultz et al., 2010).
Other recent environmental monitoring studies have identified fluoxetine concentrations that extend well beyond these background levels. In Canada, Lajeunesse et al. reported fluoxetine levels reaching up to 346 ng/l in influent and 69 ng/l in treated effluent (Lajeunesse et al., 2012). Norfluoxetine was also detected at comparable levels. Kleywegt et al. recorded fluoxetine concentrations ranging from 8 to 97 ng/l in WWTP effluents in Ontario and highlighted the persistence of fluoxetine in downstream surface waters such as Lake Ontario and the Grand River (Kleywegt et al., 2019).
In the United States, Benotti et al. documented fluoxetine concentrations as high as 560 ng/l in surface waters downstream of WWTPs (Benotti and Brownawell, 2007) while Bringolf et al. found fluoxetine levels of 104–119 ng/l in effluent discharge channels, which dropped to 10.0–14.4 ng/l at 50 m downstream and 5.1–7.3 ng/l at 100 m, demonstrating rapid dilution yet persistent detectability (Bringolf et al., 2010). Hughes et al. compiled global monitoring data and reported fluoxetine concentrations up to 596 ng/l in treated wastewater effluents from various countries (Hughes et al., 2013). Bean et al. , in a UK-based modelling study, included literature-based influent values exceeding 1,310 ng/l to assess potential ecological risks (Bean et al., 2017a).The highest measured concentration in treated effluent was reported by Salgado et al., who detected 3,645 ng/l of fluoxetine in a WWTP in Portugal (Salgado et al., 2011). Shraim et al. went further, reporting norfluoxetine concentrations of 11,700 ng/l in treated wastewater in Almadinah, Saudi Arabia (Shraim et al., 2017).

These findings demonstrate that while typical fluoxetine concentrations in surface waters range from 10–100 ng/l, specific locations near effluent discharge points can experience much higher levels, often exceeding 1,000 ng/l and, in extreme cases, 3,000–10,000 ng/l. Such

concentrations are not theoretical or based on *in-vitro* studies but are directly measured in real-world aquatic environments. Therefore, in this thesis, the term "environmentally relevant concentrations" refers to empirically observed levels of fluoxetine and norfluoxetine in surface waters and wastewater effluents, particularly near WWTP discharge points, as reported in the studies discussed above. The concentrations used in this project (ranging from 62.5 to 5,400 ng/l) were selected to reflect this spectrum: the lower and mid-range doses align with fluoxetine levels commonly detected in effluent and downstream environments, while the highest concentration (5,400 ng/l) represents a plausible upper-bound scenario. This extreme condition is intended to simulate future environmental risks that may arise from increasing pharmaceutical consumption, population growth, and water scarcity, factors expected to intensify SSRI accumulation in aquatic ecosystems, particularly in regions with limited wastewater infrastructure.

While environmental studies have primarily focused on the ecotoxicological impact of SSRIs such as fluoxetine on aquatic organisms, the implications for human health are becoming increasingly relevant. Fluoxetine has been detected in surface waters, effluents, and even drinking water supplies, raising concerns about chronic low-level exposure (Benotti and Brownawell, 2007; Lajeunesse et al., 2012; Writer et al., 2013). Populations with direct contact with natural waters, including wild swimmers, rowers, athletes, and children, represent potential at-risk groups, especially in areas downstream of wastewater treatment plants where concentrations may reach hundreds of ng/l. Occupational exposure is also a consideration for individuals working in wastewater management or recreational water services. Moreover, climate change-driven water scarcity may lead to increased fluoxetine concentrations in both recreational waters and drinking supplies, potentially elevating daily dermal exposure levels across the general population. As the skin acts as a primary barrier and plays a central role in wound healing, investigating how environmentally relevant levels of fluoxetine influence skin repair processes is crucial for understanding both ecological and public health risks

The presence of fluoxetine in most surface water sites, its environmental persistence, and its acute toxicity to non-target organisms such as fish and aquatic invertebrates (Oakes et al., 2010) make it one of if not the key SSRIs compound to study in aquatic ecosystems (Silva et al., 2012). Most of the current reports come from Europe (50%) and North America (38%) (Mole and Brooks, 2019) while as stated earlier, the problematic of SSRI presence in aquatic ecosystems is even bigger in poor and highly demographically growing areas such as Africa and Asia (Burket et al., 2018; Mole and Brooks, 2019). Changes in lifestyle, as well as a high

demographic development in those areas, suggest that the quantities of SSRIs consumed and, as a consequence, rejected in the water will increase in the future (Burket et al., 2018; Schlüsener et al., 2015). This is further compounded by the growing issue of water scarcity due to climate change, which could exacerbate the environmental impact of pharmaceutical contamination. It makes it necessary that more reports regarding the presence of SSRIs in water are conducted there in the future.

1.2.2 Impact on aquatic life: earlier research and findings.

Various aquatic species (either vertebrates or invertebrates) can be affected by the presence of SSRIs in water, and those species are sensitive to different levels of SSRIs (Sumpter et al., 2014). Not only are aquatic species sensitive to a wide range of SSRI concentrations in water, but the response to those drugs varies from one species to another.

After an exposure of 3 weeks to fluoxetine (concentrations ranging from 10 ng/l to 10,000 ng/l), *Echinogammarus marinus* (Figure 1.6) spent more time in the light (phototaxis behaviour) and were higher in the water column (geotaxis behaviour) than their non-exposed counterparts (Guler and Ford, 2010), While the highest concentration used (10,000 ng/l) exceeds environmental levels, the behavioural changes observed at lower doses (10–100 ng/l) are within environmentally relevant ranges, supporting the ecological relevance of these findings. Those changes are similar to what has been described for *Echinogammarus marinus* infected with acanthocephalans parasites. Previous studies have shown that *Gammarus* infected with that parasite had a higher predation risk and were more likely to be eaten by birds (Perrot-Minnot et al., 2007). The presence of fluoxetine in the water could potentially imply higher predation of birds on *Echinogammarus marinus* and suggest changes in the whole ecosystem. Those effects of SSRIs on small amphipod crustaceans seem to be dose-dependent. When exposed to low concentrations (1-100 ng/l) of pharmaceuticals (including fluoxetine), *Gammarus pulex* (Figure 1.6) showed increased ventilation, whereas when exposed to high concentrations (1 mg/l – 1 g/l), it showed increased locomotion (De Lange et al., 2009). Another study confirmed the difference in effects of different concentrations of drugs; when the same species *Gammarus pulex* was exposed to a low concentration of fluoxetine (100 ng/l), its swimming velocity was reduced (De Castro-Català et al., 2017), which is different to the effect observed by De Lange et al., 2009 after exposure to high concentrations (1 mg/l -1 g/l).

Another invertebrate also displays behavioural changes when exposed to antidepressants. Crayfish *Orconectes virilis* (Figure 1.6), after exposure to sertraline (424 ng/l), were more aggressive than non-exposed ones when facing each other in a bout; males exposed to sertraline initiated antagonistic interaction three times more than control males (Woodman et al., 2016). However, the number of initiations for bouts of two exposed crayfish was not significantly different from those recorded for two control animals' bouts. Sertraline affects the fighting dynamic of individuals, but since the whole population in an aquatic environment would be exposed to the same concentration, all individuals will likely experience the same increase in aggressive behaviour.

Another typical behaviour affected by SSRIs is reproduction. For example, in the water flea Daphnia magna (Figure 1.6), exposure to fluoxetine (40 µg/l) will impact reproduction behaviour similarly to the food limitation factor (Campos et al., 2016). For fingernail clams Sphaerium striatinum (Figure 1.6), SSRIs seem to induce parturition (for fluvoxamine and paroxetine) or potentiate it (for fluoxetine) even at a low concentration (3 ng/l)(Fong et al., 2017).

Taken together, it has been demonstrated that SSRIs (especially fluoxetine) have significant sublethal effects at low concentrations on small amphipods and crustaceans. Those sublethal effects can impact the predation or competition behaviours of those small species, potentially impacting ecosystems at a larger scale.

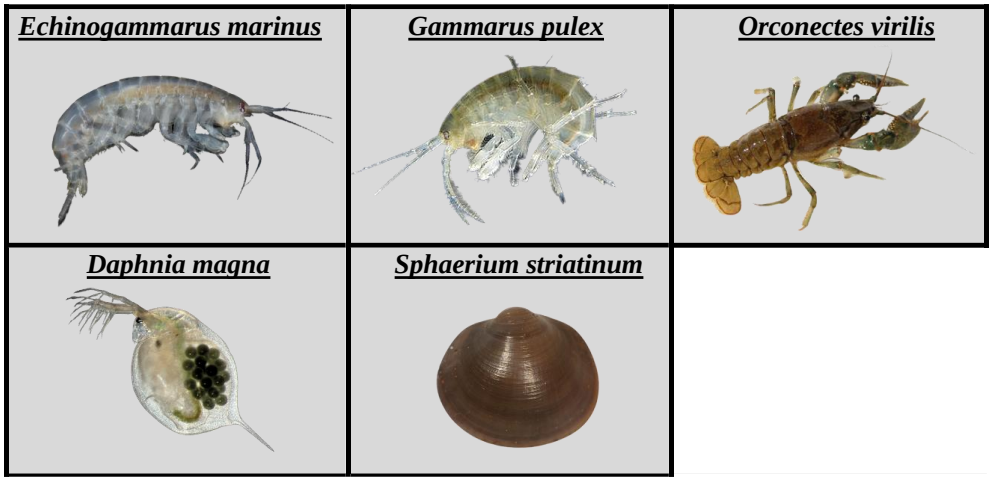

Figure 1.6: Visual representation of the various aquatic species exposed to SSRI-contaminated water. *The species depicted here were selected based on those specifically discussed in Section 1.2.2, as they have been used in published studies investigating the behavioural and physiological effects of SSRIs, particularly fluoxetine. These include Echinogammarus marinus (phototaxis and geotaxis changes, Guler and Ford, 2010), Gammarus pulex (dose-dependent behavioural changes, De Lange et al., 2009; De Castro-Català et al., 2017), Orconectes virilis (aggression modulation, Woodman et al., 2016), Daphnia magna (reproductive effects, Campos et al., 2016), and Sphaerium striatinum (early parturition, Fong et al., 2017). These invertebrates were chosen not as a comprehensive representation of all affected aquatic organisms, but because they exemplify the range of sublethal, ecologically relevant effects SSRIs can have at low concentrations. Their inclusion in the figure visually supports the discussion on how SSRI pollution can influence key ecological behaviours such as reproduction, competition, and predation.*

When it comes to fish, numerous studies have been published about the impact of SSRI-contaminated water on those species. For example, when exposed to fluoxetine at 100, 1 000 and 10 000 ng/l for 21 days, *Danio rerio* showed no changes in exploratory or social behaviour (Correia et al., 2022). However, a decrease in locomotor activity was displayed both in light and dark periods, demonstrating the ability of SSRIs to affect how this species responds to environmental stressors (change of light) (Correia et al., 2022). Similar results were observed in another study on *Danio rerio* exposed to sertraline at 10 000 ng/l (Faria et al., 2022) that identified that hypolocomotion was associated with augmented serotonin levels rather than other neurochemicals and molecular markers, highlighting the relationship between serotonin signalling and behaviour in zebrafish.

Changes in behaviour have also been described for other fish species; for instance, exposure to fluoxetine in male Siamese fighting fish caused a shift in boldness (Dzieweczynski et al., 2016). Three groups of males (0, 500 and 5000 ng/l fluoxetine) were tested in multiple boldness assays (empty tank, novel environment, and shoal) once a week for three weeks to collect baseline measures and then at three different time points postexposure. Unexposed males were bolder

in all contexts after exposure. Figure 1.7 shows the results for the novel environment assays; before exposure, all three groups had similar boldness. Still, on trial 4/5/6 after exposure to fluoxetine, groups exposed to both 500 and 5000 ng/l of fluoxetine displayed a significantly lower boldness when compared to non-exposed males (Dzieweczynski et al., 2016). When all contexts are considered, the effect of fluoxetine on boldness behaviour was dose-dependent; the higher the concentration, the greater the behavioural effect was.

Another example is how, fluoxetine affects *Pimephales promelas* (fathead minnow). At concentrations ranging from 100 ng/l, which approaches the upper limit of environmentally detected levels, to 100 000 ng/l (a high-dose exposure) a change in mating and aggression behaviours has been described (Weinberger and Klaper, 2014). Males were more aggressive and tended to be more isolated. This aggressive behaviour impacted egg production due to females' deaths after repeated aggressions. Both males and females took longer to eat and had decreased predator avoidance behaviour (Weinberger and Klaper, 2014). All those factors could affect population survival.

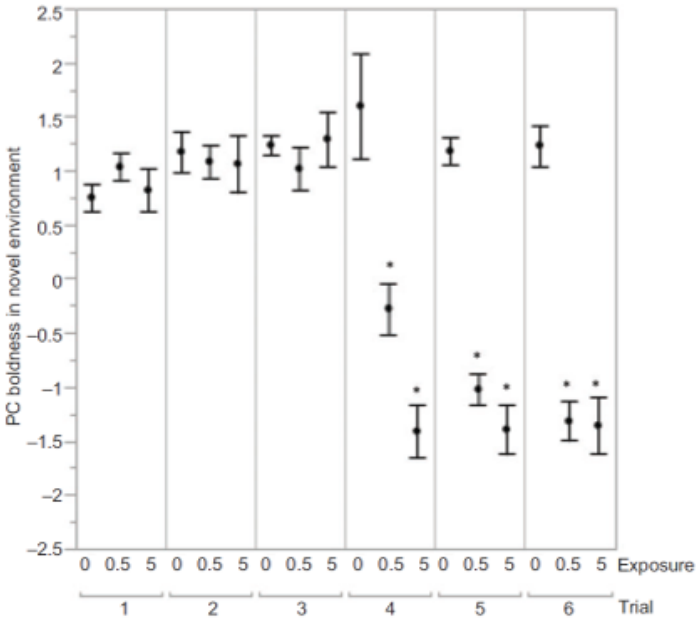

Figure 1.7: Siamese fighting fish boldness assays. *Mean boldness scores (PC B1) in all trials (1–6) for the three exposure groups (0, 0.5 and 5 μg l−1; n=20 for each group) in the novel environment assay. Error bars are ±1 s.e.m. Significant relationships are indicated by asterisks.*

1.3 Serotonin signalling

Serotonin is a neurotransmitter that plays a central role in regulating various physiological processes in the body, initially identified in the central nervous system (CNS), serotonin has since been found in numerous peripheral tissues, where it influences critical cellular functions (Berger et al., 2009; El-Merahbi et al., 2015). Serotonin signalling is a complex and tightly regulated system, mediated by multiple receptor families, transporters, and downstream signalling pathways (Boccuto et al., 2013; Zhu et al., 2011). The following sections explore serotonin production, its receptor families, and its broader physiological roles, setting the foundation for understanding its relevance to pharmacological interventions such as SSRIs.

1.3.1 Overview of serotonin production and receptor families

Serotonin synthesis begins with the amino acid tryptophan, which is hydroxylated by the enzyme tryptophan hydroxylase (TPH) to form 5-hydroxytryptophan, and subsequently decarboxylated to produce serotonin, see Figure 1.8 (Boccuto et al., 2013; Vadaq et al., 2022; Vleugels et al., 2015; Xiao et al., 2018). This process predominantly occurs in the enterochromaffin cells of the gastrointestinal tract, where approximately 95% of the serotonin of the body is produced (Vadaq et al., 2022). The remaining serotonin is synthesised in the brain, particularly in the raphe nuclei of the brainstem, where it plays a crucial role in modulating mood, cognition, and various physiological processes (Pho et al., 2022; Xiao et al., 2018).

Serotonin exerts its effects by binding to a broad range of serotonin receptors, which are classified into seven families (5-HT1 to 5-HT7), each comprising multiple subtypes with distinct functions (Boccuto et al., 2013). 5-HT1, 5-HT2, 5-HT4, 5-HT6, and 5-HT7 are key players in the transmission of serotonin signals, these receptors are distributed across various tissues in the body, including the brain, gastrointestinal tract, and cardiovascular system, regulating processes such as vasoconstriction, platelet aggregation, and gastrointestinal motility (Zhu et al., 2011).

While serotonin is primarily synthesised in the central nervous system and gastrointestinal tract, accumulating evidence suggests that keratinocytes possess the enzymatic machinery required for serotonin biosynthesis. Studies have demonstrated that keratinocytes express tryptophan hydroxylase (TPH), the rate-limiting enzyme in serotonin synthesis, as well as dopa decarboxylase (DDC), enabling local serotonin production within the epidermis (Goodwin et al., 2017; Schallreuter et al., 2012). Additionally, keratinocytes express functional serotonin

receptors (e.g., 5-HT2A, 5-HT3), suggesting that serotonin-mediated signalling is intrinsic to epidermal biology (Go et al., 2024). Furthermore, ultraviolet (UV) radiation has been shown to stimulate serotonin production in keratinocytes, linking environmental cues to serotonin availability (Edstrom et al., 2010; Slominski et al., 2024). These findings suggest that serotonin is not only present in the skin but also actively contributes to epidermal function, supporting the plausibility of serotonin-mediated effects in keratinocyte culture systems.

In addition to endogenous serotonin synthesis by keratinocytes, another potential source of serotonin in cell culture conditions is foetal bovine serum (FBS), which is widely used as a supplement in cell culture media. While direct quantification of serotonin in FBS remains limited, evidence suggests that maternal serotonin can cross the placental barrier, making its presence in foetal-derived serum plausible (Yang Li et al., 2022). Additionally, serotonin or its precursors have been detected in filtered FBS using biosensors, reinforcing the idea that even in culture conditions, serotonin could be present at biologically relevant levels (Chávez et al., 2017). Some studies have also identified enzymatic activities in serum, including amine oxidases, which may regulate serotonin availability in culture media over time (Holbert et al., 2020). Although absolute serotonin levels in FBS batches used in this study were not measured, these findings suggest that serotonin-mediated effects in keratinocyte cultures could be influenced by both intrinsic production within the cells and external serotonin sources from the culture medium.

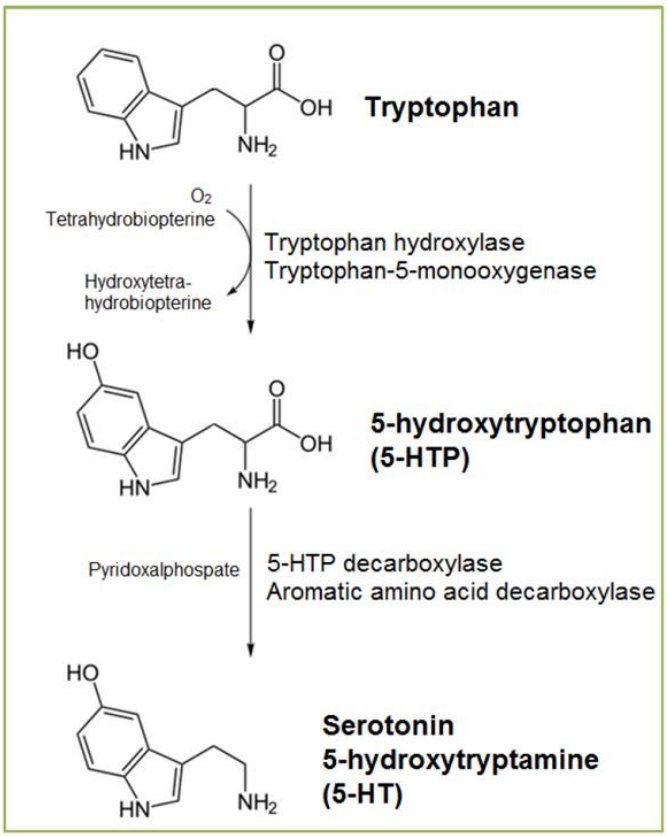

Figure 1.8: Biosynthesis of serotonin (5-HT). *Tryptophan is converted into 5-hydroxytryptamine (5-HTP) by tryptophan hydroxylase (TPH), and 5-HTP is then decarboxylated into serotonin (5-HT) by aromatic amino acid decarboxylase (AADC). From Vleugels et al. 2015.*

The mechanism by which serotonin receptors function is primarily determined by their coupling to G-proteins. 5-HT1 receptors, particularly the 5-HT1A subtype, are coupled with Gi/o proteins, which inhibit adenylyl cyclase (AC) activity (Vleugels et al., 2015). This reduces cyclic adenosine monophosphate (cAMP) levels, dampening downstream signalling pathways such as those mediated by protein kinase A (PKA), which are essential for processes like neuronal excitability and neurotransmitter release (Polter et al., 2012; Vleugels et al., 2015).
5-HT4, 5-HT6, and 5-HT7 receptors, on the other hand, are coupled with Gs proteins, which increase cAMP levels and promote functions such as memory formation, neuroplasticity, and learning. For example, activation of the 5-HT4 receptor stimulates acetylcholine release, critical for cognitive processes (Kang et al., 2019). Similarly, 5-HT6 receptor activation enhances learning and memory through modulation of cholinergic and glutamatergic mechanisms (Woods et al., 2012), the 5-HT6 receptor's ability to stimulate adenylyl cyclase activity is directly correlated with enhanced cognitive functions, as demonstrated by behavioural assays (Kendall et al., 2011). Additionally, 5-HT7 receptor activation is

noteworthy for its role in increasing cAMP levels and facilitating neuroplastic changes. Research indicates that activation of 5-HT7 receptors promotes the expression and phosphorylation of the TrkB receptor, further linking serotonin signalling to neuroplasticity and cognitive enhancement (Samarajeewa et al., 2014).

5-HT2 receptors are coupled with Gq proteins and activates phospholipase C, increasing intracellular calcium levels, this promotes physiological responses such as smooth muscle contraction and platelet aggregation (De Deurwaerdère et al., 2004; Garcia et al., 2007; Parrish and Nichols, 2006).

Serotonin signalling is further regulated by its transporters, specifically the serotonin transporter (SERT), which facilitates the reuptake of serotonin into presynaptic neurons. This process not only terminates the serotonin signal but also plays a critical role in maintaining synaptic homeostasis and regulating serotonin availability for future neurotransmission (Penkova and Nikolova, 2017). Dysregulation of SERT function can significantly affect serotonin levels, influencing mood, cognition, and overall neuronal function.

However, emerging evidence suggests that the pharmacological effects of fluoxetine extend beyond serotonin reuptake inhibition. Studies have shown that fluoxetine can interact directly with several serotonin receptor subtypes, influencing cell signalling even when serotonin levels are low. For example, fluoxetine acts as a high-affinity agonist at the 5-HT2B receptor, activating downstream pathways such as EGFR transactivation and ERK/AKT signalling in astrocytes (Peng et al., 2014). In contrast, it inhibits 5-HT3 receptor activity by binding to a different site than serotonin, reducing ion flow through the channel regardless of serotonin presence (Breitinger et al., 2001). Additional experiments showed that fluoxetine reduces the flow of sodium and calcium ions through 5-HT3 receptors when serotonin is present. This effect occurred in a dose-dependent way and was not affected by changes in electrical voltage, confirming that fluoxetine acts as a functional antagonist at this receptor (Eisensamer et al., 2003).

Fluoxetine has also been shown to block 5-HT2C receptors by competing with serotonin for the same binding site, preventing their activation even at low concentrations (Ni and Miledi, 1997). These findings highlight that fluoxetine can behave either as an agonist or an antagonist, depending on the receptor subtype. Agonists activate receptors and mimic the effects of serotonin, while antagonists bind to receptors and prevent them from being activated. This receptor-specific behaviour suggests that fluoxetine may influence cellular responses not just

by increasing serotonin levels, but also by directly modifying receptor activity. Such effects could be especially relevant in tissues like the skin, where serotonin levels may be limited, but serotonin receptors remain active and responsive. Figure 1.9 provides a schematic overview of serotonin-mediated cellular signalling and fluoxetine's interactions with its key components, including serotonin receptors, the serotonin transporter (SERT), and intracellular pathways implicated in wound healing.

In summary, serotonin signalling is shaped by local synthesis, diverse receptor subtypes, and regulation by transporters such as SERT. Fluoxetine can influence this system not only by increasing serotonin levels but also by directly interacting with specific receptors, acting as either an agonist or antagonist. These receptor-specific effects may be especially relevant in peripheral tissues like the skin, where serotonin levels are limited but receptors remain active. The following section will explore how these receptors trigger intracellular signalling pathways that regulate key cellular functions.

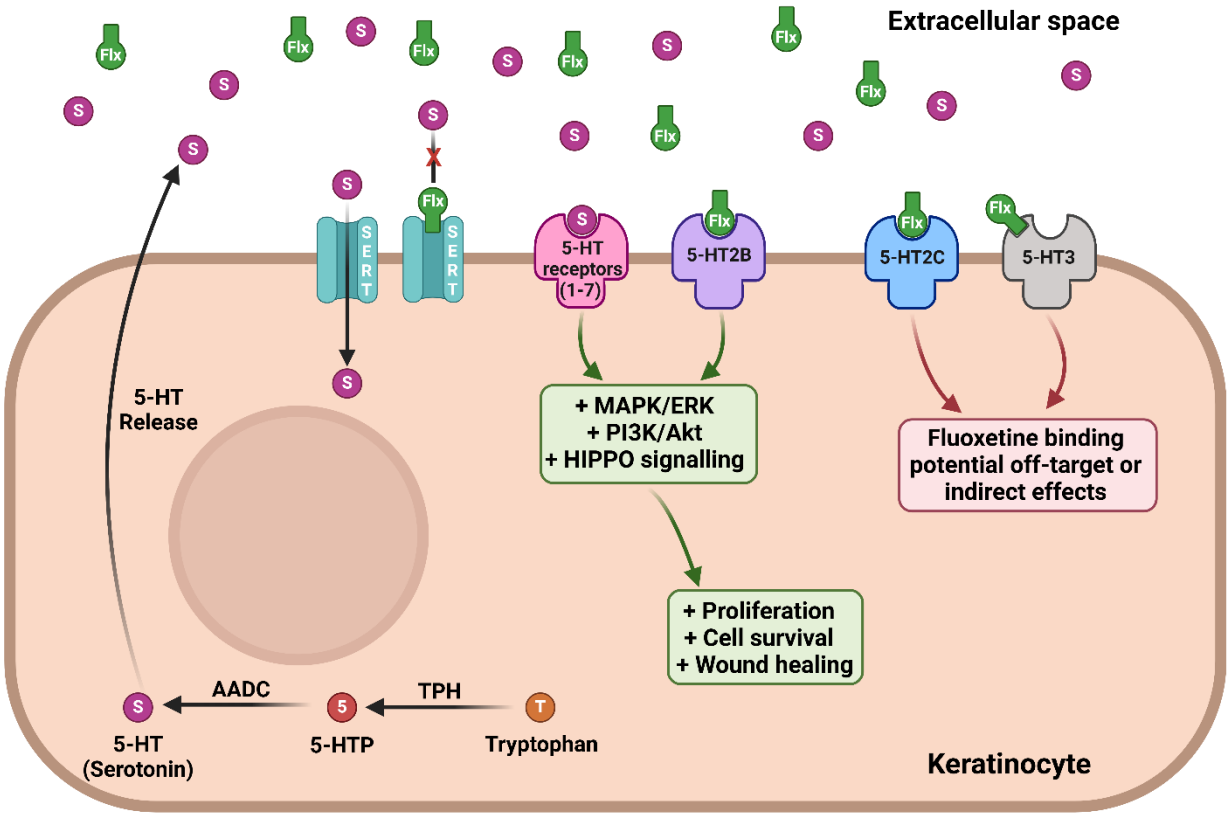

Figure 1.9: Mechanistic representation of serotonin signalling and fluoxetine activity in keratinocytes. *This schematic illustrates the proposed serotonin-mediated signalling cascade relevant to wound healing in human keratinocytes. Endogenous serotonin (S) is synthesised intracellularly from tryptophan via the enzymes tryptophan hydroxylase (TPH) and aromatic L-amino acid decarboxylase (AADC), then released into the extracellular space where it can bind to various serotonin receptor subtypes (5-HT1–7). Upon activation, these receptors stimulate intracellular signalling cascades including MAPK/ERK, PI3K/AKT, and HIPPO pathways, which promote keratinocyte proliferation, survival, and tissue repair. Fluoxetine (Flx), blocks serotonin reuptake by binding to the serotonin transporter (SERT), thereby increasing serotonin availability at the cell surface. Additionally, fluoxetine can directly bind to 5-HT receptors (5-HT2B, 5-HT2C, 5-HT3), potentially exerting receptor-specific or off-target effects that influence cellular behaviour independently of extracellular serotonin levels. This multi-pathway model integrates both serotonin-dependent and potential serotonin-independent effects of fluoxetine relevant to wound healing outcomes.*

1.3.2 Serotonin signalling pathways

As outlined in the previous section, serotonin receptors play diverse roles throughout the body, and upon activation, they initiate complex signalling pathways. These receptors are distributed across multiple tissues and systems, including the central nervous system, gastrointestinal tract, and cardiovascular system. Each receptor activates distinct intracellular signalling pathways that regulate critical processes such as cell proliferation, migration, apoptosis, neurotransmission, and immune response (Sahu et al., 2018). Given the widespread distribution and physiological importance of serotonin, understanding these pathways is key to revealing how 5-HT influences various cellular and molecular processes. The downstream effects of serotonin receptor activation are mediated by several key intracellular pathways, including the MEK/MAPK, PI3K/AKT, and JAK/STAT pathways Figure 1.9.

The activation of 5-HT2 receptors, coupled with the activation of phospholipase C (PLC), triggers the MEK/MAPK pathway. This pathway is integral to regulating gene expression and cell cycle progression and plays a crucial role in tissue repair and regeneration. Upon activation, PLC leads to the generation of inositol trisphosphate (IP3) and diacylglycerol (DAG), which mobilise intracellular calcium and activate protein kinase C (PKC). PKC, in turn, activates the MEK/MAPK pathway, promoting cellular processes such as proliferation and differentiation (Jung et al., 2006; Kimura et al., 2013; Tai and Tzeng, 2014). This signalling route highlights the significant role of serotonin in facilitating cell growth and wound healing, as explored further in later chapters. Additionally, 5-HT1 and 5-HT6 receptors are linked to the PI3K/AKT pathway, which is crucial for promoting cell survival by inhibiting pro-apoptotic factors such as CASP3 and CASP9 (Hsiung et al., 2005). This pathway is also involved in regulating autophagy, a key process in maintaining cellular homeostasis, particularly under stress conditions (Nebigil et al., 2003). Through its activation, serotonin modulates the survival of both neuronal and non-neuronal cells, such as fibroblasts and keratinocytes, which play critical roles in wound healing and tissue repair (Vleugels et al., 2015). Additionally, the PI3K/AKT pathway complements this process by preventing cell death and promoting recovery in damaged tissues. As further illustrated in Figure 1.10 from Sahu et al., 2018, the serotonin-signalling network triggers several key molecular events, including the activation of pathways such as MEK/MAPK and PI3K/AKT. This schematic represents protein-protein interactions, enzyme-catalysed reactions, and gene regulation processes initiated by serotonin receptor activation. By highlighting the downstream signalling modules enriched across various 5-HT receptor subtypes, the map demonstrates how serotonin influences critical

cellular activities, such as proliferation, survival, and apoptosis. This network underscores the multifunctional role of serotonin in both central nervous system regulation and peripheral processes like tissue repair and wound healing.

Another essential pathway influenced by serotonin is the JAK/STAT pathway, which is primarily activated by 5-HT2 receptors and is heavily involved in modulating immune responses and inflammation. Upon activation, this signalling cascade promotes the expression of pro-inflammatory cytokines, such as IL-6 and TNF-α, which are crucial for the wound healing process (Khan et al., 2020; Macrì et al., 2024). This pathway not only controls inflammation but also regulates immune responses and cellular survival (Malemud, 2017). The involvement of the JAK/STAT pathway in tissue repair underscores its critical role in broader effects of serotonin on both immune regulation and wound healing (Moon et al., 2021). Dysregulation of this pathway has been linked to chronic inflammatory disorders, highlighting the therapeutic potential of modulating JAK/STAT signalling in conditions involving excessive inflammation (Meyer and Levine, 2014; Montilla et al., 2019).

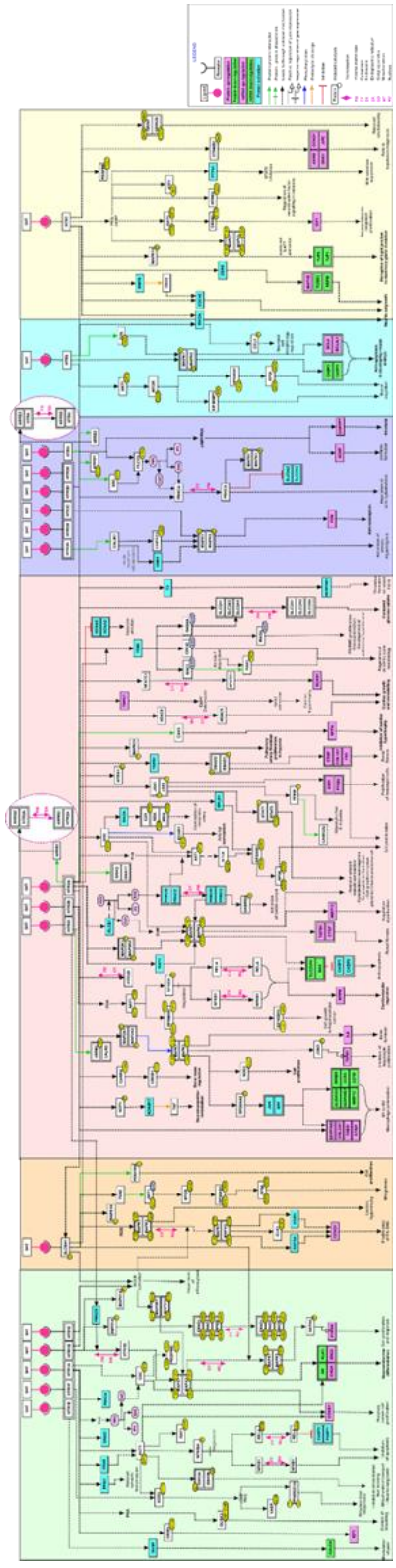

Figure 1.10: Schematic representation of the NetPath reactions induced by serotonin-serotonin receptor. *The pathway reaction map depicts molecular events induced through serotonin-serotonin receptor interaction. Pathway map represents protein-protein associations, enzyme catalysis reactions, translocation events, gene and/or protein regulation induced upon treatment with serotonin or its analogues. Legends describe the reaction events in the map. From Sahu et al., 2018.*

1.4 SSRIs and Wound Healing

As outlined in the previous section, serotonin plays a critical role in processes like cell proliferation and tissue repair, which are essential to wound healing. To fully understand how SSRIs might influence these processes, it is first important to examine the general mechanisms of wound healing. Following this, we will explore how SSRIs, whether through therapeutic use or environmental exposure, affect these pathways and their broader implications for health.

1.4.1 What is cutaneous wound healing?

A wound happens when the epidermal layer of the skin loses its integrity and exposes the dermis to the air (Ozgok Kangal and Regan, 2022). This can be accompanied by a disruption of the structure and function of the normal dermal tissue (Enoch and Leaper, 2008). A wound can result from various disruptions from precise incisions, lacerations, contusions or more extensive tissue damage (e.g. burns)(Enoch and Leaper, 2008; Reinke and Sorg, 2012).
The healing of normal wounds is a balanced process involving a complex and well-organised series of events (Cullen et al., 2002; Wilkinson and Hardman, 2020a) including repair processes to form new tissue and destructive processes to remove damaged tissue. A wound is considered fully healed when the connective tissues have been repaired, and the wound is entirely re-epithelialised, returning to a normal structure and function (Enoch and Leaper, 2008).

Wound healing occurs in four distinct but overlapping stages: the haemostasis and inflammatory phase, the proliferative phase, and the remodelling phase (Ozgok Kangal and Regan, 2022; Wilkinson and Hardman, 2020a). Each phase is tightly regulated and requires a specific set of cellular and molecular processes to occur in synchrony to achieve successful tissue repair. The timeline of these events can be influenced by numerous factors, including the wound type, the patient's health, and environmental conditions (Reinke and Sorg, 2012). Figure 1.11 illustrates these stages, the processes involved, and the time they occur at.

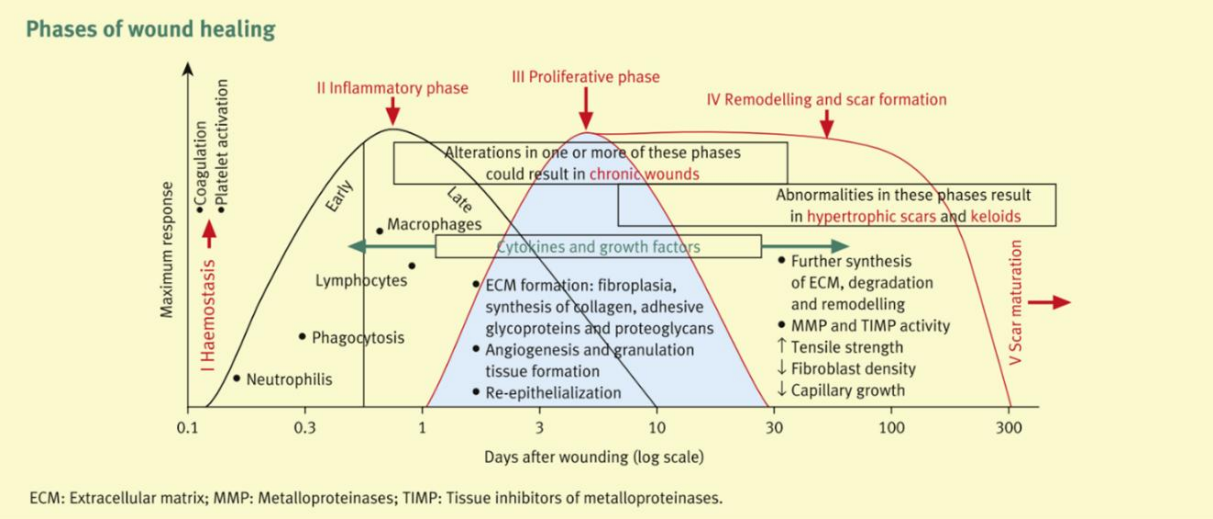

Figure 1.11: Representation of the different phases of the wound healing process. *From Enoch & Leaper, 2008*

Haemostasis:

Haemostasis is the body's initial response to tissue injury. It begins immediately after a wound occurs and serves to minimise blood loss and initiate the healing cascade. The first crucial event in haemostasis is vasoconstriction, where the blood vessels constrict to reduce blood flow to the injured site. This response is crucial for minimising blood loss. Simultaneously, platelets aggregate at the site of injury, adhering to the exposed collagen in the damaged blood vessels (Ozgok Kangal and Regan, 2022; Wilkinson and Hardman, 2020a). Figure 1.12 illustrates the involvement of various cellular components, such as platelets, neutrophils, and fibroblasts, during the haemostasis, inflammation, proliferation, and remodelling phases. Platelets release their contents, including adenosine diphosphate (ADP), thromboxane A2, and serotonin, that promote production of thrombin and further platelet aggregation and stabilise the initial clot (Horowitz and Spielvogel, 1971; Periayah MH et al., 2017). The formation of a fibrin clot occurs through the coagulation cascade, where fibrinogen is converted into fibrin. The fibrin matrix not only functions as a scaffold for cell migration but also acts as a reservoir for cytokines and growth factors that modulate the subsequent phases of healing (Hiebert and Werner, 2019).

An essential aspect of haemostasis is the release of growth factors and cytokines from the aggregated platelets. Studies demonstrate that during this phase, alpha granules in platelets release a cocktail of growth factors, including platelet-derived growth factor (PDGF), transforming growth factor-beta (TGF-β), and interleukin-1α (IL-1α) (Cognasse et al., 2008; Durante et al., 2013). These factors are essential not only for stabilising the clot but also for

initiating the inflammatory response (Hosseini et al., 2022; Reinke and Sorg, 2012). TGF-β, for instance, is crucial for attracting immune cells to the wound site, where they begin clearing dead cells and debris, setting the stage for tissue regeneration. IL-1α and PDGF play pivotal roles in orchestrating the recruitment of neutrophils and macrophages, which are key components of the inflammatory response (Hosgood, 1993; Wahl et al., 1989).

Inflammation:

The inflammatory phase begins shortly after haemostasis and is essential for protecting the wound from infection. Neutrophils (a type of granulocyte) are the first immune cells to arrive, typically within hours of the injury (Simpson and Ross, 1972). They act as the body's primary defence mechanism, engulfing and destroying invading pathogens through phagocytosis and releasing reactive oxygen species (ROS) to neutralise harmful bacteria (Reinke and Sorg, 2012; G. Schultz et al., 2011; Wilkinson and Hardman, 2020a).

The neutrophils also release enzymes such as elastase and collagenase, which help degrade damaged tissue, aiding the subsequent arrival of other immune cells (Reinke and Sorg, 2012). Neutrophils are typically active for the first 24–48 hours after injury, after which macrophages and monocytes take over., macrophages, arriving around 48–72 hours post-injury, are instrumental in clearing neutrophils and apoptotic cells, as well as dead bacteria and other debris (Savill et al., 1989). Importantly, macrophages are not only involved in tissue debridement but also play a crucial role in driving the transition from inflammation to the proliferative phase. They secrete cytokines and growth factors like TGF-β and vascular endothelial growth factor (VEGF), which promote angiogenesis and stimulate the migration and proliferation of fibroblasts (Reinke and Sorg, 2012). The late inflammatory phase is marked by the predominance of macrophages, which coordinate the repair process by inducing fibroblast proliferation and promoting the formation of new blood vessels (angiogenesis) (Enoch and Leaper, 2008; Wilkinson and Hardman, 2020a).

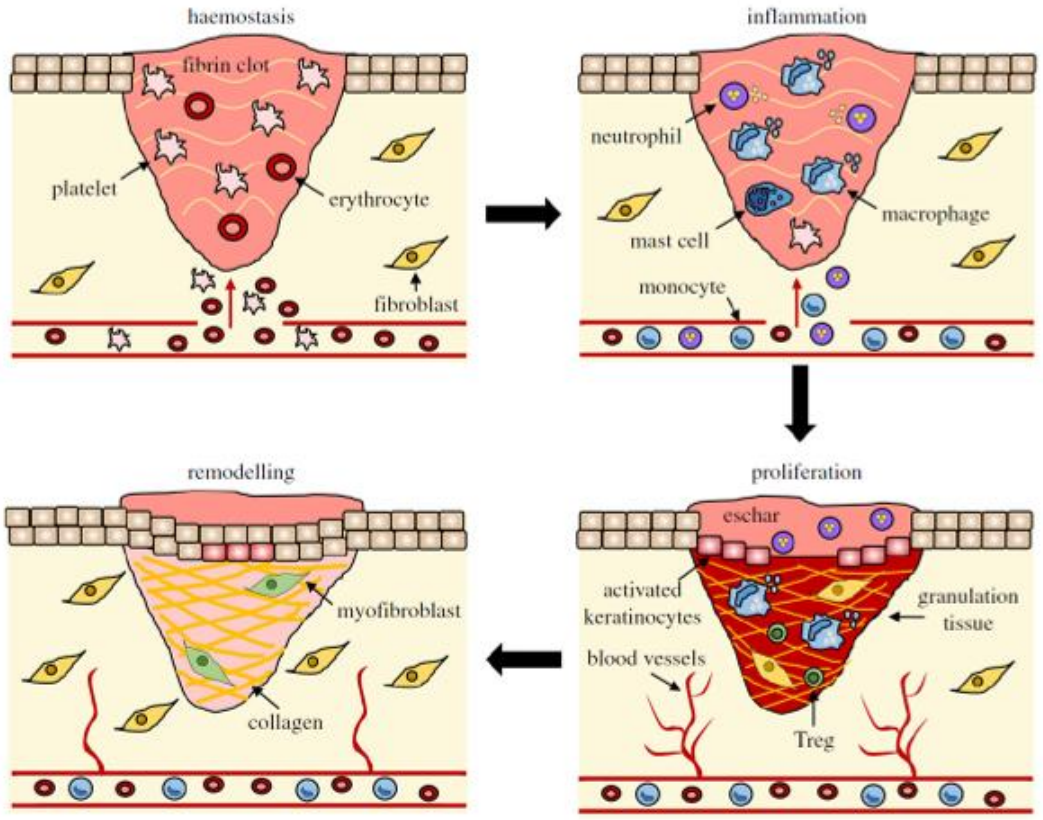

Figure 1.12: The stages of wound repair and their major cellular components. *Wound repair begins with haemostasis. Inflammation then ensues to remove debris and prevent infection, commencing with neutrophil influx, which is promoted by histamine release from mast cells. Monocytes arrive later and differentiate into tissue macrophages to clear remaining cell debris and neutrophils. During the proliferative phase, keratinocytes migrate to close the wound gap, blood vessels reform through angiogenesis, and fibroblasts replace the initial fibrin clot with granulation tissue. Macrophages and regulatory T cells (Tregs) are also vital for this stage of healing. Finally, the deposited matrix is remodelled further by fibroblasts, blood vessels regress, and myofibroblasts cause overall wound contraction. From Wilkinson and Hardman 2020.*

Proliferation:

The proliferative phase begins around 3–10 days post-injury and is characterised by extensive tissue formation, including the generation of granulation tissue and re-epithelialisation (Ozgok Kangal and Regan, 2022). Granulation tissue forms as a result of fibroblast activity, with fibroblasts migrating into the wound site and synthesising the extracellular matrix (ECM), which includes collagen type III, fibronectin, and hyaluronic acid. The ECM provides structural support to the wound bed and serves as a scaffold for cell migration and proliferation (Reinke and Sorg, 2012). Fibroblasts are stimulated by cytokines and growth factors released during the inflammatory phase, such as PDGF and TGF-β, to synthesise and secrete these ECM components (Leivonen et al., 2013; Man et al., 2012; Rosengren et al., 2010).

During the proliferative phase, the wound bed becomes rich in new blood vessels through angiogenesis, a process driven by VEGF and fibroblast growth factor (FGF-2). The formation of new blood vessels ensures an adequate supply of oxygen and nutrients to the regenerating tissues, which is crucial for sustaining cellular proliferation and collagen synthesis (Barrientos et al., 2008). The newly formed granulation tissue is pink and moist, a hallmark of active wound healing, and provides the foundation for re-epithelialisation, the process by which keratinocytes migrate from the wound edges to cover the wound bed.

Re-epithelialisation is a critical part of wound closure and involves the migration, proliferation, and differentiation of keratinocytes to re-establish the epidermal barrier (Wilkinson and Hardman, 2020a). Keratinocytes are stimulated by growth factors such as epidermal growth factor (EGF) and transforming growth factor-alpha (TGF-α) (Wilkinson and Hardman, 2020b). They proliferate at the wound margins and migrate across the wound bed, forming a new epithelial layer that covers the granulation tissue. In cases where the basement membrane is intact, re-epithelialisation proceeds rapidly. However, if the injury has disrupted the basement membrane, keratinocytes must synthesise a new one as they migrate (Enoch and Leaper, 2008).

Remodelling:

The final phase of wound healing, remodelling, can take several months to years to complete and begins approximately 21 days post-injury (Reinke and Sorg, 2012; Wilkinson and Hardman, 2020a). During this phase, the ECM undergoes extensive remodelling to increase the tensile strength of the newly formed tissue. Initially, the wound site primarily contains collagen type III, which provides a temporary scaffold. Over time, collagen type III is replaced by the stronger collagen type I, which provides greater tensile strength and stability to the tissue (Ozgok Kangal and Regan, 2022). The balance between ECM synthesis and degradation is maintained by matrix metalloproteinases (MMPs), which are secreted by fibroblasts, macrophages, and endothelial cells (Carmona-Rivera et al., 2015; Kwon et al., 2008; Pellicoro et al., 2012; Taraboletti et al., 2002). MMPs degrade excess ECM components, allowing for the precise remodelling of the tissue (Barrientos et al., 2008; Stojadinovic et al., 2007; Veves et al., 2012; Wilkinson and Hardman, 2020a). The activity of MMPs is tightly regulated by tissue inhibitors of metalloproteinases (TIMPs), ensuring that ECM degradation does not exceed synthesis and that the wound achieves optimal strength (Han et al., 2021; Lachowski et al., 2019).

During remodelling, fibroblasts differentiate into myofibroblasts, which possess contractile properties that enable them to bring the wound edges closer together, a process known as wound contraction (Darby et al., 2014). This contraction is essential for reducing the size of the wound and facilitating its closure. Myofibroblasts are characterised by the expression of alpha-smooth muscle actin (α-SMA), which gives them their contractile abilities (Sadiq et al., 2018).

Angiogenesis, which was initiated during the proliferative phase, ceases as the wound matures, and the newly formed blood vessels regress. Myofibroblasts and macrophages undergo apoptosis, and the remaining cells are reabsorbed, leaving behind a collagen-rich scar (Wilkinson and Hardman, 2020a). The scar tissue, although functional, does not possess the same strength as normal skin, with the tensile strength of healed skin reaching approximately 80% of that of unwounded skin (Hosseini et al., 2022; Hu et al., 2014).

The dynamic nature of the wound healing process means that any disruptions or delays in one phase can significantly impair overall healing. Chronic wounds, such as diabetic ulcers, are often characterised by prolonged inflammation and impaired re-epithelialisation, leading to incomplete healing (G. Schultz et al., 2011).

1.4.2 Impact of SSRIs on wound healing

Serotonin plays a vital role in regulating the activity of wound healing, mainly through its interactions with the hypothalamus and the pituitary gland (M. M. Schultz et al., 2011). The hypothalamus is a small but powerful regulatory centre in the brain that regulates many essential functions, including hunger, thirst, body temperature, and sleep. Serotonin modulates the activity of the hypothalamus by regulating the release of certain hormones, such as corticotropin-releasing hormone (CRH) and oxytocin, which are involved in stress response and social behaviour, respectively (Martins et al., 2020). Serotonin has also been described as being part of the immune signalling system (Mössner and Lesch, 1998). Certain antidepressants, such as mirtazapine, are potent antagonists of 5-HT receptors, mirtazapine antagonising specifically 5-HT2 and 5-HT3 (Watanabe et al., 2011). SSRIs inhibit the reuptake of serotonin through SERT (Lattimore et al., 2005).

Several studies have described 5-HT receptors and 5-HT transporters as present in human skin cells (Hjorth et al., 2022; Lee et al., 2011; Nordlind et al., 2008; Slominski et al., 2003, 2002; Wu et al., 2014; Zmijewski and Slominski, 2011). Those receptors and transporters can be

found in the different layers of the skin (see Figure 1.13). For example, immunohistochemistry assays in human skin showed that 5-HT1AR was present in the upper part of the epidermis, 5-HT2AR in the epidermis, 5-HT1AR was present in the upper part of the epidermis, 5-HT2AR in the epidermis and 5-HT3R in the basal epidermal skin layer (Lundeberg et al., 2002).

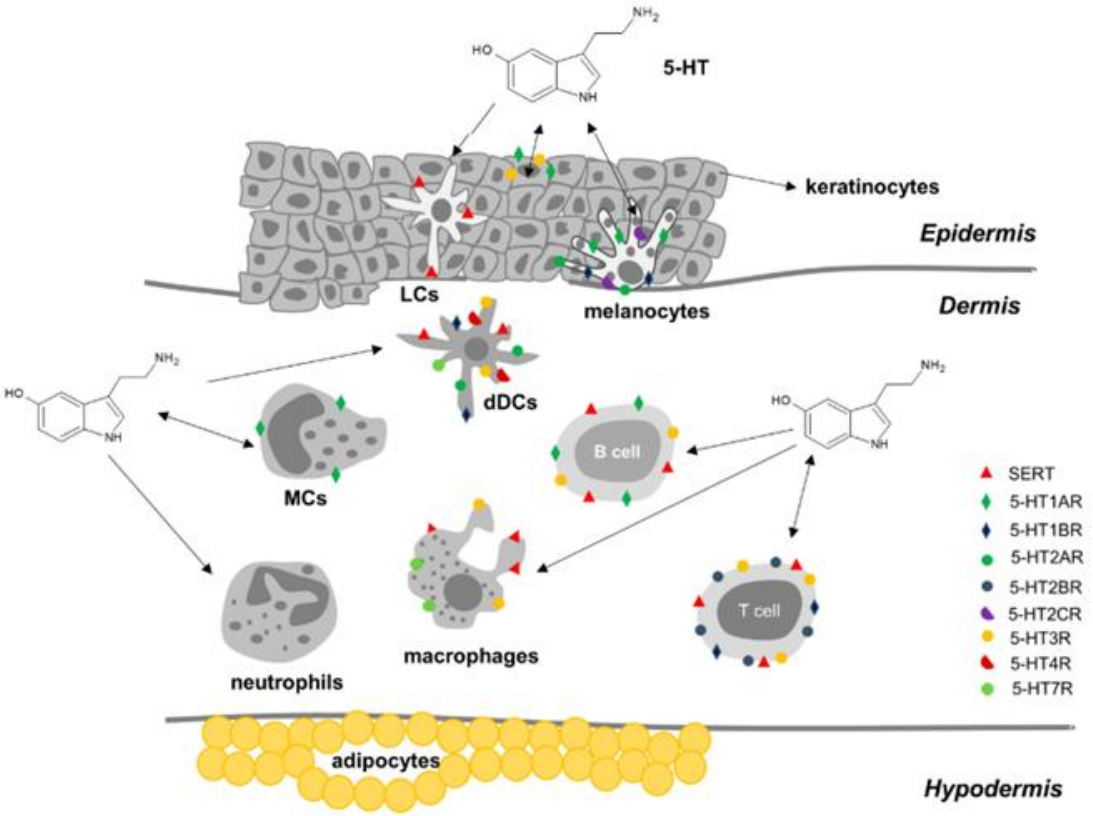

Figure 1.13: Serotonin, serotonin transporter (SERT) and serotonin receptors (5-HTRs) in human skin immunocytes and non-immunocytes. *The figure shows all the membrane proteins that may be present at any given time. Double arrows represent the production of 5-HT by the cells and the effect of 5-HT on the same cells; single arrows initiating in cells represent the production of 5-HT by these cells, while arrows initiating in 5-HT represent the direct or indirect effects of 5-HT on these cells. LCs, Langerhans cells; dDCs, dermal dendritic cells; MCs, mast cells. From Martins et al., 2020*

It has been suggested that SSRIs may be an attractive addition to the wound healing process in a review published in 2004 (Malinin et al., 2004) due to the importance of serotonin in the wound healing process (Abdouh et al., 2001; Alstergren et al., 1999; Zhang et al., 2001). Serotonin has been established to be part of various healing pathways; proinflammatory cytokines such as Interleukin 1b (IL-1b) or Interferon-c upregulate the 5-HT transporter SERT, and IL-4 also induces a reduction of 5-HT uptake (Mössner et al., 2001). Also, during the inflammatory stage, serotonin concentration is increased, as well as the synthesis of 5-HT1a receptors in B and T lymphocytes (Alstergren et al., 1999; Zhang et al., 2001). Lymphocytes are also recruited into an inflammatory focus through serotonin linked *via* secretion of IL-16

(Laberge et al., 1996). Serotonin also induces fibroblast adhesion and proliferation (Seuwen et al., 1988) by upregulating the secretion of fibroblast growth factor-2 (FGF-2).

All those interactions between the serotonergic and immune pathways lead to the belief that SSRIs would impact the healing process. This hypothesis was first tested on mammals other than humans, Kubera et al. (Kubera et al., 2000) treated mice for up to 4 weeks with citalopram (SSRI) or fluoxetine (10 mg/kg) to test the production of cytokines linked to the immune system (Interferon gamma, Il-1, Il-4 IL-2, IL-6, IL10). The results obtained in this study showed a drug-dependent and time-dependent effect of SSRIs on the production of cytokines. For citalopram, treatment for 1, 2 and 4 weeks suppressed the production of IL-4, an anti-inflammatory cytokine, and stimulated the proliferation of splenocytes (splenocytes are white blood cells originating from the spleen; they consist of a variety of cell populations such as T and B lymphocytes and macrophages). For fluoxetine, the suppressed production of IL-4 was observed only after four weeks. 4 weeks of exposure to either citalopram or fluoxetine led to increased production of IL-6 and IL-10, immunosuppressive and anti-inflammatory cytokines. This study confirmed that SSRIs have an immunomodulatory effect related to changes in the serotonergic system.

A follow-up study looked at the immunomodulatory effect of SSRIs, specifically on the wound-healing process of rats. In this study (Yuksel et al., 2014), paroxetine was injected in rats (healthy or diabetic) every day for up to 14 days at a concentration of 1 mg/kg; excision wounds were made on the skin of the rats using 4 mm biopsy punches. After 14 days of administration of paroxetine, the number of fibroblasts was significantly higher for healthy rats compared with the saline-administered healthy rats; this was not the case for diabetic rats. Complete epithelisation was also observed after 14 days only for healthy and paroxetine-administered rats. Fibroblast plays an important throughout multiple phases of wound healing, including inflammation, proliferation, and tissue remodelling. This study demonstrated that short-term exposure to certain SSRIs (specifically paroxetine) could enhance cutaneous wound healing, potentially through modulation of fibroblast activity.

Similar results were observed for chronically stressed rats (chronic social stress, 24 hours of isolation followed by 24 hours of crowding repeated for 15 days) exposed up to 14 days to fluoxetine (intraperitoneal injections of 1 mg/kg of fluoxetine diluted in sterile saline) (Farahani et al., 2007). Fluoxetine treatment increased the wound healing rate by 68% and 31% for stressed and non-stressed rats, respectively. The authors hypothesised that this improvement in wound healing after treatment with fluoxetine could be due to the fact that fluoxetine

administration increases the level of IL-1(Kubera et al., 2000). This cytokine plays a significant role in regulating inflammatory mediator production in wounds (Zhang et al., 2010).

In 2018 a study by Sadiq et al., introduced the first human experimentation. This study investigated the impact of SSRIs on the healing of burn wounds in an *in vivo* mice model and *in vitro* human fibroblast cells. Serotonin (0.3 g/l) was added to the culture media of the fibroblast this treatment significantly increased cell proliferation (Bromodeoxyuridine incorporation assays), migration, and survival (CellTiter-Glo® Luminescent cell viability assay), confirming a link between serotonergic signalling and wound healing. When treated with both serotonin and fluoxetine (3000 ng/l), a decrease in fibroblast and keratinocyte proliferation was observed. The authors estimate that inhibition of SERT may specifically affect fibroblast and keratinocyte migration and proliferation. This study (Sadiq et al., 2018) suggest that SSRIs have a deleterious effect on wound closure due to the inhibition of migration and proliferation of fibroblasts and keratinocytes, treatment with fluoxetine led to a decrease in wound closure percentage in thermal burn wounds in mice.
This seems contradictory with another study published by (Nguyen et al., 2019) where fluoxetine enhanced keratinocyte migration in scratch assays. In the presence of exogenous serotonin, neonatal human keratinocytes (isolated from human foreskin) showed improved s h scratch closure: 60.6% in the 3000 ng/l treatment group, 62.0% in the 0.3 g/l treatment group ($P = 0.01$), and 67.0% healed wound area in the 1 mmol/l FLX group ($P = 0.001$), compared to 52.2% for the non-treated cells. The authors estimated that this improved scratch closure was due to a higher migration of keratinocytes when exposed to fluoxetine, and in order to confirm this process was due to the serotonergic pathways, they replicated the scratch assays, using a 5-HT blocker (ketanserin). The use of 5-HT blockers reversed the effect of fluoxetine, confirming that the increased wound healing was due to 5-HT signalling through HTR. Fluoxetine increased keratinocyte migration and made the immune milieu less inflammatory (Nguyen et al., 2019).

The contradictory results regarding the effect of SSRIs on wound healing could be due to the different tissue/cell types used. Also, a non-linear dose-dependent effect of SSRIs may contribute to the observed discrepancies in cell culture and animal models (Stapel et al., 2021).

1.5 Phosphorylation and its role in wound healing

Phosphorylation is a critical post-translational modification that plays a central role in regulating cellular activities crucial for wound healing, such as cell proliferation and migration (Jung et al., 1997; Kimura et al., 2013; Tai and Tzeng, 2014). By adding phosphate groups to proteins, phosphorylation activates key signalling pathways, including MEK/MAPK and PI3K/AKT, which are essential for tissue repair (Flender et al., 2024). Understanding the role of phosphorylation in wound healing is important for exploring how serotonin signalling, and its modulation by SSRIs, may influence these processes.

1.5.1 Overview of PTMs and protein phosphorylation

Post-translational modifications (PTMs) are essential biochemical processes that regulate protein function, stability, localisation, and interactions, enabling cells to dynamically respond to environmental and physiological signals. Several major types of PTMs include ubiquitination, glycosylation, acetylation, and methylation (as depicted in Figure 1.14) each contributing uniquely to cellular homeostasis (Flender et al., 2024).

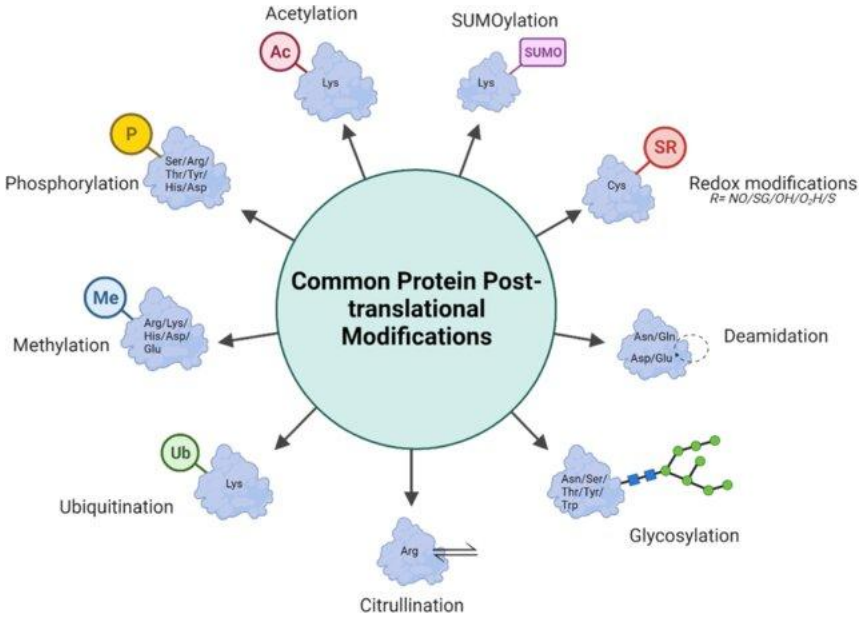

Figure 1.14: Overview of common protein post-translational modifications (PTMs) in eukaryotic cells. *The schematic representation illustrates various PTMs occurring on proteins in eukaryotic cells.*

Ubiquitination involves attaching ubiquitin molecules to lysine residues on target proteins, marking them for degradation via the proteasome pathway. This modification is critical for regulating protein turnover, cell cycle progression, and DNA repair, maintaining cellular homeostasis (Guo et al., 2012; Kawabe and Brose, 2011). Similarly, glycosylation adds

carbohydrate moieties to proteins, which is vital for proper protein folding, stability, and intercellular communication, glycosylation influences protein localisation and interaction, especially in immune responses and extracellular matrix formation, underlining its importance in cellular signalling (Ido-Kitamura et al., 2012; Zheng et al., 2014).

Acetylation and methylation of lysine residues are pivotal PTMs that play significant roles in regulating gene expression and chromatin structure. These modifications are primarily associated with histones, which help package DNA into nucleosomes and regulate its accessibility. Acetylation typically occurs on lysine residues and is catalysed by histone acetyltransferases (HATs), which neutralise the positive charge of lysine, leading to a more relaxed chromatin structure and facilitating gene transcription (Singh et al., 2010; You et al., 2012). For instance, acetylation of histone H3 at lysine 14 (H3K14ac) promotes transcription by recruiting transcription factors (Kato, 2017; Rothgiesser et al., 2010). In contrast, lysine methylation can either activate or repress gene expression, depending on the specific residue modified and the number of methyl groups added. For example, trimethylation of histone H3 at lysine 4 (H3K4me3) is linked to active transcription, while trimethylation at lysine 27 (H3K27me3) is associated with transcriptional repression (Stark et al., 2011; Zhang et al., 2022). Methylation also plays a role in stabilising protein interactions; for instance, methylation of transcription factors can enhance their DNA-binding affinity, thus modulating gene expression (Han et al., 2019). These modifications, work in concert to fine-tune gene expression, acetylation can counteract the repressive effects of methylation, allowing for a dynamic and adaptable regulation of transcription (Moore and Gozani, 2014; Stark et al., 2011). This interplay between acetylation and methylation underscores the complexity of chromatin regulation and its impact on cellular function (Wei et al., 2019).

While these PTMs are crucial for regulating protein function, phosphorylation is particularly significant due to its central role in activating key signalling pathways. Its ability to rapidly modulate cellular processes like growth and repair makes it a major focus, especially in the context of how SSRIs may affect wound healing.

Phosphorylation influences protein function through several mechanisms, firstly, phosphorylation can directly alter the conformation of a protein, either activating or inhibiting its enzymatic activity. This is particularly important for proteins such as enzymes, receptors, and transcription factors, where activity must be tightly regulated. Phosphorylation typically occurs on serine, threonine, or tyrosine residues and induces structural changes that either expose or obscure active sites or binding domains, modulating the protein's function

accordingly (Yue Li et al., 2022; Nishi et al., 2014). For example, the phosphorylation of transcription factors can enhance or inhibit their ability to bind DNA and regulate gene expression. A notable case is the oestrogen receptor, where phosphorylation enhances its transcriptional activity, particularly in cancerous tissues (Du et al., 2023). Similarly, phosphorylation of MYBL2 by GSK3-like kinase BIN2 inhibits its activity, illustrating how phosphorylation can act as a molecular switch in gene regulatory networks (Ye et al., 2012).
Secondly, phosphorylation significantly influences protein-protein interactions by either creating or disrupting binding sites, impacting processes such as signal transduction, cytoskeletal organisation, and vesicle trafficking. This modification allows cells to coordinate these functions in response to both internal signals and environmental cues. For example, phosphorylation can create docking sites for proteins with SH2 or PTB domains, which recognise phosphorylated tyrosine residues (Amanchy et al., 2011; Nishi et al., 2011). Conversely, it can disrupt binding sites, such as with the retinoblastoma protein (Rb), where phosphorylation inhibits its interaction with E2F, regulating the cell cycle (Antonucci et al., 2014; Burke et al., 2014; Lamber et al., 2013). Additionally, phosphorylation modulates protein complexes involved in mitosis and apoptosis, such as MCL-1, where it regulates interactions with apoptotic regulators (Nakajima et al., 2016).

Phosphorylation also plays a key role in regulating both subcellular localisation and complex signalling cascades. It enables proteins to move between cellular compartments in response to specific signals, such as promoting the nuclear translocation of proteins involved in cell cycle regulation or DNA repair, ensuring they are active in the correct cellular context. For example, the phosphorylation of collapsin response mediator protein 2 (CRMP2) alters its localisation in glioblastoma cells, impacting tumour growth pathways (Moutal et al., 2018). Similarly, hyperphosphorylation of tau proteins is linked to their mislocalisation, contributing to neurodegenerative diseases (Passaro et al., 2023; Yamazaki et al., 2011). Additionally, in multicellular organisms, phosphorylation regulates signalling cascades like the MEK/MAPK and PI3K/AKT pathways. In these pathways, kinases sequentially activate one another to amplify signals, ensuring rapid cellular responses. These pathways control crucial processes such as cell growth, differentiation, and apoptosis, and their dysregulation is frequently associated with diseases like cancer and neurodegenerative disorders (Kitagishi et al., 2014; Lei et al., 2023; Zhang, 2017). Aberrant phosphorylation, caused by mutations in kinases or phosphatases or external factors, plays a critical role in these diseases by disrupting signalling pathways. In cancer, overactive phosphorylation can drive uncontrolled cell growth and

survival, as seen with fibroblast growth factor receptors (FGFRs) promoting oncogenic signalling (Lih et al., 2019; Zhu et al., 2017). Similarly, in neurodegenerative diseases, hyperphosphorylation of tau protein leads to neurofibrillary tangles, contributing to neuronal dysfunction (Ardito et al., 2017; Lih et al., 2019). To target these aberrant processes, kinase inhibitors have emerged as promising therapeutic options. For example, CDK4/6 inhibitors halt cancer cell proliferation, while inhibitors of the MAPK pathway are used for cancers with BRAF or KRAS mutations (Corcoran et al., 2013; Goel et al., 2016).

Research into phosphorylation dynamics has also extended into areas such as wound healing, where protein phosphorylation and other PTMs are essential in regulating tissue repair mechanisms, further underscoring the therapeutic potential of targeting phosphorylation in diverse pathological contexts.

1.5.2 Protein phosphorylation and PTMs in wound healing

Phosphorylation is particularly crucial in wound healing, where it governs the signalling pathways responsible for coordinating cell proliferation, migration, differentiation, and survival during the repair process. Wound healing involves several tightly regulated phases, haemostasis, inflammation, proliferation, and tissue remodelling, all of which are dependent on precise phosphorylation events to ensure proper cellular responses. Phosphorylation plays a crucial role in regulating these key phases by coordinating various cellular functions, including migration and proliferation. During the haemostasis and inflammation phases, phosphorylation of signalling molecules activates platelets and inflammatory cells, initiating the wound healing cascade. For example, these phosphorylation events activate platelets, which then release cytokines and growth factors that promote an early immune response to clear the damaged tissue and prepare the wound for further healing (Gupta, 2018).

During the early inflammatory phase of wound healing, phosphorylation is critical for activating immune cells and cytokine signalling. The JAK/STAT pathway plays a crucial role in this process by regulating immune cell activation and cytokine-mediated responses. Upon cytokine binding, associated JAK kinases are activated, leading to the phosphorylation of specific tyrosine residues on STAT proteins. This phosphorylation event causes STAT proteins to dimerise and translocate to the nucleus, where they bind to DNA and initiate the transcription of genes involved in cell growth, differentiation, and immune responses (Ferrajoli et al., 2006; Mohr et al., 2012). This pathway is particularly important in hematopoietic cells, including

neutrophils and macrophages, which are critical for wound healing. Phosphorylation of STAT proteins in these immune cells drives their recruitment and activation, enabling them to clear pathogens and dead tissue at the wound site, which is essential for the inflammatory phase of healing (Ferrajoli et al., 2006). Interestingly, the JAK/STAT pathway can be activated not only by cytokines but also by environmental stressors such as hyperosmolarity, which suggests its involvement in a broad range of inflammatory responses (Gatsios et al., 1998), this flexibility enhances its role in the early stages of wound healing, where the pathway responds to various external stimuli. Additionally, the regulation of the JAK/STAT pathway is complex, involving proteins such as suppressors of cytokine signalling (SOCS) and protein inhibitors of activated STATs (PIAS), which help maintain immune homeostasis and prevent excessive immune responses that could damage tissue (Morales et al., 2010). In conclusion, phosphorylation-mediated activation of the JAK/STAT pathway plays a central role in coordinating immune cell function and cytokine signalling by inducing the expression of genes crucial for the recruitment and activation of neutrophils and macrophages during the wound healing process. The versatility of this pathway, and its ability to respond to both cytokines and environmental factors, underscores its importance in regulating the early immune response in wound healing (Ferrajoli et al., 2006; Gatsios et al., 1998; Mohr et al., 2012; Morales et al., 2010)

As the wound progresses into the proliferative phase, phosphorylation of kinases in the MAPK and PI3K/AKT pathways becomes essential for driving cell proliferation, migration, and survival (Vaiana et al., 2011). These pathways ensure that keratinocytes and fibroblasts proliferate and migrate to the wound site, facilitating re-epithelialisation and extracellular matrix (ECM) production. In particular, ERK1/2 phosphorylation in the MAPK/ERK pathway, triggered by growth factors like epidermal growth factor, promotes keratinocyte proliferation and migration, processes critical for wound closure (Kim et al., 2020; Vaiana et al., 2011). Similarly, the PI3K/AKT pathway, through AKT phosphorylation, enhances cell survival and migration while stimulating collagen production, which is crucial for ECM remodelling and scar tissue formation in the later stages of healing (Cao et al., 2019; Escuin-Ordinas et al., 2016; Wu et al., 2023), studies have highlighted the therapeutic potential of targeting these pathways to accelerate wound healing. For example, the short antimicrobial peptide Pt5-1c enhances keratinocyte migration and proliferation by inducing the phosphorylation of EGFR, Akt, ERK, p38, and STAT3, promoting both keratinocyte activation and collagen production (Wu et al., 2023). Moreover, the BRAF inhibitor vemurafenib has been shown to accelerate skin wound healing by inducing ERK phosphorylation and cell cycle progression, improving keratinocyte

function and wound closure in mouse models (Escuin-Ordinas et al., 2016). However, this benefit is reversed by the addition of MEK inhibitors, underscoring the importance of precisely regulating these phosphorylation pathways for optimal healing outcomes. In conclusion, the coordinated action of the MAPK and PI3K/AKT pathways, through ERK1/2 and AKT phosphorylation, is vital for driving cell proliferation, migration, and collagen production during the proliferative phase of wound healing, offering insights into potential therapeutic interventions (Cao et al., 2019; Escuin-Ordinas et al., 2016; Wu et al., 2023).

The importance of phosphorylation extends into the tissue remodelling phase, where it regulates critical enzymes such as matrix metalloproteinases (MMPs), which are responsible for reorganising the extracellular matrix (ECM) to form scar tissue. Phosphorylation of MMPs ensures that the ECM is appropriately remodelled, allowing for both the breakdown of excess matrix components and the proper formation of new tissue (Han et al., 2021; Lachowski et al., 2019). Additionally, phosphorylation plays a crucial role in angiogenesis, the formation of new blood vessels, which is essential for delivering oxygen and nutrients to the regenerating tissue. VEGF-induced phosphorylation of endothelial nitric oxide synthase (eNOS) at specific serine residues, particularly Ser-1177 and Ser-633, promotes angiogenesis by enhancing nitric oxide (NO) production, a key factor that drives endothelial cell migration (Aicart-Ramos et al., 2014; Chen et al., 2016; Kang et al., 2024). This cascade supports wound healing by facilitating blood vessel growth, which is crucial for tissue regeneration. The phosphorylation of eNOS exhibits a biphasic response to VEGF stimulation., initially eNOS is transiently phosphorylated at Ser-633 by protein kinase A (PKA), followed by sustained phosphorylation at Ser-1177 by Akt. This sequential activation of eNOS is critical for maintaining both short-term and long-term angiogenic responses (Chen et al., 2016; Y. Chen et al., 2017). Moreover, this phosphorylation amplifies eNOS's affinity for its cofactors, increasing NO production, which in turn not only promotes endothelial cell migration but also influences MMP activity and ECM metabolism (Kang et al., 2024). However, angiogenesis and tissue remodelling are tightly regulated processes, for instance, interactions between endothelial cells and the fibronectin-rich matrix can negatively modulate eNOS activity through a p38 MAPK-dependent pathway, potentially serving as a feedback mechanism to prevent excessive angiogenesis (Viji et al., 2009). In conclusion, VEGF-induced phosphorylation of eNOS at Ser-1177 and Ser-633 is essential for angiogenesis and ECM remodelling during wound healing. The phosphorylation of eNOS promotes NO production, endothelial cell migration, and MMP activity, ensuring the effective regeneration of tissue. These phosphorylation events are tightly regulated through various

feedback mechanisms involving ECM components, allowing for controlled tissue remodelling that balances scar formation and angiogenesis (Aicart-Ramos et al., 2014; Chen et al., 2016; Kang et al., 2024; Viji et al., 2009).

SSRIs have been shown to modulate key intracellular signalling pathways, specifically the MAPK/ERK and PI3K/AKT cascades, which are integral to cellular processes involved in wound healing, such as proliferation, migration, and survival (Bai et al., 2017; Y. X. Wang et al., 2014). Fluoxetine has been observed to enhance the phosphorylation of ERK1/2, a critical component of the MAPK/ERK pathway, which can stimulate the expression of immediate early genes like c-Fos that support cell proliferation and differentiation (Li et al., 2017). Through mechanisms such as promoting metalloproteinase activity and activating epidermal growth factor receptors (EGFR), fluoxetine enhances ERK signalling, which may also facilitate cellular responses in non-neuronal contexts relevant to wound healing (Li et al., 2017; Y. X. Wang et al., 2014). Furthermore, fluoxetine activates the PI3K/AKT pathway, crucial for cell survival and proliferation, by promoting the phosphorylation of downstream targets that regulate these processes (Bai et al., 2017). Activation of 5-HT2B receptors by fluoxetine in astrocytes transactivates EGFR, which recruits both the MAPK/ERK and PI3K/AKT pathways, potentially enhancing migration and proliferation of fibroblasts and keratinocytes necessary for wound healing (Bai et al., 2017). Additionally, the interaction between the MAPK/ERK and PI3K/AKT pathways is significant in coordinating tissue repair functions, with ERK signalling implicated in regulating matrix metalloproteinases (MMPs) crucial for extracellular matrix remodelling, while PI3K/AKT pathway supports cell survival, promoting efficient tissue healing (Y. X. Wang et al., 2014).

Recent advancements in phosphoproteomics hold the potential to reveal how SSRIs, may impact wound healing through phosphorylation-dependent mechanisms. Phosphoproteomics provides detailed mapping of phosphorylation events in key signalling pathways, particularly the MAPK/ERK and PI3K/AKT pathways, which regulate cellular functions like proliferation, migration, and survival essential for wound repair. For instance, phosphoproteomic studies have identified that ERK1/2 phosphorylation in the MAPK/ERK pathway drives fibroblast migration and proliferation by activating downstream targets like c-Fos and c-Jun, which are crucial for cellular growth and the re-epithelialization phase of wound healing (Kim and Kim, 2023). Additionally, phosphoproteomics has elucidated that AKT phosphorylation in the PI3K/AKT pathway supports cell survival and metabolism, important for tissue regeneration

(Kominato et al., 2022). This pathway's activation also enhances the expression of growth factors and cytokines involved in tissue repair (Kurashiki et al., 2022). Through comprehensive mapping of phosphorylation states, phosphoproteomics could identify how SSRIs might modulate these pathways, providing insights into their therapeutic potential. Further studies integrating phosphoproteomic data with functional assays could clarify how concurrent activation of the MAPK/ERK and PI3K/AKT pathways may enhance fibroblast and keratinocyte proliferation and migration, crucial for wound closure (Choi et al., 2021). By delineating specific phosphorylation events, phosphoproteomics could thus pave the way for understanding and optimising the role of SSRI in wound healing and tissue repair.

In conclusion, phosphorylation plays a fundamental role in wound healing by regulating the signalling pathways necessary for cell proliferation, migration, and tissue remodelling. SSRIs, through their modulation of phosphorylation, have the potential to influence these pathways, making it essential to understand their context-dependent effects on wound healing.

1.6 Hypothesis & Aims

Hypothesis: The overarching hypothesis for this thesis is that SSRIs, particularly fluoxetine, at environmentally relevant concentrations promote wound healing through serotonin signalling.

Aims:

1) **To determine the effect of environmentally relevant concentrations of fluoxetine on wound healing** by assessing cell proliferation and wound closure in a keratinocyte scratch assay model. By incorporating the serotonin receptor antagonist ketanserin, this aim will help clarify whether the impact of fluoxetine on cellular processes critical to wound repair, such as proliferation, is mediated specifically through serotonin signalling (Chapter 3).

2) **To examine transcriptional changes associated with fluoxetine exposure in keratinocytes using RNA sequencing.** This aim will explore gene expression changes comprehensively, highlighting specific pathways and biological processes affected by fluoxetine to provide insight into its influence on wound healing (Chapter 4).

3) **To investigate the biochemical mechanisms underlying the impact of fluoxetine on wound healing** through protein microarrays and phosphoproteomics, with a focus on identifying phosphorylation changes in key serotonin signalling pathways. This analysis will reveal specific targets modulated by fluoxetine that contribute to its effects on wound healing (Chapter 5).

4) **To validate findings from *in vitro* studies within an *ex-vivo* human skin biopsy model.** This aim will assess the relevance of the effects of fluoxetine in a physiologically complex environment, offering insights into the potential therapeutic use of low-dose fluoxetine for treatment of wounds (Chapter 6).

Chapter 2: Materials and Methods

2.1 Cell culture and scratch assays

2.1.1 Cell line and cell culture condition

The cell line used in these experiments is a HaCaT cell line. HaCaT cells are spontaneously transformed aneuploid immortal keratinocyte cell lines from adult human skin. Prof Matt Hardman's research group at the Centre for Atherothrombosis and Metabolic Disease, Hull York Medical School, provided this cell line.

Cells were grown in T75 flasks in high glucose, no glutamine, and no calcium Dulbecco's Modified Eagle Medium (DMEM) bought from Fisher Scientific. This DMEM was supplemented with 10% FBS, 1% antibiotic cocktail, 2 mM L-glutamine (Fisher Scientific), and 1 mM Ca^{2+}.

Once the cells were 80% confluent, the medium was taken out of the T flask, and 10 ml of phosphate-buffered saline (PBS) was used to wash the cells. Once the PBS was removed, cells were incubated at 37°C for 10 minutes with 4 ml of Trypsin 1:10 in PBS (stock: 10x Trypsin-EDTA solution from Sigma-Aldrich). After adding 6 ml of the medium, the content of the T flask was transferred to a 15 ml falcon tube and centrifuged at 300g for 3 minutes. The supernatant was removed from the tube; the pellet was resuspended in 10ml of medium. 1 ml of the resuspended cells was put in a new T75 flask with 9 ml of the medium, resulting in a 1:10 splitting.

2.1.2 Scratch assay using fluoxetine

To prepare for the scratch assays, 900 µl of a low FBS and calcium medium (same DMEM used for cell culture + 2%FBS + 0.5 mM Ca^{2+}) was added in 16 wells (4 columns out of 6) of the 24-well plates. The use of 0.5 mM Ca^{2+} in the scratch assay was chosen to optimise keratinocyte migration and proliferation rates, as adjusting calcium concentration can significantly influence cellular responses during wound healing (Pekmez and Milat, 2020; Riahi et al., 2012). The last two columns were filled with 900 µl of the 10%FBS and 1mM Ca^{2+} medium. Those two last columns were used as positive control. In every well of the plate, I added 100 µl of the cells in suspension. Cells were left at 37°C for three days until a monolayer of cells covered the entirety of the well. Using a 1000 µl pipette tip, I scratched a line in each of the wells (see Figure 2.1) the medium was removed from the wells, and PBS was used to wash. I used the following concentrations of fluoxetine: 65 ng/l, 125 ng/l, 250 ng/l, 540 ng/l,

2.5µg/L, 5400 ng/l. In the example provided in Figure 2.1, in columns 2,3,4 and 6, 1 ml of the mediums used in the previous step was added to the wells. Fluoxetine was added to the wells of the columns 3 and 4. I added a concentration of 540 ng/l in the wells of column 3 and a concentration of 5400 ng/l in the wells of column 4 (in this specific example).

For column 1 (negative control) and 5 (positive control), 500 µl of 1% Crystal violet solution was added. Plates were put back in the 37°C incubator for 5 minutes. The Crystal violet was removed, and the wells were washed with water. Plates were kept in the 37°C incubator for 36 hours to allow the cells of the column non-stained with Crystal violet to migrate and proliferate towards the middle of the scratch. After those 36 hours the Crystal violet staining was performed for all the remaining wells.

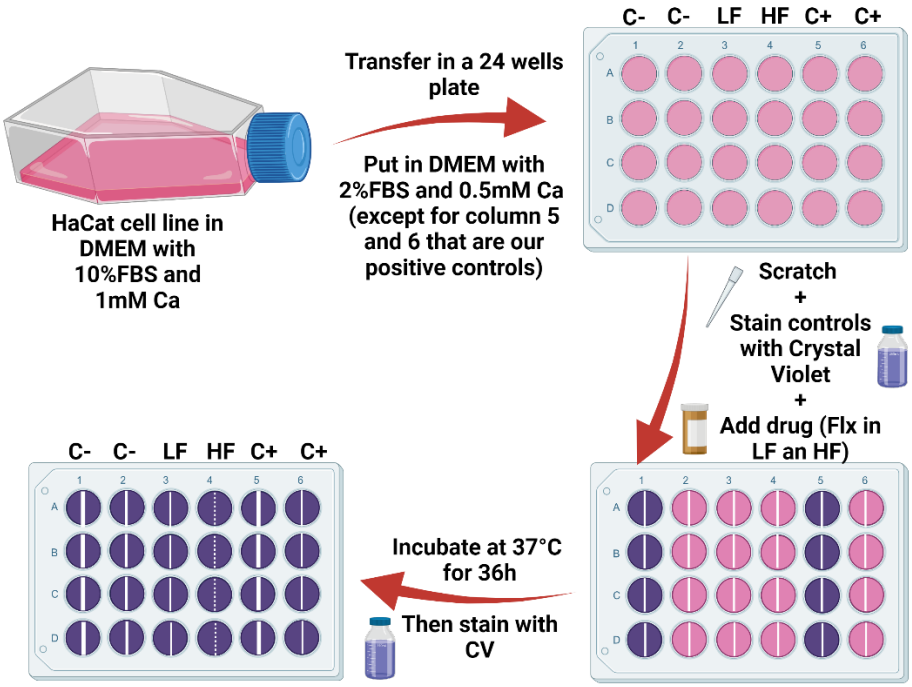

Figure 2.1: Representative diagram of the scratch assay protocol. *C-: Negative control (DMEM + 2% FBS + 0.5 mM Ca^{2+}), LF: 540 ng/l of fluoxetine, HF: 5400 ng/l of fluoxetine, C+: Positive control (DMEM + 10% FBS + 1 mM Ca^{2+})*

Pictures of the scratches were taken using the Olympus BX51 Fluorescence microscope with a 4x objective and using CellSens software. Four photos of each well were taken. The distance between the two sides of the scratch was measured using the software ImageJ (4 measurements per picture). The percentage of wound closure was calculated using the formula: 100-((wound distance/original wound distance) *100). The original wound distance was the measurements obtained for the negative controls.

2.1.3 Use of a proliferation inhibitor: Mitomycin C

In order to test if fluoxetine stimulates the migration or proliferation of HaCaT cells, leading to a higher percentage of wound closure, I decided to use a proliferation inhibitor: Mitomycin C. This antibiotic has been isolated from the *Streptomyces caespitosus*, and it inhibits the proliferation of different cell types (keratinocytes, fibroblast, etc…) through inhibition of RNA, DNA, and protein synthesis (Correa et al., 1999; Jampel, 1992; Nambu et al., 2007).
Scratch assays were performed as described in the previous section, this time using just fluoxetine (540 ng/l or 5400 ng/l), just Mitomycin C (800 µg/l), or combination of both drugs.

2.1.4 Use of Sertraline and Ketanserin

To find if the results obtained using fluoxetine could be extended to other SSRI, I decided to use another SSRI: Sertraline. I also decided to use a serotonin blocker, Ketanserin. Serotonin blockers are another common type of antidepressant, and Ketanserin targets 5-HT2 receptors.
This part of the project was done in collaboration with one master student (Tomilayo Akinmola) and a visiting PhD student (Belen Garcia-Merino) from the University of Cantabria, Spain.
The protocol of the scratch assays was similar to the one used for fluoxetine; the concentrations of Sertraline used for the scratch assays were 62.5, 125, 250, 540 and 5400 ng/l. The concentration of ketanserin used was 10 µM.

2.1.5 Statistical analysis

All statistical analyses for the scratch assays were performed using RStudio (version 2023.12.0). The normality of data distribution was assessed using the Shapiro-Wilk test. Since the data were normally distributed ($p > 0.05$), one-way ANOVA was conducted to compare fluoxetine-exposed groups with the control, followed by Tukey's post hoc test to determine pairwise differences.
Data are presented as mean ± standard deviation (SD). Statistical significance was defined as $p < 0.05$. Sample sizes (n) for each experiment are detailed in the figure legends. For boxplots, the median, interquartile range (IQR), and minimum/maximum values are displayed, with outliers defined using the 1.5×IQR rule. Statistical significance is indicated either by asterisks (*) or by different letters (A, B, C), where groups sharing the same letter are not significantly different from each other.

2.2 Protein microarrays

The kits used were Human Phospho-Kinase Array Kit purchased from the R&D system (Catalog number ARY003C). Those kits were used to detect the relative levels of phosphorylation of 37 kinase sites and 2 related total proteins.

I used different two times of exposure to fluoxetine (6 and 36 hours) and one concentration of fluoxetine (540 ng/l). For cells exposed to fluoxetine for 36 hours, I have four replicates of each of the following concentrations: 540 ng/l (LF), 0 ng/l (Control), and for cells exposed to fluoxetine for 6 hours, I have three replicates of those same concentrations.

During a splitting, HaCaT cells were transferred to a 6-well plate (3 wells were used per condition). Cells were left in an incubator at 37°C until they reached 100% confluence. The media was then removed, and the wells were washed with PBS. After removal of the PBS, 1 ml of Lysis buffer 6 (denaturing buffered solution) was added to the first well. The cells were detached from the bottom of the wells using a sterile cell scraper. The media with cells resuspended was then collected and transferred to the second well; the process was repeated, and the media was transferred to the 3rd well. After scraping the bottom of the 3rd well, the media was collected and transferred to an Eppendorf tube. The tubes were left to rock in a cold room (2-8°C) for 30 minutes. Lysates were centrifuged at 14,000xg for 5 minutes, and the supernatant was transferred to a new Eppendorf tube.

334 µl of cell lysate was added to 1666 µl of Array buffer 1 to make a total volume of 2mL.

The Proteome profiler kits are divided into two protein microarray membranes (A and B) to minimise cross-reactivity. Figure 2.2 lists the capture antibodies present on each membrane.

Membranes were blocked for one hour, and then 1 ml of the sample was added to each part of the membrane and left to incubate overnight at 2-8°C on a rocking platform. Membranes were then washed three times 10 minutes using the wash buffer provided in the kit before being incubated with 1 ml of Detection antibody A/B at room temperature for 2 hours on a rocking platform. Following three more washes of 10 minutes, Streptavidin-HRP was added to the membranes and left to incubate for 30 minutes at room temperature. After a final 10-minute wash, Clarity™ ECL western substrate (Bio-Rad) was added to the membranes; the membranes were then visualised using a ChemiDoc™ Imaging system (Bio-Rad). The densitometry was analysed using ImageJ software (Schneider et al., 2012), and the data was gathered in an Excel file. Results were analysed using Rstudio (version 2023.12.0); normality was assessed using the Shapiro-Wilk test, confirming that the dataset was non-parametric, so I used the non-

parametric equivalent of the MANOVA: a PERMANOVA. This test was computed using the Adonis function from the vegan package.

Membrane / Coordinate	Target/Control	Phosphorylation Site
A-A1, A2	Reference Spot	
B-A11, A12	Akt 1/2/3	T308
B-A13, A14	Akt 1/2/3	S473
B-A17, A18	Reference Spot	
A-B3, B4	CREB	S133
A-B5, B6	EGF R	Y1086
A-B7, B8	eNOS	S1177
A-B9, B10	ERK1/2	T202/Y204, T185/Y187
B-B11, B12	Chk-2	T68
B-B13, B14	c-Jun	S63
A-C3, C4	Fgr	Y412
A-C5, C6	GSK-3α/β	S21/S9
A-C7, C8	GSK-3β	S9
A-C9, C10	HSP27	S78/S82
B-C11, C12	p53	S15
B-C13, C14	p53	S46
B-C15, C16	p53	S392
A-D3, D4	JNK 1/2/3	T183/Y185, T221/Y223
A-D5, D6	Lck	Y394
A-D7, D8	Lyn	Y397
A-D9, D10	MSK1/2	S376/S360
B-D11, D12	p70 S6 Kinase	T389
B-D13, D14	p70 S6 Kinase	T421/S424
B-D15, D16	PRAS40	T246

Membrane/ Coordinate	Target/Control	Phosphorylation Site
A-E3, E4	p38α	T180/Y182
A-E5, E6	PDGF Rβ	Y751
A-E7, E8	PLC-γ1	Y783
A-E9, E10	Src	Y419
B-E11, E12	PYK2	Y402
B-E13, E14	RSK1/2	S221/S227
B-E15, E16	RSK1/2/3	S380/S386/S377
A-F3, F4	STAT2	Y689
A-F5, F6	STAT5a/b	Y694/Y699
A-F7, F8	WNK1	T60
A-F9, F10	Yes	Y426
B-F11, F12	STAT1	Y701
B-F13, F14	STAT3	Y705
B-F15, F16	STAT3	S727
A-G1, G2	Reference Spot	
A-G3, G4	β-Catenin	
A-G9, G10	PBS (Negative Control)	
B-G11, G12	STAT6	Y641
B-G13, G14	HSP60	
B-G17, G18	PBS (Negative Control)	

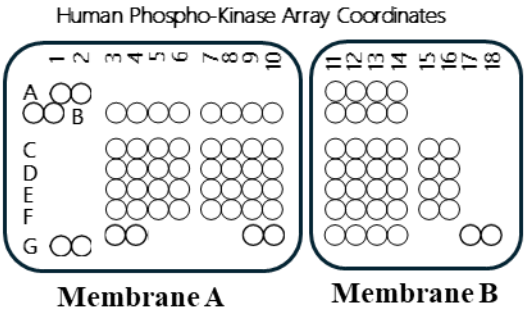

Figure 2.2: List of capture antibodies and their coordinates on the membranes, detailing the target or control proteins and their respective phosphorylation sites. *The layout provides a reference for the phosphoprotein detection array, showing the specific membrane locations and associated phosphorylation sites used to analyse the modulation of kinase activity in response to fluoxetine exposure.*

2.3 Western blots

2.3.1 Sample preparation

For the western blots I used HaCaT cells non-exposed and exposed to 540 ng/l of fluoxetine for either 6 or 36 hours. The lysis protocol was similar to the one used for the proteome profiler kits.

25 µl of 4x loading buffer was added in 75 µl of lysate and then boiled at 100°C for 5 minutes. Recipe for the 4x loading buffer: 8% SDS, 320 nM Tris HCl (pH 6.8), 40% Glycerol, 10% Mercaptoethanol, 0.04% Bromphenol blue.

2.3.2 Gel preparation

Western blot gels are composed of two parts, the resolving gel at the bottom, and the stacking gel at the top with the wells. For the western blots I used 12% gels following the recipe: 6.8 ml H_2O, 3.75 ml 1.5M Tris (pH 8.5), 4.3 ml Acrylamide, 150 µl 10% SDS, 69 µl 10% APS, 23 µl TEMED. Once the resolving gel is fully set, I prepared the stacking gel using the following recipe: 3.1 ml H_2O, 1.5 ml 0.5M Tris (pH 7.4), 500 µl Acrylamide. 50 µl 10% SDS, 30 µl 10% APS, 10 µl TEMED. Once the gel is poured between the glass plates, a 10-well comb was added. Once the gels fully set, they are ready to be used for western blotting.

2.3.3 Electrophoresis and transfer.

Gels were put in a tank full of 1X electrophoresis buffer (5x electrophoresis buffer recipe: 144 g of Glycine, 30 g Tris Base, 5 g SDS for 1 liter of buffer). 25 µl of sample was loaded in the wells, I also loaded 7.5µl of the protein ladder (Thermo Scientific™ PageRuler™ Plus Prestained Protein Ladder) in one of the wells. The electrophoresis ran at 80V for 5 minutes in order for all the samples to gather at the bottom of the wells, then the electrophoresis ran at 120V until the blue loading buffer reached the bottom of the gel (approximately one hour).

Gels were then placed in a sandwich (Figure 2.3) against a nitrocellulose membrane (Amersham™ Protan™). The transfer was run at 100V for 1 hour using transfer buffer (Glycine 111.75 g, Tris base 24.24 g, SDS 10 g for 1 liter of 10x), this 10x buffer was diluted as 8 parts 10x buffer, 1 part water, 1 part methanol.

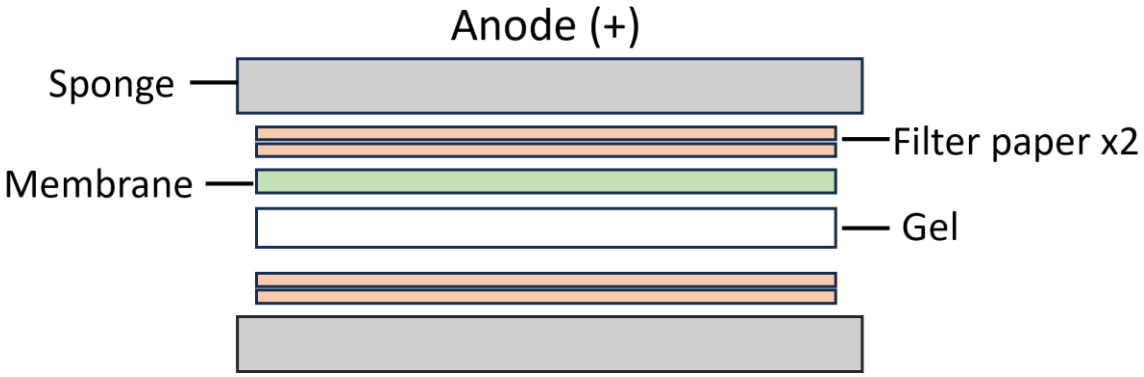

Figure 2.3: Schematic picture of western blot wet transfer sandwich. *The assembly consists of several layers designed to facilitate the transfer of proteins from the polyacrylamide gel onto the membrane. Starting from the bottom: a sponge, followed by two layers of filter paper, the polyacrylamide gel, and the membrane (typically made of nitrocellulose), all covered by another layer of filter papers and a final sponge layer. The entire assembly is placed between two electrode plates in a transfer cassette. The electric field applied across the assembly facilitates the movement of proteins from the gel onto the membrane, which can later be probed for specific proteins using antibodies*.

2.3.4 Antibodies incubation, visualisation, and analysis

After transfer membranes were blocked for one hour at room temperature in 5% milk, then placed in primary antibodies diluted in 5% milk (working concentration of 2 µg/ml) to incubate at 4°C overnight. The list of primary antibodies can be found in Table 2.1. After incubation membranes were washed 3x10 minutes with TBST before being placed to incubate in secondary antibodies for one hour at room temperature. This step is followed by three more washes of 10 minutes in TBST and a wash with TBS.

The membrane was then covered with 1 ml of HRP substrate (Millipore Immobilon Forte) and visualised using a Chemidoc (Biorad Chemidoc mp). Band intensity values were normalised against loading controls (α-tubulin or total protein levels). Statistical analysis was conducted using one-way ANOVA, followed by Tukey's post hoc test to determine significant differences between control and fluoxetine-exposed groups. Statistical significance was set at $p<0.05$, with results indicated using asterisks (*) in figures. Data are presented as mean ± standard deviation (SD).

MAB8934-SP	Human Phospho-GSK-3 beta (S9) Antibody	Rabbit	45 Kda
MAB25063-SP	Human/Mouse GSK-3 alpha / beta Antibody	Mouse	
MAB1094-SP	Human Phospho-MSK1(S376)/MSK2(S360) Antibody	Rabbit	95 Kda
AF2518-SP	Human/Mouse MSK1 Antibody	Goat	
AF2685-SP	Human Phospho-Src (Y419) Antibody	Rabbit	60 Kda
MAB3389-SP	Human/Mouse/Rat Src Antibody	Mouse	
AF8965-SP	Human/Mouse/Rat Phospho-p70 S6 Kinase (T421/S424) Antibody	Rabbit	70 + 85 Kda
MAB8962-SP	Human/Mouse/Rat p70 S6 Kinase Antibody	Mouse	

Table 2.1: List of primary antibodies used for western blotting. *The table includes details of the antibodies used to detect both total proteins and phosphorylated proteins, specifying the target proteins, phosphorylation sites, catalogue numbers, host species, and expected molecular weights. The antibodies target phospho-GSK-3β (S9), phospho-MSK1(S376)/MSK2(S360), SRC (Y419), and p70 S6K (T421/S424), as well as total protein levels of these kinases, to assess both protein expression and phosphorylation status in response to fluoxetine exposure.*

2.4 Phosphoproteomics

2.4.1 Cell lysis

I prepared one six-well plate of HaCaT cells per sample; once the cells were 100% confluent, I took the media out one well and rinsed with PBS (cold) for 5min; I then added 1 ml of the urea buffer (Buffer: 20 mM HEPES pH 8.0, 9 M Urea, 1 mM sodium orthovanadate, 2.5 mM sodium pyrophosphate, 1 mM B-glycerophosphate and cOmplete™, EDTA-free Protease Inhibitor Cocktail). Cells were detached using a sterile scraper and the plate kept tilted. After rinsing the second well with PBS, the lysate was transferred from the first well into it and I repeated the process. After scraping all six wells, the lysate was transferred to a conical Eppendorf tube.

Samples were then sonicated on a high setting for 5 minutes at 30-second intervals. After centrifuging at 20,000g for 15 minutes, the supernatant was transferred to a new Eppendorf tube.

For HaCaT cells, I used 3 replicates under 2 conditions. The two conditions were a negative control (no exposure to fluoxetine) and cells exposed to 540 ng/l of fluoxetine for 36 hours.

2.4.2 Reduction and Alkylation of Proteins

The Reduction and Alkylation process is used to break disulphide bonds within the protein and prevent the reversibility of disulphide bond forming. (Hustoft et al., 2012). This process is depicted in Figure 2.4. I added 1/278 volume of 1.25 M DTT to the cleared cell supernatant (3.6 µl of 1.25 M DTT for 1 ml of protein extract), mixed well and placed the tube into a 55ºC incubator for 30 min. After incubation, the solution was briefly cooled on ice until it reached room temperature. 1/10 volume of iodoacetamide solution was added to the cleared cell supernatant (final concentration of 50 mM of iodoacetamide) and left to incubate for 15 min at room temperature in the dark.

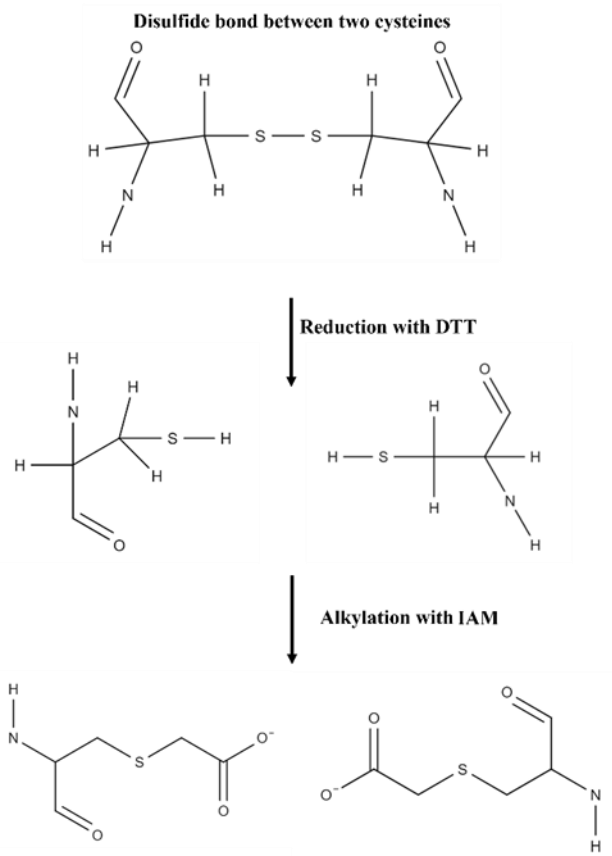

Figure 2.4: The reduction and alkylation process. *Reduction by DTT to form cysteine residues must be followed by further modification of the reactive –SH groups (to prevent reformation of the disulfide bond) by acetylation by, in this case, iodoacetamide. Adapted from (Hustoft et al., 2012)*

2.4.3 Protease digestion

Samples were diluted to a 4-fold dilution by adding 3 ml of 20 mM HEPES, pH 8.0, to 1 ml of sample. The final concentration was of 2 M urea, 20 mM HEPES, pH 8.0. Trypsin digestion allows to cleave the proteins in peptides. 40 µl of 1 mg/ml Trypsin-TPCK (Worthington,

LS003744) stock in 1 mM HCl was added to the 4 ml sample and left to digest overnight at room temperature with mixing.

2.4.4 Sep-Pak® C18 Purification of Lysate Peptides

1/20 volume of 20% TFA was added to the digest for a final concentration of 1% TFA. The pH was checked by spotting a small peptide sample on a pH strip (the pH should be under 3). After acidification, samples were placed in ice and left for 15 minutes to allow a precipitate to form. The acidified peptide solution was centrifuged for 15 min at 1780 x g at room temperature to remove the precipitate. The peptide-containing supernatant was transferred into a new 50 ml conical tube without dislodging the precipitated material.

Peptides were purified by elution through a HyperSep C18 column (Thermo Fisher). The column was pre-wet with 100% acetonitrile and washed with 3 washes of 0.1% trifluoroacetic acid. The lysate was loaded and cleaned with 3 washes of 0.1% TFA and two washes with 0.1% TFA and 5% acetonitrile. The lysate was then eluted with 0.1% TFA and 40% acetonitrile, snap-frozen in liquid Nitrogen, and lyophilised for 2 days. Samples were then sent to York University for analysis.

2.4.5 Phosphopeptides enrichment

This part of the work was done by the Centre of Excellence in Mass Spectrometry at the University of York. Phosphopeptides were enriched using MagReSyn Zr-IMAC HP beads before analysis by LC-MS/MS over 1 h acquisitions. Peptides were eluted from a 50 cm EN C18 PepMap column driven by a Waters mClass UPLC onto an Orbitrap Fusion Tribrid mass spectrometer operated in DDA mode. MS1 spectra were acquired in the Orbitrap mass analyser with parallel MS2 acquisition using the linear ion trap. Figure 2.5 depicts the enrichment process, adapted from (Galán et al., 2018).

Resulting data in .raw format were imported into PEAKS StudioXPro for peak picking, database searching, chromatographic alignment and relative label-free peak area quantification.

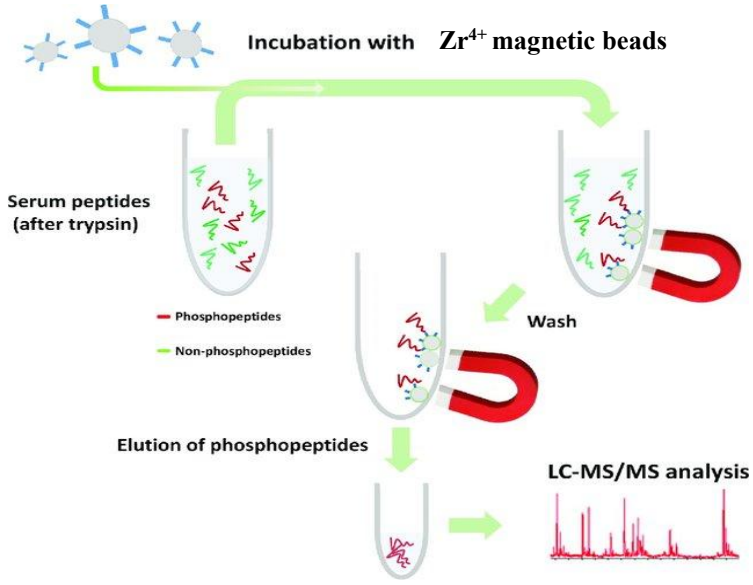

Figure 2.5: Phosphopeptides enrichment scheme. *Magnetic Zr4+ beads were used. Samples containing (phospho) peptides were mixed with the beads, and several washes were applied using magnets to retain beads at the bottom of each tube. In a final step, enriched phosphopeptides were eluted from beads by adding a high pH acetonitrile solution. Adapted from (Galán et al., 2018)*

2.5 *Ex-vivo* experiments.

The *ex-vivo* experiments were performed following the protocol described by Wilkinson et al., 2021. Human skin was obtained from patients undergoing reconstructive surgery at Castle Hill Hospital and Hull Royal Infirmary (Hull, UK) under fully informed, written patient consent, institutional guidelines, and ethical approval (LRECs: 17/SC/0220 and 19/NE/0150). Skin was collected from patients undergoing routine surgery. Samples from surgery were transported in holding media and processed immediately upon arrival at the laboratory. All experimental steps using unfixed human tissue were performed at Biosafety Level-2 (BSL-2) in a class II laminar flow biosafety cabinet.

2.5.1 Preparation of skin for wounding

In a class II laminar biosafety cabinet, skin was placed dermis-side down in a 90mm sterile Petri dish, and adipose tissue was removed using sterile scissors. Once the adipose tissue was removed, the skin was placed in 25 ml of HBSS (Hank's balanced salt solution with 4% (v/v) antibiotic-antimycotic solution) and left to incubate for 10 min at room temperature.

The skin was then placed in a new 50 ml falcon tube with 25 ml of HBSS, this time without any antibiotic solution, and left to incubate for 10 minutes at room temperature. During those

incubation phases, the tubes were shaken regularly. Finally, the skin was placed in a new tube containing 25 ml of Dulbecco's phosphate-buffered saline (9.6 g of DPBS powder per litre of distilled water). The 50 ml Falcon tube was autoclaved to sterilise it.

2.5.2 Creating *ex-vivo* human skin wounds

The dermis side of the skin was dried using sterile gauze. The skin was then placed dermis-side down on a 90mm Petri dish lid and dabbed with fresh sterile gauze.

The skin was held using curved-toothed tissue forceps, and the wound was created by pressing a 2mm biopsy punch against the skin and twisting gently. The 2mm wound was cut out and removed using forceps and curved iris scissors. A 6mm biopsy punch was then used to create a 6mm explant around a 2mm partial thickness wound in the middle (Figure 2.6 panel A).

The wound explants were placed epidermis-side up on a stack of two sterile absorbent pads and a nylon filter membrane in a 60mm Petri dish containing 4 ml of human skin media (DMEM with 2 mM L-glutamine, 1% (v/v) antibiotic-antimycotic solution, and 10% (v/v) foetal bovine serum) as showed in Figure 2.6 panel B.

In this experiment, I used a control condition (human skin media) and six exposures to drug conditions:

- Human skin media + 2500 ng/l of fluoxetine => 11 replicates
- Human skin media + 5400 ng/l of fluoxetine => 11 replicates
- Human skin media + 1.5mg/l of mirtazapine => 4 replicates
- Human skin media + 5400 ng/l of fluoxetine + 1.5mg/l of mirtazapine => 4 replicates
- Human skin media + 10µM of ketanserin => 3 replicates
- Human skin media + 5400 ng/l of fluoxetine + 10µM of ketanserin => 3 replicates

The biopsies were incubated at 37 °C and 5% CO2 in a humidified atmosphere (90-95%) for 48 hours (Wilkinson et al., 2021).

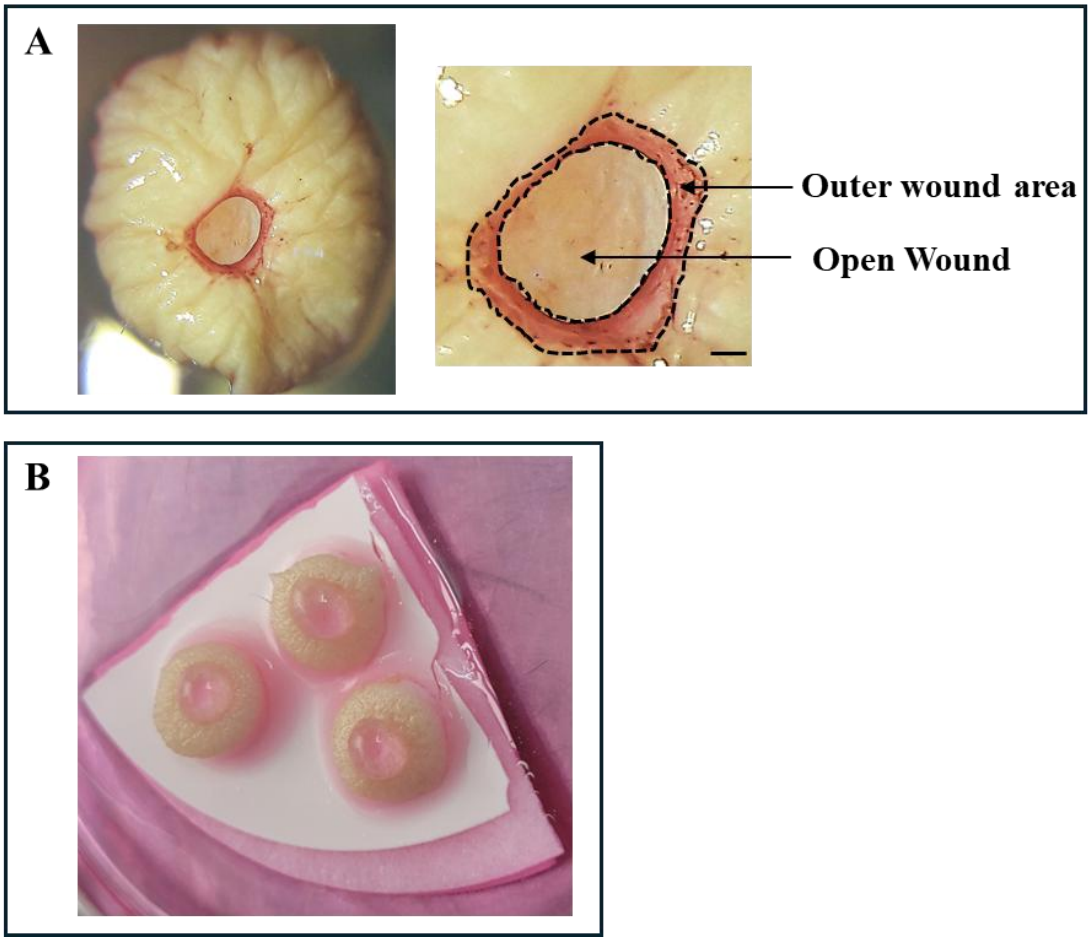

Figure 2.6: Wound creation and explant placement in a Petri dish. (A) *Brightfield image of a 2 mm partial-thickness wound created in human skin tissue using a biopsy punch. The dashed line indicates the boundary of the 6 mm explant surrounding the central wound. Scale bar = 300 µm. (B) Example of how the 6 mm wound explants were placed in the Petri dish. Explants were placed epidermis-side up on a stack of two sterile absorbent pads and a nylon filter membrane in a 60 mm Petri dish containing human skin media (DMEM with 2 mM L-glutamine, 1% (v/v) antibiotic-antimycotic solution, and 10% (v/v) fetal bovine serum). Adapted from* (Wilkinson et al., 2021).

2.5.3 Whole-mount staining of *ex-vivo* wounds.

Wound explants were placed on the epidermis face down in a 42-well plate (one explant per well). 500 µl of skin fixative (450 ml of dH2O + 40 ml of formaldehyde solution + 10 ml of glacial acetic acid + 4.5 g of sodium chloride and 0.25 g of alkyltrimethylammonium bromide) was added to every well. Explants were left to incubate at 4 °C overnight. The skin fixative was removed and replaced with 1 ml of staining wash buffer (PBS and 0.5% (v/v) Triton X-100). This buffer was removed, and another wash was performed using 1 ml of staining wash buffer.

All staining buffer was removed from the plate, and 150 µl of blocking buffer (staining wash buffer + 0.2% (w/v) sodium azide and 2% (v/v) animal serum) was added to every well. The plates were left to incubate at room temperature for 1 hour.

The blocking buffer was removed, and 150 µl primary antibody (Anti-mouse keratin 14 diluted 1:1000 in blocking buffer) was added to each well (Wilkinson et al., 2021). The plates were left to incubate overnight at 4°C. The following day, the primary antibody solution was removed, and 500 µl of staining wash buffer +0.2 % sodium azide was added to every well. Explants were left to incubate for 1 hour at room temperature. This step was followed by three washes (using staining wash buffer), every wash lasting 30 minutes.

Once the wash process was completed, all buffer was removed, and 150 µl of secondary antibody (goat anti-mouse 488 diluted 1:400 in staining wash buffer) was added to every well. Explants were left to incubate for 1 hour at room temperature in the dark. Secondary antibodies and 3 washes of 30 min using staining wash buffer were performed.

Once the washes were done, all buffers were removed. 150 µL of DAPI working solution (5 µg/ml) was then added to every well. The plates were incubated in the dark at room temperature for 10 minutes. The DAPI solution was removed, and two more 30-minute washes were performed.

2.5.4 Imaging, quantification and statistical analysis

Wound explants were transferred to a 60mm Petri dish filled with 1 mL of DBPS and placed epidermis-side down using small tissue forceps. Images were acquired using a confocal microscope (Zeiss LSM 710) and the ZEN software. Focus was done for each channel (DAPI and K14) before acquisition of the image.

The quantification was performed using the ImageJ software. Using the freehand shape tool, the outside of the re-epithelialised wound where it meets the normal skin was measured. Then, using the same tool, the wound area was measured, this time where the open wound meets the inside edge of the re-epithelializing tissue. Values were copied in an Excel file, and the percentage of wound re-epithelialization/closure was calculated using the following formula: % Closure = (Outer Wound Area - Inner Wound Area) / (Outer Wound Area) x 100.

All statistical analyses for the scratch assays were performed using RStudio (version 2023.12.0). The normality of data distribution was assessed using the Shapiro-Wilk test. Since the data were normally distributed ($p > 0.05$), one-way ANOVA was conducted to compare

fluoxetine-exposed groups with the control, followed by Tukey's post hoc test to determine pairwise differences.

Data are presented as mean ± standard deviation (SD). Statistical significance was defined as $p < 0.05$. Sample sizes (n) for each experiment are detailed in the figure legends. For boxplots, the median, interquartile range (IQR), and minimum/maximum values are displayed, with outliers defined using the 1.5×IQR rule. Statistical significance is indicated either by asterisks (*) or by different letters (A, B, C), where groups sharing the same letter are not significantly different from each other.

2.6 RNA sequencing

2.6.1 Cell lysis and RNA isolation

RNA sequencing (RNAseq) was performed using HaCaT cells not exposed to any drugs and exposed to 540 ng/l of fluoxetine. Cells from both conditions were lysed at two different time points: 6 hours and 36 hours. I used four replicates of each condition for each time point, giving a total of 16 samples.

Total RNA was isolated from HaCaT cells using the PureLink™ RNA Mini Kit (Thermo Fisher Scientific, Catalog number 12183020) following the manufacturer's instructions. The procedure was performed under RNase-free conditions to ensure RNA integrity. Before every RNA isolation, Wash Buffer II (60 ml of 96–100% ethanol added to the Wash Buffer II mix) and Lysis Buffer (10 µl of 2-mercaptoethanol per 1 ml of Lysis Buffer) were made freshly.

I prepared half a 6-well plate of HaCaT cells per sample; once the cells were 100% confluent, I removed the media from one well and rinsed it with PBS (cold). 350 µl of Lysis Buffer was added to the first well with 350 µl of 70% ethanol. The well was scraped using a cell scraper. Lysate was transferred to the second well before scraping, and finally, it was transferred to the third well for scraping. The 700 µl of lysate obtained was then transferred to a spin column.

Columns were centrifuged at 12,000 x g for 15 seconds at room temperature. Any liquid was discarded. 700 µl of Wash Buffer I was added to the column and another 15-second cycle at 12,000 x g was performed.

The liquid was removed again, and 500 µl of Wash Buffer II was added to the column. The samples were centrifuged for 15 seconds at 12,000 x g, and this step was repeated once more.

Finally, all liquid was removed, and columns were centrifuged for 2 minutes at 12,000 x g to dry.

30 µl of DH_2O was added to the column and left to incubate for 1 minute at room temperature. The columns were then centrifuged for 2 minutes at 12,000 x g. The liquid obtained from that process is the sample (Elute RNA in Figure 2.7). After concentrations of RNA were measured using a spectrophotometer (ThermoFisher NanoDrop™ Lite), the samples in Eppendorf tubes were frozen using liquid nitrogen and stored at -80°C.

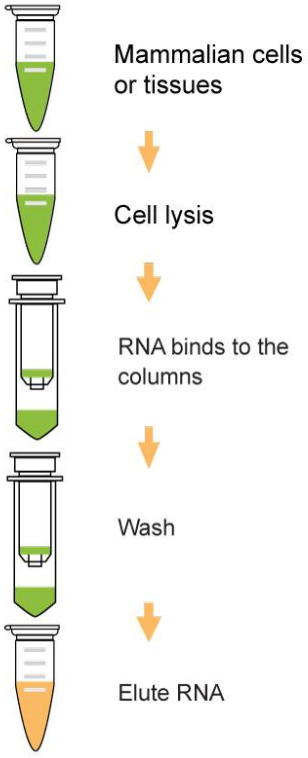

Figure 2.7: Overview of RNA extraction process. *Starting with mammalian cells or tissues, the cells are lysed to release RNA. The RNA binds to the silica membrane in the columns, while other cellular components are washed away. After a series of wash steps, the purified RNA is eluted and collected in a final tube for downstream applications. Figure from EpigenTek.*

2.6.2 RNA sequencing and data analysis

Samples were sent to Novogene (Cambridge, UK) where Human mRNAseq was performed using the Illumina NovaSeq 6000 platform. Raw data were processed, including quality control, alignment, and gene expression analysis. Reads were aligned to the human reference genome using HISAT2, and the expression of genes was quantified using FPKM (Fragments Per Kilobase of transcript per Million mapped reads). Differential expression analysis was conducted using the DESeq2 R package. A Benjamini-Hochberg correction was applied to adjust for false discovery rate (padj ≤ 0.05). Gene expression data, including significantly differentially expressed genes, were log2 transformed for further analysis. The RNAseq data have been deposited in the NCBI Gene Expression Omnibus (GEO) under the accession number GSE268987 (Rodriguez-Barucg et al., 2024).

2.7 Edu Cell proliferation assay

To evaluate the proliferative activity of keratinocytes, an EdU (5-ethynyl-2'-deoxyuridine) incorporation assay was performed using the Click-iT EdU Imaging Kit (Thermo Fisher, #BCK-EDU488). Cells were seeded in 6-well plates at 80% confluence and exposed to fluoxetine at concentrations of 62.5, 125, 250, 540, and 5400 ng/l for 36 hours. A second round of experiments was conducted using either 540 or 5400 ng/l fluoxetine alone, or in combination with mitomycin C (800 µg/l). After the exposure period, cells were incubated with 10 µM EdU for 2 hours. Following the EdU incubation, cells were fixed in 3.7% formaldehyde for 15 minutes at room temperature and permeabilised with 0.5% Triton X-100 in PBS for 20 minutes.

EdU detection was achieved through the Click-iT reaction cocktail, as per the manufacturer's protocol, using 500 µl of reaction cocktail per well. Following a 30-minute incubation at room temperature, protected from light, cells were washed with 3% BSA in PBS. Counterstaining was performed using Hoechst 33342 for nuclear visualisation. Cells were imaged using an Olympus BX51 microscope using a Zeiss fluorescence LDA-Plan x5 lens and the software CellSens, and quantification of EdU-positive cells was performed with ImageJ software. Each condition was tested with three biological replicates.

Chapter 3: Investigating the effects of fluoxetine in a scratch closure keratinocyte model.

3.1 Introduction

The recent emergence of studies indicating the connection of Selective Serotonin Reuptake Inhibitors (SSRIs) to environmental and biological systems has led to research on their broader biological impact, particularly in human health, outside of their traditional psychiatric applications (Brooks et al., 2003; Daughton and Ternes, 1999; Schultz et al., 2010). Due to their widespread presence in aquatic environments and human water systems, understanding how SSRIs such as fluoxetine interact with human cells has become essential. This chapter will explore the possible impact of SSRIs on scratch closure in a keratinocyte model based on the hypothesis that SSRIs could impact critical cellular processes involved in wound healing.

The rationale for this study arises from the previous research showing that serotonin beyond its neurological functions, plays a critical role in processes essential for wound healing, such as inflammation, cell migration, and tissue repair. These processes are regulated through serotonin signalling pathways, which are modulated by SSRIs (Kreke and Dietrich, 2008; Lattimore et al., 2005; Nguyen et al., 2019; Sadiq et al., 2018; Tate et al., 2021).

Serotonin receptors and transporters are present and functionally active in keratinocytes and other skin cells (Lundeberg et al., 2002; Nordlind et al., 2008). While SSRIs such as fluoxetine are best known for inhibiting the serotonin transporter (SERT) in neuronal systems, they can also interact directly with serotonin receptors. For instance, fluoxetine is a reversible antagonist of the 5-HT2C receptor (Ni and Miledi, 1997), which is relevant given the presence of 5-HT receptor subtypes in skin. This raises the possibility that SSRIs may influence skin physiology through both transporter-dependent and receptor-mediated mechanisms.

Based on the established knowledge of the effects of SSRIs on neuronal systems, this study further explores the effects on skin physiology. Keratinocytes are one of the main cells involved in wound healing, and upon injury, they migrate and proliferate to close the wound (Wilkinson and Hardman, 2020a). The mechanism of action of SSRIs on serotonin pathways implies that these processes can be affected in a way that could either promote or hinder skin repair. This

aspect is of particular interest given the fact that human populations are being exposed to SSRIs through environmental vectors (González Alonso et al., 2010; Schlüsener et al., 2015).
Studying the influence of fluoxetine on keratinocyte function will help to expand the knowledge of the environmental impact of SSRIs, which is the intersection of pharmacology, environmental science, and public health.

3.2 Aims & Objectives

The aim of this chapter is to investigate how exposure to environmentally relevant concentrations of fluoxetine impacts scratch closure in a keratinocyte model.

The objectives of this chapter are the following:

1) **To determine the effect of fluoxetine on scratch closure in a keratinocyte model** by using an environmentally relevant range of concentrations of fluoxetine in scratch assays.

2) **To understand the mechanisms underlying changes in scratch closure** by using mitomycin C (a cell proliferation inhibitor) and EdU assays.

3) **To identify the relationship between changes in scratch closure and serotonin signalling** by using another SSRI (Sertraline) and a serotonin antagonist (Ketanserin)

3.3 Results

3.3.1 Fluoxetine promotes keratinocyte model scratch closure in a dose-dependent manner

The first objective of this chapter was to determine the effect of fluoxetine on scratch closure in a keratinocyte model. I performed a scratch assay on human keratinocytes (HaCaT cells) and used six concentrations of fluoxetine (62.5, 125, 250, 540, 2700, and 5400 ng/l); scratch closure was assessed at 36 hours post-scratch.

Figure 3.1 shows representative images of the scratch assays. Visual observation indicated that exposure to fluoxetine had a notable impact on the scratch-healing process of HaCaT cells. Specifically, cells exposed to fluoxetine (Figure 3.1b-f) exhibited enhanced scratch closure compared to control cells (Figure 3.1a). This effect was particularly evident at higher fluoxetine concentrations (Figure 3.1f) where the scratch was almost completely closed, indicating a strong positive response to fluoxetine.

In order to validate these observations, I measured the percentage of scratch closure. The averages for each condition were calculated across four biological replicates (n=4, four different cell passages) and are presented in Figure 3.2. The data passed the Shapiro-Wilk test for normality (p-value=0.2374), allowing to use a one-way ANOVA, which highlighted the significant impact of fluoxetine on scratch closure (p-value=4.688e-15). Post-hoc analysis was conducted using Tukey's HSD test to further identify the differences between the fluoxetine-exposed groups and the control group.

After statistical analysis, I observed an apparent dose-dependent effect of fluoxetine on the HaCaT cells' scratch closure percentage. In the control group, the mean scratch closure was 66% ± 2.41, serving as the baseline for comparison. At the lowest fluoxetine concentration (62.5 ng/l), a slight decrease in scratch closure was calculated (64.59% ± 1.90), but this difference was not statistically significant when compared to control (p-value=0.861). However, at 125 ng/l, the enhancement in would closure became significant, with the average scratch closure percentage increasing to 70.85% ± 0.17 (p-value=0.00356 when compared to control). This trend continued at higher fluoxetine concentrations with a dose-dependent effect. For cells exposed to 250 ng/l, 540 ng/l and 2700 ng/l, scratch closure increased to 72.62% ± 1.02, 75.52% ± 0.43 and 79.78% ± 0.6186, respectively, with p-values<0.001.

Cells exposed to the highest concentration of fluoxetine (5400 ng/l) resulted in the most substantial percentage of scratch closure, with an average of 86.36% ± 1.7 (p-value<0.001 when compared to control). This increase highlighted the dose-dependent nature of the impact of fluoxetine on HaCaT cell's scratch closure. The variability within each treatment group was relatively low (around ± 1%), indicating consistent responses among HaCaT cells exposed to fluoxetine.

In conclusion, the results from both visual inspection (Figure 3.1) and statistical analysis (Figure 3.2) demonstrate that fluoxetine has a dose-dependent effect on HaCaT cells scratch healing. With the most pronounced increase in scratch healing being observed at higher concentrations.

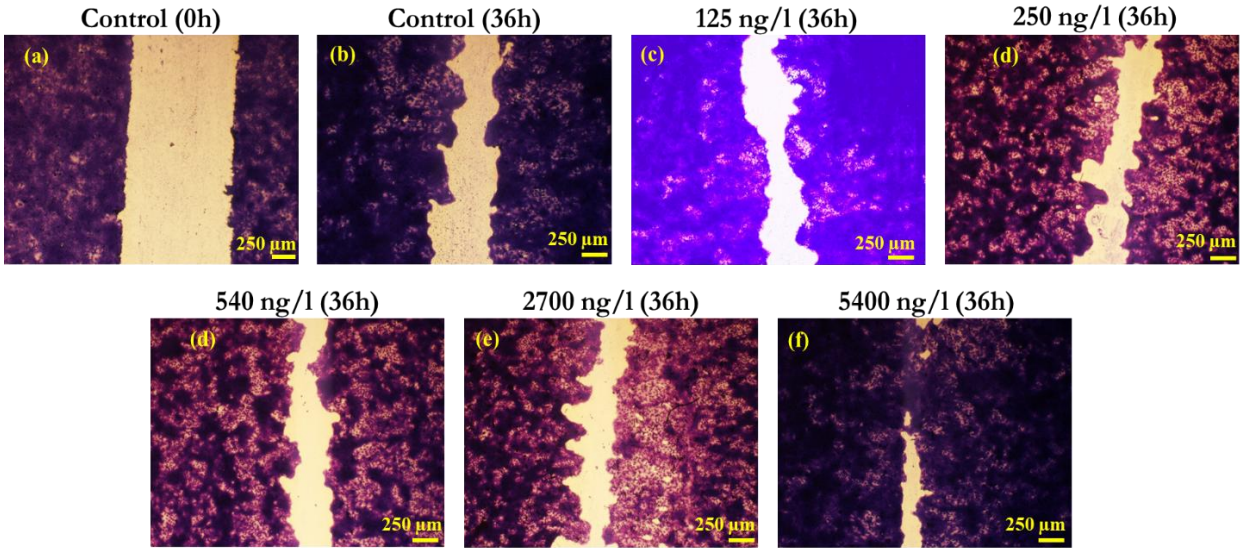

Figure 3.1: Representative images of scratch assays in the presence of fluoxetine. *At the indicated concentrations, at 36 hours after scratching (Figure 3.1b-f) or at the time of scratching (Figure 3.1a), with n=4 for each condition. Images were captured at 4× magnification, and the scale bars indicate 250µm.*

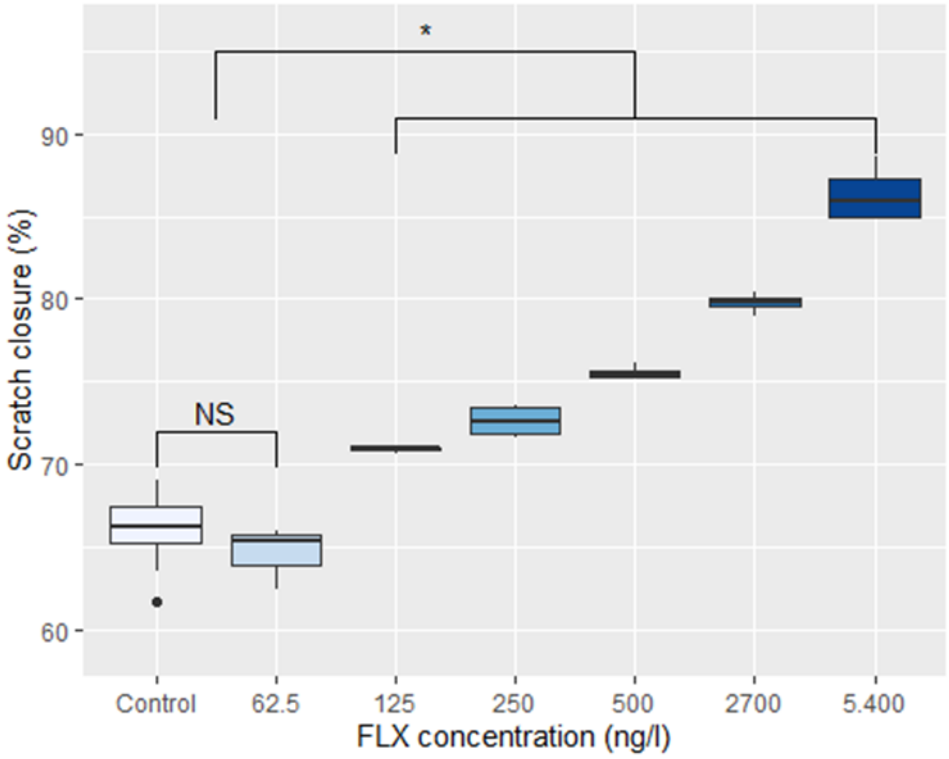

Figure 3.2: Boxplot of the percentage of scratch closure after 36 hours of exposure to fluoxetine. *The x-axis represents the fluoxetine concentrations (62.5 ng/l to 5400 ng/l), and the y-axis shows the percentage of scratch closure. X-axis not to scale. Each box represents the interquartile range (IQR), where the top and bottom of the box indicate the 75th and 25th percentiles, respectively. The horizontal line within each box represents the median. The whiskers extend to the minimum and maximum values, excluding outliers, and the dots represent individual data points. Statistical significance compared to the control group is indicated by asterisks (* $p < 0.05$), NS: non-significant. Statistical analysis was performed using one-way ANOVA followed by Tukey's post hoc test (n>4 biological replicates per condition).*

3.3.2 Mechanistic insights: fluoxetine-induced keratinocyte proliferation

Having established that fluoxetine significantly enhances scratch closure in a dose-dependent manner in HaCaT cells, the next aim was to understand the mechanisms underlying these changes. In the following section I will explore the results from Mitomycin C and EdU assays. These assays are designed to determine if the increase in scratch closure in HaCaT cells is caused mainly by increase in cell proliferation or cell migration. These experiments were conducted in collaboration with Belen Garcia-Merino, a visiting PhD student from the University of Cantabria, Spain, whom I trained and supervised throughout the process.

First, I conducted a series of experiments using Mitomycin C, a known inhibitor of cell proliferation, for this experiment I used HaCaT cells exposed to either just fluoxetine at two different concentration (540 and 5400 ng/l), cells exposed to only Mitomycin C (800 µg/l),

cells exposed to a combination of both drugs (540 ng/l fluoxetine+ 800 µg/l Mitomycin C and 5400 ng/l fluoxetine + 800 µg/l Mitomycin C) as well as control cells.

Initial visual observation indicated that cells exposed to 800 µg/l of Mitomycin C seemed to have a similar scratch closure when compared to control cells (Figure 3.3 a&d). Visual observation of cells exposed to the combination of both drugs showed less scratch closure when compared to cells exposed to only fluoxetine (Figure 3.3 b/e and c/f) at both 540 and 5400 ng/l.

After statistical analysis I confirmed that the presence of Mitomycin C completely abrogated the fluoxetine-induced enhancement of scratch closure (Figure 3.4). When Mitomycin C was introduced, the scratch closure percentage was significantly reduced when compared to cells exposed to only the equivalent concentration of fluoxetine (p-values<0.05). Cells exposed to combination of both Mitomycin C and fluoxetine had a percentage of scratch closure comparable to the control cells (p-values>0.05).

This finding suggests that fluoxetine promotes scratch closure through a mechanism that is at least partially dependent on cell proliferation, as pre-treatment with Mitomycin C reversed this effect. However, it cannot be concluded from this experiment alone whether fluoxetine and Mitomycin C act through the same proliferative signalling pathways.

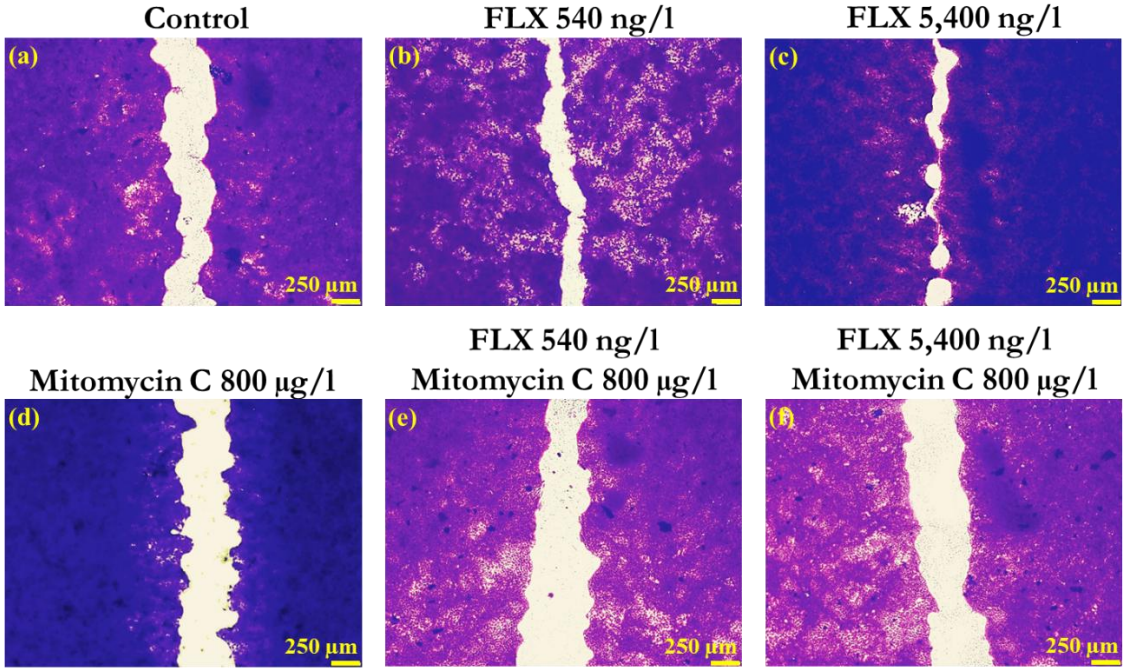

Figure 3.3: Representative images of scratch assays in the presence of fluoxetine. *At the indicated concentrations, at 36 hours after scratching with n=4 for each condition. Images were captured at 4× magnification, and the scale bars indicate 250µm.*

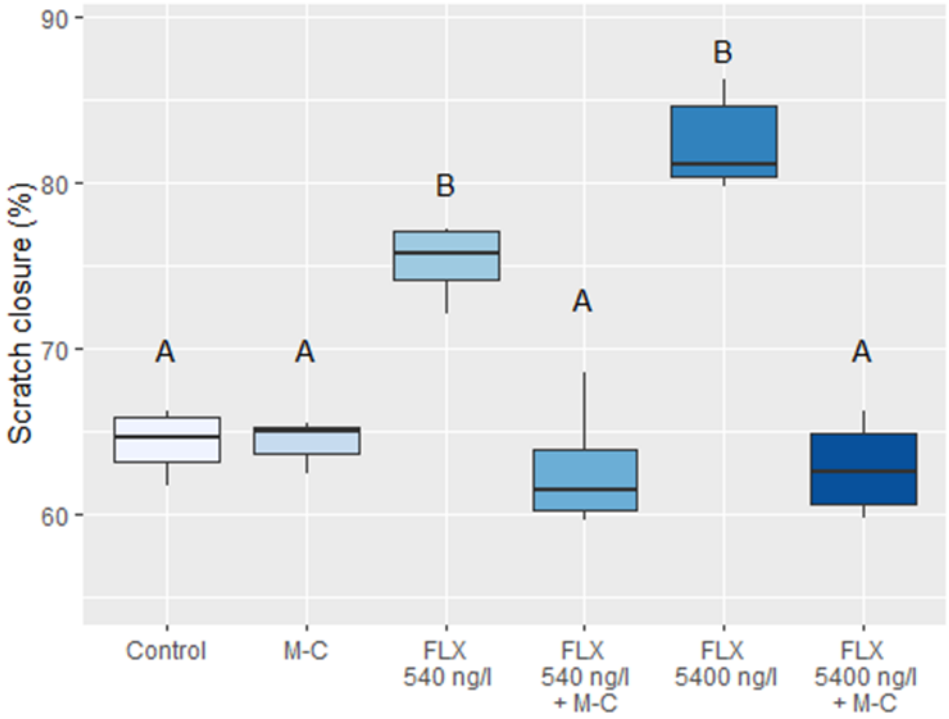

Figure 3.4: Boxplot of the percentage of scratch closure after exposure to Mitomycin C, fluoxetine or a combination of both. *The x-axis represents the fluoxetine concentrations (540 ng/l and 5400 ng/l) in combination with or without Mitomycin C, and the y-axis shows the percentage of scratch closure 36 hours after scratching. X-axis not to scale. Each box represents the interquartile range (IQR), where the top and bottom of the box indicate the 75th and 25th percentiles, respectively. The horizontal line within each box represents the median. The whiskers extend to the minimum and maximum values, excluding outliers, and the dots represent individual data points. Groups labelled A and B represent statistically significant differences between conditions, where different letters indicate a significant difference ($p < 0.05$), and the same letter indicates no significant difference. Statistical analysis was performed using one-way ANOVA followed by Tukey's post hoc test (n>4 biological replicates per condition).*

In order to confirm that the faster scratch closure after exposure to fluoxetine is due to an increase in cell proliferation, I performed EdU (5-ethynyl-2'-deoxyuridine) incorporation assays. This assay allows to measure the number of proliferating cells. For this experiment I used the range of environmentally relevant concentrations of fluoxetine (62.5 to 5400 ng/l) and EdU was added to label the proliferating cells.

After visualisation using a Zeiss fluorescence and a LD A-Plan x5 lens I measured the number of proliferating cells for each condition. Raw pictures are depicted in Figure 3.5. The pictures suggest a dose-dependent impact to fluoxetine on scratch closure, the higher the concentration, the smaller the scratch is after 28 hours. Due to experimental variation across different time

points and cell passages, the timeframe was adjusted to 28 hours for this set of experiments to ensure consistent scratch closure in control cells.

The measurement results are depicted in Figure 3.6. Fluoxetine increases the number of proliferating cells in the scratch area in a dose dependant manner. The difference in the number of proliferating cells between control cells and those exposed to fluoxetine was statistically significant only at the two highest concentrations, 540 ng/l (p-value = 0.01) and 5400 ng/l (p-value = 0.0023). Although there was an increase in proliferation at lower concentrations, these changes were not statistically significant (p-values > 0.05).
Those findings suggest that exposure to fluoxetine increases cell proliferation that in consequences increases scratch closure. To confirm these results, I repeated the EdU assays in the presence of Mitomycin C. The number of EdU-positive cells in the presence of both fluoxetine and Mitomycin C was significantly lower than with fluoxetine alone, as shown in Figure 3.7 and did not differ significantly from the control group (p-values> 0.05). This further supports the conclusion that fluoxetine enhances scratch closure primarily through the stimulation of keratinocyte proliferation.

In summary the results from both the Mitomycin C and EdU assays provided strong evidence that the exposure to fluoxetine at environmentally relevant concentrations promotes scratch closure of HaCaT cells by increasing cell proliferation. These findings do not only corroborate my previous findings but also offer a deeper understanding of the mechanisms involved in how fluoxetine may influence cellular processes involved in scratch healing.

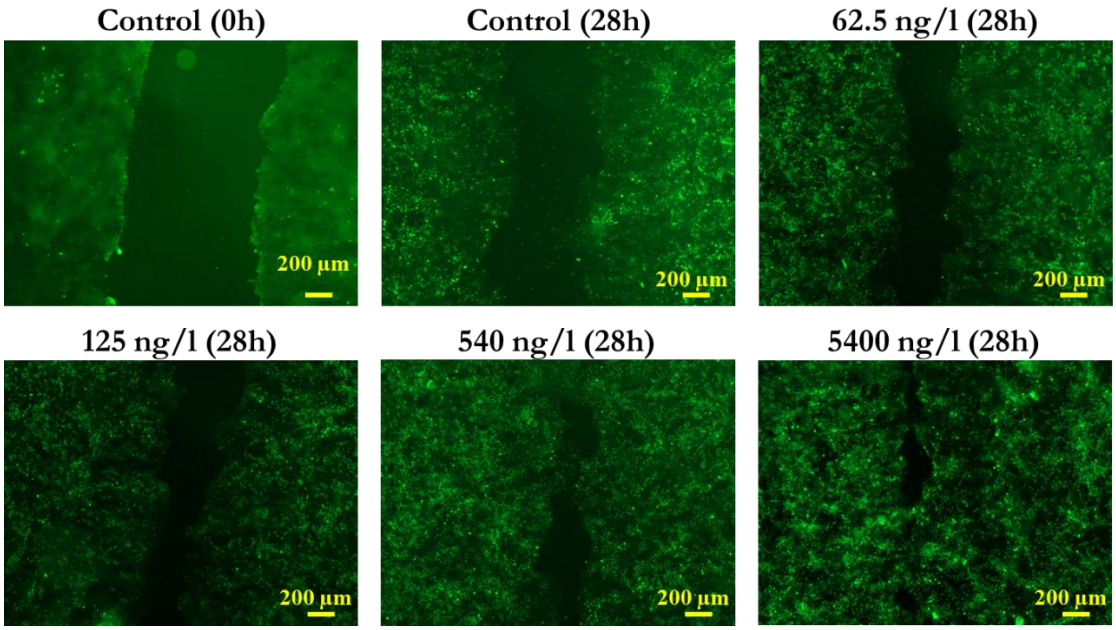

Figure 3.5: Representative images of EdU assays in the presence of fluoxetine *At the indicated concentrations, EdU incorporation was assessed at 28 hours after scratching, with n > 3 biological replicates per condition. Images were captured at 5× magnification, and the scale bars indicate 200 µm. EdU-positive cells were quantified using ImageJ software, where fluorescence thresholding was applied to identify EdU+ nuclei, and the percentage of EdU-positive cells was calculated relative to the total number of Hoechst-stained nuclei.*

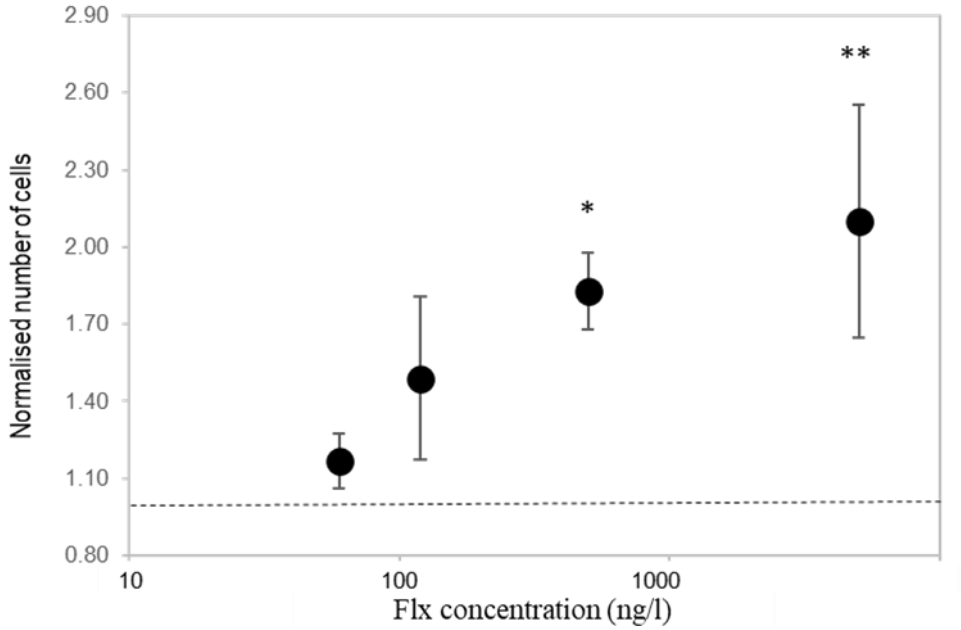

Figure 3.6: Dose-response dependence of the number of proliferating cells. *The x-axis represents fluoxetine concentrations (62.5 ng/l to 5400 ng/l), and the y-axis shows the normalized number of proliferating cells, measured by EdU incorporation 28 hours after scratching. Data are normalised to the Control condition, meaning that a value of 2.0 indicates twice as many proliferating cells compared to the non-treated Control group. EdU-positive cells were counted using ImageJ software. The data are presented as mean ± standard deviation (SD), and statistical significance compared to the control group is indicated by asterisks (*p-value=0.01, **p-value=0.0023).*

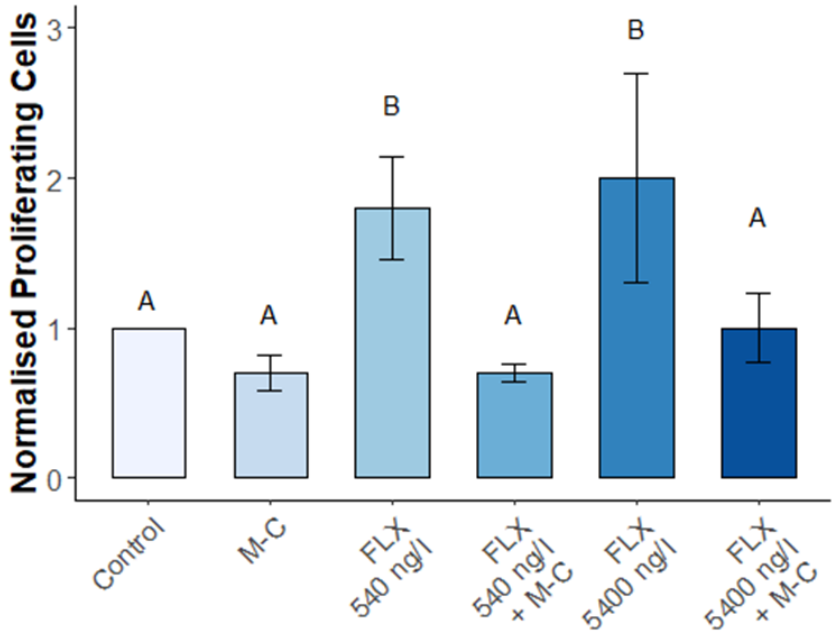

Figure 3.7: Barplot of the number of proliferating cells after exposure to Mitomycin C, fluoxetine or a combination of both. *The y-axis represents the normalised count of proliferating cells, as measured by EdU incorporation 28 hours after scratching. Data are normalised to the Control condition, meaning that a value of 2.0 indicates twice as many proliferating cells compared to the non-treated Control group. The x-axis represents the experimental conditions of fluoxetine, Mitomycin C, and their combination (not to scale). Each bar represents the mean, with error bars indicating the standard deviation. Statistical significance between groups is indicated by letters, where different letters denote significantly different groups ($p < 0.05$). Statistical analysis was performed using one-way ANOVA followed by Tukey's post hoc test (n>4 biological replicates per condition).*

3.3.3 Sertraline and ketanserin modulate keratinocyte scratch healing: insights into serotonin receptor involvement

In the previous sections I demonstrated that fluoxetine enhances keratinocyte scratch healing through an increase in cell proliferation. I will in this section aim to determine the relationship between changes in scratch closure and serotonin signalling. I will be testing another SSRI (Sertraline) to determine if the findings from my fluoxetine experiments can be extended to other SSRIs. Additionally, I will be using a serotonin receptor antagonist called Ketanserin to identify which specific receptors are involved in scratch-healing These experiments were conducted in collaboration with Tomilayo Akinmola a Master's student from the University of Hull, whom I trained and supervised throughout the process.

First, in order to investigate whether the enhanced scratch healing observed in the HaCaT model after exposure to fluoxetine is a general characteristic of SSRIs or specific to fluoxetine,

I conducted similar scratch assays using sertraline, another commonly used SSRI. I used the same range of concentrations as the one used in the fluoxetine experiments: 62.5 ng/l to 5400 ng/l. Examples of the images obtained are shown in Figure 3.8, visual observation indicates that sertraline worked in the same way that fluoxetine did, with an increase in scratch-closure after exposure to the drug.

The statistical analysis validates the visual observations, exposure to sertraline at 125, 540 and 5400 ng/l enhances the scratch closure of scratched HaCaT cells in a dose-dependent manner, as shown in Figure 3.9 (p-values<0.05 when compared to control cells). The lowest concentration of sertraline showed no significant changes in the percentage of scratch closure when compared to the control cells (p-value=0.999). Unlike fluoxetine, where the increase in scratch closure followed a clear dose-dependent pattern, the sertraline-induced enhancement in wound closure did not show a statistically significant difference between the three highest concentrations (p-values > 0.05), suggesting that a more complex relationship might be involved.

These findings suggest that the scratch healing enhancement may be a common feature of SSRIs, most likely due to alteration of 5-HT signalling.

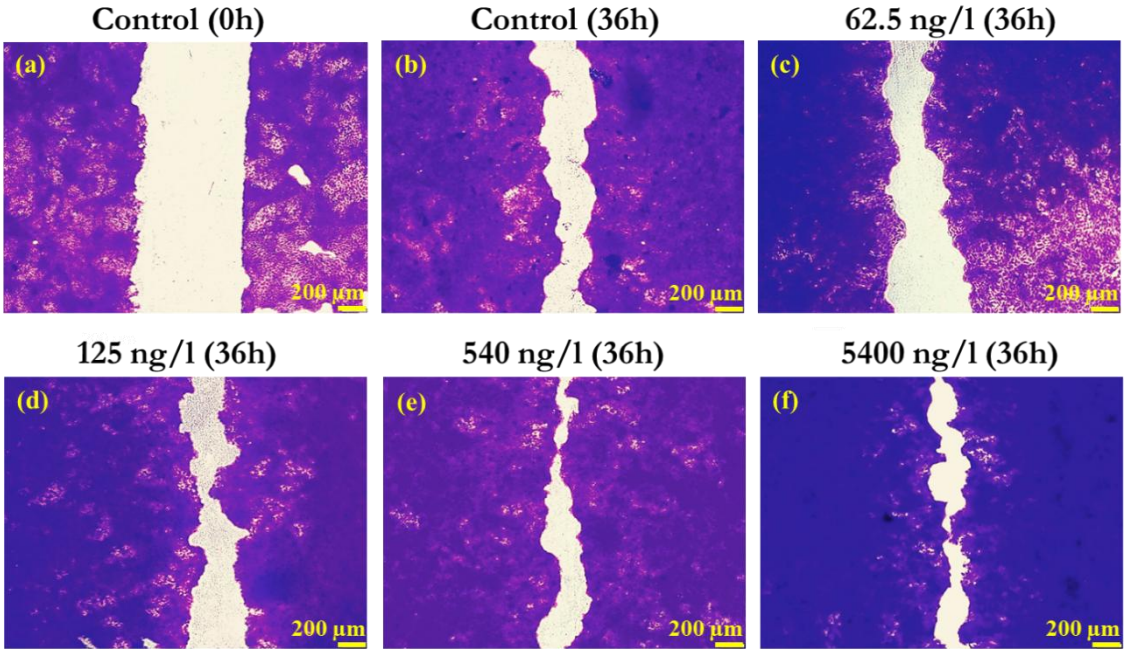

Figure 3.8: Representative images of scratch assays in the presence of sertraline. *At the indicated concentrations, at 28 hours after scratching (Figure 1.1b-f) or at the time of scratching (Figure 1.8a), with n=4 for each condition. Images were captured at 4× magnification, and the scale bars indicate 200µm.*

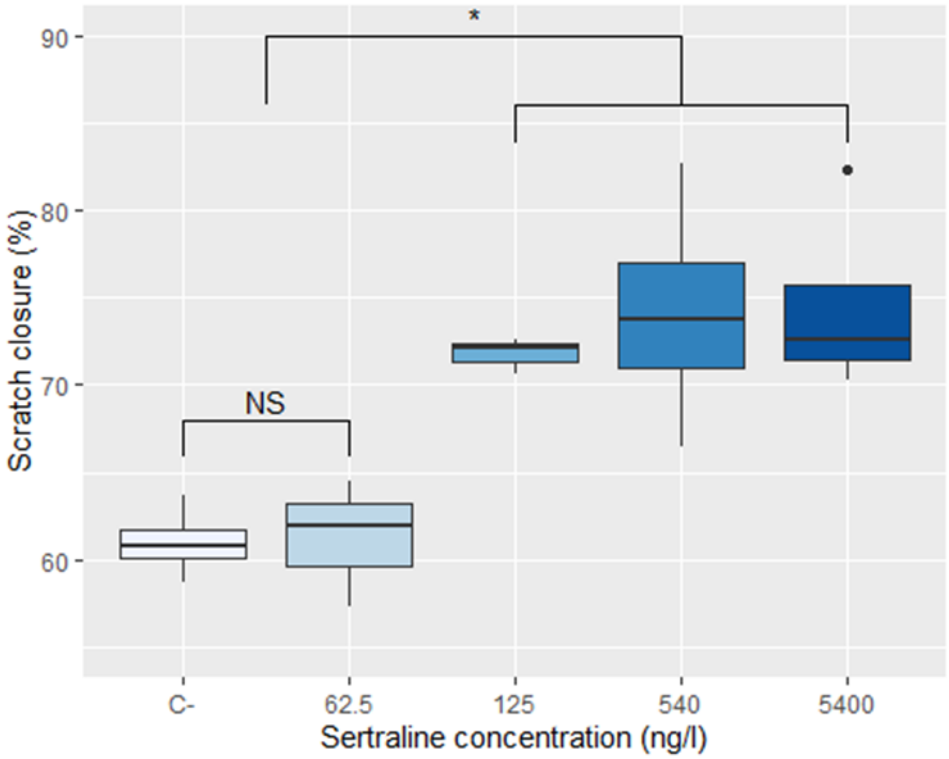

Figure 3.9: Boxplot of the percentage of scratch closure after 28 hours of exposure to sertraline. *The x-axis represents the concentrations of sertraline (62.5 ng/l to 5400 ng/l), and the y-axis shows the percentage of scratch closure 28 hours after scratching. X-axis not to scale. Each box represents the interquartile range (IQR), where the top and bottom of the box indicate the 75th and 25th percentiles, respectively. The horizontal line within each box represents the median. The whiskers extend to the minimum and maximum values, excluding outliers, and the dots represent individual data points. Statistical significance compared to the control group is indicated by asterisks (* $p < 0.05$), NS: non-significant. Statistical analysis was performed using one-way ANOVA followed by Tukey's post hoc test (n=4 biological replicates per condition).*

In order to determine the role of alteration of 5-HT signalling in mediating the wound healing effects of SSRIs I performed a series of scratch assays in which HaCaT cells were exposed to fluoxetine in combination with ketanserin. Ketanserin is an antagonist of 5HTR2a and 5HTR2c that has been previously used to investigate the role of 5-HT in wound healing (Nguyen et al., 2019; Sadiq et al., 2018).

Figure 3.10 illustrates the effect of ketanserin (10 µM) on fluoxetine-induced scratch healing. The co-administration of ketanserin with fluoxetine resulted in a significant reduction in scratch closure compared to fluoxetine alone (p-value=0.003). The addition of ketanserin reduced the percentage of scratch closure from 58.21% ± 5.84 to 45.99% ± 4.00 indicating

that the activation of 5-HT2 receptors is crucial for the observed effects and that the 5-HT2 receptor plays a pivotal role in mediating the scratch healing effects of SSRIs.

To identify the serotonin receptors involved in mediating these effects, RNAseq was performed to assess the expression of 5-HT receptors in HaCaT cells. The analysis detected the expression of 5-HT receptors from all seven receptor families (HTR1 to HTR7), as shown in Table 3.1. The RNAseq results, along with further details and analysis, will be provided in Chapter 4.

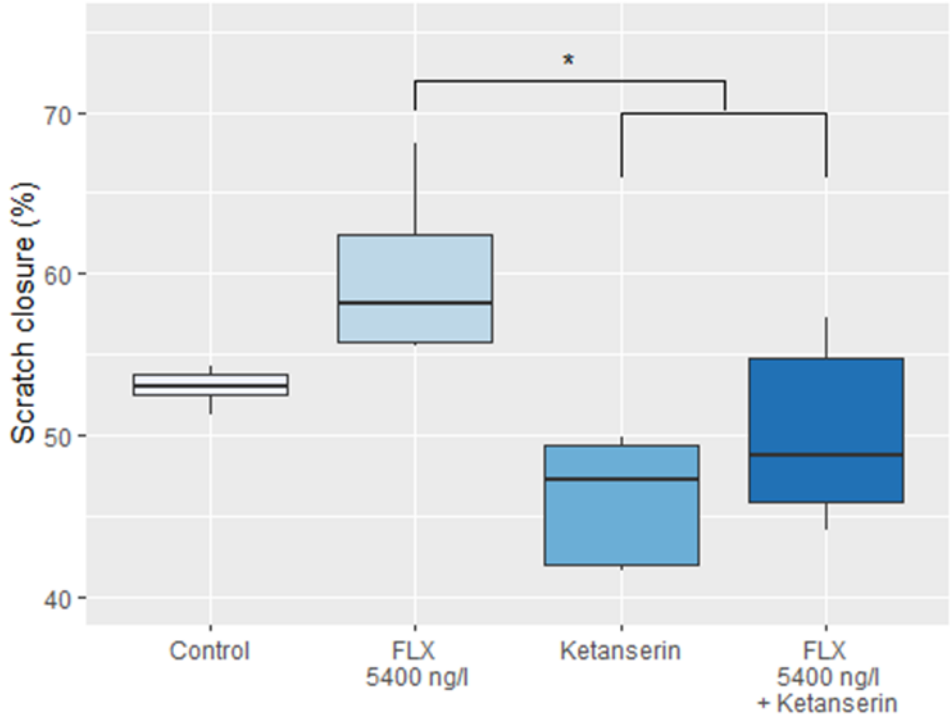

Figure 3.10: Boxplot of the percentage of scratch closure after exposure to fluoxetine, ketanserin or a combination of both. *The x-axis represents the conditions of fluoxetine, Ketanserin, and the combination of both, and the y-axis shows the percentage of scratch closure 28 hours after scratching. X-axis not to scale. Each box represents the interquartile range (IQR), where the top and bottom of the box indicate the 75th and 25th percentiles, respectively. The horizontal line within each box represents the median. The whiskers extend to the minimum and maximum values, excluding outliers, and the dots represent individual data points. Statistical significance between groups is indicated by asterisks (* $p < 0.05$). Statistical analysis was performed using one-way ANOVA followed by Tukey's post hoc test (n>5 biological replicates per condition).*

Gene ID	Gene Name	Chromosome	Gene Biotype	Description
ENSG00000158748	HTR6	1	protein_coding	5-hydroxytryptamine receptor 6
ENSG00000179546	HTR1D	1	protein_coding	5-hydroxytryptamine receptor 1D
ENSG00000135914	HTR2B	2	protein_coding	5-hydroxytryptamine receptor 2B
ENSG00000179097	HTR1F	3	protein_coding	5-hydroxytryptamine receptor 1F
ENSG00000186090	HTR3D	3	protein_coding	5-hydroxytryptamine receptor 3D
ENSG00000178084	HTR3C	3	protein_coding	5-hydroxytryptamine receptor 3C
ENSG00000186038	HTR3E	3	protein_coding	5-hydroxytryptamine receptor 3E
ENSG00000178394	HTR1A	5	protein_coding	5-hydroxytryptamine receptor 1A
ENSG00000164270	HTR4	5	protein_coding	5-hydroxytryptamine receptor 4
ENSG00000135312	HTR1B	6	protein_coding	5-hydroxytryptamine receptor 1B
ENSG00000168830	HTR1E	6	protein_coding	5-hydroxytryptamine receptor 1E
ENSG00000157219	HTR5A	7	protein_coding	5-hydroxytryptamine receptor 5A
ENSG00000147246	HTR2C	X	protein_coding	5-hydroxytryptamine receptor 2C
ENSG00000149305	HTR3B	11	protein_coding	5-hydroxytryptamine receptor 3B
ENSG00000166736	HTR3A	11	protein_coding	5-hydroxytryptamine receptor 3A
ENSG00000148680	HTR7	10	protein_coding	5-hydroxytryptamine receptor 7
ENSG00000102468	HTR2A	13	protein_coding	5-hydroxytryptamine receptor 2A

Table 3.1: Expression of serotonin (5-HT) receptors in HaCaT cells. *The table displays the gene identifiers, names, chromosomal locations, and biotypes of the serotonin receptors expressed in HaCaT cells, as detected by RNAseq. The gene biotypes indicate whether the genes are functional, protein-coding receptors*.

3.4 Discussion

This chapter aimed to investigate the effects of environmentally relevant concentrations of fluoxetine on wound closure, more specifically on how fluoxetine will influence a keratinocyte model. The results demonstrated a dose-dependent enhancement of wound closure, which appears to be mainly due to an increase in cell proliferation.

This discussion will delve into the specific underlying mechanisms in fluoxetine-mediated scratch closure.

3.4.1 Fluoxetine-induced scratch closure via serotonin signalling.

The dose-dependent scratch closure observed in this study confirms the role of serotonin signalling in promoting keratinocyte activity. At the highest concentration of fluoxetine (5400 ng/l), near-complete wound closure was achieved after 36 hours, suggesting that serotonin receptor activation drives keratinocyte behaviour. RNAseq results further reinforced this, showing the expression of serotonin receptors from all seven receptor families (HTR1 to HTR7) in HaCaT cells, with notable expression of HTR2A and HTR2C, receptors known to regulate cell proliferation and tissue repair.

These findings align with a previous study (Nguyen et al., 2019), who demonstrated that fluoxetine improved wound healing in diabetic mice, primarily through promoting keratinocyte migration. However, while Nguyen et al. focused on migration in Normal Human Epidermal Keratinocytes (NHEK), my results suggest that fluoxetine promotes scratch closure in HaCaT cells via proliferation. Both studies underscore the importance of 5-HT2 receptors, though the specific cellular responses (migration versus proliferation) may vary based on the experimental model and fluoxetine concentrations (Nguyen et al., 2019).

Sertraline, another SSRI tested in this chapter, also enhanced scratch closure, with a more complex dose-response relationship, unlike fluoxetine, the sertraline-induced enhancement in wound closure did not show statistically significant differences between the three highest concentrations (125, 540, and 5400 ng/L). This suggests that while both SSRIs act via serotonin signalling, the wound-healing effects of sertraline may plateau at higher doses or involve additional factors beyond 5-HT2 receptor activation. These findings are consistent with the general role of SSRIs in modulating skin cell function but also suggest distinct mechanisms of action between fluoxetine and sertraline that warrant further investigation.

The critical role of 5-HT2 receptors in skin cells is well-established in the literature. In a study published in 2008 it was showed that 5-HT2 receptors are highly expressed in human keratinocytes and play an essential role in regulating inflammation and wound healing (Nordlind et al., 2008). My findings confirm that fluoxetine, through 5-HT2 receptor activation, enhances keratinocyte proliferation, which accelerates wound closure. The RNAseq results in my study align with the findings from Nordlind et al., demonstrating that serotonin receptor expression in HaCaT cells contribute to skin regeneration.

The broader regulatory role of serotonin signalling in skin cells has also been previously emphasised (Martins et al., 2020). Their work on psoriasis highlighted how 5-HT2 receptors modulate inflammation and tissue regeneration, roles consistent with fluoxetine's effects on keratinocyte proliferation in my study. These combined findings suggest that serotonin signalling through 5-HT2 receptors is central to maintaining keratinocyte function and promoting tissue repair in a variety of contexts.

The relevance of 5-HT2 receptors in wound healing was also confirmed by other teams, who showed that serotonin receptor activation enhances keratinocyte proliferation after thermal

injury (Sadiq et al., 2018). Their study mirrors my findings, where fluoxetine-driven 5-HT2 receptor activation significantly boosted keratinocyte proliferation, underscoring the potential therapeutic applications of fluoxetine for skin repair.

However, while the data support a role for serotonin signalling, it is important to acknowledge that serotonin was not supplemented in the culture media, and its endogenous levels were not directly measured. Although keratinocytes express the enzymes necessary for serotonin biosynthesis (Goodwin et al., 2017; Schallreuter et al., 2012) and FBS been shown to contain trace amounts of serotonin or its precursors (Chávez et al., 2017), these potential sources may not provide sufficient levels to fully activate serotonin receptors. Therefore, the contribution of serotonin itself remains uncertain. An alternative and plausible explanation is that fluoxetine may act directly on serotonin receptors, independently of serotonin availability. Fluoxetine is a competitive and reversible antagonist at the 5-HT2C receptor, a non-competitive antagonist at 5-HT3 receptors, and an agonist at 5-HT2B receptors (Peng et al., 2014), all of which are expressed in skin. These receptor-mediated mechanisms may account for the observed effects and suggest that fluoxetine could modulate receptor activity directly, without requiring high extracellular serotonin concentrations.

3.4.2 Cell proliferation as the primary mechanism of action of fluoxetine

The Mitomycin C experiments provided crucial mechanistic insights, confirming that fluoxetine enhances wound closure by stimulating keratinocyte proliferation. Mitomycin C, which inhibits DNA synthesis and cell proliferation, effectively blocked the wound-healing effects of fluoxetine, indicating that proliferation, rather than migration, is the primary driver of the observed wound closure. This finding complements studies that used Mitomycin C to block cell proliferation in keratinocytes, such as Ribeiro et al. (De Andrade Quintanilha Ribeiro et al., 2004) who demonstrated that Mitomycin C significantly delayed wound healing in rats by inhibiting fibroblast activity, and Wang et al. (Wang et al., 2012) who showed that Mitomycin C inhibited the proliferation of both fibroblasts and HaCaT cells *in vitro*, with higher concentrations of Mitomycin C resulting in stronger antiproliferative effects. Both studies align with my findings, where fluoxetine's ability to accelerate wound closure was fully abrogated when proliferation was inhibited by Mitomycin C, highlighting the critical role of cell proliferation in the action of fluoxetine.

The dose-dependent increase in keratinocyte proliferation observed in the EdU incorporation assays further supports this conclusion. Higher concentrations of fluoxetine resulted in greater cell proliferation, indicating that fluoxetine directly influences the cell cycle in HaCaT cells. While a previous study (Nguyen et al., 2019) found that fluoxetine primarily enhanced keratinocyte migration in their *in vivo* model, my study shows that fluoxetine promotes proliferation in HaCaT cells, which is the key driver of scratch closure in this *in vitro* system. Although the exact cellular responses differ between migration and proliferation, both studies reinforce the role of fluoxetine in promoting wound healing via serotonin receptor activation, particularly 5-HT2 receptors.

3.4.3 Serotonin receptor activation as a key driver of scratch closure

The role of serotonin receptor activation in fluoxetine-mediated scratch closure was further clarified by the use of ketanserin, a 5-HT2A receptor antagonist. Co-administration of ketanserin significantly reduced the wound-healing effects of fluoxetine, confirming that 5-HT2 receptors are essential mediators of the action of fluoxetine. This finding complements earlier work (Nordlind et al., 2008; Sadiq et al., 2018), who identified 5-HT2 receptors as critical in modulating keratinocyte function and tissue repair. In my study, the reduction in wound closure when 5-HT2 receptors were blocked underscores the importance of serotonin signalling in driving keratinocyte proliferation.

The RNAseq results, which showed strong expression of 5-HT2A and 5-HT2C receptors in HaCaT cells, provide molecular support for the involvement of these receptors in mediating the effects of fluoxetine. However, the mechanism underlying their activation in this context remains open to interpretation. No serotonin was supplemented in the culture system, and although keratinocytes can produce serotonin endogenously, and foetal bovine serum may contain trace levels (Chávez et al., 2017; Goodwin et al., 2017), the presence of serotonin under these conditions was not directly confirmed. This raises the possibility that fluoxetine may act through serotonin-independent mechanisms by binding directly to serotonin receptors. Indeed, fluoxetine has been shown to modulate receptor activity independent of serotonin, functioning as a 5-HT2C antagonist, a 5-HT2B agonist, and a 5-HT3 non-competitive antagonist (Breitinger et al., 2001; Eisensamer et al., 2003; Ni and Miledi, 1997; Peng et al., 2014). These direct receptor interactions could explain the effects on keratinocyte proliferation even in the absence of high extracellular serotonin.

Importantly, although these effects are not mediated by serotonin itself, they still fall within the scope of serotonin receptor signalling. Thus, fluoxetine may modulate skin physiology through receptor-specific signalling events, even in the absence of classical serotonergic activation.

In this light, the inhibition of the effects of fluoxetine by ketanserin supports the importance of 5-HT2 receptor engagement but does not necessarily confirm serotonin-mediated signalling. Further studies are required to determine whether the action of fluoxetine is dependent on endogenous serotonin levels or arises from direct modulation of serotonin receptors in keratinocytes.

3.5 Conclusion

In this chapter, I have demonstrated that fluoxetine, a widely prescribed SSRI that is frequently detected in freshwater systems, significantly enhances scratch closure in keratinocyte models through a dose-dependent mechanism. This effect is primarily driven by increased cell proliferation, as confirmed by the Mitomycin C and EdU assays. My findings suggest that the impact of fluoxetine on scratch closure is mediated through the activation of serotonin receptors, particularly 5-HT2A and 5-HT2C, which regulate key processes in cell proliferation and tissue repair. The use of ketanserin, a 5-HT2 receptor antagonist, further confirmed the essential role of 5-HT2 receptors in mediating these effects.

RNAseq revealed the expression of 5-HT receptors from all seven receptor families (HTR1 to HTR7) in HaCaT cells, with notable expression of HTR2A and HTR2C, providing molecular evidence for the mechanism of action of fluoxetine. These results emphasise that serotonin signalling, particularly through 5-HT2 receptors, plays a central role in skin physiology and wound healing. However, serotonin itself was not supplemented in the culture system, and its concentration was not measured. While keratinocytes can synthesise serotonin and FBS may contain trace levels, the precise contribution of endogenous serotonin to receptor activation remains uncertain. Given this, it is plausible that fluoxetine acts directly on serotonin receptors to promote downstream signalling, independent of serotonin availability. Fluoxetine is known to act as an agonist or antagonist at several 5-HT receptor subtypes, including 5-HT2B, 5-HT2C, and 5-HT3, which could account for the observed cellular effects. This still falls within the scope of serotonin receptor signalling, but not classical serotonin-mediated signalling, and highlights the need for further mechanistic dissection.

Furthermore, the effects of sertraline, another SSRI, mirrored those of fluoxetine, suggesting that these wound-healing properties may be a broader characteristic of SSRIs. These findings expand the understanding of the biological effects of SSRIs beyond their psychiatric applications, indicating potential therapeutic uses for skin repair and regeneration.

These findings have important implications, particularly in the context of the environmental presence of SSRIs. Fluoxetine has been detected in surface waters at concentrations ranging from low ng/l to several hundred ng/l, depending on location and treatment efficacy (Lajeunesse et al., 2012; Schultz et al., 2010). The concentrations used in this chapter include levels that bracket environmentally relevant exposures, with 540 ng/l falling well within the upper range found in contaminated effluents. Although accelerated wound healing may not inherently pose a health risk, the ability of SSRIs to modulate cellular processes such as proliferation raises broader ecotoxicological questions, particularly regarding chronic, low-level exposure through environmental vectors. Populations such as wild swimmers, rowers, and children who regularly use lakes and rivers may be more directly exposed to SSRIs like fluoxetine. In parallel, increasing water scarcity due to climate change may lead to higher concentrations of pharmaceuticals in drinking water supplies. Additionally, occupational exposure in wastewater-related jobs may represent another under-recognised risk. Whether through indirect serotonin-mediated pathways or direct receptor engagement, SSRIs have the potential to disrupt skin physiology under environmentally relevant exposure scenarios.

In conclusion, this chapter provides new insights into the role of SSRIs in scratch closure, revealing the complex interplay between serotonin receptor signalling and keratinocyte function. Although the presence of serotonin in the culture system remains uncertain, the consistent expression of serotonin receptors and the effects of fluoxetine and ketanserin together suggest a receptor-driven mechanism. These results not only enhance the understanding of the broader biological effects of SSRIs but also underscore the need for further research into their environmental and health impacts.

Chapter 4: Transcriptomic insights into fluoxetine-induced wound healing in keratinocytes

4.1 Introduction

In the previous chapter, I determined that exposure to environmentally relevant concentrations of fluoxetine promoted scratch closure in HaCaT cells, primarily through activation of serotonin signalling and increased keratinocyte proliferation. These findings align with existing literature (Yoon et al., 2021), which demonstrated that fluoxetine accelerates re-epithelialization in chronic wounds by influencing both inflammatory and proliferative pathways. The molecular mechanisms behind these, particularly at low environmentally relevant fluoxetine concentrations, are however less well understood.

The main mode of action of fluoxetine as an SSRIs involves the inhibition of serotonin reuptake, leading to elevated levels of extracellular serotonin. Downstream pathways that regulate cellular proliferation, tissue repair and inflammation control are activated due to the increase in serotonin levels (Nordlind et al., 2008; Sahu et al., 2018). While the connection between serotonin and keratinocyte activity has begun to be reported (Nguyen et al., 2019), the precise transcriptomic changes that occur in keratinocytes exposed to fluoxetine, particularly at lower, environmentally relevant concentrations, remain largely unexplored.

To address this knowledge gap, this chapter uses RNAseq to determine the transcriptional modifications caused by fluoxetine in keratinocytes. By analysing the gene expression changes and pathway enrichment I aim to identify the main genes and pathways involved in the fluoxetine-induced proliferation and wound healing processes. These insights will offer a deeper understanding of the mechanisms by which fluoxetine influences skin regeneration and its broader environmental implications.

4.2 Aims & Objectives

The aim of this chapter is to investigate the molecular mechanisms underlying fluoxetine-induced wound healing in keratinocytes through transcriptomic analysis. Specifically, RNA sequencing was employed to identify differentially expressed genes (DEGs) that are involved in the process of cell proliferation and wound healing in response to fluoxetine exposure.

The objectives of this chapter are:

1) **To characterise the transcriptomic response of keratinocytes exposed to environmentally relevant concentrations of fluoxetine,** by identifying differentially expressed genes through RNA sequencing analysis.

2) **To analyse the biological pathways modulated by fluoxetine in keratinocytes,** by performing Gene Ontology (GO) and KEGG pathway enrichment analyses.

3) **To investigate the molecular interactions influencing fluoxetine-induced keratinocyte proliferation,** through protein-protein interaction (PPI) network analysis.

4.3 Results

4.3.1 RNA sequencing overview

To assess the transcriptomic changes in keratinocytes exposed to fluoxetine, RNAseq was performed on HaCaT cells. The concentration of fluoxetine used was environmentally relevant (540 ng/l) and exposure time was 36 hours. High-throughput sequencing generated a robust dataset, with an average of 51,076,758 reads per sample, and the average clean read count was 50,048,716 per sample. Quality control checks ensured high confidence in the data, with more than 95.39% of the reads aligning to the reference genome, with 96.36% mapping to exonic regions, 2.39% to intronic regions, and 1.25% to intergenic regions. The high proportion of exonic reads highlights the quality of the data. This is further demonstrated by the sector diagram (Figure 4.1), showing the distribution of reads across exonic, intronic, and intergenic regions.

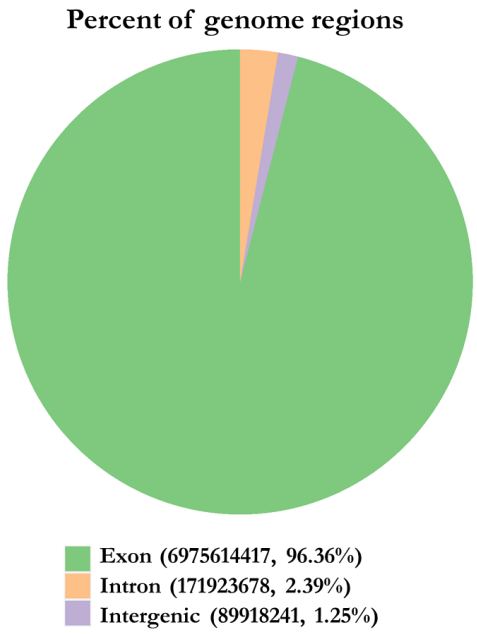

Figure 4.1: Sequencing reads in the genomic region. *The pie chart displays the distribution of RNAseq reads across exonic, intronic, and intergenic regions in the HaCaT cell line.*

The RNAseq data revealed some gene expression changes in response to fluoxetine exposure, identifying a total of 350 differentially expressed genes, comprising both upregulated and downregulated genes. This comprehensive dataset provided the foundation for further analysis to explore the biological pathways affected by fluoxetine and how these transcriptomic alterations relate to wound healing.

Serotonin receptors were among the key transcripts identified, reflecting the expected role of serotonin signalling in keratinocytes. As noted in Chapter 3, Table 3.1, 5-HT receptors, including 5-HTR2q and 5-HTR2c, were expressed in HaCaT cells, providing further evidence of the involvement of serotonin signalling in the molecular pathways activated by fluoxetine. These results are consistent with the idea that fluoxetine mediates its effects on wound healing by modulating serotonin receptor activity, subsequently affecting downstream signalling pathways involved in cellular proliferation and tissue repair.

This section sets the stage for a detailed examination of differentially expressed genes, pathway enrichment, and protein-protein interactions in subsequent sections of the results.

4.3.2: Differential gene expression and pathway enrichment analysis after fluoxetine exposure

RNAseq identified a total of 350 DEGs in HaCaT exposed to fluoxetine. Of these, exactly 100 genes were upregulated while 250 genes were downregulated. The volcano plot in Figure 4.2 is the visual representation of the magnitude and significance of the DEGs. The red dots represent genes that are significantly upregulated, while the green dots indicate genes that are significantly downregulated. Genes with non-significant changes are depicted in blue, providing a clear distinction between those that were highly affected by fluoxetine and those that were not. The volcano plot demonstrates a strong segregation between upregulated and downregulated genes, reflecting the distinct transcriptional response to fluoxetine exposure.
Figure 4.3 is a heatmap that further illustrate the global transcriptional changes induced by fluoxetine. The red regions on the heatmap represent genes that were upregulated, while the blue regions depict downregulated genes. The heatmap visually highlights the overall gene expression patterns in response to fluoxetine exposure, demonstrating clear clustering of upregulated and downregulated genes. This figure underscores the transcriptional impact of fluoxetine treatment on keratinocytes, setting the stage for further analysis of the affected biological pathways.

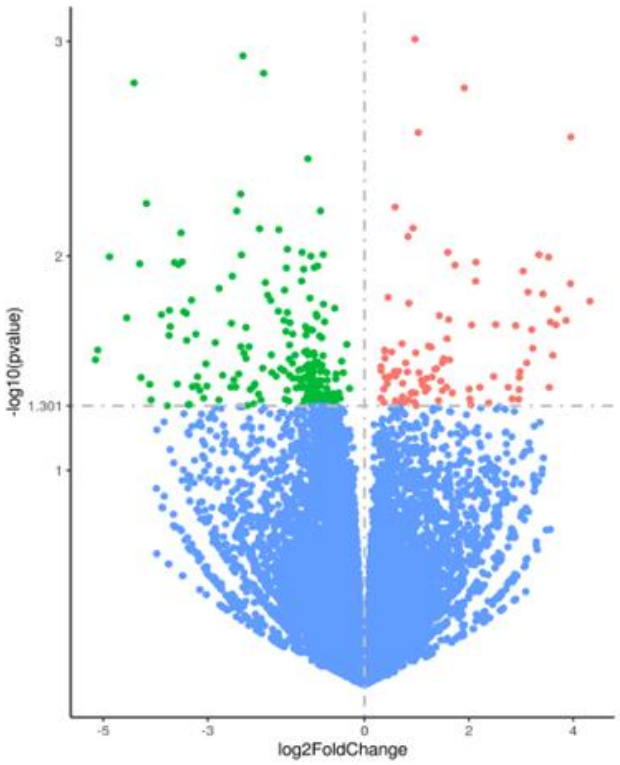

Figure 4.2: Volcano plot of differentially expressed genes (DEGs) in HaCaT cells keratinocytes exposed to fluoxetine (540 ng/l) for 36 hours. *The plot visualises the significance and magnitude of gene expression changes. Red dots represent significantly upregulated genes, green dots indicate significantly downregulated genes, and blue dots represent genes with non-significant changes. The x-axis displays the log2 fold change, indicating the magnitude of expression changes, while the y-axis shows the -log10(p-value), representing the statistical significance of these changes.*

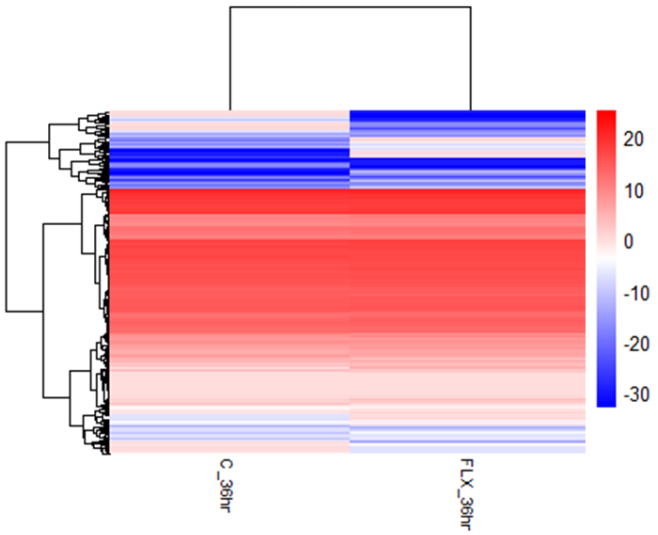

Figure 4.3: Heatmap of differentially expressed genes (DEGs) in HaCaT keratinocytes exposed to 540 ng/l fluoxetine for 36 hours. *The heatmap visualises the global transcriptional response to fluoxetine treatment, with red regions indicating significantly upregulated genes and blue regions representing significantly downregulated genes. The clustering in the heatmap highlights the distinct molecular responses in keratinocytes exposed to fluoxetine.*

To understand the biological significance of the identified DEGs, Gene Ontology (GO) analysis was performed. Figure 4.4 illustrates the top enriched GO terms for upregulated and downregulated gene. In Figure 4.4 panel A the key GO terms for downregulated genes are presented, including NADH dehydrogenase activity, ATP metabolic process, and mitochondrial membrane part. The downregulated genes were significantly enriched in GO terms related to mitochondrial function, oxidative phosphorylation and energy metabolism.

For the upregulated genes (Figure 4.4 panel B), GO analysis identified top enriched GO terms such as growth factor beta receptor binding, scaffold protein binding, and co-receptor binding. Upregulated genes were significantly enriched in GO terms linked to tissue morphogenesis, cell proliferation and cell cycle progression.

Together, these GO analyses highlight the dual impact of fluoxetine: promoting cell proliferation through upregulated signalling pathways and downregulating mitochondrial processes that modulate energy metabolism. These findings suggest that fluoxetine may shift the energy balance in keratinocytes towards increased proliferation while modulating energy production.

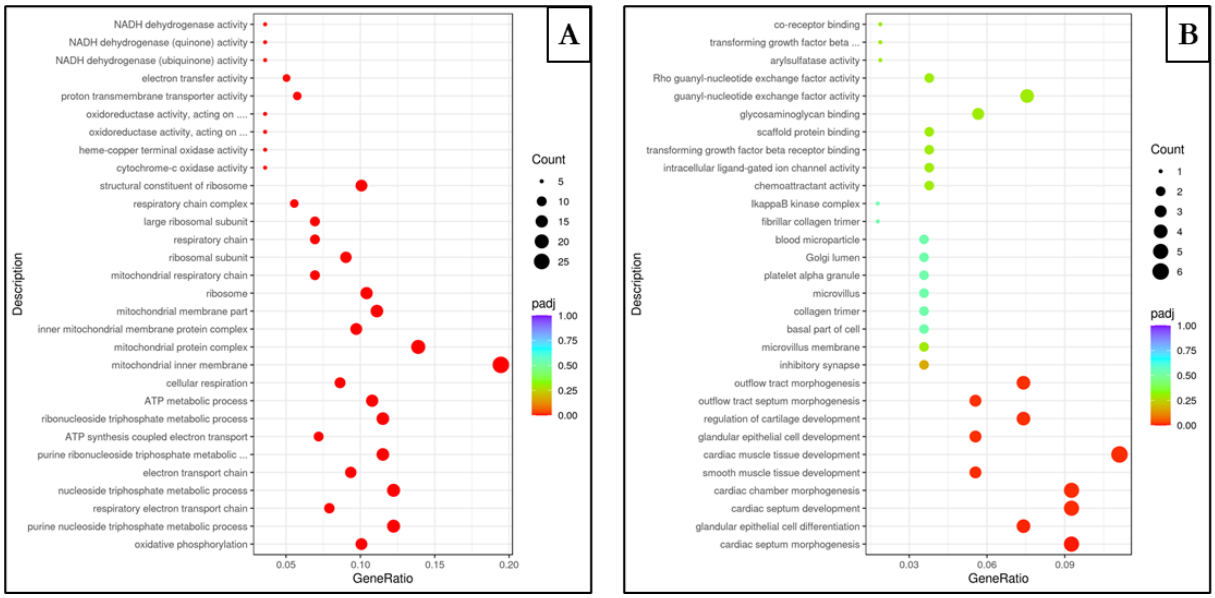

Figure 4.4: Gene Ontology (GO) analysis of differentially expressed genes (DEGs) in HaCaT cells after 36 hours of fluoxetine exposure. *The dot plot visualises the most significantly enriched GO terms for both upregulated and downregulated genes. (A) GO terms enriched in downregulated genes. (B): GO terms enriched in upregulated genes. The dot size represents the number of genes associated with each GO term, while the colour scale indicates the statistical significance (with red representing the most significant terms). The gene ratio reflects the proportion of DEGs involved in each biological process.*

Following the GO analysis, KEGG pathway enrichment analysis was conducted to further explore the specific biological pathways modulated by fluoxetine in HaCaT cells. The results of this analysis reveal distinct pathways enriched for both downregulated and upregulated genes, providing deeper insight into the molecular processes affected by fluoxetine exposure.

The top downregulated pathways are presented in Figure 4.5 panel A. Some of the top downregulated pathways include oxidative phosphorylation, thermogenesis, and chemical carcinogenesis – reactive oxygen species. Oxidative phosphorylation, one of the most significantly enriched pathways, involves a series of mitochondrial processes critical for ATP production, the downregulation of this pathway, as shown by the large dot size and intense red colouring, suggests that fluoxetine may have a suppressive effect on mitochondrial energy production. Other energy-related pathways such as thermogenesis and ROS production are also significantly downregulated, further indicating a reduction in mitochondrial activity and the potential modulation of oxidative stress levels in fluoxetine-exposed cells. Each dot represents the number of genes involved in the pathway, with the colour intensity reflecting the adjusted p-values, showing a strong statistical significance for these findings. The distribution of gene ratios for these pathways suggests that a considerable proportion of downregulated genes are involved in energy metabolism, mitochondrial function, and stress responses, reflecting a substantial impact of fluoxetine on these processes.

The pathways presented in Figure 4.5 panel B exhibit upregulation trends, although none reached statistical significance, as indicated by the adjusted p-value (padj) of 0.5. These upregulated pathways include those involved in cell cycle regulation, ECM-receptor interaction, and signalling pathways regulating pluripotency of stem cells. While these upregulated pathways suggest a potential role for fluoxetine in cellular proliferation and wound healing processes in keratinocytes, further investigation is needed to confirm these effects. For instance, pathways such as Basal cell carcinoma and Arginine biosynthesis showed enrichment, which might reflect the role of fluoxetine in enhancing cellular growth and metabolic activity. The ECM-receptor interaction pathway, involved in cell adhesion and communication, also suggests that fluoxetine could affect keratinocyte migration and adhesion, both of which are essential for effective wound healing. Overall, while these trends point to the potential impact of fluoxetine on processes related to wound healing, such as cell proliferation and tissue morphogenesis, further validation is required to determine their significance.

The size of the dots across both panels represents the number of genes involved in each pathway, while the colour scale indicates the statistical significance, with more intense red hues representing higher significance levels (adjusted p-values). This visual representation highlights the most prominent biological processes modulated by fluoxetine, with panel A underscoring the downregulation of mitochondrial and energy-related pathways, and panel B suggesting the upregulation of pathways critical for cell cycle progression, protein synthesis, and cell adhesion.

In summary, the KEGG pathway enrichment analysis confirms the dual impact of fluoxetine on HaCaT cells, with significant downregulation of mitochondrial processes and oxidative phosphorylation pathways, alongside upregulation of pathways that drive cellular proliferation, protein synthesis, and tissue regeneration.

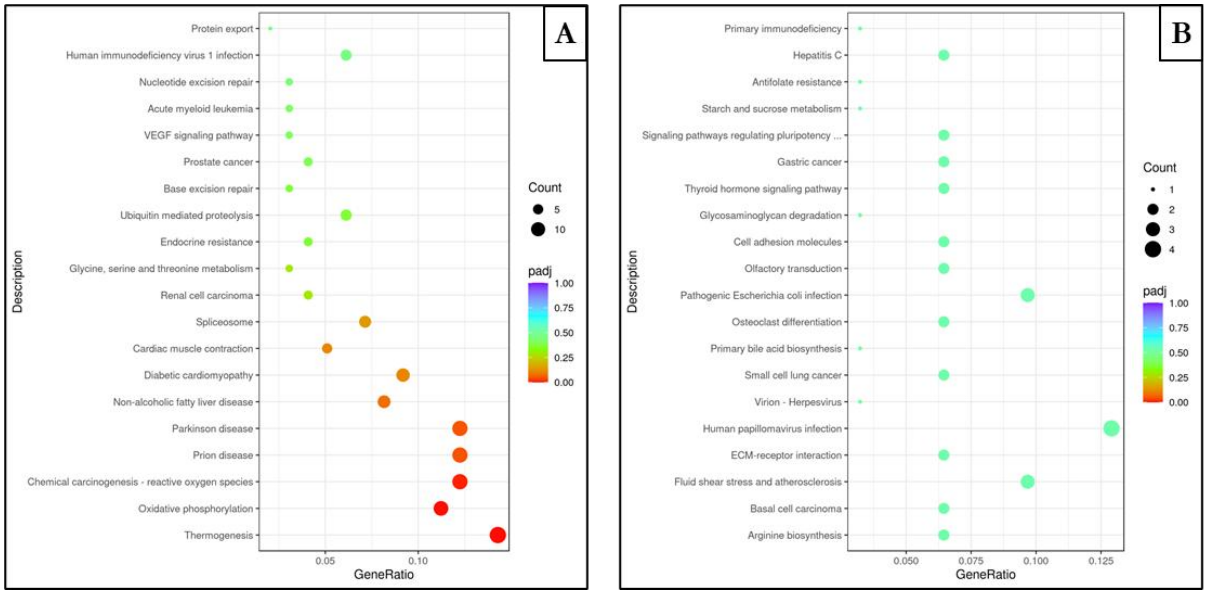

Figure 4.5: KEGG pathway enrichment analysis of downregulated and upregulated genes after 36-hour fluoxetine exposure. *The dot plot visualises the most significantly enriched KEGG pathways for both upregulated and downregulated genes. (A): KEGG pathways enriched in downregulated genes. (B): KEGG pathways enriched in upregulated genes. The dot size represents the number of genes associated with each pathway, while the colour scale indicates the statistical significance (with red representing the most significant pathways). The gene ratio reflects the proportion of DEGs involved in each pathway.*

4.3.3 Protein-protein interaction networks

To further explore the functional relationships between the differentially expressed genes identified after fluoxetine exposure, a protein-protein interaction network was generated using the STRING database. This analysis provides insights into how proteins encoded by these DEGs may interact and cooperate in biological processes. The PPI network (Figure 4.6) included 58 out of the 350 DEGs with high-confidence interactions (interaction score > 0.9), illustrating the complex interaction landscape among fluoxetine-modulated proteins. A total of 132 edges were identified, significantly more than the 71 edges expected by chance (PPI enrichment p-value = 6.69E-11), indicating strong functional associations between these DEGs.

The PPI network revealed two major clusters of interacting proteins. The first major cluster consists of proteins related to mitochondrial function and energy metabolism, including multiple subunits of the oxidative phosphorylation machinery (Figure 4.6). Notably, proteins such as NDUFB10, NDUFA2, COX5B, COX6C, and ATP5PO, all involved in oxidative phosphorylation, formed tight interactions. This is consistent with the KEGG pathway analysis results that showed downregulation of oxidative phosphorylation and mitochondrial ATP synthesis pathways. These proteins are critical components of the electron transport chain, where their downregulation suggests a significant reduction in mitochondrial energy production.

The second major cluster of the PPI network was composed of proteins involved in ribosomal function and protein synthesis (Figure 4.6). Proteins such as RPL39, RPL35, RPS9, and MRPL11 were highly interconnected, forming a dense network linked to ribosome biogenesis and translation. This cluster aligns with the upregulation of pathways associated with protein biosynthesis and cell cycle progression observed in the KEGG pathway enrichment analysis. The upregulation of ribosomal proteins reflects the increased protein synthesis requirements during cell proliferation and tissue regeneration in response to fluoxetine treatment. The enrichment of ribosomal function is, thus, likely to support the keratinocyte proliferation observed in the wound healing process.

A smaller cluster of interacting proteins included POLR2J, which is involved in RNA polymerase II-mediated transcription, along with RBX1, ANAPC10, UBE2S, H4C6, and

ANAPC11. These proteins are part of the ubiquitin-proteasome system and the anaphase-promoting complex (APC/C). The APC/C regulates cell cycle progression by tagging specific proteins with ubiquitin, marking them for degradation by the proteasome. For example, the APC/C targets cyclins, whose degradation helps reset the cell's regulatory machinery, enabling the cell to exit mitosis and enter the G1 phase. Although not directly involved in the ubiquitin-proteasome system, the APC/C plays a crucial role in protein turnover during cell division (Chowdhury and Enenkel, 2015; Fhu and Ali, 2021; Wang et al., 2017). The interactions observed in this cluster suggest that fluoxetine exposure may influence cell cycle control and protein turnover, potentially contributing to the observed increase in keratinocyte proliferation

In summary, the PPI network analysis highlights the effects of fluoxetine on mitochondrial activity, protein synthesis, and cell cycle regulation. The downregulation of mitochondrial proteins involved in oxidative phosphorylation reflects changes in energy metabolism, while the upregulation of ribosomal proteins points to an increase in protein synthesis. Additionally, proteins such as RBX1, ANAPC10, UBE2S, H4C6, and ANAPC11, interacting with POLR2J, suggest involvement in the ubiquitin-proteasome system and protein degradation pathways. These interactions indicate the role of fluoxetine in modulating processes linked to cell cycle regulation and protein turnover, supporting the observed transcriptional changes.

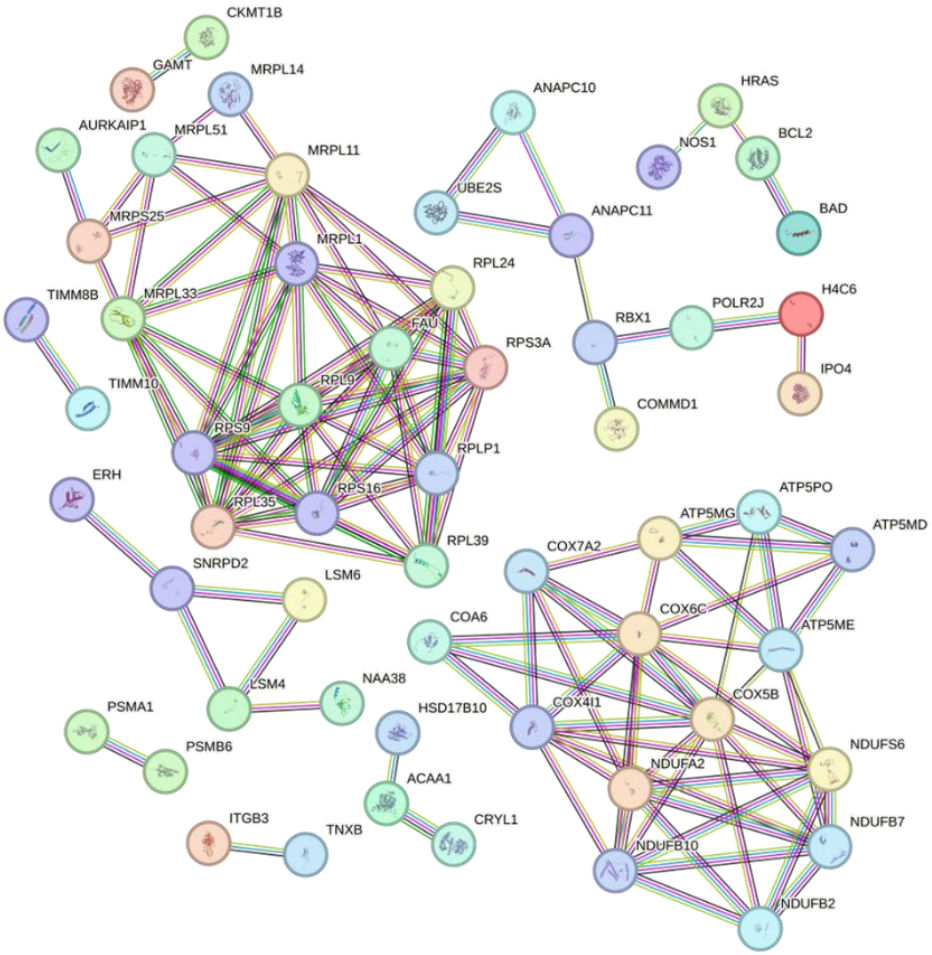

Figure 4.6: STRING analysis of all differentially expressed genes (DEGs) identified after 36-hour fluoxetine (540 ng/l) exposure in HaCaT keratinocytes. *Only the highest confidence interactions (interaction score > 0.9) are displayed, showing connections between 58 of the 350 DEGs. A total of 132 edges are present in the network, compared to the 71 expected, indicating significant protein-protein interactions (p-value = 6.69E-11).*

4.3.4 Time-dependent gene expression changes

To gain insights into the early transcriptional changes induced by fluoxetine, gene expression was analysed at a 6-hour time point in addition to the 36-hour exposure. The 6-hour time point was specifically chosen to explore whether early molecular responses precede the cell proliferation observed at 36 hours. RNAseq was performed on HaCaT cells exposed to 540 ng/l of fluoxetine, revealing distinct patterns of differentially expressed genes (DEGs) at both time points.

At 6 hours, a total of 165 DEGs were identified, with 76 genes upregulated and 89 genes downregulated. Figure 4.7 is a volcano plot that highlights the statistical significance and

magnitude of these changes, with upregulated genes shown in red and downregulated genes in green.

Figure 4.8 presents a heatmap illustrating the gene expression changes at the 6-hour time point following fluoxetine exposure. In this heatmap, red regions correspond to upregulated genes, while blue regions represent downregulated genes. The visual clustering in the heatmap highlights the distinct transcriptional profiles induced by fluoxetine, with clear differentiation between upregulated and downregulated gene sets. The heatmap provides an overview of the global transcriptional shifts, setting the foundation for further exploration of the specific biological pathways involved through Gene Ontology (GO) analysis.

Gene Ontology (GO) enrichment analysis for the downregulated genes (Figure 4.9 panel A) suggested enrichment in processes related to oxidative stress and mitochondrial function, including glutathione transferase activity, phospholipase inhibitor activity, and mitochondrial proton-transporting ATP synthase complex. This suggests that fluoxetine impacts mitochondrial activity and stress response pathways early in the exposure. Other enriched terms included transferase activity, lipase inhibitor activity, and anaphase-promoting complex, reflecting changes in cellular metabolic processes and possibly cell cycle regulation at the 6-hour mark. For the upregulated genes (Figure 4.9 panel B), the GO enrichment analysis suggested potential involvement of pathways such as potassium ion channel activity, filamentous actin, vascular endothelial growth factor receptor signalling, and guanylate cyclase activity (which are linked to early cellular signalling and cytoskeletal organisation), although these did not show strong statistical support. However, adenylate cyclase binding was significantly enriched, suggesting that cAMP-mediated signalling, which regulates key processes like cell proliferation, migration, and tissue repair, may play a central role in fluoxetine's influence on early cellular responses and cytoskeletal organisation.

Comparing the transcriptional changes at 6 hours with those observed at 36 hours, the early responses primarily target mitochondrial function and stress pathways, while later transcriptional changes suggest a shift towards processes involved in cellular proliferation and tissue regeneration, though this was not strongly supported by statistically significant upregulation. This time-dependent shift from early metabolic and stress adaptations to potential proliferation-related processes highlights the evolving impact of fluoxetine on keratinocytes, where early responses may prime the cells for later regenerative processes.

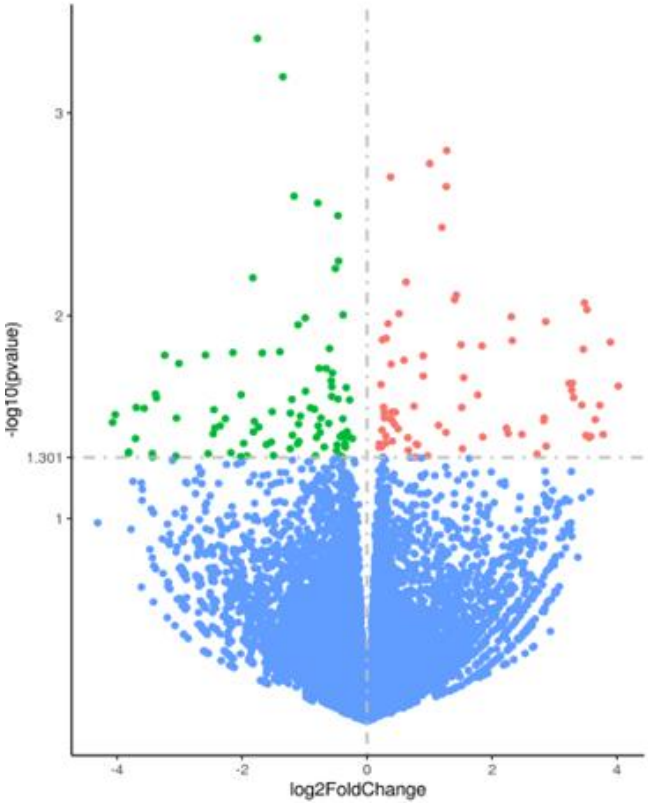

Figure 4.7: Volcano plot showing differentially expressed genes (DEGs) in HaCaT cells after 6 hours of exposure to 540 ng/l fluoxetine. *The x-axis represents the log2 fold change in gene expression, and the y-axis displays the -log10(p-value), indicating the statistical significance of the changes. Red dots represent significantly upregulated genes, while green dots indicate significantly downregulated genes. blue dots correspond to genes with non-significant expression changes.*

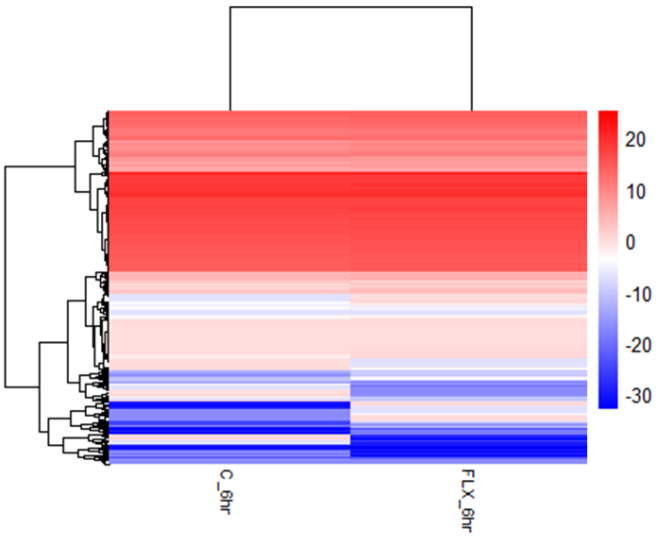

Figure 4.8: Heatmap of differentially expressed genes (DEGs) in HaCaT keratinocytes exposed to 540 ng/l fluoxetine for 6 hours. *The heatmap visualises the global transcriptional response to fluoxetine treatment, with red regions indicating significantly upregulated genes and blue regions representing significantly downregulated genes. The clustering in the heatmap highlights the distinct molecular responses in keratinocytes exposed to fluoxetine.*

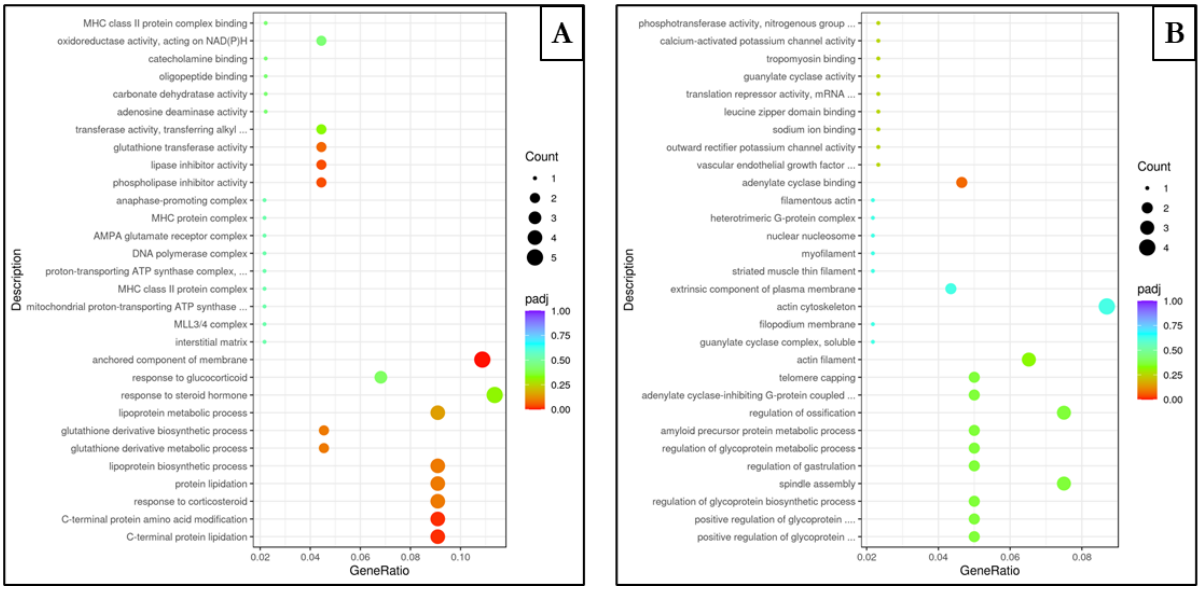

Figure 4.9: Gene Ontology (GO) enrichment analysis of differentially expressed genes (DEGs) in HaCaT cells after 6 hours of fluoxetine exposure. *The dot plot visualises the most significantly enriched GO terms for both upregulated and downregulated genes. (A) GO terms enriched in downregulated genes. (B): GO terms enriched in upregulated genes. The dot size represents the number of genes associated with each GO term, while the colour scale indicates the statistical significance (with red representing the most significant terms). The gene ratio reflects the proportion of DEGs involved in each biological process.*

4.4 Discussion

This chapter aimed to investigate the molecular mechanisms by which fluoxetine enhances wound healing in keratinocytes at environmentally relevant concentrations. Using transcriptomic analysis, I identified key differentially expressed genes and pathways that are involved in cellular proliferation, energy metabolism, and wound healing following fluoxetine exposure. The results suggests that fluoxetine may influence keratinocyte proliferation, through pathways that modulate cellular signalling and mitochondrial function, as well as protein turnover, although no direct associations with serotonin signalling were observed in the GO terms.

This discussion will explore the specific underlying molecular mechanisms involved in fluoxetine-mediated wound healing and examine the implications of these findings for potential therapeutic applications and environmental risks.

4.4.1 Fluoxetine promotes keratinocyte proliferation and wound healing through serotonin signalling

The results from this chapter suggest that fluoxetine promotes keratinocyte proliferation and wound healing through the modulation of pathways related to cell cycle regulation, energy metabolism, and protein synthesis. RNAseq analysis highlighted significant changes in the expression of genes involved in these key processes, supporting the conclusion that fluoxetine enhances cellular proliferation and wound healing by influencing multiple biological pathways critical for wound healing.

RNAseq analysis also detected the presence of several serotonin receptors in HaCaT cells, including 5-HTR2a and 5-HTR2c, which are known to regulate cell proliferation and tissue repair (Nordlind et al., 2008). While the expression of these receptors was not significantly upregulated in my datataset, their presence suggests that fluoxetine could potentially influence keratinocyte proliferation through serotonin receptor-mediated signalling. This is consistent with findings from Chapter 3, where fluoxetine enhanced scratch closure in a dose-dependent manner. Previous studies have shown that serotonin modulates key wound healing processes, including inflammation and cell migration (Kim et al., 2018; Sahu et al., 2018; Welsh et al., 2004). Although my findings do not conclusively demonstrate serotonin receptor-mediated signalling as a primary mechanism, they align with the study by Nguyen et al. (2019), which suggests that fluoxetine improves wound healing through pathways involving serotonin receptors in other models, such as diabetic mouse models.

Gene Ontology analysis further supports the observation that fluoxetine influences pathways related to cell cycle regulation, tissue morphogenesis, and cell proliferation among the upregulated genes. This suggests that fluoxetine shifts the balance in keratinocytes towards increased cellular proliferation and tissue regeneration, corroborating the phenotypic outcomes of enhanced scratch closure observed in Chapter 3. The increased expression of ribosomal proteins such as RPL39 and RPS9 also points towards enhanced protein synthesis, further supporting the proliferative effect of fluoxetine. These results are consistent with previous studies showing the ability of fluoxetine to promote proliferation in various cell types, such as brain cells and fibroblasts (Imoto et al., 2015; C. C. Wang et al., 2014).

4.4.2 Modulation of energy metabolism by fluoxetine

Fluoxetine exposure also led to significant downregulation of pathways involved in mitochondrial function and oxidative phosphorylation, as identified through both GO and KEGG pathway analyses. The observed reduction in mitochondrial activity, particularly downregulation of components of the electron transport chain (NDUFB10, NDUFA2, COX5B, and COX6C), suggests that fluoxetine induces a metabolic shift in keratinocytes. This shift could be analogous to the Warburg effect, where cells reduce oxidative phosphorylation in favour of glycolysis to support rapid proliferation (Arciuch et al., 2012; Chandel, 2021). Although my study did not directly measure glycolytic activity (which could be assessed through the Seahorse glycolytic assay, which measures the extracellular acidification rate (ECAR) as an indicator of glycolysis as part of future work), the transcriptomic data suggest that fluoxetine may promote a similar metabolic reprogramming in keratinocytes, which could be necessary for increased cell proliferation. This is consistent with research demonstrating that fluoxetine promotes glycolysis in various cellular contexts, including in neuronal cells (Pan et al., 2022). This metabolic modulation is critical in the context of wound healing, where rapid tissue regeneration requires not only increased cellular proliferation but also substantial alterations in energy metabolism to support the biosynthetic demands of new tissue formation. The downregulation of mitochondrial pathways suggests that fluoxetine might reduce energy production through oxidative phosphorylation while enhancing processes that support biosynthesis and growth. This is supported by the upregulation of cell cycle-related pathways and proteins involved in ribosomal biogenesis, pointing to a cellular environment primed for rapid proliferation. Similar effects of fluoxetine on enhancing growth and cellular proliferation through metabolic reprogramming have been observed in other studies, such as those involving brain and cancer cells (Ballou et al., 2018; Imoto et al., 2015).

4.4.3 Protein interactions and the role of the ubiquitin-proteasome system

The protein-protein interaction network analysis highlighted two major clusters of interacting proteins. One cluster was composed of ribosomal proteins, which are essential for protein synthesis, further corroborating the enhanced cellular proliferation observed in fluoxetine-treated keratinocytes. The second cluster involved proteins linked to the ubiquitin-proteasome system (UPS), such as RBX1, ANAPC10, and UBE2S, which are crucial in regulating the cell cycle through targeted protein degradation. The UPS functions by tagging damaged or not needed proteins with ubiquitin, marking them for degradation by the proteasome. This

regulated degradation is vital for maintaining protein homeostasis, especially during cell division, as it removes cyclins and other key regulatory proteins to ensure timely cell cycle progression (Chowdhury and Enenkel, 2015; Fhu and Ali, 2021). Specifically, the anaphase-promoting complex/cyclosome (APC/C) targets proteins like cyclin B for degradation, allowing the cell to transition from mitosis to the G1 phase, a process essential for proper cell cycle progression and the proliferative effect observed in fluoxetine-treated keratinocytes (Fhu and Ali, 2021). The role of the UPS in cell proliferation is well-supported, as evidenced by UBE2C's involvement in regulating cell cycle progression through its interaction with APC/C and its role in tumorigenesis across various cancers, including gastric adenocarcinoma (Wang et al., 2017).

In addition to these protein degradation mechanisms (Chowdhury and Enenkel, 2015; Fhu and Ali, 2021), the influence of fluoxetine extends to transcriptional activity. The upregulation of POLR2J, a component of RNA polymerase II, alongside UPS-related proteins, suggests that fluoxetine affects both transcriptional activity and protein degradation pathways. These processes are tightly regulated during cell cycle progression, especially in the context of wound healing, where rapid cellular turnover and regeneration are required. These findings provide mechanistic insight into how fluoxetine influences keratinocyte proliferation at the molecular level and extend previous research on the effects of fluoxetine on different cell types ((Ballou et al., 2018; Brandes et al., 1992; Sousa-Ferreira et al., 2014).

4.4.4 Time-dependent effects of fluoxetine

My time-dependent analysis of fluoxetine exposure provided valuable insights into the early and late transcriptional responses in keratinocytes. This aligns with findings from a previous study (Correia et al., 2023), which reported the impact of fluoxetine on oxidative stress pathways in other biological systems, showing similar gene expression changes related to oxidative stress and mitochondrial function. At 6 hours, the downregulation of mitochondrial function and oxidative stress-related genes was already apparent, suggesting that fluoxetine induces an early metabolic shift in keratinocytes. This was accompanied by the upregulation of genes involved in cytoskeletal organisation, potassium ion channel activity, and signalling pathways related to vascular endothelial growth factor, pointing to an early response that likely primes cells for proliferation and migration.

By 36 hours, the effects of fluoxetine on keratinocyte proliferation were much more pronounced, as indicated by the significant upregulation of genes involved in cell cycle regulation and tissue morphogenesis. The increased expression of ribosomal and cell cycle-related genes at this later time point suggests that fluoxetine drives sustained cellular proliferation and tissue regeneration. These findings are consistent with other studies that have demonstrated the proliferative effects of fluoxetine in brain cells (Imoto et al., 2015) and breast cancer cells (Ballou et al., 2018), highlighting the broad influence of fluoxetine on cell proliferation.

This time-dependent analysis underscores the dynamic nature of the effects of fluoxetine on keratinocytes, where early metabolic and signalling changes pave the way for later proliferative responses. The early transcriptional changes at 6 hours likely prime keratinocytes for the enhanced cellular proliferation observed at the later time point, supporting the conclusion that fluoxetine has both immediate and sustained effects on wound healing processes.

4.4.5 Implications for fluoxetine as a wound healing therapy

The findings from this chapter have significant implications for understanding how low-dose fluoxetine exposure affects skin physiology, particularly in the context of environmental contamination. This is especially relevant given that fluoxetine, like other SSRIs, is frequently detected in surface waters and wastewater effluents, where human exposure may occur through recreational contact or water reuse. The ability of fluoxetine to enhance keratinocyte proliferation at low, sub-therapeutic concentrations, including levels that bracket those reported in environmental settings, suggests that such compounds may have unanticipated effects on skin homeostasis and tissue repair.

Previous studies have shown that fluoxetine enhances wound healing in various models, including diabetic mice and human keratinocytes (Nguyen et al., 2019; Yoon et al., 2021), but my study provides new insights into the molecular mechanisms underpinning these effects, likely through the modulation of several pathways involved in cellular proliferation and tissue regeneration, rather than being exclusively mediated through serotonin signalling and energy metabolism modulation.

These findings suggest that fluoxetine enhances wound healing, likely through its modulation of several pathways involved in cellular proliferation and tissue regeneration, rather than being

exclusively mediated through serotonin signalling. Crucially, this observation originates from a toxicological perspective, by examining environmentally relevant concentrations of fluoxetine, this work helps uncover how SSRIs, even at low doses, can modulate non-neuronal systems such as the skin. These data not only raise awareness of the potential risks of long-term, low-level pharmaceutical exposure but also uncover molecular pathways that could, in a different context, be harnessed therapeutically. Thus, while this is not a therapeutic proposal, it demonstrates how environmental pharmacology can reveal new biological interactions with translational relevance. Although the concentration used in this chapter (540 ng/l) is higher than typical surface water levels, it aligns with concentrations reported in contaminated wastewater effluents and pharmaceutical discharge zones (Salgado et al., 2011; Shraim et al., 2017). This dose allows for the assessment of potential cellular and molecular effects under conditions that may reflect high-exposure scenarios or environmental hotspots, as well as potential future conditions, including increased pharmaceutical load due to water reuse, climate-related scarcity, or poor infrastructure. Moreover, these findings highlight the relevance of chronic low-level exposure for specific subpopulations, including wild swimmers, children, athletes in open water, or workers frequently in contact with effluent-impacted environments. In such groups, repeated dermal or incidental ingestion exposure may be more significant than in the general population.

However, the potential risks of chronic exposure to fluoxetine, particularly in the context of environmental contamination, should not be overlooked. The observed downregulation of mitochondrial pathways and possible induction of a Warburg-like metabolic state raise concerns about the long-term consequences of fluoxetine exposure, particularly in terms of uncontrolled cell proliferation, which is a hallmark of cancer (Hanahan and Weinberg, 2011). Further research, such as long-term *in vitro* and *in vivo* studies, would be necessary to determine whether chronic exposure to fluoxetine induces oncogenic transformation. *In vitro* studies using immortalised keratinocyte cell lines could assess changes in cell morphology, proliferation rates, and the expression of key oncogenic markers following prolonged fluoxetine exposure. *In vivo* studies using animal models, such as genetically modified mice prone to tumorigenesis, could help elucidate the potential tumorigenic effects of fluoxetine at environmentally relevant concentrations (Sahu et al., 2021). Additionally, proteomic and metabolomic profiling could provide further insight into the metabolic shifts and signalling pathways involved in fluoxetine-induced proliferation (Fang et al., 2022; Önal et al., 2023; Shao et al., 2022; Zhao et al., 2018).

4.5 Conclusion

This chapter explored the molecular mechanisms by which fluoxetine promotes wound healing in keratinocytes at environmentally relevant concentrations. Using RNAseq and pathway analysis, I identified that fluoxetine enhances keratinocyte proliferation primarily through serotonin signalling, with key upregulation of genes involved in cell cycle regulation and protein synthesis. The modulation of energy metabolism, particularly the downregulation of mitochondrial function and oxidative phosphorylation, suggests that fluoxetine induces a Warburg-like metabolic shift, facilitating rapid cell proliferation.

Protein-protein interaction analysis further highlighted the role of the ubiquitin-proteasome system and ribosomal biogenesis in fluoxetine-driven cell cycle regulation and protein turnover. Time-dependent transcriptional changes showed that fluoxetine triggers early metabolic shifts and cytoskeletal rearrangement, followed by sustained cellular proliferation and tissue regeneration at later time points.

The results from this chapter provide strong evidence that fluoxetine, even at low concentrations, enhances wound healing by modulating key molecular pathways. However, the potential risks associated with chronic environmental exposure to fluoxetine, including the possibility of uncontrolled cell proliferation, warrant further investigation.

Chapter 5: Phosphoproteomics insights into the effect of fluoxetine on kinase activity in wound healing.

5.1 Introduction

The findings from the previous chapters underscore the significant impact of fluoxetine on wound healing in keratinocytes, particularly its ability to modulate gene expression related to cellular proliferation and mitochondrial function. However, while transcriptomic data provided valuable insights into the early transcriptional changes, further investigation into the post-translational modifications is necessary to fully understand the molecular pathways activated during fluoxetine-induced wound healing.

Proteome profiler arrays were chosen as the first approach to explore the specific proteins and pathways affected by fluoxetine at a broader level, with a focus on key proteins involved in wound healing, proliferation, and cell migration. This method provides a semi-quantitative analysis of multiple proteins simultaneously, offering a snapshot of the key signalling molecules modulated by fluoxetine exposure. Studies have demonstrated that kinase phosphorylation assays, like the proteome arrays used here, are particularly effective in uncovering the broader impact of drug treatments on signalling pathways, including those involved in cellular stress responses and metabolism (Zheng et al., 2009).

Following the results from the proteome profiling, phosphoproteomics was employed to investigate the phosphorylation status of key kinases and signalling proteins, as phosphorylation plays a critical role in the activation and regulation of various cellular pathways. This method allows for the identification of phosphorylation sites on proteins that are crucial for cell proliferation, survival, and migration. By examining these post-translational modifications, the aim is to gain a deeper understanding of how fluoxetine modulates key signalling pathways. Investigating phosphorylation dynamics is essential for comprehending the broader effects of fluoxetine on keratinocyte proliferation and wound healing.

A specific focus was placed on the ERK and MAPK pathways, given their established roles in 5HT signalling, cellular proliferation, differentiation, and wound healing (Shi and Sun, 2020; Shishido and Nguyen, 2016). These pathways are critical targets for investigating how

fluoxetine affects skin cell regeneration due to their involvement in promoting cell survival and growth. Studies have shown that serotonin can promote keratinocyte proliferation and migration via the 5-HT2B receptor and ERK pathways, suggesting a potential mechanism by which fluoxetine, as a serotonin reuptake inhibitor, could modulate these processes in skin cells (Kim et al., 2018). Additionally, studies have shown the involvement of MAPK signalling in mediating the role of serotonin in various cell types, including cardiomyocytes, suggesting its relevance to skin cells (Nebigil et al., 2003). The phosphorylation status of ERK1/2 and other MAPK-related proteins will help elucidate whether fluoxetine promotes keratinocyte proliferation through these pathways.

In summary, this chapter integrates proteome profiling and phosphoproteomics to comprehensively explore the signalling pathways activated by fluoxetine, with particular emphasis on the ERK and MAPK pathways. These analyses aim to reveal the post-translational mechanisms driving the proliferative effects observed in previous chapters, offering deeper insights into how fluoxetine influences keratinocyte proliferation and wound healing.

5.2 Aims & Objectives

The aim of this chapter is to investigate how fluoxetine modulates post-translational modifications, with a particular focus on phosphorylation events, to understand their influence on keratinocyte proliferation, migration, and wound healing.

The objectives of this chapter are as follows:

1) **To explore the modulation of the ERK and MAPK pathways, as well as other key signalling proteins involved in wound healing,** by using proteome and kinase arrays.

2) **To validate the effects of fluoxetine on specific proteins, particularly within the ERK and MAPK pathways,** by using western blot analysis.

3) **To assess phosphorylation changes and the modulation of signalling pathways,** by fluoxetine through comprehensive phosphoproteomics analysis.

5.3 Results

5.3.1 Protein microarrays result after 36-hour exposure to fluoxetine

To investigate the phosphorylation status of key kinases involved in wound healing, cell proliferation, and migration, I employed a protein kinase array. This array allowed us to simultaneously monitor the relative phosphorylation levels of 37 kinase sites and two related total proteins. Phosphorylation plays a crucial regulatory role in many signalling pathways, and this approach provided a comprehensive snapshot of the molecular effects induced by fluoxetine at the protein level.

I chose a single fluoxetine concentration of 540 ng/l, reflecting environmentally relevant exposure levels, to explore its effects on keratinocytes after 36 hours of treatment. The array included key kinases known to play critical roles in cellular stress responses, proliferation, and survival pathways, such as ERK1/2, PDGF Rβ, STAT1.

Figure 5.1 shows representative membranes from the protein kinase array. The dots in the corners of each membrane are reference spots, which allow us to normalise the pixel density of the capture antibody spots across all membranes. These reference spots serve a similar role to loading control antibodies used in western blotting. While the raw phosphorylation data are shown here, the red and green boxes indicate key findings from the quantitative analysis that follows. Specifically, the red boxes highlight reduced phosphorylation levels for GSK3β (Ser9) in box 1, MSK1/2 (Ser376/Ser360) in box 2, and SRC Tyr419 in box 3, while the green box indicates increased phosphorylation of p70 S6K (Thr421/Ser424) in box 4. These differences were confirmed through the subsequent analysis of the pixel density values, which were transferred to an Excel sheet. The values for each kinase (each duplicated on the membrane) were averaged, and following normalisation to the reference spots, these values were saved as the final dataset for further interpretation.

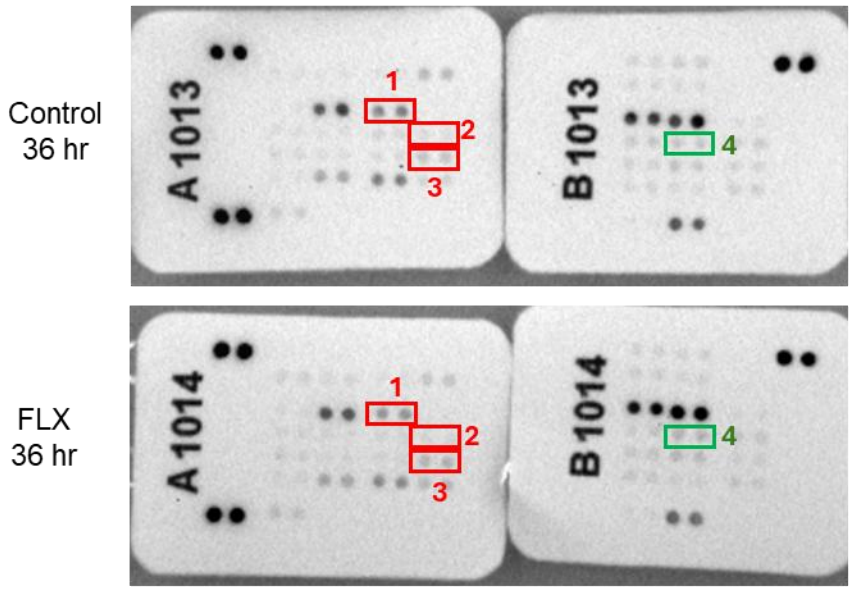

Figure 5.1: Example of protein microarrays membranes showing relative phosphorylation levels after 36 hours of exposure to 540 ng/l fluoxetine in HaCaT cells. *Reference spots in the corners were used for normalisation. Red boxes indicate reduced phosphorylation of GSK3B (Ser9) (box 1), MSK1/2 (Ser376/Ser360) (box 2), and SRC Tyr419 (box 3), while the green box shows increased phosphorylation of p70 S6K (Thr421/Ser424) (box 4). These changes were identified through quantitative analysis of the normalised pixel densities.*

Using the software RStudio, I initially aimed to perform a MANOVA (Multivariate Analysis of Variance) to compare the phosphorylation profiles of keratinocytes exposed to fluoxetine versus control cells. However, the Shapiro-Wilk test for normality returned a p-value of 2.2e-16, indicating that the data did not meet the assumption of normality ($p < 0.05$). As a result, I employed the non-parametric equivalent of MANOVA, the PERMANOVA, using the Adonis function from the vegan package in R.

The PERMANOVA test was conducted to compare the phosphorylation profiles of the control group, and the group exposed to an environmentally relevant concentration of fluoxetine (540 ng/l). The results, as summarised in Table 5.1, indicated that there was no statistically significant difference between the two groups (p-value=0.125). This suggests that the overall composition of the phosphorylation profiles in both groups was not different, although there may be a trend (p value close to 0.1).

To further investigate the position of the samples and the centroids of each treatment, I utilised a two-dimensional principal component analysis (2D PCA), as shown in Figure 5.2. This PCA plot illustrates the control and 540 ng/l of fluoxetine samples based on their phosphorylation

profiles. The percentages on the axes indicate the variance explained by each principal component, with PC1 accounting for 41.9% and PC2 for 32.8% of the total variation.
The confidence intervals around the treatment centroids (black bars) extend widely across the graph, indicating that there are no statistically significant differences between the two treatments. The control samples (yellow squares) cluster closely together, while the exposed samples (teal circles) show more variability, with one sample spread further along the PC2 axis. These findings are consistent with the non-significant result from the PERMANOVA analysis (p-value=0.125), suggesting that the phosphorylation profiles of the proteins did not differ significantly between the control and fluoxetine-exposed groups, while allowing to speculate that there may be a trend towards differences between the treatments in terms of specific phosphorylation events in specific proteins.

When visualised in three dimensions, as shown in Figure 5.3, the 3D PCA plot reveals that the low fluoxetine samples are clustered more closely together, while the control (C) samples display greater variability across the PC2 and PC3 axes. The positioning of the control and fluoxetine-exposed groups in different planes along the PC3 axis may suggest a trend towards separation between the treatments, although the differences are not statistically significant, as indicated by the PERMANOVA analysis (p-value=0.125). This visual trend aligns with the non-significant p-value, indicating that while there may be some potential differentiation, it is not conclusive at this stage across all the phosphosites.

PERMANOVA of proteins

	Df	SumsOfSqs	MeanSqs	F.Model	R2	Pr..F.
Treatment	1	0.1044	0.1044	1.8735	0.238	0.125
Residuals	6	0.3342	0.0557	NA	0.762	NA
Total	7	0.4386	NA	NA	1.000	NA

Table 5.1: Results of the PERMANOVA analysis comparing the phosphorylation profiles of control cells and cells exposed to fluoxetine (540 ng/l). *The test was performed using the Adonis function from the vegan package in R, and no statistically significant difference was observed between the groups (p-value=0.125, F=1.8735). The R^2 value indicates that 23.8% of the variation in kinase activity can be attributed to the treatment.*

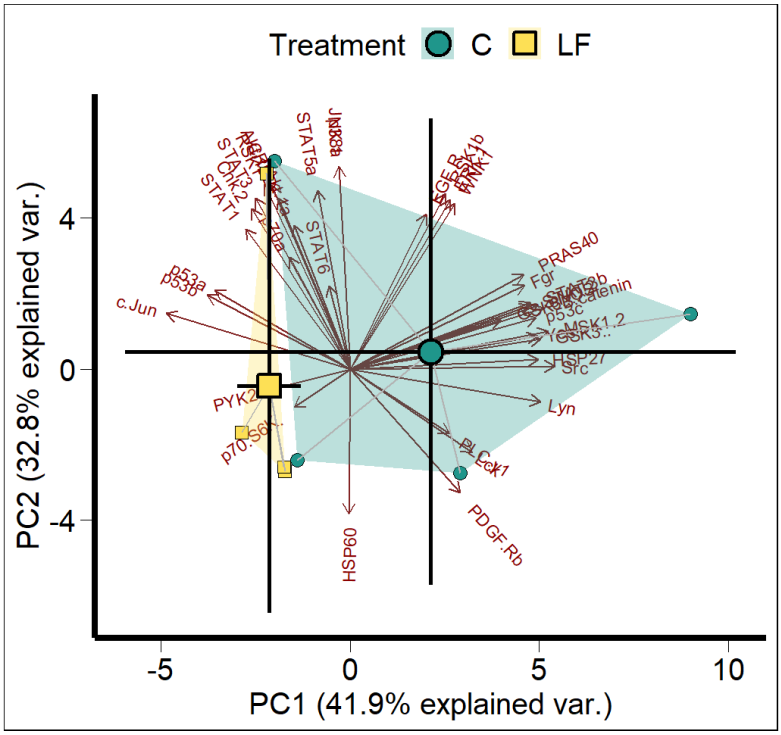

Figure 5.2: Two-dimensional principal component analysis (2D PCA) plot for 36-hour exposure. *Illustrating the phosphorylation profiles of keratinocytes exposed to fluoxetine (540 ng/l) and control cells (C) after 36 hours of exposure. The percentages on the axes represent the variance explained by each principal component. Control samples are represented by yellow squares, fluoxetine-exposed samples are represented in teal circles. Confidence intervals are displayed using black bars.*

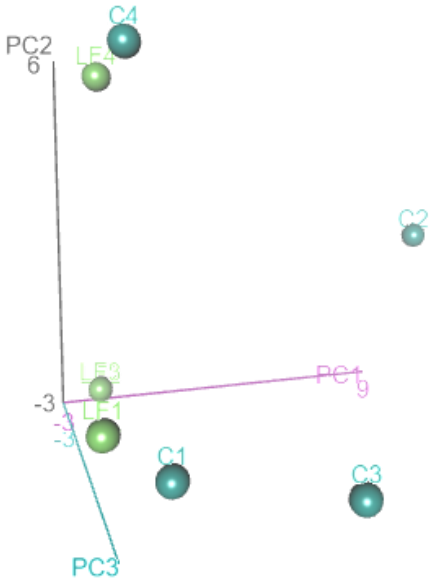

Figure 5.3: Three-dimensional principal component analysis (3D PCA) plot for 36-hour exposure. *Showing the phosphorylation profiles of control (C, teal) and fluoxetine-exposed (LF, green) keratinocytes after 36 hours of exposure. The axes represent the first three principal components, with PC2 and PC3 highlighting potential trends in separation between the two treatment groups.*

I had therefore collected weak evidence that there may be trends towards differences between treatments, but this still warranted further investigation for each protein. To explore any potential differences, I performed post-hoc tests for all kinases to compare their phosphorylation levels between the control and fluoxetine-exposed groups. From this analysis, I decided to focus on kinases with a p-value of less than 0.1, including both those that were significantly affected (p-value<0.05) and those that showed a trend toward significance (p-value< 0.1), as they were most likely to be biologically relevant.

Boxplots were generated to visualise the distribution of phosphorylation levels for these selected proteins, including GSK3β (Ser9), MSK1/2 (Ser376/Ser360), SRC Tyr419, and p70-S6K (Thr421/Ser424). The boxplots in Figure 5.4 demonstrate the variance across replicates for each treatment condition. Statistical analysis revealed significant reductions in the phosphorylation of GSK3β (p-value=0.0286) and p70-S6K (p-value=0.0213) in the fluoxetine-exposed group. Although SRC showed an increase in phosphorylation, and MSK1/2 showed a reduction, these changes were borderline statistically significant (p = 0.0525 for both). Given these findings, I selected both the significantly affected proteins and those with a p-value of less than 0.1 for further validation via western blotting (see section 5.3.2).

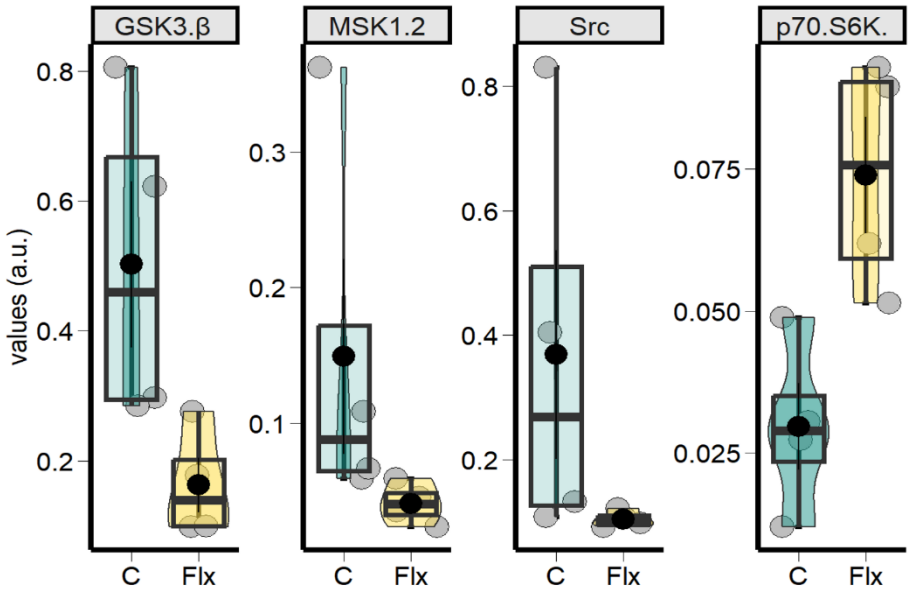

Figure 5.4: Boxplots illustrating the phosphorylation levels of selected kinases in control (C) and fluoxetine-exposed (Flx, 540 ng/l) keratinocytes after 36 hours of exposure. *The selected kinases include GSK3β (Ser9), MSK1/2 (Ser376/Ser360), SRC Tyr419, and p70-S6K (Thr421/Ser424), which were chosen for further analysis based on their post-hoc test results (p-value<0.1). The black horizontal lines within each box represent the median values, while the vertical lines (whiskers) denote the range of data within 1.5 times the interquartile range (IQR). Black circles represent the mean values for each group, and the grey dots represent individual replicates.*

5.3.2 Protein microarrays result after 6-hour exposure to fluoxetine

To investigate the immediate effects of fluoxetine exposure on kinase activity, I conducted a protein microarray analysis after 6 hours of treatment with 540 ng/l fluoxetine. This early time point was chosen to capture rapid phosphorylation events that might be transient and potentially crucial for initiating key cellular processes, such as proliferation and stress responses.

Following the same approach as in the 36-hour analysis, the phosphorylation levels of 37 kinase sites were measured and normalised to reference spots. By analysing this shorter time point, I aimed to identify which signalling pathways were activated or modulated shortly after fluoxetine exposure. This could provide a deeper understanding of the immediate molecular changes that precede the longer-term effects observed at the 36-hour time point.

To statistically assess the overall differences between the control and fluoxetine-exposed groups, I performed a PERMANOVA test on the phosphorylation data. The results, shown in Table 5.2, indicate that the differences between the control and fluoxetine-exposed groups were non-significant (p-value=0.1). Although the R^2 value was relatively high (0.6233), suggesting a substantial proportion of variance might be associated with fluoxetine treatment, this cannot be confidently interpreted without statistical significance. Nonetheless, the data suggest a potential trend towards early changes in phosphorylation patterns that warrants further investigation with increased replicates or alternative time points

To further visualise the differences in phosphorylation profiles between the control and fluoxetine-exposed groups at the 6-hour time point, I performed a two-dimensional principal component analysis (2D PCA). This method allows us to assess the distribution of samples based on their overall phosphorylation patterns. The results, shown in Figure 5.5, revealed clustering of the LF samples along the PC1 axis, which explained 66.9% of the total variance. In contrast, the control samples showed more variability along the PC2 axis, which accounts for 16.6% of the variance. While the centroids for the two treatment groups appeared separated, there was some overlap in the variability, as indicated by the confidence intervals around the centroids (black bars).

Key kinases such as GSK3β, WNK1, and STAT5a showed notable contributions to the separation between the control and exposed groups, as depicted by the vector loadings. These

results aligned with the PERMANOVA analysis, suggesting that, although there were observable trends in phosphorylation changes, the overall difference between the groups remained marginally non-significant (p-value=0.1).

To further explore the potential differences in phosphorylation profiles between control and fluoxetine-exposed groups, I performed a three-dimensional principal component analysis (3D PCA). This analysis provides a more comprehensive view of the variance across the samples by incorporating an additional principal component (PC3), allowing for a more detailed examination of the underlying trends. As shown in Figure 5.6, the 3D PCA plot revealed the spatial distribution of the samples along the three principal components. Similar to the 2D analysis, PC1 explained the majority of the variance, with PC2 and PC3 capturing additional variability. LF samples cluster more closely together, while the control samples are spread along both PC2 and PC3 axes. This pattern suggests potential differentiation between the two groups, though further analysis was needed to confirm the significance of these trends.

PERMANOVA of proteins

	Df	SumsOfSqs	MeanSqs	F.Model	R2	Pr..F.
Treatment	1	0.1485	0.1485	6.6175	0.6233	0.1
Residuals	4	0.0897	0.0224	NA	0.3767	NA
Total	5	0.2382	NA	NA	1.0000	NA

Table 5.2: Results of the PERMANOVA analysis comparing the phosphorylation profiles of control cells and cells exposed to fluoxetine (540 ng/l) after 6 hours. *The test was performed using the Adonis function from the vegan package in R. While the differences between the groups were marginally non-significant (p-value=0.1, F = 6.6175), the R^2 value indicates that 62.3% of the variation in kinase activity can be attributed to the treatment.*

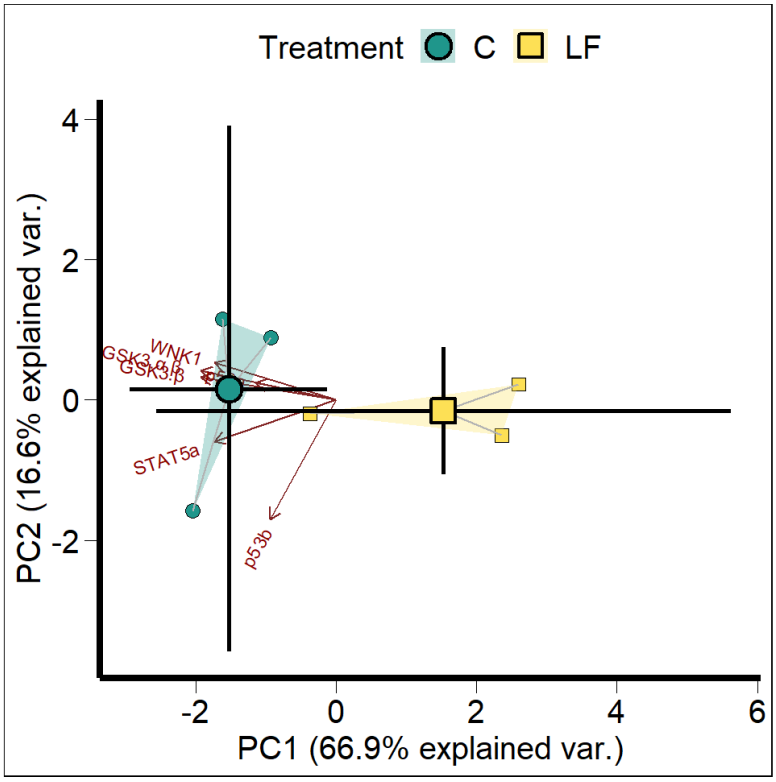

Figure 5.5: Two-dimensional principal component analysis (2D PCA) plot for 6 hours exposure. *Illustrating the phosphorylation profiles of keratinocytes exposed to fluoxetine (540 ng/l) and control cells (C) after 6 hours of exposure. The percentages on the axes represent the variance explained by each principal component. Control samples are represented by yellow squares, fluoxetine-exposed samples are represented in teal circles. Confidence intervals are displayed using black bars.*

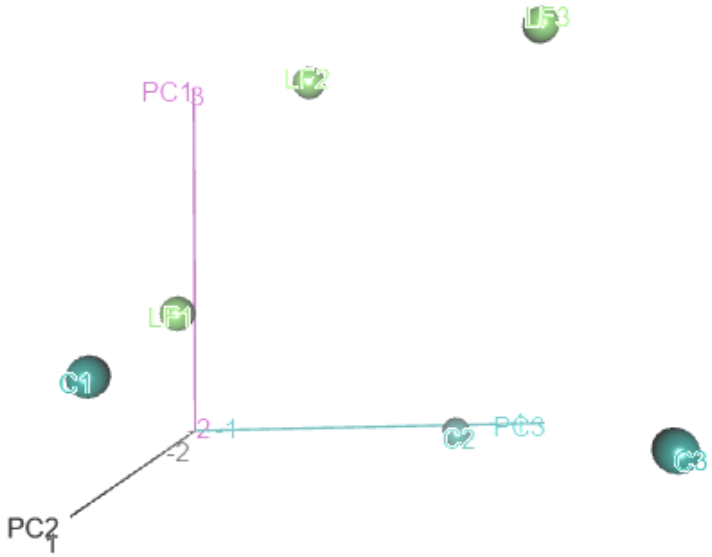

Figure 5.6: Three-dimensional principal component analysis (3D PCA) plot for 6-hour exposure. *Showing the phosphorylation profiles of control (C, teal) and fluoxetine-exposed (LF, green) keratinocytes after 6 hours of exposure. The axes represent the first three principal components, with PC2 and PC3 highlighting potential trends in separation between the two treatment groups.*

To assess these potential differences between treatments, I performed post-hoc tests on all kinases to compare phosphorylation levels between the control and fluoxetine-exposed groups, selecting those with p-values of 0.1 or lower for further analysis. Boxplots were generated for the kinases GSK3α/β (Ser21/Ser9), GSK3β (Ser9), and WNK1. As shown in Figure 5.7, there was a trend toward reduced phosphorylation in fluoxetine-exposed cells for all three kinases compared to the control. Although these changes did not reach conventional levels of statistical significance, the p-value of 0.1 indicates that these trends are worth further investigation.

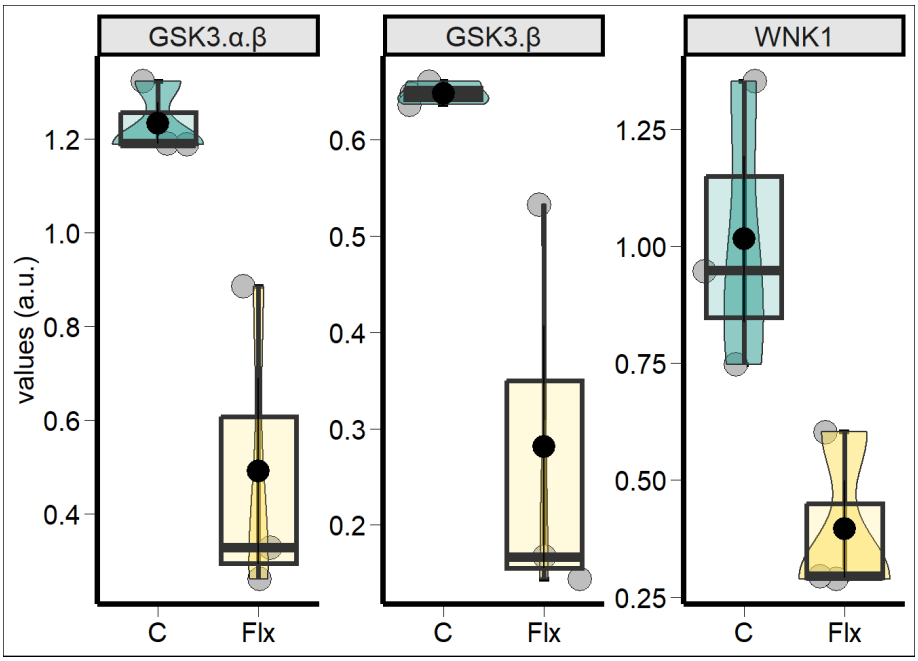

Figure 5.7: Boxplots illustrating the phosphorylation levels of selected kinases in control (C) and fluoxetine-exposed (Flx, 540 ng/l) keratinocytes after 6 hours of exposure. *The selected kinases include GSK3α/β (Ser21/Ser9), GSK3β (Ser9) and WNK1, which were chosen for further analysis based on their post-hoc test results (p-value=0.1). The black horizontal lines within each box represent the median values, while the vertical lines (whiskers) denote the range of data within 1.5 times the interquartile range (IQR). Black circles represent the mean values for each group, and the grey dots represent individual replicates.*

5.3.3 Western blot validation of key signalling proteins

To further validate the phosphorylation changes observed in the protein microarrays, I conducted western blot analyses. This method was employed to examine both total protein levels and the specific phosphosites identified in the microarray analysis. Western blotting provides a more direct, quantitative method for confirming the trends observed in phosphorylation, offering a clearer view of how fluoxetine modulates kinase activity at specific sites.

For the western blots, I focused on the key kinases GSK3β (Ser9), MSK1/2 (Ser376/Ser360), SRC (Tyr419), and p70 S6K (Thr421/Ser424), all of which showed phosphorylation changes in the earlier analyses. The antibodies used for these analyses, along with their respective molecular weights, are presented in Table 2.1. I used both phospho-specific antibodies and total protein antibodies to determine whether changes in phosphorylation were independent of changes in overall protein levels.

This approach allows us to differentiate between changes in protein expression and modifications at specific phosphorylation sites, helping to clarify the impact of fluoxetine on kinase signalling. Due to technical limitations, such as non-specific antibody binding and failure to detect the target protein, I was unable to obtain reliable results for SRC and p70 S6K, and as such, no graphs are presented for these proteins. The results for MSK1/2 and GSK3 are shown below.

The western blot results for the 36-hour exposure are presented in Figure 5.8, with the corresponding raw western blot data presented in Figure 5.9, detailing both total protein levels and phosphorylation states for MSK1 and GSK3.

For MSK1, total protein levels in fluoxetine-exposed cells showed a significant reduction compared to the control group, the raw western blot data, shown in Figure 5.9, illustrate the reduced band intensity in the fluoxetine-exposed group compared to the control, corroborating the quantitative data. The boxplot displays a clear separation between the two conditions, with the fluoxetine-exposed group exhibiting notably lower median protein levels. The ANOVA analysis confirmed that this reduction was statistically significant (p-value=0.00757). Similarly, phosphorylation levels of MSK1/2 at Ser376/Ser360 were reduced in the fluoxetine-exposed cells relative to the control. The boxplot for phosphorylated MSK1/2 shows a distinct decrease in phosphorylation levels for the fluoxetine-exposed group, with lower median values and a narrower distribution. This decrease was also found to be statistically significant based on the ANOVA test (p-value=0.00346).

In the case of GSK3α/β, total protein levels were significantly lower in the fluoxetine-exposed group compared to the control. The raw western blot data in Figure 5.9 show visibly reduced band intensity in the fluoxetine-treated samples, supporting the quantitative results. The boxplot reflects this difference, with the fluoxetine group showing a much lower median for total protein levels of GSK3α/β. The statistical analysis confirmed this reduction as significant (p-value=0.00226). Phosphorylation of GSK3β at Ser9, an inhibitory site, was also

significantly reduced in fluoxetine-exposed cells. The boxplot highlights a substantial decrease in phosphorylation levels, with the fluoxetine group displaying a considerably lower median value compared to the control group. The ANOVA analysis demonstrated that this reduction in GSK3β (Ser9) phosphorylation was statistically significant (p-value=0.0738).

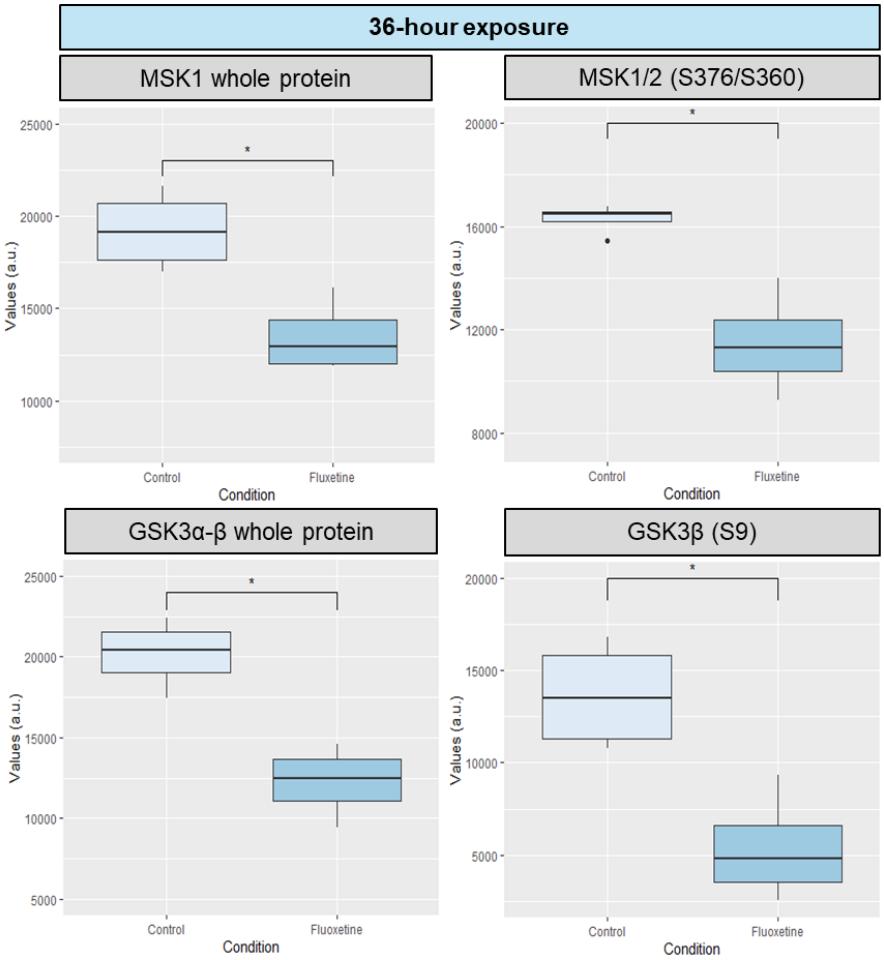

Figure 5.8: Western blot quantification of total protein levels and phosphorylation of MSK1 and GSK3 in keratinocytes after 36-hour exposure to fluoxetine (540 ng/l). *Boxplots represent normalised values (a.u.) for both total protein and specific phosphorylation sites: MSK1 whole protein, MSK1/2 (Ser376/Ser360), GSK3α/β whole protein, and GSK3β (Ser9). The black lines within each box represent the median values, and the whiskers indicate the full range of the data. Statistical significance between control and fluoxetine-exposed groups is indicated by an asterisk (*). Statistical analysis was performed using one-way ANOVA followed by Tukey's post hoc test (n>4 biological replicates per condition).*

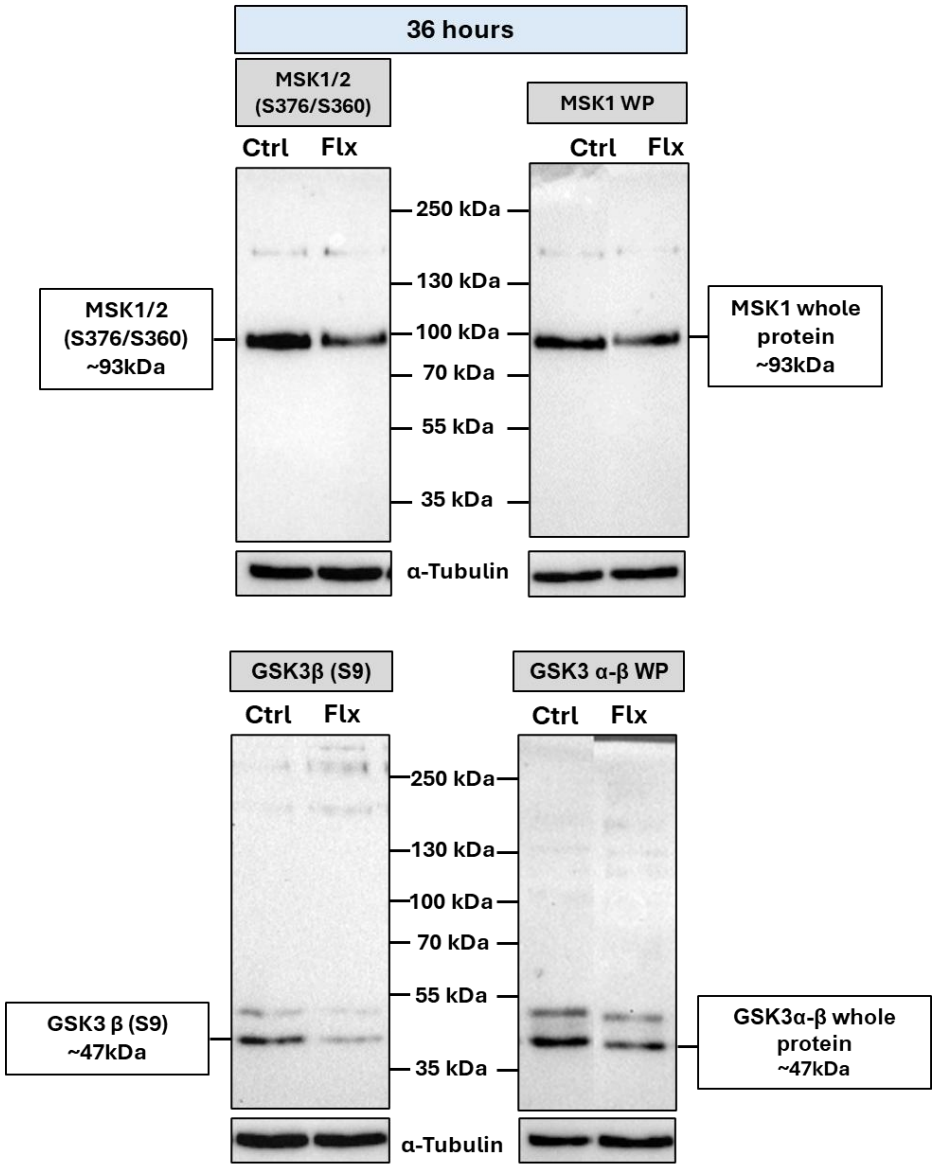

Figure 5.9: Representative western blot images after 36-hour exposure to fluoxetine (540 ng/l) in keratinocytes. *For MSK1 total protein (WP), MSK1/2 phosphorylation (S376/S360), GSK3α/β total protein (WP) and GSK3β phosphorylation (Ser9) The images depict the protein bands for control and fluoxetine-exposed samples. The bottom bands represent the loading control (α-tubulin).*

Western blot results for the 6-hour exposure are shown in Figure 5.11 and the corresponding raw western blot data is presented in Figure 5.10, focusing on GSK3 protein levels. Due to technical issues, reliable results were only obtained for GSK3α/β total protein and GSK3β (Ser9) phosphorylation, while results for other kinases were inconclusive and are not presented here.

The raw western blots in Figure 5.10 clearly show a reduction in signal intensity for both total GSK3α/β and phosphorylated GSK3β (Ser9) in fluoxetine-exposed cells compared to the control group. This visual decrease in band intensity is reflected in the box plot data. For

GSK3α/β total protein, there is a noticeable reduction in the fluoxetine-exposed group compared to the control (Figure 5.11). The boxplot shows a clear decrease in total protein levels after 6 hours of exposure to fluoxetine, with the fluoxetine-exposed group displaying lower median values. The ANOVA analysis revealed that this reduction was statistically significant (p-value=0.000039).

Similarly, GSK3β phosphorylation at Ser9, an inhibitory site, was significantly reduced in fluoxetine-exposed cells compared to the control. The box plot illustrates a substantial decrease in phosphorylation levels, with the fluoxetine-exposed group having a much lower median value. The ANOVA test confirmed the statistical significance of this reduction (p-value=0.000350).

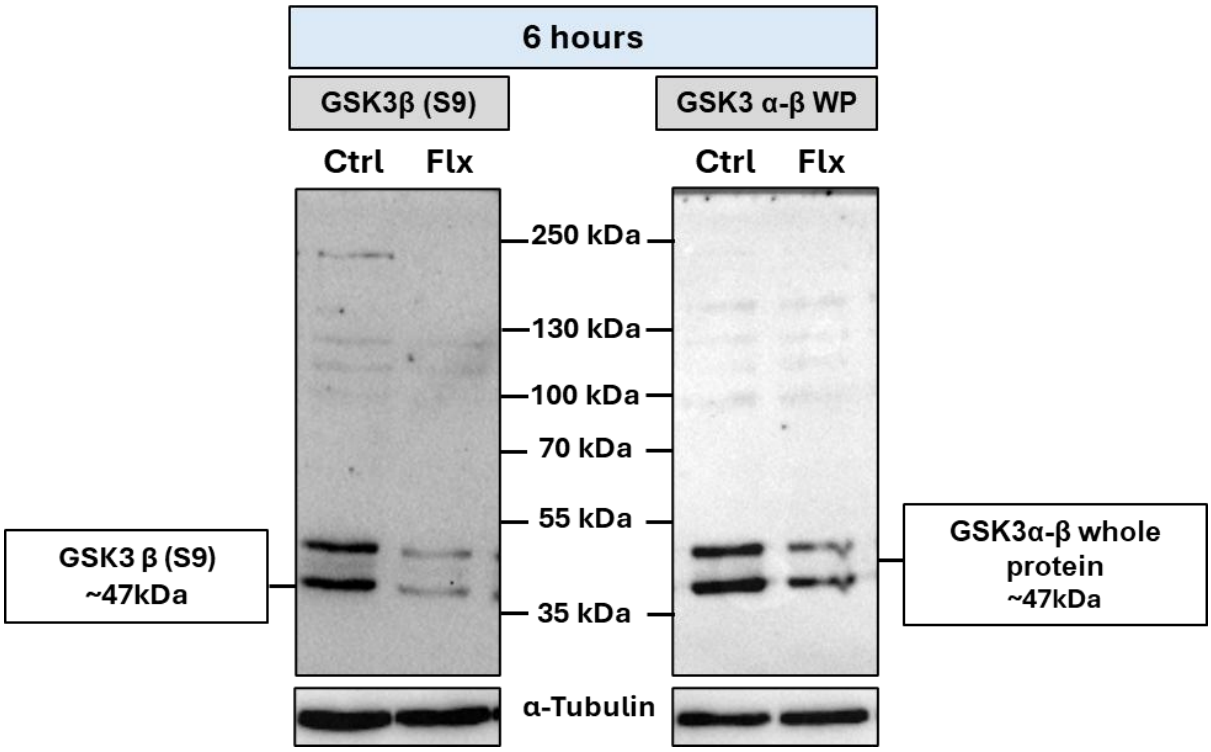

Figure 5.10: Representative western blot images after 6-hour exposure to fluoxetine (540 ng/l) in keratinocytes. *For GSK3α/β total protein (WP) and GSK3β phosphorylation (Ser9) The images depict the protein bands for control and fluoxetine-exposed samples. The bottom bands represent the loading control (α-tubulin).*

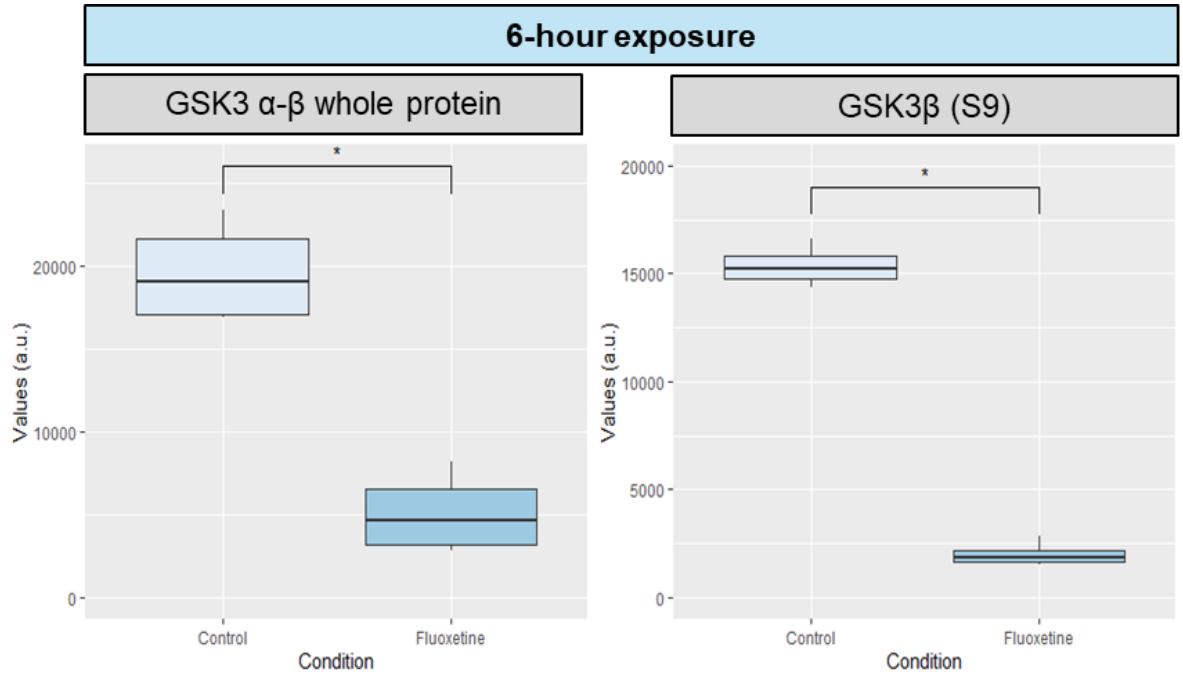

Figure 5.11: Western blot quantification of total protein levels and phosphorylation of MSK1 and GSK3 in keratinocytes after 6-hour exposure to fluoxetine (540 ng/l). *Boxplots represent normalised values (a.u.) for both total protein and specific phosphorylation sites: MSK1 whole protein, MSK1/2 (Ser376/Ser360), GSK3α/β whole protein, and GSK3β (Ser9). The black lines within each box represent the median values, and the whiskers indicate the full range of the data. Statistical significance between control and fluoxetine-exposed groups is indicated by an asterisk (*). Statistical analysis was performed using one-way ANOVA followed by Tukey's post hoc test (n>4 biological replicates per condition).*

5.3.4 Phosphoproteomics: analysis of phosphorylation dynamics in keratinocytes

Phosphoproteomics analysis was performed to explore the post-translational modifications induced by fluoxetine in keratinocytes. Given the observed changes in kinase activation from previous analyses, this study aimed to investigate phosphorylation changes across the proteomic landscape to understand how fluoxetine modulates cellular signalling at a broader level. In this study, HaCaT cells were exposed to 540 ng/l of fluoxetine for 36 hours, after which cell lysates were processed for phosphoproteomics analysis. Proteins were digested and enriched for phosphopeptides before being analysed using mass spectrometry. Out of the 3,204 phosphorylated proteins detected, 414 proteins were identified as having significant phosphorylation changes, with a p-value below 0.001. These 414 proteins were exclusively phosphorylated in either the control or fluoxetine-exposed groups. After filtering based on statistical significance (padj < 0.00001 and log2 fold change > 5), the final dataset comprised 45 proteins with decreased phosphorylation in fluoxetine-exposed cells and 190 proteins with increased phosphorylation compared to controls. The volcano plot (Figure 5.12) illustrates the

phosphorylation changes between fluoxetine-exposed and control cells, showing proteins with increased phosphorylation in fluoxetine-exposed cells on the right and decreased phosphorylation on the left.

Following this, the heatmap (Figure 5.13) provides a detailed comparison of the phosphorylation profiles across three replicates of fluoxetine-exposed and control cells. In this heatmap, each row represents a distinct phosphosite, while the columns correspond to individual replicates from both treatment conditions. The control samples (CTROL1-3) are shown on the right, and the fluoxetine-exposed samples (FLX1-3) are on the left. The heatmap reveals distinct clustering patterns, with groups of proteins showing differential phosphorylation between the two conditions. A large cluster of phosphosites shows increased phosphorylation in the fluoxetine-exposed samples, forming a distinct pattern on the left side of the heatmap. In contrast, a smaller cluster of proteins shows reduced phosphorylation in the fluoxetine-exposed samples compared to controls, appearing on the right side of the heatmap. This visualisation clearly distinguishes the phosphorylation dynamics between the control and fluoxetine-exposed groups, highlighting the shifts in phosphorylation levels across multiple proteins.

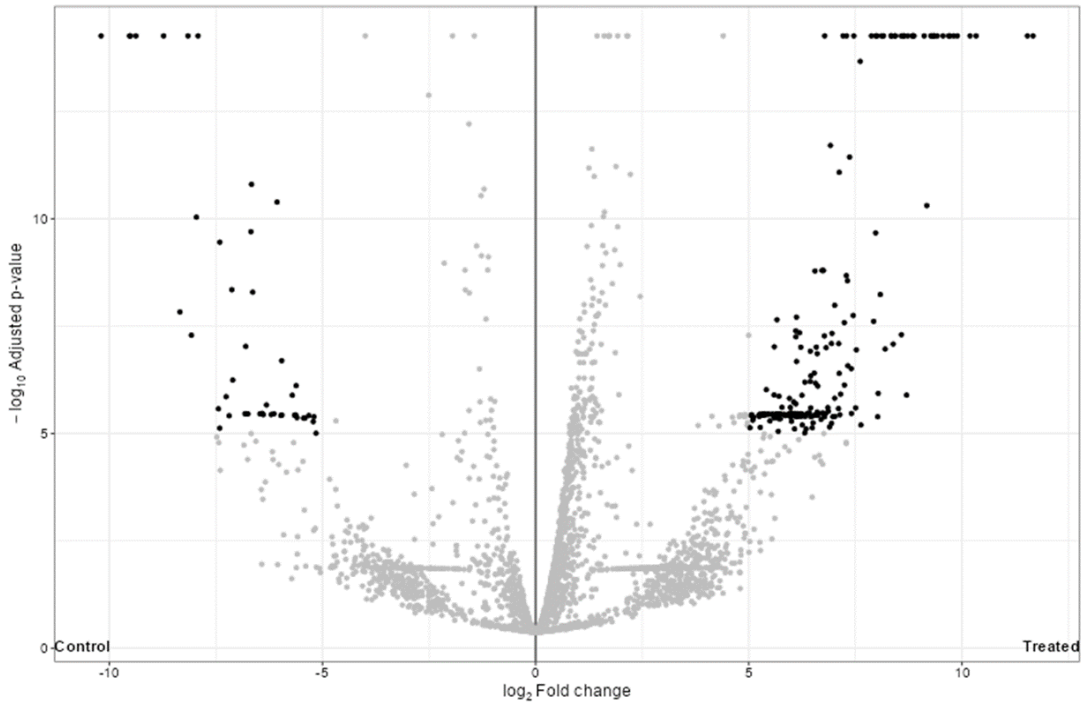

Figure 5.12: Volcano plot illustrating 190 upregulated and 45 downregulated phosphosites after 36-hour exposure to 540 ng/l fluoxetine. *The x-axis represents the log2 fold change in phosphorylation, with positive values indicating increased phosphorylation in fluoxetine-exposed cells and negative values indicating decreased phosphorylation. The y-axis shows the -log10 p-value, with higher values indicating greater statistical significance. Phosphosites meeting the adjusted p-value threshold of padj < 0.00001 are highlighted.*

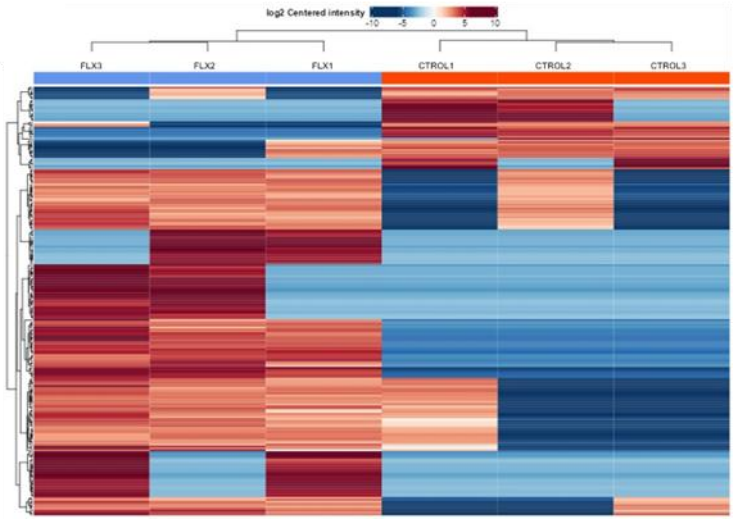

Figure 5.13: Heatmap comparing phosphosites in HaCaT cells exposed to 540 ng/l of fluoxetine for 36 hours versus control cells. *Three individual replicates are shown for control (CTROL1-3, right) and fluoxetine-exposed (FLX1-3, left) samples. The colour scale represents the level of phosphorylation, with red indicating higher phosphorylation levels and blue indicating lower phosphorylation levels.*

To further explore the functional relationships between the phosphoproteins identified as upregulated in fluoxetine-exposed cells, a protein-protein interaction network was constructed using STRING Figure 5.14. The analysis focused on the proteins with significantly increased phosphorylation levels upon fluoxetine exposure, displaying only the highest-confidence interactions (STRING interaction score > 0.9) for clarity. The network reveals several distinct clusters of interacting proteins, suggesting functional groupings relevant to the cellular response to fluoxetine. Cluster 1 includes proteins involved in DNA repair, cell signalling, and structures associated with epithelial cell fate, indicating that these processes may be influenced by fluoxetine exposure. Cluster 2, consists of ribonucleoproteins, suggesting that RNA processing and transport are affected by fluoxetine treatment. Cluster 3, contains proteins associated with chromosome organisation, pointing to the regulation of chromatin structure and gene expression as potential targets of fluoxetine. Finally, Cluster 4, features proteins related to elongation initiation factors, which are essential for protein synthesis, suggesting that fluoxetine may also affect translational mechanisms.

No significant protein-protein interactions were observed among the proteins with downregulated phosphorylation levels events.

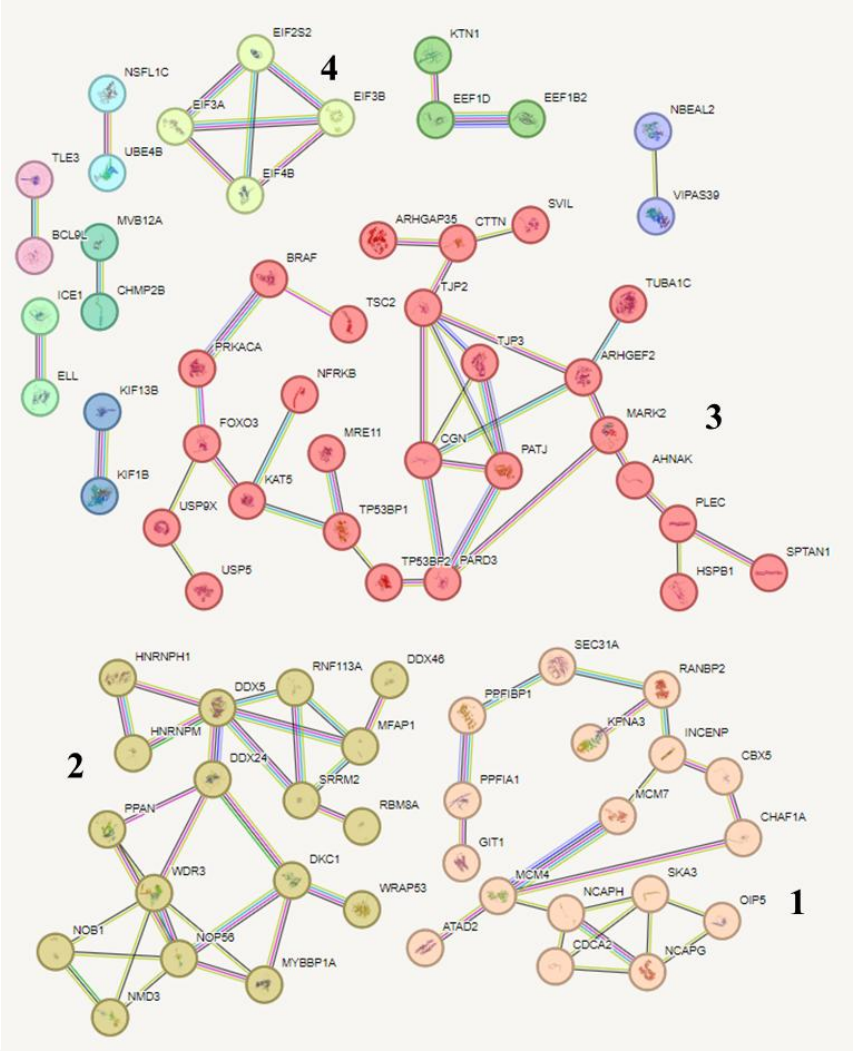

Figure 5.14: Protein-protein interaction network of proteins with upregulated phosphorylation after 36-hour exposure to fluoxetine (540 ng/l). *The network was generated using STRING with a high-confidence interaction score (>0.9). Four distinct clusters are shown: Cluster 1 includes proteins related to DNA repair, cell signalling, and structures associated with epithelial cell fate; Cluster 2 consists of ribonucleoproteins involved in RNA processing and transport; Cluster 3 is associated with chromosome organisation; and Cluster 4 contains proteins related to elongation initiation factors and protein synthesis. Only the highest confidence interactions are displayed for clarity.*

In addition to identifying the differentially phosphorylated proteins, functional enrichment analyses were conducted to explore the biological pathways and molecular functions specifically associated with proteins exhibiting altered phosphorylation after fluoxetine exposure. These analyses help contextualise the significance of both upregulated and downregulated phosphorylation levels in response to fluoxetine, providing a broader understanding of the cellular processes impacted by this treatment.

Focusing first on the upregulated phosphoproteins, the Gene Ontology (GO) analysis using ShinyGO revealed that proteins with increased phosphorylation in the fluoxetine-exposed group were significantly enriched in terms associated with structural and signalling roles (Figure 5.15). The top enriched terms included "anaphase-promoting complex," "apical junction complex," and "cell junction," indicating that fluoxetine exposure alters proteins critical for maintaining cell structure, cell adhesion, and signal transduction. These GO terms suggest that fluoxetine-induced phosphorylation enhances the function of proteins involved in cellular architecture and the regulation of keratinocyte proliferation.

Similarly, the Ingenuity Pathway Analysis (IPA) (Table 5.3) revealed several canonical pathways that were significantly impacted by proteins with upregulated phosphorylation. Notably, the HIPPO signalling pathway, which regulates cell growth and apoptosis, was the most enriched pathway (p-value=6.13E-05, 5.8% overlap), followed by pathways such as ATM signalling and tight junction signalling, both of which are crucial for maintaining genomic stability and epithelial barrier function, respectively.

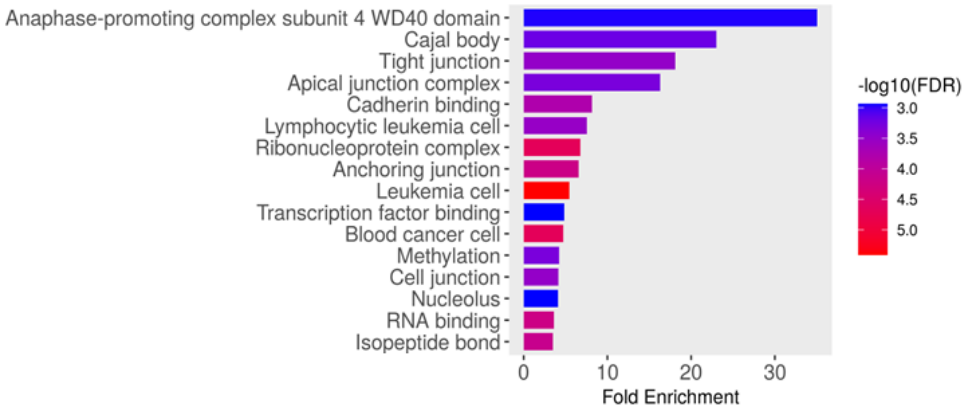

Figure 5.15: Gene Ontology (GO) enrichment analysis of proteins with upregulated phosphorylation after 36 hours of fluoxetine exposure (540 ng/l). *The graph displays the top GO terms enriched for molecular function and cellular components. The x-axis represents the fold enrichment of each term, while the colour scale represents the -log10 of the false discovery rate (FDR), with red indicating stronger statistical significance.*

Top Canonical Pathways		
Name	p-value	Overlap
HIPPO signaling	6.13E-05	5.8 % 5/86
ATM Signaling	1.26E-04	5.0 % 5/100
Kinetochore Metaphase Signaling Pathway	2.05E-04	4.5 % 5/111
Tight Junction Signaling	2.37E-04	3.4 % 6/179
Agrin Interactions at Neuromuscular Junction	3.50E-04	5.8 % 4/69

Table 5.3: Top canonical pathways enriched for proteins with upregulated phosphorylation after 36 hours of fluoxetine exposure (540 ng/l), identified using Ingenuity Pathway Analysis (IPA). *The table displays the pathway names, associated p-values, and the percentage overlap between the identified proteins and the total proteins in each pathway.*

Focusing next on the downregulated phosphoproteins, the Gene Ontology (GO) analysis using ShinyGO highlighted several biological processes that were significantly affected by decreased phosphorylation levels in the fluoxetine-exposed group (Figure 5.16). The top enriched terms for these proteins included “polarised epithelial cell differentiation,” “maintenance of epithelial cell apical/basal polarity,” and “morphogenesis of a polarised epithelium.” These GO terms are crucial for the structural organisation and differentiation of epithelial cells, suggesting that the downregulation of phosphorylation at these sites may disrupt the structural integrity and differentiation of keratinocytes, potentially affecting their ability to maintain proper cellular architecture under fluoxetine exposure.

Additionally, the Ingenuity Pathway Analysis (IPA) (Table 5.4) provided further insights into the canonical pathways impacted by downregulated phosphorylation. The Germ Cell-Sertoli Cell Junction Signalling pathway emerged as the most significantly affected, followed by pathways related to mismatch repair in eukaryotes and UVC-induced MAPK signalling. These pathways play essential roles in DNA repair, cell cycle regulation, and cellular stress responses, implying that fluoxetine may hinder the cells' capacity to manage genomic stability and effectively respond to stress.

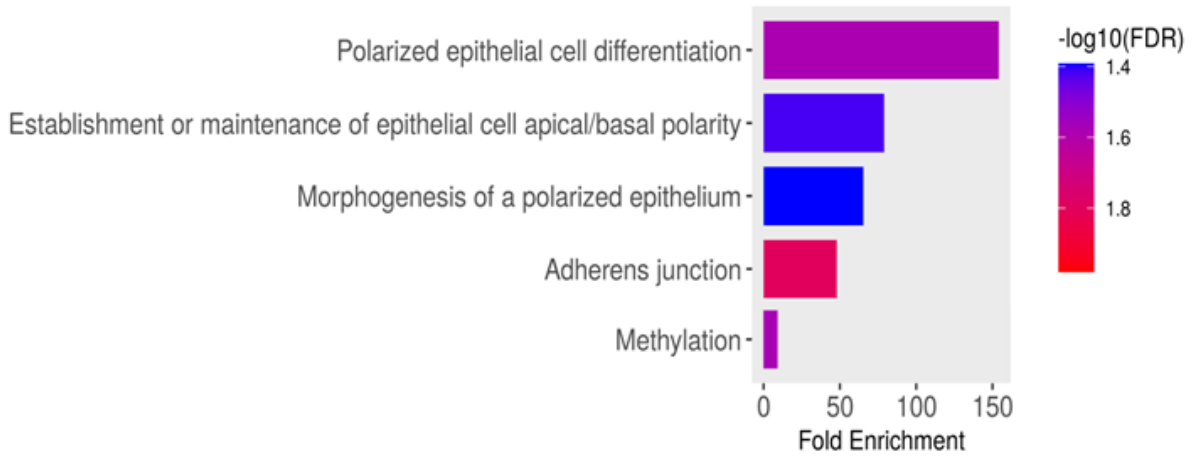

Figure 5.16: Gene Ontology (GO) enrichment analysis of proteins with downregulated phosphorylation after 36 hours of fluoxetine exposure (540 ng/l).*The graph displays the top GO terms enriched for molecular function and cellular components. The x-axis represents the fold enrichment of each term, while the colour scale represents the -log10 of the false discovery rate (FDR), with red indicating stronger statistical significance.*

Top Canonical Pathways

Name	p-value	Overlap
Germ Cell-Sertoli Cell Junction Signaling	1.41E-02	1.2 % 2/170
Mismatch Repair in Eukaryotes	1.91E-02	5.6 % 1/18
BER (Base Excision Repair) Pathway	4.60E-02	2.3 % 1/44
UVC-Induced MAPK Signaling	5.31E-02	2.0 % 1/51
Role of CHK Proteins in Cell Cycle Checkpoint Control	6.02E-02	1.7 % 1/58

Table 5.4: Top canonical pathways enriched for proteins with downregulated phosphorylation after 36 hours of fluoxetine exposure (540 ng/l), identified using Ingenuity Pathway Analysis (IPA). *The table displays the pathway names, associated p-values, and the percentage overlap between the identified proteins and the total proteins in each pathway.*

5.4 Discussion

The objective of this chapter was to investigate how fluoxetine modulates phosphorylation events in keratinocytes, particularly in the context of wound healing and cellular signalling. By employing protein kinase arrays, phosphoproteomics, and western blot validation, I aimed to uncover key signalling pathways affected by fluoxetine exposure, with a particular focus on the ERK/MAPK pathway. This chapter builds upon the findings of previous chapters, which highlighted the impact of fluoxetine on keratinocyte proliferation and mitochondrial function. In this discussion, I interpret the phosphorylation changes observed and place them within the broader context of wound healing and signalling regulation in keratinocytes.

5.4.1 Fluoxetine alters key signalling pathways: insights from protein microarray and western blot analysis

The results of the protein microarray analysis revealed significant changes in the phosphorylation status of key kinases involved in keratinocyte proliferation and stress responses, particularly after 36 hours of fluoxetine exposure. To further validate these findings, western blot analysis was conducted, focusing on GSK3β and MSK1/2, which emerged as central players in the regulation of wound healing and cellular signalling. Importantly, both the total protein levels and phosphorylation states of these kinases were evaluated to provide a comprehensive view of the impact of fluoxetine.

After 36 hours of fluoxetine exposure, both total protein levels and phosphorylation were significantly reduced in key kinases, including GSK3β and MSK1/2. The protein microarray data indicated a marked reduction in the phosphorylation of GSK3β at Ser9, an inhibitory site that plays a critical role in regulating the activity of the kinase. This reduction was confirmed by western blot analysis, which not only showed a decrease in phosphorylation but also revealed a significant reduction in the total GSK3β protein levels. The concurrent decrease in both total protein and phosphorylation levels suggests that fluoxetine affects GSK3β through multiple mechanisms: by reducing the overall abundance of the protein and by modulating its phosphorylation status. The reduction in total protein levels could indicate that fluoxetine downregulates the expression of GSK3β at the transcriptional or translational level, or it may enhance the degradation of GSK3β through proteasomal pathways. This impact on total protein availability may reduce the pool of GSK3β available for phosphorylation, leading to the observed decrease in phosphorylation at Ser9. Phosphorylation at Ser9 typically inhibits

GSK3β activity (Molz et al., 2011; Nishimoto et al., 2008), and thus, a decrease in both total GSK3β and its phosphorylation could suggest a broader suppression of its regulatory roles in apoptosis, proliferation, and migration. Studies have shown that reduced GSK3β levels contribute to diminished kinase activity, as seen in various models, such as cancer cell lines and neurodegenerative disorders (Ma et al., 2015; Yao et al., 2016). In addition, a study (Lang et al., 2013) highlighted that GSK3β plays a central role in regulating cellular survival and stress response, which may be relevant to keratinocytes under fluoxetine exposure. Another study (Zeng et al., 2014) discussed how fluoxetine modulates pathways associated with GSK3β to influence cellular behaviour, further supporting these observations of reduced kinase activity in response to fluoxetine.

A similar pattern was observed for MSK1/2, where both total protein levels and phosphorylation at Ser376/Ser360 were reduced in fluoxetine-exposed cells compared to controls. MSK1/2 is a key downstream target of the ERK/MAPK signalling pathway, which plays a critical role in regulating cellular stress responses, chromatin remodelling, and proliferation (Reyes et al., 2014; Sawicka et al., 2014).

In addition to the observed changes in GSK3β phosphorylation, our phosphoproteomics analysis revealed hyperphosphorylation of key MAPK kinases, including MAP3K3, MAP3K4, and MAP4K5, in fluoxetine-exposed keratinocytes. These findings highlight the involvement of the MAPK signalling pathway in mediating the effect of fluoxetine on cellular stress responses and cell fate decisions. MAPK signalling, particularly through these kinases, plays a critical role in modulating cell proliferation and survival, processes essential for efficient wound healing. The hyperphosphorylation of these kinases suggests that fluoxetine not only modulates GSK3β activity but also affects upstream MAPK components, further amplifying its impact on cellular signalling dynamics.

The observed reduction in total MSK1/2 protein levels after 36 hours suggests that fluoxetine may be modulating the ERK/MAPK pathway, but this reduction likely occurs after an earlier activation of the pathway. Given the role of MAPK in early signalling events, it is likely that fluoxetine initially activates the ERK/MAPK pathway, and the reduction at 36 hours reflects a later phase of downregulation after the primary effects have already taken place. MSK1 has been shown to influence transcriptional regulation in response to cellular stress through the phosphorylation of histone H3 (Zhang and Wu, 2020), which further highlights its importance in maintaining proper cellular functions during wound healing and tissue repair processes(P. Chen et al., 2017; Choi et al., 2012; Ukil et al., 2011).

The implications of a reduction in both total protein and phosphorylation are significant. Since phosphorylation is dependent on the presence of the protein itself, it stands to reason that a decrease in total protein would lead to reduced phosphorylation levels. However, the fact that both total protein and phosphorylation are reduced suggests a more comprehensive mechanism at play, where fluoxetine may be downregulating the production of these proteins as part of a larger cellular response. This could be a way for keratinocytes to tightly regulate signalling pathways, ensuring that excessive activity does not lead to uncontrolled proliferation or stress responses during wound healing.

The ability of fluoxetine to suppress both the abundance and activity of GSK3β and MSK1/2 hints at its broader role in modulating cellular signalling at multiple levels. Interestingly, since no changes were observed in the RNA levels of these proteins, it is likely that fluoxetine promotes protein degradation rather than affecting transcription, at least after 36 hours. By reducing the overall levels of these proteins, fluoxetine may be downregulating pathways involved in cell cycle control, stress responses, and DNA repair, thereby modulating the balance between cell survival and death during the wound healing process. The reduction of GSK3β levels has been shown to influence key pathways involved in cell survival and apoptosis, as serotonin signalling through 5-HT1A receptors regulates GSK3 activity via the PI3K/Akt pathway, impacting various downstream effects on cell fate (Polter et al., 2012). Similarly, MSK1/2, which are activated by both MAPK and SAPK2/p38 pathways, play a critical role in the cellular response to stress, and their inhibition by fluoxetine could further modulate stress responses and transcriptional regulation (Deak et al., 1998).

At the 6-hour time point, the western blot analysis revealed early reductions in both GSK3β total protein levels and phosphorylation at Ser9, though the effects were less pronounced compared to the 36-hour exposure. This suggests that fluoxetine begins to modulate GSK3β activity relatively early, with reductions in both the amount of the protein and its phosphorylation state becoming more pronounced over time. The early decrease in GSK3β phosphorylation could be a key event in initiating the effects of fluoxetine on keratinocyte behaviour (Polter et al., 2012).

Despite the successful validation of GSK3β, the western blot analysis encountered technical challenges when validating other kinases, such as SRC and p70-S6K. Issues with antibody

specificity may have limited the ability to detect changes in these proteins. However, the consistent findings in GSK3β provide strong evidence that fluoxetine modulates critical signalling pathways involved in keratinocyte proliferation, survival, and wound healing.

5.4.2 Influence of fluoxetine on cellular signalling networks: phosphoproteomic insights

To further explore the molecular mechanisms by which fluoxetine modulates keratinocyte behaviour, I performed a comprehensive phosphoproteomics analysis. This technique allowed for a broader examination of phosphorylation events across the proteome, offering deeper insights into how fluoxetine influences key signalling pathways involved in wound healing, cellular proliferation, and stress responses.

The phosphoproteomics analysis conducted in this study provides comprehensive insights into the role of fluoxetine in modulating phosphorylation dynamics, which are crucial for cellular signalling during the wound healing process. The identification of 235 differentially phosphorylated peptides between fluoxetine-exposed and control keratinocytes suggests that fluoxetine has a measurable impact fluoxetine has on the cellular phosphoproteome. This modulation of kinase activity has significant implications for processes such as cell proliferation, migration, stress response, and DNA repair, all of which are integral to efficient tissue regeneration.

A key observation from this study was the significant upregulation of 190 phosphosites in fluoxetine-exposed cells, suggesting that fluoxetine triggers activation of signalling networks involved in keratinocyte function. These phosphosites were predominantly linked to pathways that promote keratinocyte proliferation and migration, both of which are fundamental for wound healing. This aligns with previous research showing that fluoxetine enhances cellular survival and proliferation by regulating phosphorylation of critical proteins, such as GSK3β, which is central to the PI3K/AKT pathway (Hui et al., 2015; Yang et al., 2020). This pathway plays a pivotal role in promoting keratinocyte survival by inhibiting pro-apoptotic signals and driving the expression of genes involved in cell growth and tissue repair.

The upregulation of the PI3K/AKT pathway in fluoxetine-exposed keratinocytes suggests that this signalling cascade may be one of the primary mechanisms through which fluoxetine exerts its pro-regenerative effects. The activation of PI3K/AKT signalling has been widely implicated in promoting cell proliferation and inhibiting apoptosis, which is critical for efficient wound closure. By enhancing the phosphorylation of downstream effectors within this pathway,

fluoxetine may help maintain a favourable environment for keratinocyte survival and division, facilitating the wound healing process (Yang et al., 2020).

Interestingly, fluoxetine also appeared to downregulate phosphorylation in several pathways related to stress responses and DNA repair. Specifically, proteins involved in mismatch repair and UVC-induced MAPK signalling exhibited reduced phosphorylation in fluoxetine-exposed cells. This downregulation is consistent with the known ability of fluoxetine to modulate cellular stress responses by inhibiting key kinases such as GSK3β and p38 MAPK (Hui et al., 2015; Zhao et al., 2018). The inhibition of stress-related pathways could be an adaptive mechanism, allowing cells to prioritise proliferation and migration over the activation of DNA repair processes, which might otherwise delay wound closure. The suppression of stress responses likely reduces excessive inflammation and prevents prolonged cell cycle arrest, both of which are detrimental to timely tissue regeneration.

The balance between promoting cell proliferation and suppressing stress signalling is a critical aspect of the role of fluoxetine role in wound healing. On one hand, the ability of fluoxetine to upregulate phosphosites involved in proliferation-related pathways supports its role in enhancing keratinocyte migration and tissue repair. On the other hand, the suppression of stress-related kinases, such as p38 MAPK, may limit the cellular energy spent on managing DNA damage and instead direct resources towards tissue regeneration. This selective modulation of signalling pathways reflects the dual capacity of fluoxetine to stimulate cellular growth while curbing excessive stress responses that could otherwise impede wound healing (Maingrette et al., 2015).

Another critical aspect of the impact of fluoxetine on phosphorylation dynamics is its modulation of the HIPPO signalling pathway, a key regulator of cell proliferation, organ size, and tissue regeneration (Yu et al., 2015; Zhao et al., 2011). The upregulation of fluoxetine of phosphosites within this pathway suggests its potential influence on keratinocyte architecture and growth control mechanisms, which are essential for efficient wound healing. The HIPPO pathway primarily regulates the balance between cell growth and apoptosis by modulating YAP and TAZ activity, ensuring that tissue expansion occurs in a controlled manner (Duan, n.d.; Mia and Singh, 2022; Misra and Irvine, 2018). This influence on HIPPO signalling likely helps maintain tissue integrity, enhancing keratinocyte proliferation and migration, which are critical for timely wound closure (Mia and Singh, 2022; Yu et al., 2015).

Future experiments could investigate whether fluoxetine inhibits upstream kinases such as MST1/2 and LATS1/2, potentially promoting YAP/TAZ nuclear translocation and thereby activating transcriptional programs that support keratinocyte proliferation and survival (Misra and Irvine, 2018; Pan, 2007). To test this hypothesis, experiments could involve assessing YAP/TAZ localisation and activity following fluoxetine exposure, using specific inhibitors or genetic knockdowns of MST1/2 and LATS1/2 to observe any changes in keratinocyte proliferation and survival.

The STRING network analysis also revealed distinct clusters of proteins involved in both the structural maintenance of keratinocytes and the regulation of DNA repair mechanisms. These findings are in line with previous reports on the ability of fluoxetine to modulate signalling pathways that govern cellular architecture, particularly in contexts where rapid tissue repair is required. The activation of pathways such as PI3K/AKT and HIPPO, alongside the suppression of DNA repair processes, highlights the capacity of fluoxetine to fine-tune cellular responses to injury. This dynamic regulation of phosphorylation allows fluoxetine to promote tissue repair while maintaining cellular homeostasis (Polter et al., 2012; Zheng et al., 2009).

The phosphoproteomics analysis highlights the significant enrichment of proteins involved in structural maintenance, shedding light on the role of fluoxetine role in stabilising keratinocyte architecture during the wound healing process. Ensuring structural integrity is essential for effective cell migration and tissue remodelling, both of which are vital for wound closure. The modulation of phosphosites within these pathways underscores the potential of fluoxetine not only to promote keratinocyte proliferation but also to ensure the resilience and strength of the newly formed tissue (Mia and Singh, 2022; Yang et al., 2020).

In conclusion, the phosphoproteomics data provide compelling evidence that fluoxetine has a broad and multifaceted impact on phosphorylation dynamics in keratinocytes. By selectively modulating key signalling pathways such as PI3K/AKT, HIPPO, and MAPK, fluoxetine enhances keratinocyte proliferation and wound healing, while simultaneously downregulating stress responses and DNA repair mechanisms. These findings align with existing literature on the role of fluoxetine in cellular proliferation and survival (Hui et al., 2015; Shi and Sun, 2020; Yang et al., 2020), highlighting its potential for therapeutic applications in tissue repair and regenerative medicine.

5.5 Conclusion

The work presented in this chapter provides crucial insights into the broader effects of fluoxetine on keratinocyte behaviour, especially through its impact on post-translational modifications. This chapter explored the impact of fluoxetine on the modulation of kinase activity and phosphorylation dynamics through a combination of proteome profiling, phosphoproteomics, and western blot validation. Collectively, these findings underscore the multifaceted role of fluoxetine in promoting wound healing by influencing key signalling pathways.

The proteome profiler arrays highlighted significant changes in the phosphorylation of proteins critical to cellular stress responses, proliferation, and migration. Specifically, fluoxetine was shown to reduce the phosphorylation of GSK3β and MSK1/2, central regulators of cell survival and stress responses, thereby suggesting a broad suppression of these pathways during wound healing. Western blot analysis validated these findings, showing that both the total protein levels and phosphorylation status of GSK3β and MSK1/2 were significantly reduced. These reductions highlight the ability of fluoxetine to modulate these proteins at multiple regulatory levels, possibly through transcriptional or translational downregulation, in addition to direct phosphorylation changes.

Additionally, the phosphoproteomics analysis offered a more detailed view of the post-translational modifications occurring under fluoxetine exposure. By identifying differentially phosphorylated proteins, this analysis revealed the capacity of fluoxetine to trigger phosphorylation of proteins involved in keratinocyte migration and proliferation. Pathways such as PI3K/AKT and HIPPO were particularly enriched, further demonstrating the role of fluoxetine in promoting cellular proliferation and ensuring proper tissue remodelling during wound healing. This phosphorylation-driven modulation of cellular architecture aligns with the transcriptional and mitochondrial observations made in previous chapters.

Linking these findings to the results from Chapter 3, which focused on the role of fluoxetine in keratinocyte proliferation and wound healing through serotonin signalling, I can see a clear connection between early gene expression changes and subsequent post-translational modifications. In Chapter 3, fluoxetine was shown to enhance keratinocyte proliferation and wound closure, driven by transcriptional changes related to serotonin receptors and cell growth

pathways. The current chapter builds on these findings by demonstrating how phosphorylation events reinforce these gene expression changes at the protein level, further regulating keratinocyte behaviour through post-translational control.

Chapter 4 explored how fluoxetine modulates signalling pathways tied to energy metabolism and stress responses, particularly through mitochondrial function. This chapter complements those findings by showing how fluoxetine also affects kinase signalling pathways such as ERK/MAPK and potentially PI3K/AKT, which are crucial for managing cellular stress and facilitating tissue repair. The reduction in stress-related phosphorylation, especially in DNA repair and MAPK signalling pathways, highlights the capacity of fluoxetine to prioritise keratinocyte proliferation over stress management, ensuring efficient tissue regeneration.

Together, this chapter extends the insights from Chapters 3 and 4, revealing the critical role of fluoxetine in both transcriptional and post-translational regulation. Through a detailed examination of phosphorylation dynamics, fluoxetine is shown to enhance keratinocyte proliferation and tissue remodelling, while effectively managing cellular stress responses. These findings underscore the potential of fluoxetine in wound healing and regenerative medicine.

In conclusion, Chapter 5 highlights the importance of integrating multiple molecular approaches, such as proteome profiling, phosphoproteomics, and western blotting, to fully understand the broad impact of fluoxetine on cellular signalling. The combined insights from these techniques illustrate the multi-level regulation of keratinocyte behaviour by fluoxetine, from transcriptional changes to phosphorylation-driven pathways, positioning fluoxetine as a promising candidate for therapeutic interventions in tissue repair.

Chapter 6: *Ex-vivo* model to investigate the effects of fluoxetine on human skin

6.1 Introduction

The previous chapters established that fluoxetine modulates key signalling pathways involved in cellular stress, proliferation, and apoptosis, providing a foundation for understanding its potential therapeutic effects in wound healing. These findings suggest that fluoxetine may play a significant role in promoting tissue regeneration and enhancing healing outcomes.

To further explore these possibilities, this chapter investigates the effects of fluoxetine on human skin repair using *ex-vivo* models. These models serve as an intermediary between *in vitro* cell cultures and *in vivo* studies, offering a more accurate representation of physiological conditions. Human skin biopsies, in particular, provide an ideal platform for studying wound healing, as they preserve the wound microenvironment and interactions between different cell types, such as keratinocytes, fibroblasts, and immune cells, which are crucial for the wound healing process (Sorg et al., 2017; Wilkinson and Hardman, 2020a). This approach allows to assess the effects of fluoxetine in a context that closely mimics *in vivo* conditions, providing relevant insights into its potential therapeutic and adverse effects.

To elucidate the mechanisms underlying the effects of fluoxetine, I also employed two serotonin blockers: mirtazapine and ketanserin. Mirtazapine acts as an antagonist at key serotonin receptors, including 5-HT2 and 5-HT3 receptors. Given that my study suggests fluoxetine may impact serotonin signalling, understanding the effect of mirtazapine is essential for evaluating how serotonergic pathways influence wound healing outcomes (Chang et al., 2010; Lalani et al., 2023). Ketanserin is an antagonist of 5-HT2A and 5-HT2C that has previously been used to investigate the role of 5-HT in wound healing (Nguyen et al., 2019; Sadiq et al., 2018). In order to confirm that fluoxetine impacts wound healing through serotonin signalling, I used fluoxetine in combination with these two blockers. This approach allows to dissect the contributions of serotonergic signalling to the modulation of wound healing processes more effectively.

6.2 Aims & Objectives

This chapter investigates the effects of fluoxetine on wound healing using human skin biopsies in *ex-vivo* models to elucidate the underlying mechanisms of tissue repair.

The objectives are as follows:

1) **To evaluate the effects of fluoxetine on human skin wound healing,** by using *ex-vivo* human skin biopsies.

2) **To investigate the role of serotonin signalling in the modulation of wound healing** by employing mirtazapine and ketanserin to block serotonin receptors.

6.3 Materials and methods: clinical data of skin donors

The clinical data of the skin donors used in this chapter are presented in Table 6.1. Samples were obtained from individuals undergoing surgical procedures, with an average age of 53 years, and included mostly female donors (except one male donor). The donors had various comorbidities, such as squamous cell carcinoma of the hypopharynx, bilateral breast cancer, hypertension, and others. Medications taken by the donors included tamoxifen and Amitriptyline, while some were not on any medication. Skin biopsies were primarily collected from the abdomen, except for one sample from an anterolateral thigh flap (ALT).

Experiments	Sex	Co-morbidities	Medication	Skin location
Fluoxetine	Female	No information	No information	abdomen
Fluoxetine	Male	Squamous Cell Carcinoma hypopharynx, Continuous Cycler Peritoneal Dialysis, Hypertension	Fosinopril	ALT (Anterolateral thigh flap)
Fluoxetine	Female	Hypertension, Gout, Type 2 Diabetes Mellitus	Letrozole, Allopurinol, Amitriptyline, Calceos, Fluoxetine, Gabapentin, Indapamide, Lansoprazole, Morphine, Ozemnpic, Perindopril, Simvastatin	Abdomen
Fluoxetine	Female	Bilateral breast cancer	Tamoxifen	Abdomen
Fluoxetine	Female	No information	Amitriptyline	Abdomen
Fluoxetine, Mirrtazapine	Female	No information	No information	Abdomen
Fluoxetine, Mirtazapine	Female	Bilateral idiopathic uveitis	Prednisolone, Mycophenolate, Adalimumab	Abdomen
Fluoxetine, Mirtazapine	Female	Fit and well	Nil	Abdomen
Fluoxetine, Mirtazapine, Ketanserin	Female	Breast Cancer	Anastrozole, Ibandronic acid	Abodomen
Fluoxetine, Ketanserin	Female	no information	No information	Abodomen
Fluoxetine, Ketanserin	Female	Breast Cancer	Ventafaxine	Abdomen

Table 6.1: Clinical data of skin donors used in the ex-vivo experiments. *The table details the sex, comorbidities, medication history, and anatomical location of the biopsy. The "Experiments" column specifies the types of experiments conducted using each sample.*

6.4 Results

6.4.1 Wound closure in human skin biopsies: fluoxetine treatment

Fluoxetine exposure was tested at two concentrations (2500 ng/l and 5400 ng/l) to evaluate its impact on wound healing in an *ex-vivo* human skin model. These concentrations were selected to reflect the upper end of environmentally reported levels, particularly those found in wastewater effluents and near pharmaceutical discharge points, where concentrations have been measured up to 596 ng/l (Hughes et al., 2013), 1310 ng/l (Bean et al., 2017b), and even 3645 ng/l (Salgado et al., 2011). While these concentrations exceed typical levels found in surface waters, they are environmentally relevant for modelling high-exposure scenarios, including direct contact with contaminated effluent, accidental dermal exposure, or conditions of limited water dilution due to infrastructure, geography, or climate-related water scarcity. These higher concentrations also align with previous experimental studies (Correia et al., 2022; Dzieweczynski et al., 2016; Guler and Ford, 2010; Weinberger and Klaper, 2014) and allow detection of robust biological responses in human skin tissue, providing a valuable model for assessing potential health impacts under worst-case exposure conditions. By using these concentrations, the study aimed to assess the biological effects of fluoxetine within a range that mirrors environmental exposure and potentially produces noticeable effects on wound healing. Representative images show the extent of wound closure for each treatment (Figure 6.1), with control samples exhibiting minimal epithelial coverage over the wound area. In contrast, samples treated with fluoxetine demonstrated significant increases in wound closure, particularly at the higher concentration of 5400 ng/l, where re-epithelialisation was visibly enhanced, with dense keratinocyte. This was accompanied by dense epithelial activity around the wound margins, suggesting increased cellular processes. However, without specific assays or markers, it remains unclear whether this enhancement was primarily due to proliferation and migration, or a combination of both.

To validate these observations measurements of wound area were taken, the averages for each condition were calculated across eleven biological replicates (n=11, 11 different donors) and with three to four technical replicates per donor. The wound closure percentage was normalised across donors, due to the high variability of response between donors in *ex-vivo* biopsies model (Wilkinson et al., 2021). The quantitative analysis of wound closure percentage is depicted in Figure 6.2. Normality was tested using a Shapiro-Wilk test and homoscedasticity using a Levene test, both were proven true with p-values>0.05, allowing the usage of a one-way

ANOVA. This ANOVA highlighted the significant impact of fluoxetine on wound closure in the *ex-vivo* samples, with p-value=1.357e-09. Post-hoc analysis using Tukey's HSD test was performed to identify the differences between control biopsies and the biopsies exposed to fluoxetine. The control biopsies had a percentage of wound closure after 48 hours of 55.1% ± 0.859, biopsies exposed to 2500 ng/l of fluoxetine had an average wound closure of 62.61% ± 2.59 that was significantly higher when compared to control biopsies (p-value=5.31e-04). Finally, biopsies exposed to 5400 ng/l had an average percentage of 71.43% ± 7.37, which was significantly higher than the other two groups (p-values<0.001). All groups were statistically different to the other. These results indicate that fluoxetine effectively stimulates wound healing processes in an *ex-vivo* human skin model, with the higher concentration (5400 ng/l) showing the most pronounced effects on wound closure.

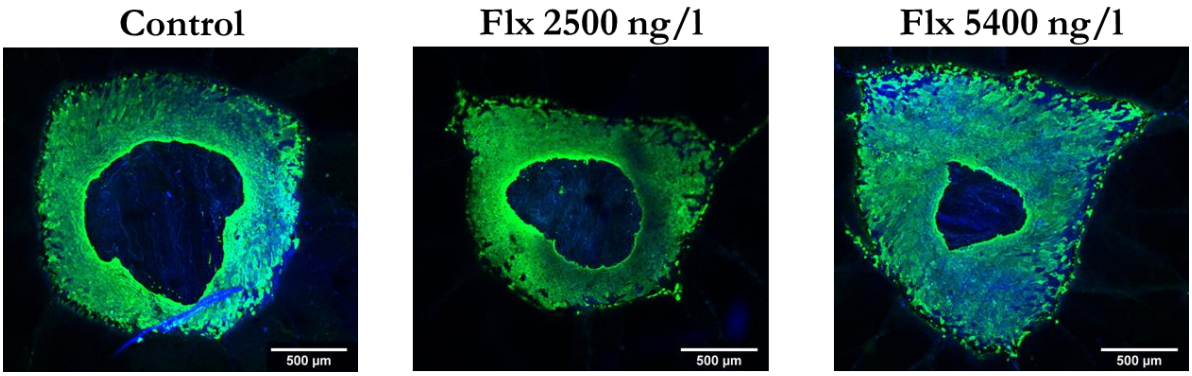

Figure 6.1: Representative images of the effects of fluoxetine on ex-vivo human skin biopsies. *Images showing keratin 14 (K14, green) expression and nuclear staining (DAPI, blue) in control and fluoxetine-exposed samples at concentrations of 2500 ng/l and 5400 ng/l. The scale bar represents 500 µm.*

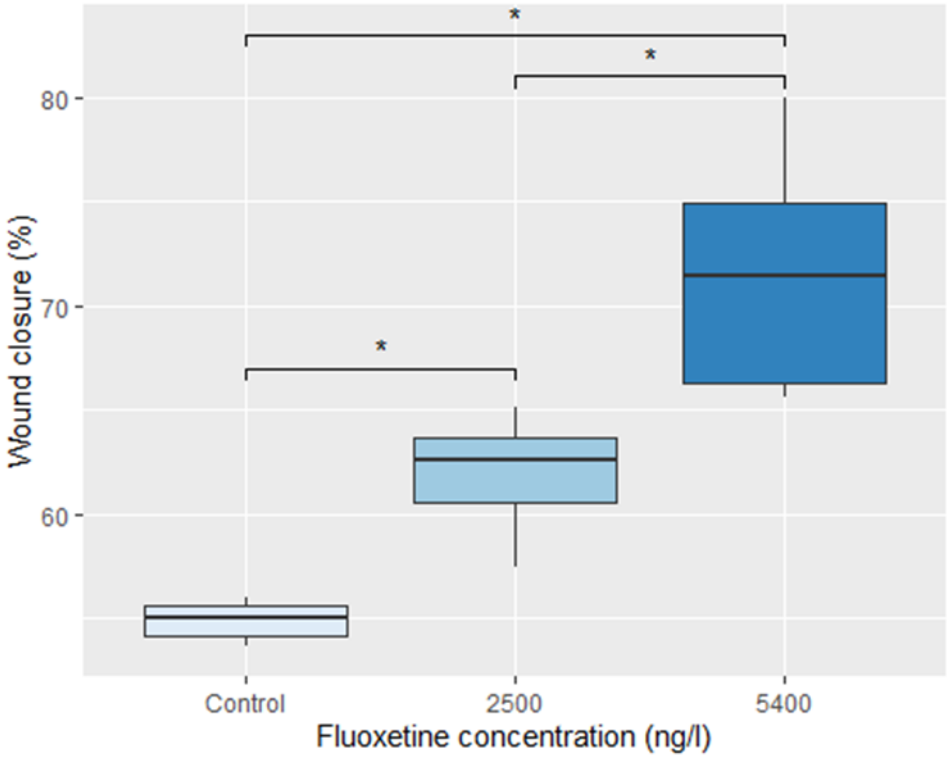

Figure 6.2: Boxplot of the percentage of wound closure after 48 hours of exposure to fluoxetine. *The x-axis represents the fluoxetine concentrations (2500 ng/l and 5400 ng/l), and the y-axis shows the percentage of wound closure. X-axis not to scale. Each box represents the interquartile range (IQR), where the top and bottom of the box indicate the 75th and 25th percentiles, respectively. The horizontal line within each box represents the median. The whiskers extend to the minimum and maximum values, excluding outliers, and the dots represent individual data points. Statistical significance between groups is indicated by asterisks (* p< 0.05). Statistical analysis was performed using one-way ANOVA followed by Tukey's post hoc test (n=11 biological replicates per condition).*

6.4.2 Fluoxetine and mirtazapine: investigating serotonin signalling

Fluoxetine was administered in combination with mirtazapine to elucidate whether the effects of fluoxetine on keratinocyte behaviour are mediated through serotonin pathways. Mirtazapine and fluoxetine were also administered on their own as controls.

Representative images illustrate the extent of wound closure following exposure to fluoxetine, treatment with mirtazapine or exposure to both drugs (Figure 6.3). Similar to the results described in the previous section, biopsies exposed to fluoxetine seemed to have more epithelial coverage over the wound area when compared to control biopsies. Biopsies treated only with mirtazapine visually had a lower wound closure, in an order similar to what was visible in control biopsies. Finally, biopsies exposed to a combination to both drugs amongst

visual inspection presented wound closure similar to what was visible in the fluoxetine-exposed biopsies.

To quantify these observations, wound area measurements were taken, and averages for each condition were calculated across biological replicates (n=4, representing different donors), with three technical replicates per donor. The wound closure percentage was normalised across donors to account for variability inherent in *ex-vivo* biopsies as before. After validation of both normality and homoscedasticity of the date (p-values>0.05 for both Shapiro-Wilk and Levene tests) a one-way ANOVA was performed. This revealed a significant difference in percentage of wound closure across the different conditions (p-value= 0.002526).

Post-hoc analysis using Tukey's HSD test identified significant differences between the control group and biopsies exposed to fluoxetine only. Control biopsies demonstrated a percentage of wound closure after 48 hours of 55.1% ± 1.47.

Biopsies treated with fluoxetine alone achieved an average wound closure of 65.55% ± 5.0, significantly higher than controls (p-value=0. 0215853). Samples treated with fluoxetine and mirtazapine exhibited the greatest wound closure, averaging 67.63% ± 2.9, which was significantly greater than the control (p-value=0. 0207458) but not significantly different than the fluoxetine-only group (p-values=0.999). Finally, biopsies treated with only mirtazapine showed a percentage of wound closure (54.0% ± 4.99) similar to the control group (p-value=0.873) and significantly lower than both fluoxetine-exposed and fluoxetine+mirtazapine-treated groups (both p-values<0.01). Groups with statistically different percentage of wound closure were classified as groups A and B in the figure.

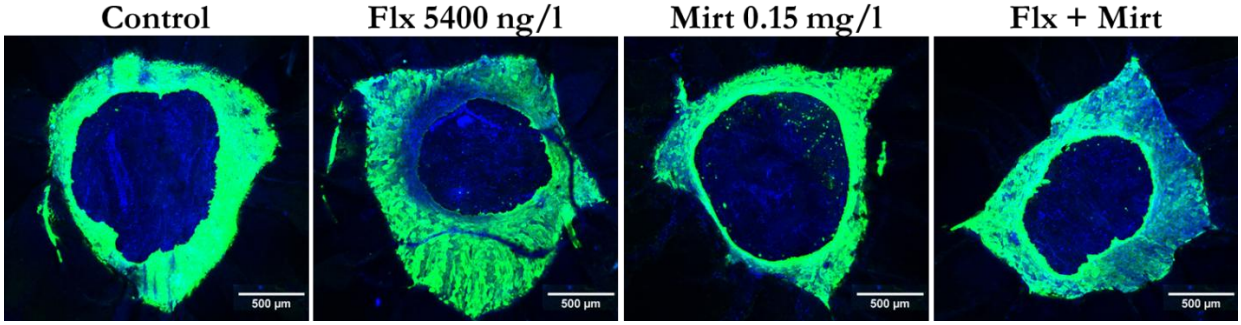

Figure 6.3: Representative images of the effects of fluoxetine and mirtazapine on ex-vivo human skin biopsies. *Images showing keratin 14 (K14, green) expression and nuclear staining (DAPI, blue) in control, fluoxetine-exposed (5400 ng/l) and mirtazapine-treated samples (0.15 mg/l) as well as samples exposed to a combination of both drugs (5400 ng/l of fluoxetine + 0.15 mg/l of mirtazapine). The scale bar represents 500 µm.*

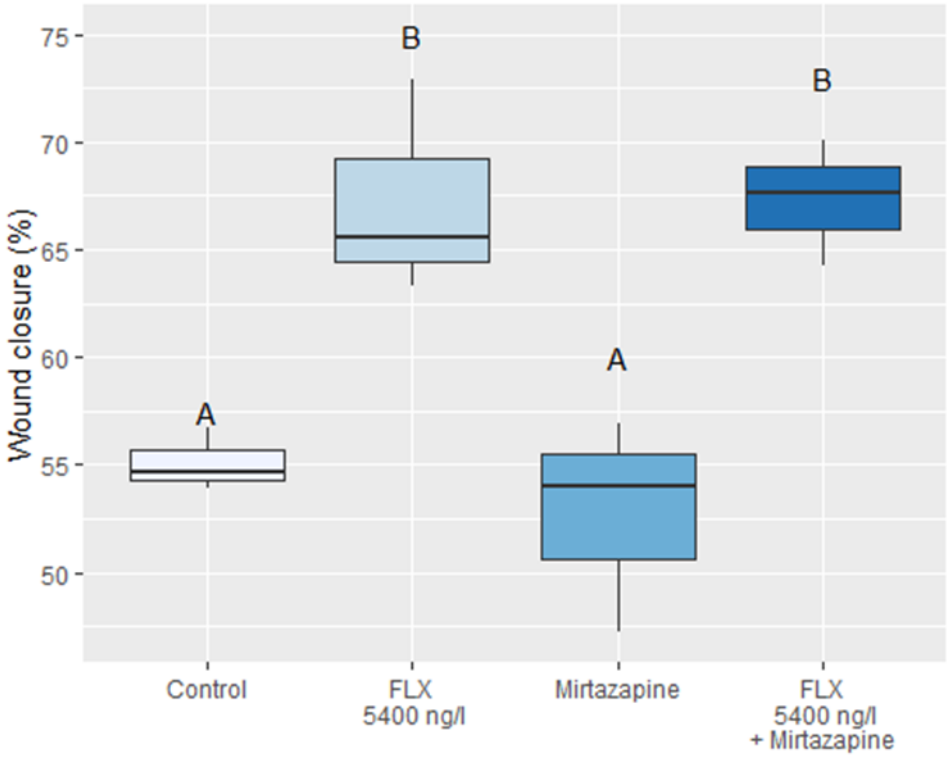

Figure 6.4: Boxplot of the percentage of wound closure after 48 hours of exposure to fluoxetine, mirtazapine or combination of both. *The x-axis represents the conditions: fluoxetine (5400 ng/l) in combination with or without mirtazapine (0.15 mg/l) and mirtazapine alone. The y-axis shows the percentage of wound closure. X-axis not to scale. Each box represents the interquartile range (IQR), where the top and bottom of the box indicate the 75th and 25th percentiles, respectively. The horizontal line within each box represents the median. The whiskers extend to the minimum and maximum values, excluding outliers, and the dots represent individual data points. Groups labelled with different letters (A, B) indicate significant differences between conditions ($p < 0.05$). Conditions sharing the same letter are not significantly different from each other. For example, groups labelled "A" (Control, Mirtazapine) are statistically similar to each other but significantly different from those labelled "B" (Fluoxetine, Fluoxetine + Mirtazapine). Statistical analysis was performed using one-way ANOVA followed by Tukey's post hoc test (n=4 biological replicates per condition).*

6.4.3 Using ketanserin to further investigate the impact of fluoxetine on wound-healing *ex-vivo* via serotonin signalling.

Fluoxetine was administered in combination with ketanserin to determine whether the effects of fluoxetine on wound healing were mediated through serotonin signalling. Figure 6.5 presents representative images of the wound closure of the biopsies following exposure to fluoxetine, treatment with ketanserin or combination of both. Visual inspection seems to indicate that biopsies exposed to fluoxetine had greater epithelial coverage over the wound area compared to control samples. In contrast, those treated only with ketanserin exhibited wound closure similar to that of the control group, showing minimal epithelialisation. Finally, biopsies

treated with both fluoxetine and ketanserin presented wound closure comparable to those exposed to ketanserin alone and the control group. Statistical analysis using a one-way ANOVA was performed after validation of the normality and homoscedasticity of the data, this ANOVA revealed that the percentage of wound closure was different depending on the group, with a p-value of 0.0004256.

In order to identify the differences between each groups a post-hoc analysis was performed using a Tukey's HSD test. The control group had significantly lower percentage of wound closure (55.1%± 1.347219) then the group exposed to only fluoxetine (75.55% ± 7.52) with p-value=0.00078, this is relevant with results from the two previous sections of the *ex-vivo* chapter.

Biopsies treated with only ketanserin, and biopsies treated with fluoxetine and ketanserin showed no significant difference between them (53.07% ± 2.02 and 63.4 ± 2.8 average wound closure respectively) with p-value=0.111. Those two groups were also not statistically different from the control group (p-value=0.985 and p-value=0.172 respectively) and had an average percentage of wound closure significantly lower than the fluoxetine-exposed group (p-value=0.005 and p-value=0.0109 respectively).

Groups with statistically different percentages of wound closure were classified as groups A and B in Figure 6.6.

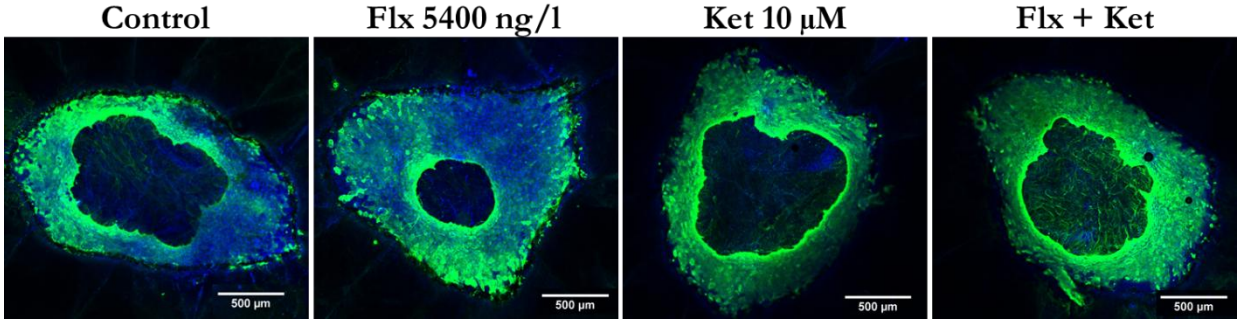

Figure 6.5: Representative images of the effects of fluoxetine and ketanserin on ex-vivo human skin biopsies. *Images showing keratin 14 (K14, green) expression and nuclear staining (DAPI, blue) in control, fluoxetine-exposed (5400 ng/l) and ketanserin-treated samples (10 µM) as well as samples exposed to a combination of both drugs (5400 ng/l of fluoxetine + 10 µM of ketanserin). The scale bar represents 500 µm.*

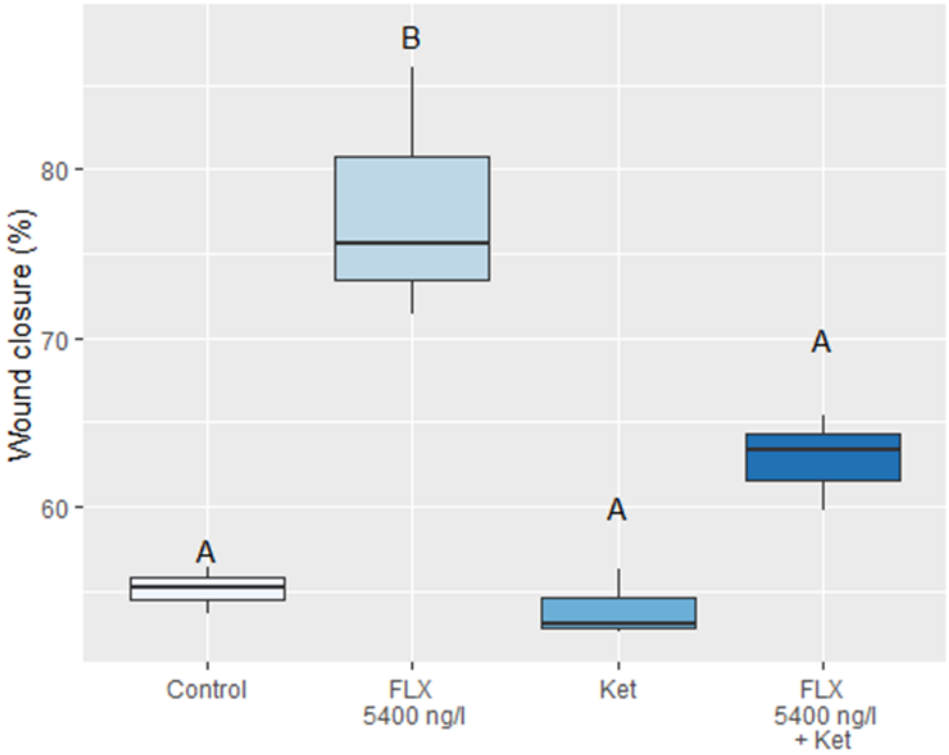

Figure 6.6: Boxplot of the percentage of wound closure after 48 hours of exposure to fluoxetine, ketanserin or combination of both. *The x-axis represents the conditions: fluoxetine (5400 ng/l) in combination with or without ketanserin (10 µM) and ketanserin alone. The y-axis shows the percentage of wound closure. X-axis not to scale. Each box represents the interquartile range (IQR), where the top and bottom of the box indicate the 75th and 25th percentiles, respectively. The horizontal line within each box represents the median. The whiskers extend to the minimum and maximum values, excluding outliers, and the dots represent individual data points. Groups labelled with different letters (A, B) indicate statistically significant differences between conditions ($p < 0.05$). Conditions sharing the same letter are not significantly different from each other. Specifically, Control, ketanserin, and fluoxetine+Ketanserin (A) are not significantly different from each other but differ significantly from fluoxetine (B). Statistical analysis was performed using one-way ANOVA followed by Tukey's post hoc test (n=4 biological replicates per condition).*

6.5 Discussion

This chapter aimed to investigate the effects of fluoxetine on wound healing using an *ex-vivo* human skin model, focusing on the role of serotonin signalling pathways. The results demonstrated that fluoxetine significantly enhanced wound closure, aligning with the hypothesis that fluoxetine may influence tissue repair processes through serotonin signalling. Additionally, serotonin antagonists, mirtazapine and ketanserin, were employed to test whether blocking serotonin receptors could reverse the effects observed with fluoxetine. This discussion explores the significance of these findings, integrates and compares them with previous literature, and highlights the potential clinical implications and limitations.

6.5.1 Fluoxetine increases wound-healing in *ex-vivo* samples

To assess the impact of fluoxetine on wound healing, two concentrations were selected: 2500 ng/l and 5400 ng/l. These concentrations were chosen based on upper limits reported for environmentally relevant fluoxetine levels. Several studies have used these as benchmark levels to investigate the effects of fluoxetine in various biological systems, demonstrating their relevance for environmental exposure scenarios. For example, on study looking at the chronic effects of fluoxetine on *Danio rerio* used fluoxetine concentrations ranging between 0.4 to 3600 ng/l (Correia et al., 2022), another study looking at the dose-dependent effects of fluoxetine on boldness in male Siamese fighting fish used 5000 ng/l as their environmentally relevant concentration. Other various studies used environmentally relevant concentrations of fluoxetine ranging from 10 to 10 000 ng/l to look at its impact on different models(Al Shuraiqi et al., 2021; Guler and Ford, 2010; Weinberger and Klaper, 2014). By employing these concentrations, our aim was to evaluate the impact of fluoxetine on wound healing within a realistic exposure range, which adds ecological and translational relevance to the findings.

My findings indicate that fluoxetine significantly enhances wound healing, as demonstrated by increased epithelial coverage and wound closure in treated biopsies compared to controls. This is consistent with my previous *in-vitro* work using HaCaT cells, where fluoxetine promoted keratinocyte proliferation and migration. The use of an *ex-vivo* model offers a more physiologically relevant environment by retaining the three-dimensional architecture and cell diversity of human skin, allowing to observe the effects of fluoxetine in a setting that closely mimics clinical conditions (Wilkinson et al., 2021).

This role of fluoxetine in promoting wound healing has been further supported by several studies. For instance, Farahani et al. investigated the effects of fluoxetine and paroxetine on wound healing in stressed rat models by administering these SSRIs systemically for 14 days. They found that fluoxetine-treated rats exhibited a significant increase in fibroblast proliferation and epithelialisation compared to controls, indicating that these SSRIs promoted the healing process. The study also highlighted that fluoxetine modulated levels of pro-inflammatory cytokines, such as IL-1, which are crucial during the inflammatory phase of wound healing, suggesting that the effects of fluoxetine are partly mediated through enhancing immune cell recruitment and activity, ultimately accelerating tissue repair (Farahani et al., 2007). Similarly, Yüksel et al. conducted a study using rat excision wound models to evaluate

the impact of fluoxetine on wound healing. They administered fluoxetine daily for two weeks and observed a marked increase in fibroblast proliferation and wound closure rates compared to the control group. The study further demonstrated that fluoxetine treatment led to enhanced collagen deposition, which is essential for tissue strength and integrity during the repair process. Additionally, the authors noted that fluoxetine modulated inflammatory responses by reducing pro-inflammatory cytokine levels, indicating that serotonin signalling plays a vital role in balancing the inflammatory and proliferative phases of wound healing, thus promoting optimal tissue regeneration (Yuksel et al., 2014). My *ex-vivo* findings expand upon these studies by demonstrating that the effects of fluoxetine are not limited to *in-vitro* or animal models but are also effective in human skin biopsies.

My results suggest that serotonin-related signalling may influence cellular behaviour and inflammatory responses during wound healing, although the precise mechanisms remain to be fully validated in this *ex-vivo* context. In the wound healing process, particularly during the inflammatory and proliferative phases, the role of serotonin has been previously described. For example, one study found that serotonin receptor expression is significantly upregulated in immune cells, such as macrophages and lymphocytes, within inflamed tissue sites (Zhang et al., 2001). This upregulation facilitates the recruitment of these immune cells to the wound area, which is crucial for initiating the healing response. The recruited immune cells release pro-inflammatory cytokines like IL-1 and TNF-α, which not only help to clear pathogens but also activate the subsequent stages of wound healing by promoting fibroblast activity and extracellular matrix deposition (Alstergren et al., 1999). Similarly, Zhang et al. observed that the activation of serotonin receptors enhanced the production of these cytokines, further supporting their role in the inflammatory and early proliferative phases of wound healing. Their study indicated that serotonin signalling modulates the behaviour of immune cells, enhancing their ability to sustain an inflammatory response critical for the formation of new tissue. Also, during the proliferative phase, serotonin has been shown to regulate fibroblast proliferation and extracellular matrix (ECM) deposition. Seuwen et al. demonstrated that serotonin significantly induces fibroblast proliferation by activating specific serotonin receptors, leading to the upregulation of fibroblast growth factor-2 (FGF-2) secretion. FGF-2 is a crucial component that facilitates cell proliferation, angiogenesis, and ECM formation, all vital for wound healing (Seuwen et al., 1988). The study also highlighted that serotonin stimulates the production of essential ECM components like collagen, which are necessary for maintaining tissue strength and providing a scaffold for re-epithelialisation (Seuwen et al., 1988).

My *ex-vivo* findings align with these studies, as fluoxetine treatment led to enhanced epithelial coverage. However, the mechanism may not depend solely on serotonin levels. While keratinocytes are capable of producing serotonin (Goodwin et al., 2017; Schallreuter et al., 2012), and serotonin may be present in foetal bovine serum (Chávez et al., 2017), direct activation of serotonin receptors by fluoxetine itself is also plausible. As shown in earlier chapters, fluoxetine can function as a receptor agonist or antagonist independent of serotonin availability (Ni and Miledi, 1997; Peng et al., 2014). Therefore, the observed effects in this tissue model could reflect either serotonin-mediated signalling or direct modulation of receptor activity by fluoxetine. This dual possibility must be considered when interpreting the mechanism behind improved wound closure.

6.5.2 Role of serotonin signalling in how fluoxetine impacts wound-healing *ex-vivo*

To confirm the role of serotonin pathways in fluoxetine-mediated wound healing, serotonin blockers mirtazapine and ketanserin were utilised. The divergent outcomes with these blockers provide essential insights into the complexity of the role of serotonin in wound healing. The concentration of mirtazapine used in this study was 0.15 mg/l, chosen to align with plasma concentrations observed in therapeutic use. Timmer et al. reported that therapeutic doses of mirtazapine (15-45 mg/day) yield plasma levels ranging from 0.05 to 0.1 mg/l (Timmer et al., 2000), additionally, Kirkton et al. identified a therapeutic range of 0.18 to 0.2 mg/l (Kirkton and McIntyre, 2006), further supporting the relevance of our selected dose for *ex-vivo* application. However, the differing effects observed, with ketanserin reversing the impact of fluoxetine while mirtazapine did not, suggest that receptor specificity, compound stability, or off-target effects may have influenced the outcomes. Although both drugs are serotonin receptor antagonists, their distinct pharmacological profiles and metabolic behaviours highlight the need for caution in interpreting these results as direct evidence of serotonin signalling.

Mirtazapine, an atypical antidepressant that antagonises the 5-HT2A and 5-HT2C receptors, was expected to reverse the effects of fluoxetine if serotonin signalling was involved. However, mirtazapine did not significantly alter wound closure when administered alone or in combination with fluoxetine. This outcome was unexpected, as the pharmacological profile of mirtazapine profile suggests it could inhibit serotonin pathways involved in wound healing.

One possible explanation is that the observed effects of fluoxetine in this system may not be fully dependent on serotonin signalling. Given the broad pharmacological profile of mirtazapine, it is possible that off-target effects unrelated to serotonin pathways limited its specificity in this model. Mirtazapine not only antagonises 5-HT2A and 5-HT2C receptors, but also interacts with noradrenergic and histaminergic systems, and antagonises central alpha-2 adrenergic receptors (Anttila and Leinonen, 2001). These neurotransmitter systems may not play significant roles in keratinocyte function, which could explain the limited impact observed. In addition, mirtazapine undergoes extensive metabolism via cytochrome P450 enzymes, potentially contributing to variability in its efficacy depending on tissue type and receptor context. Altogether, this makes mirtazapine a challenging tool for specifically interrogating serotonin signalling in skin tissue.

Another contributing factor for these unexpected results may be the stability of mirtazapine under experimental conditions. Research by Fang et al. demonstrated that mirtazapine is sensitive to light exposure and temperature fluctuations, which can lead to degradation over time. The study found that when mirtazapine was stored at room temperature and exposed to light, its chemical structure broke down, significantly reducing its pharmacological activity. Conversely, storing mirtazapine in dark, temperature-controlled environments (below 8°C) preserved its integrity (Fang et al., 2012). Similarly, Fitzpatrick et al. investigated the impact of formulation and storage practices on the stability of mirtazapine. They found that high humidity levels or non-airtight containers led to significant chemical degradation of the drug, diminishing its efficacy. The study also highlighted that brief UV light exposure could alter the pharmacological properties of mirtazapine properties, making it less effective. They. emphasised the importance of using light-resistant packaging and maintaining low-humidity, temperature-controlled storage to preserve the drug's effectiveness (Fitzpatrick et al., 2018). Given these findings, experimental conditions such as prolonged exposure to light, humidity, or elevated temperature in the current study may have reduced the bioactivity of mirtazapine, limiting its ability to antagonise serotonin receptors effectively.

This suggests that mirtazapine may not be the most reliable candidate for assessing the role of serotonin in wound healing, as its complex pharmacological interactions may not provide the specificity needed for clear conclusions. Exploring other serotonin antagonists with more selective mechanisms may offer a more precise understanding of the pathways involved. Future studies should focus on optimising the storage and handling conditions for mirtazapine to maintain its efficacy and consider alternative, more stable antagonists for exploring the role of serotonin in tissue repair.

Given the results with mirtazapine, ketanserin, a well-documented 5-HT2A receptor antagonist, was employed. Ketanserin has been extensively used in wound healing studies to modulate inflammatory responses and fibroblast activity. For instance, Quatresooz et al. investigated the effects of ketanserin in diabetic leg ulcers, a model characterised by impaired microcirculation and chronic inflammation. They found that ketanserin application significantly improved wound healing by enhancing blood flow and reducing inflammation in the affected tissues. The study highlighted the drug's capacity to modulate microcirculation, leading to better oxygen and nutrient delivery to the wound site, which is critical for effective tissue repair. These results underscore the therapeutic potential of ketanserin in wounds where inflammation and poor blood supply are predominant issues (Quatresooz et al., 2006). My study aligns with these findings, as ketanserin treatment successfully reversed the enhancement of wound closure by fluoxetine in my *ex-vivo* model. This suggests that the antagonistic effect of ketanserin on serotonin pathways effectively counteracts the positive influence of fluoxetine on wound healing, providing evidence that the effects of fluoxetine are indeed serotonin-mediated. Similarly, Hong et al. explored the anti-inflammatory properties of ketanserin and its impact on wound healing mechanisms. Their study demonstrated that ketanserin effectively reduced inflammation by targeting serotonin-mediated pathways, particularly those involving NF-κB and MAPK signalling. By inhibiting these pathways, ketanserin was shown to decrease the release of pro-inflammatory cytokines, thus creating a more conducive environment for wound healing. These findings suggest that the anti-inflammatory effects of ketanserin play a pivotal role in its ability to modulate wound healing processes. In my study, the antagonistic action of ketanserin led to a noticeable reduction in wound closure when combined with fluoxetine, which aligns with Hong et al.'s findings on its anti-inflammatory properties. The reduction in wound closure in the fluoxetine–ketanserin combination indicates that ketanserin likely inhibits the pathways that fluoxetine activates, supporting the involvement of serotonin receptors in mediating the effects of fluoxetine on wound healing. However, given the pharmacological complexity of ketanserin and fluoxetine, the possibility of off-target effects influencing the results cannot be ruled out. Both compounds interact with additional receptor systems and signalling pathways, and further validation using more selective tools or genetic approaches would be required to definitively confirm serotonin-specific mechanisms.

These findings collectively demonstrate that the modulation of serotonin pathways can have dual outcomes depending on the experimental conditions and receptor targets. While fluoxetine

can enhance wound healing through serotonin receptor activation, the antagonistic action of ketanserin on the same pathways results in the inhibition of these beneficial effects. This duality underscores the complexity of SSRI mechanisms in tissue repair, where receptor-specific interactions play a critical role in determining the overall outcome of treatment. By integrating the results from my study with those of Quatresooz et al., and Hong et al, a more comprehensive understanding of the role of serotonin signalling in wound healing emerges, highlighting the importance of context and receptor specificity in therapeutic applications.

6.5.3 Clinical implications, limitations, and future directions

The consistency between my *ex-vivo* results and earlier *in-vitro* findings suggests that the mechanisms induced by fluoxetine-exposure are conserved across different experimental models. The use of *ex-vivo* human skin biopsies allows for the preservation of cellular diversity and tissue architecture, providing a more clinically relevant model for studying drug effects on wound healing. This is crucial for translating laboratory findings into therapeutic strategies applicable in clinical settings, as *ex-vivo* models bridge the gap between in-vitro studies and in-vivo clinical outcomes. The variability between the responses to mirtazapine and ketanserin highlights the importance of drug stability and receptor specificity. The consistent effects of ketanserin suggest that it is a reliable tool for investigating the role of serotonin in tissue repair, while the variability of mirtazapine indicates a need for further optimisation. Exploring additional serotonin antagonists with higher specificity for relevant receptors could provide clearer evidence of the mechanisms of fluoxetine in wound healing. Furthermore, understanding the pharmacokinetics and stability of these drugs in various biological environments is crucial. Studies like those by Rikki et al. emphasise the need to control storage conditions and formulations to maintain drug efficacy (Fitzpatrick et al., 2018). Future research should focus on optimising these parameters for mirtazapine and exploring its effects under controlled conditions to determine its true impact on wound healing.

To deepen our understanding of the role of fluoxetine and serotonin, molecular analyses such as transcriptomics and proteomics on *ex-vivo* human skin biopsies should be incorporated. Identifying specific genes or proteins influenced by fluoxetine and serotonin blockers would offer a comprehensive view of the pathways involved and enable the development of targeted therapies. Comparing the effects of fluoxetine with other SSRIs, such as sertraline or

paroxetine, across different models (e.g., diabetic wounds or chronic ulcers) would also provide insights into the broader applicability of serotonin modulation in wound healing.

Despite the promising findings, several limitations must be addressed. The variability in donor skin samples and the sample size may influence the reproducibility of results. Standardising clinical parameters for donor skin and expanding the study cohort would help validate these findings further. Additionally, while my study used fluoxetine concentrations based on previous studies on other models, it is worth noting that these concentrations are significantly lower than those used in studies in human (Nguyen et al., 2019; Yoon et al., 2021) where much higher doses were tested. The use of these lower, environmentally relevant concentrations in my study not only provides ecological relevance but also highlights the potential for therapeutic applications at lower doses, minimising potential side effects. This approach may offer an innovative pathway for developing safe and effective treatments for wound healing. Further exploration of this lower dose range could clarify the dose-dependent effects of fluoxetine and determine its optimal therapeutic window.

Chapter 7: General Discussion

7.1 Overview of findings and implications

This study investigates the potential of fluoxetine as a therapeutic agent in wound healing, particularly at environmentally relevant concentrations (62.5-5400 ng/l). The results indicate that fluoxetine enhances keratinocyte proliferation, which is critical for effective wound closure and tissue regeneration. By focusing on the cellular mechanisms underlying this effect, the research provides valuable insights into how fluoxetine might be utilised in clinical settings for improving wound healing outcomes.

The exploration of molecular pathways revealed significant activation of serotonin signalling in keratinocytes exposed to fluoxetine. This was confirmed through the use of the serotonin antagonist ketanserin, which demonstrated that the wound healing effects of fluoxetine are likely mediated through its action on serotonin receptors. These findings not only highlight the pharmacological efficacy of fluoxetine in promoting cellular activities essential for wound repair but also underscore the importance of serotonin in this process.

In addition to its therapeutic implications, the persistence of fluoxetine in the environment raises critical concerns. While this study primarily focuses on its benefits in wound healing, it is essential to recognise the broader context of the presence of fluoxetine in aquatic systems. The increasing detection of fluoxetine and other SSRIs in water bodies suggests a need for enhanced monitoring to assess potential risks to aquatic ecosystems. Although this project did not directly address the ecological consequences of fluoxetine exposure in non-target organisms, the environmental implications warrant attention and further investigation.

Overall, this chapter will elaborate on the cellular mechanisms involved in the action of fluoxetine on keratinocytes and its effects observed in *ex-vivo* models, its potential therapeutic applications in chronic wound management, and the necessity for continued environmental surveillance of SSRIs. The subsequent sections will provide a detailed analysis of the findings, contextualised within the existing body of literature, to fully capture the multifaceted implications of this research.

7.2 Mechanisms of action of fluoxetine in wound healing

7.2.1 Integrated pathways of proliferation, metabolism, and cellular resilience in fluoxetine-mediated wound repair

This study demonstrates that fluoxetine, even at environmentally relevant low concentrations, enhances keratinocyte proliferation and accelerates wound healing through a network of cellular pathways rather than a single dominant mechanism. The combined findings from scratch assays, RNAseq, and pathway analyses suggest that fluoxetine engages multiple systems that collectively contribute to wound repair. The investigation into the effects of fluoxetine on wound healing elucidates a multifaceted role in keratinocyte proliferation and the modulation of key cellular pathways. Through comprehensive analysis of phosphoproteomic data and validation in *ex-vivo* models, this study demonstrates that fluoxetine enhances wound repair mechanisms through a combination of kinase signalling activation and effective protein regulation.

Initial insights from the scratch assays indicated the role of fluoxetine in promoting wound closure, as fluoxetine-exposed keratinocytes consistently showed increased proliferation, closing wound gaps more effectively than unexposed cells. This enhancement of cell proliferation directly supports early wound healing, providing the groundwork to explore how the molecular effects of fluoxetine facilitate keratinocyte function.

Further molecular insights from RNAseq identified the influence of fluoxetine on a variety of gene expression changes linked to cellular proliferation and metabolic regulation. Several upregulated genes were associated with cell growth and energy production, indicating that fluoxetine optimises conditions necessary for keratinocyte survival and replication. Among the affected pathways, serotonin signalling was one notable component, though it likely works in tandem with other systems rather than serving as the central driver. This serotonin-related modulation hints at the known pharmacological interactions of fluoxetine, yet here it seems to act as part of a larger, multi-pathway response.

Fluoxetine exposure resulted in significant phosphorylation of several key proteins within the ERK/MAPK signalling pathway, which is critical for mediating cellular responses to growth stimuli. The activation of ERK1/2 suggests that fluoxetine facilitates cell proliferation and survival, enabling keratinocytes to respond more robustly to the demands of wound repair.

Figure 7.1 illustrates this pathway's role, highlighting the ERK/MAPK pathway's activation as part of the effects of fluoxetine on keratinocyte proliferation and tissue growth, which are essential for wound healing. Additionally, the use of protein microarrays and western blotting analysis revealed phosphorylation changes in other kinases, including MSK1 and GSK3. The phosphorylation of MSK1, involved in cell survival and proliferation, indicates that fluoxetine may enhance the survival of keratinocytes under stress conditions, while GSK3 modulation suggests a role in energy metabolism and regulation of cellular functions necessary for wound healing. The HIPPO pathway, also activated by fluoxetine, further supports cell proliferation and survival by promoting growth and inhibiting apoptosis, phosphorylation of key components within this pathway, such as MST1/2 and LATS1/2, underscores the influence of fluoxetine in maintaining cellular viability during early repair stages, an effect illustrated in Figure 7.1. This activation of the HIPPO pathway, together with ERK/MAPK, suggests that fluoxetine coordinates multiple signalling mechanisms to support wound healing effectively.

The inclusion of serotonin signalling pathways is particularly noteworthy, as fluoxetine, an SSRI, enhances wound healing partly through serotonin receptor activation, which plays a crucial role in keratinocyte migration and immune modulation. This integration of serotonin signalling is confirmed by the use of serotonin antagonists like ketanserin in this study, which mitigated the effects of fluoxetine, highlighting the pivotal function of serotonin in coordinating cellular activities during wound repair. In Figure 7.1, the serotonin pathway is illustrated as central in the multi-pathway action of fluoxetine, positioning it as an initiator of downstream molecular effects that support wound healing. Although serotonin may be present in culture via endogenous production by keratinocytes or from components in FBS it was not directly measured in this study. As such, an alternative but not mutually exclusive explanation is that fluoxetine directly binds to serotonin receptors to trigger intracellular signalling cascades. Studies have shown that fluoxetine can act as an agonist or antagonist at specific 5-HT receptor subtypes, including 5-HT2A, 5-HT2B, 5-HT2C, and 5-HT3, even in the absence of serotonin (Breitinger et al., 2001; Eisensamer et al., 2003; Ni and Miledi, 1997; Peng et al., 2014). This direct receptor engagement could activate the same downstream pathways (e.g., PI3K/Akt, MAPK/ERK) typically stimulated by serotonin. Therefore, whether fluoxetine exerts its effects by increasing serotonin availability or by acting directly on serotonin receptors, these outcomes can still be understood within the framework of serotonin receptor-mediated signalling. Additionally, the modulation of metabolic pathways by fluoxetine is crucial in facilitating the energy demands of wound healing. RNAseq data revealed

upregulation of mitochondrial and ATP production pathways, suggesting that fluoxetine supports the energetic demands of rapidly proliferating keratinocytes. By facilitating increased energy availability, fluoxetine enables keratinocytes to maintain the metabolic flexibility required for wound repair, especially in resource-constrained environments typical of healing tissue. Additionally, the modulation of the ubiquitin-proteasome system by fluoxetine provides a potential mechanism for maintaining protein quality during cellular proliferation. By promoting the degradation of damaged proteins, fluoxetine helps sustain keratinocyte functionality, preventing the buildup of cellular stress that can arise during rapid cell growth.

The role of fluoxetine in enhancing cellular resilience aligns with its broader impact on cellular health, aiding keratinocyte activity through multiple phases of the wound healing process. Notably, the observed effects of fluoxetine appear to be time-dependent: early impacts primarily engage cell growth pathways, while extended exposure broadens its influence to include metabolic and protein regulatory systems. This temporal modulation suggests a coordinated response, where fluoxetine adapts its cellular engagement over time to meet the specific needs of each stage in wound repair.

In the *ex-vivo* human skin model, the improvements in wound closure corroborated the molecular findings, indicating that the effects of fluoxetine observed in simpler cell systems translate effectively to more complex tissue environments. The *ex-vivo* model provided valuable insights into how fluoxetine operates within the layered architecture of skin, where it can interact with multiple cell types and extracellular matrix components. The ability of fluoxetine to enhance keratinocyte function and support wound closure in this context highlights its translational relevance for clinical applications. The integration of findings from the phosphoproteomic analysis with the functional outcomes in the *ex-vivo* model suggests that fluoxetine operates through a multifactorial approach, engaging multiple pathways that collectively contribute to wound healing.

Together, the pathways illustrated in Figure 7.1 reflect the synergy between increased kinase activity, serotonin-receptor signalling, and metabolic support. This multi-pathway action of fluoxetine positions it as a promising candidate for low-dose, localised therapies that could effectively target chronic wounds. Such a therapeutic approach, by minimising systemic exposure, addresses a critical need in wound management while providing a targeted solution for cell proliferation, survival, and energy metabolism. Coordinated engagement of signalling by fluoxetine, metabolic, and regulatory pathways, as depicted in Figure 7.1, suggests it could overcome key obstacles in chronic wound healing, enhancing tissue repair through a robust network of cellular responses.

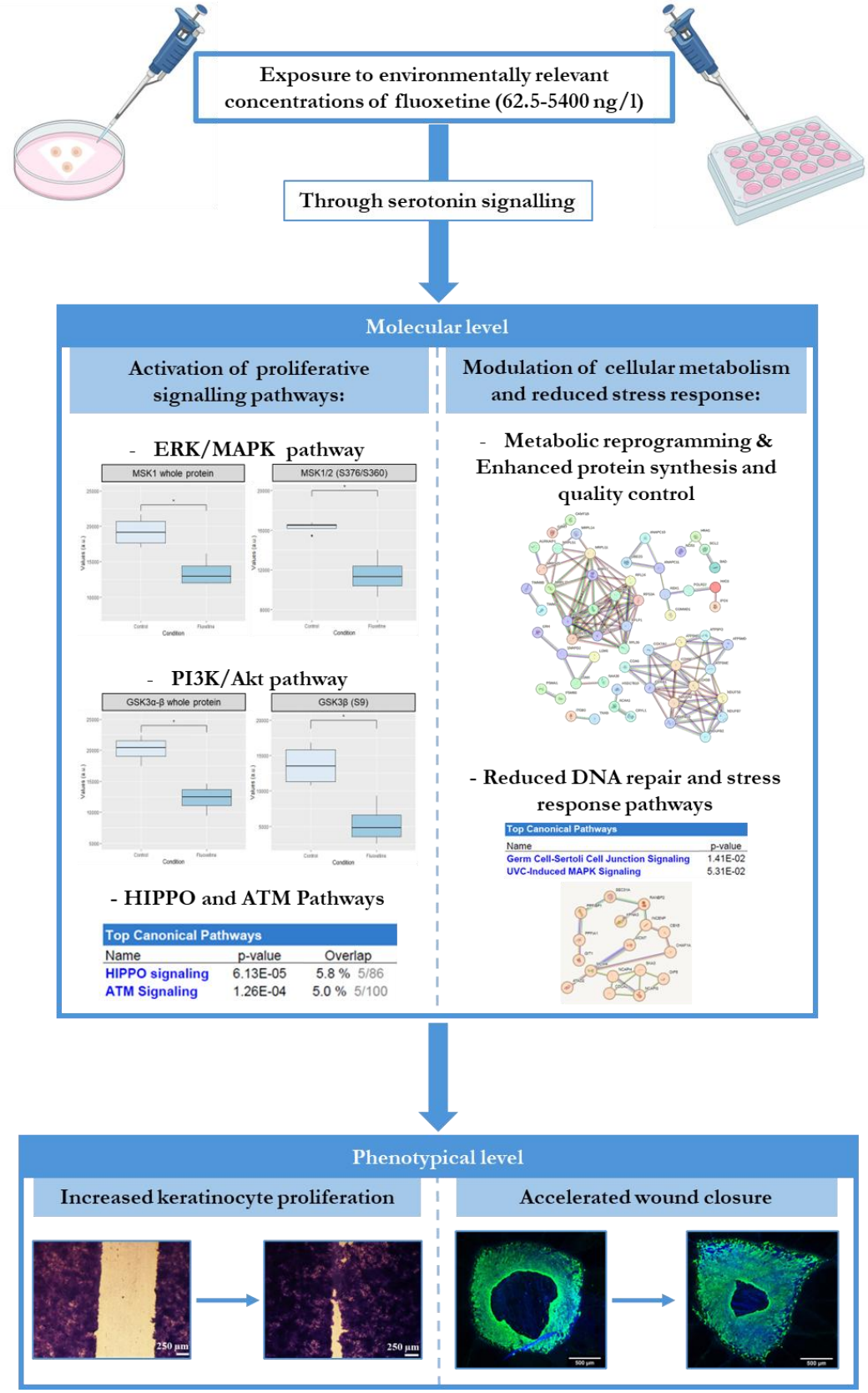

Figure 7.1: Effects of fluoxetine on wound healing at phenotypical and molecular levels. *Overview of the role of fluoxetine in promoting keratinocyte proliferation, wound closure, and activation of key signalling pathways (ERK/MAPK, HIPPO, ATM) involved in cell growth, metabolism, and protein regulation.*

7.2.2 Comparison with key literature

Nguyen et al. (2018): Topical fluoxetine as a novel therapeutic that improves wound healing in diabetic mice

Nguyen et al. investigated the impact of fluoxetine on wound healing, focusing on its ability to enhance keratinocyte migration and alter the local inflammatory environment (Nguyen et al., 2019). Using both *in vitro* and *in vivo* models, their study demonstrated that fluoxetine facilitates wound closure by promoting keratinocyte migration and reducing inflammation. In their *in vitro* scratch assay, Nguyen et al. showed that fluoxetine significantly increased neonatal human keratinocytes migration, enabling more extensive wound coverage by migrating cells. This migration-promoting effect was observed at the tested fluoxetine concentration (3000 to 300,000 ng/l) and was attributed to serotonin signalling pathways, as fluoxetine functions as a selective serotonin reuptake inhibitor.

In vivo, fluoxetine similarly improved wound closure in a diabetic mouse model, not only by enhancing keratinocyte migration but also by shifting the immune profile within the wound site toward a less inflammatory state. Lower levels of pro-inflammatory cytokines were observed in fluoxetine-treated wounds, suggesting that fluoxetine supports a balanced immune response conducive to faster tissue repair. Nguyen et al. proposed that the dual action of fluoxetine, promoting keratinocyte migration and moderating inflammation, creates an optimal environment for wound healing, which is particularly advantageous in cases of chronic wounds where excessive inflammation impedes effective repair.

Yoon et al. (2021): Topical fluoxetine as a potential nonantibiotic adjunctive therapy for infected wounds

Yoon et al. (2021) investigated the therapeutic potential of fluoxetine in wound healing, particularly focusing on its effects in infected wound models (Yoon et al., 2021). The study used *in vitro*, *in vivo*, and *ex-vivo* models, including cultured human keratinocytes, *ex-vivo* human skin, and a murine wound infection model, to evaluate the effects of fluoxetine on re-epithelialisation, biofilm reduction, and immune modulation. In addition to its known antimicrobial activity, the study explored how fluoxetine affects keratinocyte migration and shifts the wound environment from pro-inflammatory to anti-inflammatory, making it a promising non-antibiotic adjunctive therapy for chronic wounds.

In their *ex-vivo* human skin model, Yoon et al. observed that daily topical application of 0.2% fluoxetine significantly improved wound re-epithelialisation and reduced biofilm formation of

Staphylococcus aureus, a common pathogen in chronic wounds. The treatment decreased pro-inflammatory cytokines, such as IL-6 and TNF-α, and upregulated keratinocyte markers associated with migration, including keratin 17 (K17). These molecular changes contributed to a more pro-reparative wound environment that supported wound closure. Additionally, fluoxetine diminished the expression of key virulence factors in *S. aureus*, lowering biofilm mass and pathogen viability, which are major barriers to effective wound healing.

In their *in vivo* murine wound model, fluoxetine further demonstrated its efficacy by enhancing re-epithelialisation and reducing bacterial translocation to systemic sites, like the spleen, indicating its potential to contain infection locally. The study's findings highlighted the capacity of fluoxetine to improve wound healing outcomes by promoting keratinocyte migration, reducing inflammatory markers, and mitigating infection-related barriers to wound closure.

Sadiq et al. (2018): The role of serotonin during skin healing in post-thermal injury

The study by Sadiq et al. examined the role of serotonin in wound healing, using both *in vitro* and *in vivo* models to explore how fluoxetine impacts key cellular processes such as proliferation, migration, and differentiation in keratinocytes and fibroblasts (Sadiq et al., 2018). The study specifically addressed how serotonin signalling influences wound repair and the effects of inhibiting this pathway with fluoxetine adding valuable insights into the dual roles of serotonin in wound closure.

In the *in vitro* component of their study, Sadiq et al. used cultured human fibroblasts and neonatal keratinocytes to assess the influence of serotonin, fluoxetine, and ketanserin migration and proliferation. Serotonin, when applied at a concentration of 10^{-8}M, significantly promoted cell survival, reduced apoptosis, and stimulated keratinocyte migration and proliferation. In scratch assays, serotonin-treated cells demonstrated faster scratch closure compared to controls, highlighting the role of serotonin in accelerating wound closure. Conversely, exposure to fluoxetine at the same concentration markedly inhibited these serotonin-mediated effects. Fluoxetine exposure reduced keratinocyte migration, resulting in slower scratch closure, suggesting that the inhibition of serotonin reuptake by fluoxetine impedes the natural healing-promoting effects of serotonin on these cells. Additionally, ketanserin was found to have similar effects as fluoxetine, further indicating that the wound healing process is driven primarily through 5-HT2A receptors. These findings imply that serotonin plays an essential role in maintaining wound repair mechanisms, while SSRIs, by inhibiting serotonin availability, may disrupt these processes.

In the *in vivo* component, Sadiq et al. used a mouse model to assess the effects of fluoxetine on wound healing following scald injuries. Mice with burn wounds were systemically administered fluoxetine and ketanserin at a dose of 10 mg/kg. The untreated control group, which retained natural serotonin signalling, exhibited notably smaller wounds and faster re-epithelialisation, as well as a well-organised granulation tissue structure, indicating efficient wound repair. In contrast, fluoxetine-treated mice showed a significant delay in wound closure, evidenced by larger wound areas, slower epithelial migration, and reduced cellular density within granulation tissues. The presence of fluoxetine correlated with premature keratinocyte differentiation, indicating that while serotonin promotes early-stage keratinocyte migration and proliferation, fluoxetine disrupts these pathways, potentially by causing keratinocytes to enter differentiation prematurely. Additionally, the study underscored the importance of serotonin receptor activity, particularly the 5-HT2A receptor, in modulating these effects. Sadiq et al. concluded that the influence of serotonin on wound healing occurs through 5-HT receptor-mediated pathways, with the 5-HT2A receptor playing a central role in maintaining cell migration, adhesion, and proliferation essential for wound closure. The similarity in the inhibitory effects observed with both fluoxetine and ketanserin underscores the critical role of serotonin and suggests that therapeutic strategies involving SSRIs could unintentionally interfere with wound repair by inhibiting this pathway.

Sadiq et al. thus provides a comprehensive analysis of the beneficial effects of serotonin on wound healing and the inhibitory impact of SSRIs like fluoxetine. While serotonin itself promotes wound closure through receptor-driven mechanisms, the reuptake inhibition by fluoxetine impairs these cellular responses, suggesting that SSRIs may negatively affect wound healing in clinical settings.

Comparative Synthesis and Implications:

The findings of this thesis, together with those of Sadiq et al. (2018), Yoon et al. (2021), and Nguyen et al. (2018), deepen the understanding of the mechanisms of fluoxetine in wound healing, revealing both similarities and context-specific effects. Across studies, fluoxetine has shown promise in enhancing cellular activities crucial for wound repair. For example, both this thesis and Yoon et al. observed enhanced keratinocyte function; however, my project demonstrated increased cell proliferation, while Yoon et al. focused on migration and re-epithelialisation in infected wound models. Similarly, Nguyen et al. highlighted the anti-

inflammatory benefits of fluoxetine, which support wound closure in a diabetic context, aligning with the immunomodulatory aspects seen in my study.

Differences between these studies primarily arise from the concentrations of fluoxetine used, the model environments, and methodological approaches. While Yoon et al. and Nguyen et al. employed higher concentrations of fluoxetine, relevant to pharmacological applications, this thesis uniquely focused on environmentally relevant, low-dose concentrations, demonstrating that fluoxetine can support wound healing without the potential side effects associated with higher doses. Although some of the higher concentrations used in this thesis (5400 ng/l in ex-vivo models) exceed average environmental levels, mid-range doses such as 540 ng/l, used in the transcriptomic analyses, closely reflect concentrations observed in contaminated wastewater effluents or surface water hotspots (Salgado et al., 2011; Shraim et al., 2017). Given that these concentrations elicited measurable biological effects, the findings remain highly relevant to environmental exposure scenarios. Importantly, while many of these studies attribute the effects of fluoxetine to increased serotonin signalling, recent evidence, including data discussed in this thesis, suggests that fluoxetine can directly modulate serotonin receptor activity. It may act as a functional agonist or antagonist at 5-HT2A, 5-HT2B, 5-HT2C and 5-HT3 receptors, even in the absence of measurable serotonin in the culture system (Breitinger et al., 2001; Eisensamer et al., 2003; Ni and Miledi, 1997; Peng et al., 2014). This receptor-specific engagement could account for the observed wound-healing effects and helps reconcile discrepancies between in vitro and in vivo findings.

Together, these studies suggest that the role of fluoxetine in wound healing likely operates through a multifaceted mechanism that includes serotonin receptor activation, MAPK/ERK signalling, and inflammatory modulation. The unique focus of this thesis on low-dose fluoxetine provides critical insights relevant to both therapeutic and environmental contexts. The effectiveness of fluoxetine at these lower doses supports its potential for safe, localised wound therapy, with minimal systemic impact, making it suitable for prolonged treatment scenarios. Additionally, by demonstrating bioactivity at environmentally relevant concentrations, this study underscores the importance of monitoring fluoxetine in aquatic systems to mitigate potential ecological impacts on non-target organisms.

7.3 Potential therapeutic and environmental implications of low-dose fluoxetine exposure

7.3.1 Fluoxetine as a potential treatment for chronic wounds

Chronic wounds present a significant challenge in clinical management due to prolonged healing times and the complexities involved in restoring tissue integrity. Current wound healing therapies face numerous limitations, especially in the context of chronic wounds, which can persist for months or even years without adequate closure, the treatment landscape includes a variety of approaches, ranging from traditional dressings to advanced bioengineered solutions, but each therapy presents significant challenges in terms of cost, effectiveness, and accessibility.

Table 7.1, adapted from Gardikiotis et al., summarises current wound healing therapies, detailing their mechanisms, advantages, and limitations. This table highlights gaps in existing treatments, such as high costs, limited efficacy, and accessibility issues, especially for chronic wound care. Conventional therapies, including biopolymer dressings, PRP derivatives, growth factors, and topical antibiotics, often target singular aspects of wound healing (e.g., creating a moist environment, modulating inflammation, or controlling infection).

Treatment type	Mechanism of Action	Benefits	Limitations
Commercial dressings (e.g., Aquacel, Kaltostat, Carboflex)	Provide a moist environment, promote autolytic debridement, prevent bacterial contamination	Readily available and easy to use; waterproof and impermeable; highly absorbent; may be used on infected wounds	May adhere to wound bed; not effective for moist wound healing; frequent changes needed, increasing costs; potential residue can cause infection
Biopolymer dressings	Bioactive materials interact with wound tissue, supporting healing processes	Unique biochemical properties; biocompatible with human tissue; biodegradable	Poor mechanical strength; rapid degradation in vivo, requiring frequent replacement
PRP derivatives	Release growth factors and cytokines to stimulate cell proliferation and wound repair	Cost-effective; low immunological risk; promotes regenerative effects in wound healing	Lack of standardization; risk of contamination; requires optimization in preparation; limited large-scale studies
Growth factors	Stimulate cell proliferation, migration, and differentiation for tissue regeneration	Enhance wound healing and skin regeneration; regulate cellular responses	Low stability in vivo; high cost; potential side effects, including allergic reactions
Topical antibiotics	Reduce bacterial load to prevent infection and promote wound healing	Effective for managing infected wounds; can reduce risk of wound infection	Potential for antibiotic resistance; limited effectiveness in non-infected wounds
Hyperbaric Oxygen Therapy	Increases oxygen supply to enhance healing	Useful in diabetic ulcers	Costly; limited availability; not suitable for all patients

Table 7.1: Current therapeutic approaches for wound healing. *Summary of wound healing therapies, highlighting mechanisms of action, advantages, and limitations, with a focus on areas where fluoxetine could address treatment gaps. Adapted from Gardikiotis et al (2022).*

Standard wound dressings, such as commercial dressings (e.g., Aquacel, Kaltostat) and biopolymer-based materials, are widely used for wound care but often lack bioactive properties that promote tissue repair. While some of these dressings create a moist environment favourable for healing and protect against infection, they do not actively engage in cell signalling or proliferation necessary for chronic wound repair, this limitation is particularly problematic in cases of impaired healing, as seen in chronic wounds where cell function is already compromised. Furthermore, these dressings often require frequent replacement, adding to patient burden and increasing healthcare costs (Gardikiotis et al., 2022).

Growth factors and platelet-rich plasma (PRP) derivatives are among the more advanced biological therapies used to stimulate wound healing at a molecular level. Growth factors, such as fibroblast growth factor and epidermal growth factor, aim to accelerate tissue regeneration by activating cell proliferation pathways, however, they suffer from low stability *in vivo* and are typically expensive, limiting their accessibility and use on a large scale. PRP therapies, while relatively cost-effective, lack standardisation and consistency in preparation, which affects their reliability and therapeutic outcomes. Additionally, the application of growth factors and PRP alone may not address all facets of wound healing, particularly in complex cases where metabolic and immune support are also needed.

Antibiotic treatments are frequently employed to manage wound infections, but they do not directly contribute to tissue repair, repeated use of topical antibiotics can contribute to antibiotic resistance, which presents a long-term risk for patients and the broader healthcare system. Antimicrobial resistance is especially concerning in chronic wound care, where bacterial biofilms can impede healing and further complicate treatment strategies.

Given these limitations, there is a need for a therapeutic solution that not only promotes cell proliferation but also provides metabolic and immune support to facilitate comprehensive wound healing. The findings of my study highlight the potential of fluoxetine as a therapeutic agent for chronic wound treatment, particularly at low, environmentally relevant concentrations. In vitro scratch assays demonstrated that fluoxetine exposure enhanced keratinocyte proliferative activity, resulting in faster wound closure. However, chronic wounds are often characterised by a hyperproliferative yet dysfunctional epidermis, where excessive cell proliferation does not necessarily translate into effective re-epithelialisation (Eming et al., 2014). This underscores the importance of targeting multiple pathways, beyond proliferation alone, to support proper wound resolution. In this context, the ability of fluoxetine to modulate not only cell growth but also cellular metabolism and inflammatory signalling becomes

particularly relevant. Chronic wounds often stuffer from impaired cellular metabolism, which can hinder the healing process by limiting the energy resources available for cell growth and repair. This study found that fluoxetine upregulates pathways involved in energy metabolism, particularly mitochondrial function and ATP production, suggesting that fluoxetine provides keratinocytes with the metabolic support needed to sustain proliferative activity. By enhancing cellular energy resources, fluoxetine not only bolsters the capacity of keratinocytes to proliferate but also reinforces their resilience in energy-demanding wound healing scenarios. These findings align with the observed benefits of fluoxetine in promoting wound closure, offering a promising perspective on its role in addressing metabolic limitations that contribute to chronic wound challenges.

The multi-pathway activation by fluoxetine, which includes the ERK/MAPK, HIPPO, and serotonin signalling pathways, aligns with established pharmaceutical targets in other medical contexts, such as cancer and regenerative medicine. The ERK/MAPK pathway, known for regulating cell proliferation and survival in oncology, plays a central role in controlled cell growth, as seen in studies on gastric and colorectal cancer (Pandian et al., 2020; Tian et al., 2017). Targeting this pathway has shown effects on cell cycle progression and apoptosis regulation (Meigui et al., 2022), suggesting that its activation by fluoxetine could similarly support regenerative processes in wound healing. The HIPPO signalling pathway, a key regulator of tissue growth and regeneration, supports cell proliferation and survival through the activity of YAP and TAZ transcriptional co-activators (Chen et al., 2019; Juan and Hong, 2016). When the pathway is inactive, YAP/TAZ translocate to the nucleus, promoting gene expression associated with regenerative processes (Lu et al., 2018). The activation of this pathway by fluoxetine suggests potential benefits for keratinocyte survival and function in chronic wound settings. Additionally, serotonin signalling, a primary pathway in the mechanism of action of fluoxetine as an SSRI, provides an immune-modulating effect, supporting keratinocyte migration and inflammation control essential to wound repair, importantly, these effects may occur either through serotonin directly binding to its receptors or by fluoxetine itself interacting with and modulating receptor activity.

The multifaceted nature of the action of fluoxetine suggests a synergistic effect that could significantly benefit patients with chronic wounds. Unlike conventional therapies that may focus on singular aspects of healing, the dual mechanism of action of fluoxetine, promoting proliferation while simultaneously regulating inflammation, positions it as a promising

candidate for adjunctive therapies in wound management. This holistic approach may enhance the overall effectiveness of treatment strategies, ultimately leading to better patient outcomes. Moreover, the established safety profile of fluoxetine, coupled with its widespread clinical use as an antidepressant, makes it an attractive option for repurposing in wound care. The prospect of low-dose fluoxetine formulations, perhaps delivered topically to minimise systemic exposure, offers a practical avenue for enhancing chronic wound treatment. Such an approach could provide a cost-effective solution that leverages the therapeutic properties of fluoxetine directly at the site of injury, maximising its benefits while reducing the risks typically associated with higher doses. The multi-pathway action of fluoxetine positions it as a promising adjunctive therapy, potentially addressing gaps in chronic wound care.

7.3.2 Ecological impact and monitoring needs for fluoxetine

Fluoxetine, widely recognised for its therapeutic benefits in treating various psychiatric conditions, is increasingly detected as an environmental contaminant in aquatic ecosystems. The findings of this study, which underscore the efficacy of fluoxetine in promoting keratinocyte proliferation and wound healing, necessitate a comprehensive understanding of its ecological implications. As fluoxetine persists in the environment, it raises important questions regarding its potential impact on non-target organisms and overall ecosystem health. Environmental monitoring studies have consistently reported the presence of fluoxetine in rivers, lakes, and wastewater effluents, often at concentrations that exceed those considered safe for aquatic life. These concentrations can lead to bioaccumulation in various organisms, such as fish and invertebrates, which are crucial components of aquatic ecosystems. The introduction of fluoxetine into these environments can disrupt normal biological processes, leading to unintended consequences on population dynamics and biodiversity.

One significant concern is the potential of fluoxetine to interfere with endocrine systems in aquatic organisms. Research has shown that exposure to SSRIs, including fluoxetine, can alter hormone levels and disrupt reproductive processes in fish, leading to changes in spawning success, growth rates, and overall fitness. Such disruptions can have far-reaching effects, not only on individual species but also on entire food webs and community structures. For instance, reductions in fish populations due to reproductive impairment can lead to imbalances in predator-prey relationships, affecting species diversity and ecosystem stability.

In addition to endocrine disruption, fluoxetine can influence behaviour in aquatic organisms. Studies have indicated that exposure to fluoxetine can alter locomotion, feeding patterns, and predator avoidance, thereby impacting survival rates. These behavioural changes could compromise the ability of affected species to thrive in their natural habitats, ultimately leading to shifts in community composition and ecosystem function.

Given these potential ecological risks, it is imperative to establish comprehensive monitoring programs that track the presence and concentrations of fluoxetine in aquatic environments. Such programs should employ advanced analytical techniques to accurately assess fluoxetine levels in various water sources, including surface water and effluents from wastewater treatment facilities. Understanding the spatial and temporal distribution of fluoxetine is crucial for identifying hotspots of contamination and evaluating the effectiveness of current water treatment processes in removing pharmaceutical residues. Furthermore, regulatory frameworks should be developed to limit the release of fluoxetine into the environment, promoting responsible pharmaceutical production and disposal practices. This includes incentivising the adoption of environmentally sustainable practices in the manufacturing of pharmaceuticals and improving waste management strategies to prevent the introduction of contaminants into natural water bodies.

Public awareness campaigns can also play a vital role in mitigating the ecological impact of fluoxetine, educating healthcare professionals, patients, and the public about the proper disposal of unused medications can reduce the likelihood of these substances entering the environment. Encouraging the use of drug take-back programs and promoting the proper disposal of pharmaceuticals can significantly decrease the accumulation of fluoxetine in aquatic systems.

In summary, while this study highlights the therapeutic potential of fluoxetine in wound healing, it also brings to light the pressing need for environmental stewardship. The dual role of fluoxetine, as a beneficial therapeutic agent and an ecological concern, underscores the necessity for a balanced approach that prioritises human health while safeguarding aquatic ecosystems. By implementing robust monitoring strategies and regulatory measures, it is possible to harness the benefits of fluoxetine for wound care while minimising its ecological footprint and protecting the integrity of our natural environments.

7.4 Future directions and concluding remarks

This study lays the groundwork for understanding the multifaceted role of fluoxetine in promoting wound healing, highlighting its potential therapeutic applications at low, environmentally relevant concentrations. However, several avenues for future research remain to be explored, which could enhance our understanding of the effects of fluoxetine and inform clinical practices in wound management. Future studies should focus on elucidating the precise molecular mechanisms through which fluoxetine exerts its effects on keratinocytes. While this research identified key pathways, including the ERK/MAPK signalling cascade and energy metabolism, further investigations are warranted to explore additional signalling networks that may be involved. Techniques such as advanced proteomics and transcriptomics could provide deeper insights into the temporal dynamics of gene and protein expression following fluoxetine treatment, allowing for a more comprehensive understanding of its action over different time frames and concentrations.

Additionally, exploring the effects of fluoxetine effects in other wound models is essential for assessing its therapeutic potential across different contexts. Future research could include studies on diabetic skin biopsies and other chronic wound types to determine how the efficacy of fluoxetine may vary based on the specific wound environment. This would not only contribute to a broader understanding of its application in clinical settings but also identify the optimal dosing regimens and delivery methods, such as topical formulations, that could maximise its benefits while minimising systemic exposure.

Investigating the interactions between fluoxetine and other therapeutic agents could also yield valuable insights. Combination therapies that incorporate fluoxetine with other growth factors or anti-inflammatory agents may enhance wound healing outcomes by targeting multiple pathways simultaneously. Research into the synergistic effects of such combinations could open new avenues for more effective chronic wound treatments, providing a holistic approach to wound care.

Furthermore, as fluoxetine is increasingly recognised for its environmental implications, future research should focus on its long-term ecological impact and the risks associated with its presence in aquatic environments. Understanding the concentration thresholds that affect non-target organisms, coupled with investigations into the mechanisms of action in these species,

will be crucial for developing effective monitoring strategies and regulatory frameworks. Studies that assess the bioaccumulation potential of fluoxetine in aquatic food webs will provide critical data to inform ecological risk assessments and conservation efforts.

In conclusion, this study underscores the potential of fluoxetine as a versatile agent in wound healing, particularly at low doses that promote keratinocyte proliferation and support cellular metabolism. The integration of findings from *in vitro* and *ex-vivo* models establish a compelling case for the therapeutic applications of fluoxetine in chronic wound care. As we advance our understanding of the mechanisms and effects of fluoxetine, it is imperative to balance its clinical benefits with ecological considerations. Through continued research and monitoring efforts, fluoxetine can be positioned not only as a valuable therapeutic tool but also as a compound that can be managed responsibly within our environment.

References

Abdouh, M., Storring, J.M., Riad, M., Paquette, Y., Albert, P.R., Drobetsky, E., Kouassi, E., 2001. Transcriptional Mechanisms for Induction of 5-HT1A Receptor mRNA and Protein in Activated B and T Lymphocytes. J. Biol. Chem. 276, 4382–4388. https://doi.org/10.1074/jbc.M004559200

Aicart-Ramos, C., Sánchez-Ruiloba, L., Gómez-Parrizas, M., Zaragoza, C., Iglesias, T., Rodríguez-Crespo, I., 2014. Protein kinase D activity controls endothelial nitric oxide synthesis. J. Cell Sci. 127, 3360–3372. https://doi.org/10.1242/jcs.148601

Al Shuraiqi, A., Al-Habsi, A., Barry, M.J., 2021. Time-, dose- and transgenerational effects of fluoxetine on the behavioural responses of zebrafish to a conspecific alarm substance. Environ. Pollut. 270, 116164. https://doi.org/10.1016/j.envpol.2020.116164

Albert, P.R., Lemonde, S., 2004. 5-HT1A Receptors, Gene Repression, and Depression: Guilt by Association. Neurosci. 10, 575–593. https://doi.org/10.1177/1073858404267382

Alstergren, P., Ernberg, M., Kopp, S., Lundeberg, T., Theodorsson, E., 1999. TMJ Pain in Relation to Circulating Neuropeptide Y, Serotonin, and Interleukin-1β in Rheumatoid Arthritis. J. Orofac. Pain 13, 49–55.

Amanchy, R., Kandasamy, K., Mathivanan, S., Periaswamy, B., Reddy, R., Yoon, W.H., Joore, J., Beer, M.A., Cope, L., Pandey, A., 2011. Identification of novel phosphorylation motifs through an integrative computational and experimental analysis of the human phosphoproteome. J. Proteomics Bioinforma. 4, 22–35. https://doi.org/10.4172/jpb.1000163

Antonucci, L.A., Egger, J. V., Krucher, N.A., 2014. Phosphorylation of the Retinoblastoma protein (RB) on serine-807 is required for association with Bax. Cell Cycle 13, 3611–3617. https://doi.org/10.4161/15384101.2014.964093

Anttila, S.A.K., Leinonen, E.V.J., 2001. A review of the pharmacological and clinical profile of mirtazapine. CNS Drug Rev. 7, 249–264. https://doi.org/10.1111/j.1527-3458.2001.tb00198.x

Arciuch, V.G.A., Elguero, M.E., Poderoso, J.J., Carreras, M.C., 2012. Mitochondrial regulation of cell cycle and proliferation. Antioxidants Redox Signal. 16, 1150–1180. https://doi.org/10.1089/ars.2011.4085

Ardito, F., Giuliani, M., Perrone, D., Troiano, G., Muzio, L. Lo, 2017. The crucial role of protein phosphorylation in cell signalingand its use as targeted therapy (Review). Int. J. Mol. Med. 40, 271–280. https://doi.org/10.3892/ijmm.2017.3036

Atmaca, M., 2020. Selective Serotonin Reuptake Inhibitor-Induced Sexual Dysfunction: Current Management Perspectives. Neuropsychiatr. Dis. Treat. Volume 16, 1043–1050. https://doi.org/10.2147/NDT.S185757

Bai, Q., Song, D., Gu, L., Verkhratsky, A., Peng, L., 2017. Bi-phasic regulation of glycogen content in astrocytes via Cav-1/PTEN/PI3K/AKT/GSK-3β pathway by fluoxetine. Psychopharmacology (Berl). 234, 1069–1077. https://doi.org/10.1007/s00213-017-4547-3

Ballou, Y., Rivas, A., Belmont, A., Patel, L., Amaya, C., Lipson, S., Khayou, T., Dickerson, E., Nahleh, Z., Bryan, B., 2018. 5-HT serotonin receptors modulate mitogenic signaling and impact tumor cell viability. Mol. Clin. Oncol. 243–254. https://doi.org/10.3892/mco.2018.1681

Barbui, C., Esposito, E., Cipriani, A., 2009. Selective serotonin reuptake inhibitors and risk of suicide: A systematic review of observational studies. C. Can. Med. Assoc. J. 180, 291–297. https://doi.org/10.1503/cmaj.081514

Barrientos, S., Stojadinovic, O., Golinko, M.S., Brem, H., Tomic-Canic, M., 2008. Growth factors and cytokines in wound healing. Wound Repair Regen. 16, 585–601. https://doi.org/10.1111/j.1524-475X.2008.00410.x

Bayes, A., Parker, G., 2019. How to choose an antidepressant medication. Acta Psychiatr. Scand. 139, 280–291. https://doi.org/10.1111/acps.13001

Bean, T.G., Arnold, K.E., Lane, J.M., Bergström, E., Thomas-Oates, J., Rattner, B.A., Boxall, A.B.A., 2017a. Predictive framework for estimating exposure of birds to pharmaceuticals. Environ. Toxicol. Chem. 36, 2335–2344. https://doi.org/10.1002/etc.3771

Bean, T.G., Arnold, K.E., Lane, J.M., Bergström, E., Thomas-Oates, J., Rattner, B.A., Boxall, A.B.A., 2017b. Predictive framework for estimating exposure of birds to pharmaceuticals. Environ. Toxicol. Chem. 36, 2335–2344. https://doi.org/10.1002/etc.3771

Benotti, M.J., Brownawell, B.J., 2007. Distributions of Pharmaceuticals in an Urban Estuary during both Dry- and Wet-Weather Conditions. Environ. Sci. Technol. 41, 5795–5802. https://doi.org/10.1021/es0629965

Berger, M., Gray, J.A., Roth, B.L., 2009. The Expanded Biology of Serotonin. Annu. Rev. Med. 60, 355–366. https://doi.org/10.1146/annurev.med.60.042307.110802

Bhatia, V., Dhingra, A.K., Dass, R., Chopra, B., Guarve, K., 2022. Formulation, Development, and in-vitro Evaluation of Escitalopram Fast Dissolving Tablets. Cent. Nerv. Syst. Agents Med. Chem. 22, 198–213. https://doi.org/10.2174/1871524922666220624113719

Björkenstam, C., Möller, J., Ringbäck, G., Salmi, P., Hallqvist, J., Ljung, R., 2013. An

Association between Initiation of Selective Serotonin Reuptake Inhibitors and Suicide - A Nationwide Register-Based Case-Crossover Study. PLoS One 8, 1–6. https://doi.org/10.1371/journal.pone.0073973

Boccuto, L., Chen, C.F., Pittman, A.R., Skinner, C.D., McCartney, H.J., Jones, K., Bochner, B.R., Stevenson, R.E., Schwartz, C.E., 2013. Decreased tryptophan metabolism in patients with autism spectrum disorders. Mol. Autism 4, 1–10. https://doi.org/10.1186/2040-2392-4-16

Bogowicz, P., Curtis, H.J., Walker, A.J., Cowen, P., Geddes, J., Goldacre, B., 2021. Trends and variation in antidepressant prescribing in English primary care: a retrospective longitudinal study. BJGP Open 5, 1–12. https://doi.org/10.3399/BJGPO.2021.0020

Bokor, G., Anderson, P.D., 2014. Obsessive-compulsive disorder. J. Pharm. Pract. 27, 116–130. https://doi.org/10.1177/0897190014521996

Bossus, M.C., Guler, Y.Z., Short, S.J., Morrison, E.R., Ford, A.T., 2014. Behavioural and transcriptional changes in the amphipod Echinogammarus marinus exposed to two antidepressants, fluoxetine and sertraline. Aquat. Toxicol. 151, 46–56. https://doi.org/10.1016/j.aquatox.2013.11.025

Bouckaert, F., 2021. Clinical aspects of deprescribing process in affective disorders. Eur. Psychiatry 64, S58–S59. https://doi.org/10.1192/j.eurpsy.2021.183

Brandes, L.J., Arron, R.J., Patricia Bogdanovic, R., Tong, J., Zaborniak, C.L.F., Hogg, G.R., Warrington, R.C., Fang, W., LaBella, F.S., 1992. Stimulation of Malignant Growth in Rodents by Antidepressant Drugs at Clinically Relevant Doses. Cancer Res. 52, 3796–3800.

Breitinger, H.G.A., Geetha, N., Hess, G.P., 2001. Inhibition of the serotonin 5-HT3 receptor by nicotine, cocaine, and fluoxetine investigated by rapid chemical kinetic techniques. Biochemistry 40, 8419–8429. https://doi.org/10.1021/bi0106890

Bringolf, R.B., Heltsley, R.M., Newton, T.J., Eads, C.B., Fraley, S.J., Shea, D., Cope, W.G., 2010. Environmental occurrence and reproductive effects of the pharmaceutical fluoxetine in native freshwater mussels. Environ. Toxicol. Chem. 29, 1311–1318. https://doi.org/10.1002/etc.157

Brooks, B.W., Chambliss, C.K., Stanley, J.K., Ramirez, A., Banks, K.E., Johnson, R.D., Lewis, R.J., 2005. Determination of select antidepressants in fish from an effluent-dominated stream. Environ. Toxicol. Chem. 24, 464–469. https://doi.org/10.1897/04-081R.1

Brooks, B.W., Turner, P.K., Stanley, J.K., Weston, J.J., Glidewell, E.A., Foran, C.M., Slattery, M., La Point, T.W., Huggett, D.B., 2003. Waterborne and sediment toxicity of fluoxetine

to select organisms. Chemosphere 52, 135–142. https://doi.org/10.1016/S0045-6535(03)00103-6

Bülow, P., 2022. The Infamous SSRIs. J. Sci. Humanit. Arts - JOSHA 9. https://doi.org/10.17160/josha.9.6.864

Burke, J.R., Liban, T.J., Restrepo, T., Lee, H.W., Rubin, S.M., 2014. Multiple mechanisms for E2F binding inhibition by phosphorylation of the retinoblastoma protein C-terminal domain. J. Mol. Biol. 426, 245–255. https://doi.org/10.1016/j.jmb.2013.09.031

Burket, S.R., Sapozhnikova, Y., Zheng, J.S., Chung, S.S., Brooks, B.W., 2018. At the Intersection of Urbanization, Water, and Food Security: Determination of Select Contaminants of Emerging Concern in Mussels and Oysters from Hong Kong. J. Agric. Food Chem. 66, 5009–5017. https://doi.org/10.1021/acs.jafc.7b05730

Campos, B., Piña, B., Carlos, B.C., 2012. Mechanisms of action of selective serotonin reuptake inhibitors in Daphnia magna. Environ. Sci. Technol. 46, 2943–2950. https://doi.org/10.1021/es203157f

Campos, B., Rivetti, C., Kress, T., Barata, C., Dircksen, H., 2016. Depressing Antidepressant: Fluoxetine Affects Serotonin Neurons Causing Adverse Reproductive Responses in Daphnia magna. Environ. Sci. Technol. 50, 6000–6007. https://doi.org/10.1021/acs.est.6b00826

Cao, Z., Liao, Q., Su, M., Huang, K., Jin, J., Cao, D., 2019. AKT and ERK dual inhibitors: The way forward? Cancer Lett. 459, 30–40. https://doi.org/10.1016/j.canlet.2019.05.025

Carmona-Rivera, C., Zhao, W., Yalavarthi, S., Kaplan, M.J., 2015. Neutrophil extracellular traps induce endothelial dysfunction in systemic lupus erythematosus through the activation of matrix metalloproteinase-2. Ann. Rheum. Dis. 74, 1417–1424. https://doi.org/10.1136/annrheumdis-2013-204837

Chandel, N.S., 2021. Metabolism of proliferating cells. Cold Spring Harb. Perspect. Biol. 13. https://doi.org/10.1101/CSHPERSPECT.A040618

Chang, F.L., Ho, S.T., Sheen, M.J., 2010. Efficacy of mirtazapine in preventing intrathecalmorphine-induced nausea and vomiting after orthopaedic surgery. Anaesthesia 65, 1206–1211. https://doi.org/10.1111/j.1365-2044.2010.06561.x

Chávez, J.L., Hagen, J.A., Kelley-Loughnane, N., 2017. Fast and selective plasmonic serotonin detection with Aptamer-gold nanoparticle conjugates. Sensors (Switzerland) 17. https://doi.org/10.3390/s17040681

Chen, M., Yi, B., Zhu, N., Wei, X., Zhang, G.X., Huang, S., Sun, J., 2016. Pim1 kinase promotes angiogenesis through phosphorylation of endothelial nitric oxide synthase at

Ser-633. Cardiovasc. Res. 109, 141–150. https://doi.org/10.1093/cvr/cvv250

Chen, P., Xu, W., Luo, Y., Zhang, Y., He, Y., Yang, S., Yuan, Z., 2017. MicroRNA 543 suppresses breast cancer cell proliferation, blocks cell cycle and induces cell apoptosis via direct targeting of ERK/MAPK. Onco. Targets. Ther. 10, 1423–1431. https://doi.org/10.2147/OTT.S118366

Chen, Y.-A., Lu, C.-Y., Cheng, T.-Y., Pan, S.-H., Chen, H.-F., Chang, N.-S., 2019. WW Domain-Containing Proteins YAP and TAZ in the Hippo Pathway as Key Regulators in Stemness Maintenance, Tissue Homeostasis, and Tumorigenesis. Front. Oncol. 9. https://doi.org/10.3389/fonc.2019.00060

Chen, Y., Jiang, B., Zhuang, Y., Peng, H., Chen, W., 2017. Differential effects of heat shock protein 90 and serine 1179 phosphorylation on endothelial nitric oxide synthase activity and on its cofactors. PLoS One 12, 1–14. https://doi.org/10.1371/journal.pone.0179978

Choi, S.H., Won, K.J., Lee, R., Cho, H.S., Hwang, S.H., Nah, S.Y., 2021. Wound healing effect of gintonin involves lysophosphatidic acid receptor/vascular endothelial growth factor signaling pathway in keratinocytes. Int. J. Mol. Sci. 22. https://doi.org/10.3390/ijms221810155

Choi, Y.S., Karelina, K., Alzate-Correa, D., Hoyt, K.R., Impey, S., Arthur, J.S., Obrietan, K., 2012. Mitogen- and stress-activated kinases regulate progenitor cell proliferation and neuron development in the adult dentate gyrus. J. Neurochem. 123, 676–688. https://doi.org/10.1111/jnc.12035

Chowdhury, M., Enenkel, C., 2015. Intracellular Dynamics of the Ubiquitin-Proteasome-System [version 1 ; referees : 3 approved] Referee Status : 367, 1–13.

Christensen, A.M., Faaborg-Andersen, S., Ingerslev, F., Baun, A., 2007. Mixture and single-substance toxicity of selective serotonin reuptake inhibitors toward algae and crustaceans. Environ. Toxicol. Chem. 26, 85–91. https://doi.org/10.1897/06-219R.1

Cipriani, A., Furukawa, T.A., Salanti, G., Chaimani, A., Atkinson, L.Z., Ogawa, Y., Leucht, S., Ruhe, H.G., Turner, E.H., Higgins, J.P.T., Egger, M., Takeshima, N., Hayasaka, Y., Imai, H., Shinohara, K., Tajika, A., Ioannidis, J.P.A., Geddes, J.R., 2018. Comparative efficacy and acceptability of 21 antidepressant drugs for the acute treatment of adults with major depressive disorder: a systematic review and network meta-analysis. Lancet 391, 1357–1366. https://doi.org/10.1016/S0140-6736(17)32802-7

Clevenger, S.S., Malhotra, D., Dang, J., Vanle, B., IsHak, W.W., 2018. The role of selective serotonin reuptake inhibitors in preventing relapse of major depressive disorder. Ther. Adv. Psychopharmacol. 8, 49–58. https://doi.org/10.1177/2045125317737264

Cognasse, F., Hamzeh-Cognasse, H., Lafarge, S., Delezay, O., Pozzetto, B., McNicol, A., Garraud, O., 2008. Toll-like receptor 4 ligand can differentially modulate the release of cytokines by human platelets. Br. J. Haematol. 141, 84–91. https://doi.org/10.1111/j.1365-2141.2008.06999.x

Corcoran, R.B., Rothenberg, S.M., Hata, A.N., Faber, A.C., Piris, A., Nazarian, R.M., Brown, R.D., Godfrey, J.T., Winokur, D., Walsh, J., Mino-Kenudson, M., Maheswaran, S., Settleman, J., Wargo, J.A., Flaherty, K.T., Haber, D.A., Engelman, J.A., 2013. TORC1 Suppression Predicts Responsiveness to RAF and MEK Inhibition in BRAF- Mutant Melanoma. Sci. Transl. Med. 5. https://doi.org/10.1126/scitranslmed.3005753

Correa, A.J., Reinisch, L., Sanders, D.L., Huang, S., Deriso, W., Duncavage, J.A., Garrett, C.G., 1999. Inhibition of subglottic stenosis with mitomycin-C in the canine model. Ann. Otol. Rhinol. Laryngol. 108, 1053–1060. https://doi.org/10.1177/000348949910801106

Correia, D., Domingues, I., Faria, M., Oliveira, M., 2023. Effects of fluoxetine on fish: What do we know and where should we focus our efforts in the future? Sci. Total Environ. 857. https://doi.org/10.1016/j.scitotenv.2022.159486

Correia, D., Domingues, I., Faria, M., Oliveira, M., 2022. Chronic Effects of Fluoxetine on Danio rerio: A Biochemical and Behavioral Perspective. Appl. Sci. 12. https://doi.org/10.3390/app12042256

Cullen, B., Smith, R., Mcculloch, E., Silcock, D., Morrison, L., 2002. Original research articles Mechanism of action of PROMOGRAN , a protease modulating matrix , for the treatment of diabetic foot ulcers 16–25.

Darby, I.A., Laverdet, B., Bonté, F., Desmoulière, A., 2014. Fibroblasts and myofibroblasts in wound healing. Clin. Cosmet. Investig. Dermatol. 7, 301–311. https://doi.org/10.2147/CCID.S50046

Daughton, C.G., Ternes, T.A., 1999. Pharmaceuticals and personal care products in the environment: Agents of subtle change? Environ. Health Perspect. 107, 907–938. https://doi.org/10.1289/ehp.99107s6907

De Andrade Quintanilha Ribeiro, F., Guaraldo, L., De Pádua Borges, J., Silva Zacchi, F.F., Eckley, C.A., 2004. Clinical and Histological Healing of Surgical Wounds Treated with Mitomycin C. Laryngoscope 114, 148–152. https://doi.org/10.1097/00005537-200401000-00027

De Castro-Català, N., Muñoz, I., Riera, J.L., Ford, A.T., 2017. Evidence of low dose effects of the antidepressant fluoxetine and the fungicide prochloraz on the behavior of the keystone freshwater invertebrate Gammarus pulex. Environ. Pollut. 231, 406–414.

https://doi.org/10.1016/j.envpol.2017.07.088

De Deurwaerdère, P., Navailles, S., Berg, K.A., Clarke, W.P., Spampinato, U., 2004. Constitutive Activity of the Serotonin2C Receptor Inhibits In Vivo Dopamine Release in the Rat Striatum and Nucleus Accumbens. J. Neurosci. 24, 3235–3241. https://doi.org/10.1523/JNEUROSCI.0112-04.2004

De Lange, H.J., Peeters, E.T.H.M., Lürling, M., 2009. Changes in nentilation and locomotion of Gammarus pulex (Crustacea, Amphipoda) in response to low concentrations of pharmaceuticals. Hum. Ecol. Risk Assess. 15, 111–120. https://doi.org/10.1080/10807030802615584

Deak, M., Clifton, A.D., Lucocq, J.M., Alessi, D.R., 1998. Mitogen- and stress-activated protein kinase-1 (MSK1) is directly activated by MAPK and SAPK2/p38, and may mediate activation of CREB. EMBO J. 17, 4426–4441. https://doi.org/10.1093/emboj/17.15.4426

Diniz, J.B., Malavazzi, D.M., Fossaluza, V., Belotto-Silva, C., Borcato, S., Pimentel, I., Miguel, E.C., Shavitt, R.G., 2011. Risk factors for early treatment discontinuation in patients with obsessive-compulsive disorder. Clinics 66, 387–393. https://doi.org/10.1590/S1807-59322011000300004

Domingues, R.R., Fricke, H.P., Sheftel, C.M., Bell, A.M., Sartori, L.C., Manuel, R.S.J., Krajco, C.J., Wiltbank, M.C., Hernandez, L.L., 2022. Effect of Low and High Doses of Two Selective Serotonin Reuptake Inhibitors on Pregnancy Outcomes and Neonatal Mortality. Toxics 10. https://doi.org/10.3390/toxics10010011

Du, Z., Wang, H., Wu, C., Buck, M., Zheng, W., Hansen, A.L., Kao, H.-Y., Yang, S., 2023. Phosphorylation modulates estrogen receptor disorder by altering long-range hydrophobic interactions.

Duan, X., n.d. Interaction between envelope protein of Jaagsiekte Sheep Retrovirus and Hippo signaling pathway is inferred from transcriptome analysis of naturally infected Ovine Pulmonary Adenomatosis 34.

Dubovsky, S.L., 2015. The usefulness of genotyping cytochrome P450 enzymes in the treatment of depression. Expert Opin. Drug Metab. Toxicol. 11, 369–379. https://doi.org/10.1517/17425255.2015.998996

Durante, C., Agostini, F., Abbruzzese, L., Toffola, R.T., Zanolin, S., Suine, C., Mazzucato, M., 2013. Growth factor release from platelet concentrates: Analytic quantification and characterization for clinical applications. Vox Sang. 105, 129–136. https://doi.org/10.1111/vox.12039

Dzieweczynski, T.L., Campbell, B.A., Kane, J.L., 2016. Dose-dependent fluoxetine effects on boldness in male Siamese fighting fish. J. Exp. Biol. 219, 797–804. https://doi.org/10.1242/jeb.132761

Edinoff, A.N., Akuly, H.A., Hanna, T.A., Ochoa, C.O., Patti, S.J., Ghaffar, Y.A., Kaye, A.D., Viswanath, O., Urits, I., Boyer, A.G., Cornett, E.M., Kaye, A.M., 2021. Selective serotonin reuptake inhibitors and adverse effects: A narrative review. Neurol. Int. 13, 387–401. https://doi.org/10.3390/neurolint13030038

Edstrom, D.W., Linder, J., Wennersten, G., Brismar, K., Ros, A.M., 2010. Phototherapy with ultraviolet radiation: A study of hormone parameters and psychological effects. J. Eur. Acad. Dermatology Venereol. 24, 403–409. https://doi.org/10.1111/j.1468-3083.2009.03423.x

Eisensamer, B., Rammes, G., Gimpl, G., Shapa, M., Ferrari, U., Hapfelmeier, G., Bondy, B., Parsons, C., Gilling, K., Zieglgänsberger, W., Holsboer, F., Rupprecht, R., 2003. Antidepressants are functional antagonists at the serotonin type 3 (5-HT3) receptor. Mol. Psychiatry 8, 994–1007. https://doi.org/10.1038/sj.mp.4001314

El-Merahbi, R., Löffler, M., Mayer, A., Sumara, G., 2015. The roles of peripheral serotonin in metabolic homeostasis. FEBS Lett. 589, 1728–1734. https://doi.org/10.1016/j.febslet.2015.05.054

Eming, S.A., Martin, P., Tomic-Canic, M., 2014. Wound repair and regeneration: Mechanisms, signaling, and translation. Sci. Transl. Med. 6. https://doi.org/10.1126/scitranslmed.3009337

Enoch, S., Leaper, D.J., 2008. Basic science surgery 26:2 31 Basic science of wound healing 26, 37–42.

Escuin-Ordinas, H., Li, S., Xie, M.W., Sun, L., Hugo, W., Huang, R.R., Jiao, J., de-Faria, F.M., Realegeno, S., Krystofinski, P., Azhdam, A., Komenan, S.M.D., Atefi, M., Comin-Anduix, B., Pellegrini, M., Cochran, A.J., Modlin, R.L., Herschman, H.R., Lo, R.S., McBride, W.H., Segura, T., Ribas, A., 2016. Cutaneous wound healing through paradoxical MAPK activation by BRAF inhibitors. Nat. Commun. 7, 12348. https://doi.org/10.1038/ncomms12348

Fang, C.K., Chen, H.W., Chiang, I.T., Chen, C.C., Liao, J.F., Su, T.P., Tung, C.Y., Uchitomi, Y., Hwang, J.J., 2012. Mirtazapine inhibits tumor growth via immune response and serotonergic system. PLoS One 7. https://doi.org/10.1371/journal.pone.0038886

Fang, Y., Ding, X., Zhang, Y., Cai, L., Ge, Y., Ma, K., Xu, R., Li, S., Song, M., Zhu, H., Liu, J., Ding, J., Lu, M., Hu, G., 2022. Fluoxetine inhibited the activation of A1 reactive

astrocyte in a mouse model of major depressive disorder through astrocytic 5-HT2BR/β-arrestin2 pathway. J. Neuroinflammation 19, 1–20. https://doi.org/10.1186/s12974-022-02389-y

Farahani, R.M.Z., Sadr, K., Rad, J.S., Mesgari, M., 2007. Fluoxetine enhances cutaneous wound healing in chronically stressed Wistar rats. Adv. Skin Wound Care 20, 157–165. https://doi.org/10.1097/01.ASW.0000262710.59293.6b

Faria, M., Bellot, M., Soto, O., Prats, E., Montemurro, N., Manjarrés, D., Gómez-Canela, C., Raldúa, D., 2022. Developmental exposure to sertraline impaired zebrafish behavioral and neurochemical profiles. Front. Physiol. 13, 1–15. https://doi.org/10.3389/fphys.2022.1040598

Fava, G.A., Gatti, A., Belaise, C., Guidi, J., Offidani, E., 2015. Withdrawal symptoms after selective serotonin reuptake inhibitor discontinuation: A systematic review. Psychother. Psychosom. 84, 72–81. https://doi.org/10.1159/000370338

Ferguson, J.M., 2001. SSRI Antidepressant Medications. Prim. Care Companion CNS Disord. 3. https://doi.org/10.4088/PCC.v03n0105

Ferrajoli, A., Faderl, S., Ravandi, F., Estrov, Z., 2006. The JAK-STAT Pathway: A Therapeutic Target in Hematological Malignancies. Curr. Cancer Drug Targets 6, 671–679. https://doi.org/10.2174/156800906779010227

Fhu, C.W., Ali, A., 2021. Dysregulation of the ubiquitin proteasome system in human malignancies: A window for therapeutic intervention. Cancers (Basel). 13. https://doi.org/10.3390/cancers13071513

Fineberg, N.A., Baldwin, D.S., Drummond, L.M., Wyatt, S., Hanson, J., Gopi, S., Kaur, S., Reid, J., Marwah, V., Sachdev, R.A., Pampaloni, I., Shahper, S., Varlakova, Y., Mpavaenda, D., Manson, C., O'Leary, C., Irvine, K., Monji-Patel, D., Shodunke, A., Dyer, T., Dymond, A., Barton, G., Wellsted, D., 2018. Optimal treatment for obsessive compulsive disorder. Int. Clin. Psychopharmacol. 33, 334–348. https://doi.org/10.1097/YIC.0000000000000237

Fitzpatrick, R.L., Quimby, J.M., Benson, K.K., Ramirez, D., Sieberg, L.G., Wittenburg, L.A., Gustafson, D.L., 2018. In vivo and in vitro assessment of mirtazapine pharmacokinetics in cats with liver disease. J. Vet. Intern. Med. 32, 1951–1957. https://doi.org/10.1111/jvim.15237

Flender, D., Vilenne, F., Adams, C., Boonen, K., Valkenborg, D., Baggerman, G., 2024. Exploring the dynamic landscape of immunopeptidomics: Unravelling posttranslational modifications and navigating bioinformatics terrain. Mass Spectrom. Rev. 1–31.

https://doi.org/10.1002/mas.21905

Fong, P.P., Bury, T.B.S., Donovan, E.E., Lambert, O.J., Palmucci, J.R., Adamczak, S.K., 2017. Exposure to SSRI-type antidepressants increases righting time in the marine snail Ilyanassa obsoleta. Environ. Sci. Pollut. Res. 24, 725–731. https://doi.org/10.1007/s11356-016-7855-y

Galán, A., Horvatić, A., Kuleš, J., Bilić, P., Gotić, J., Mrljak, V., 2018. LC-MS/MS analysis of the dog serum phosphoproteome reveals novel and conserved phosphorylation sites: Phosphoprotein patterns in babesiosis caused by Babesia canis, a case study. PLoS One 13. https://doi.org/10.1371/journal.pone.0207245

Garcia, E.E., Smith, R.L., Sanders-Bush, E., 2007. Role of Gq protein in behavioral effects of the hallucinogenic drug 1-(2,5-dimethoxy-4-iodophenyl)-2-aminopropane. Neuropharmacology 52, 1671–1677. https://doi.org/10.1016/j.neuropharm.2007.03.013

Gardikiotis, I., Cojocaru, F.D., Mihai, C.T., Balan, V., Dodi, G., 2022. Borrowing the Features of Biopolymers for Emerging Wound Healing Dressings: A Review. Int. J. Mol. Sci. 23. https://doi.org/10.3390/ijms23158778

Gatsios, P., Terstegen, L., Schliess, F., Häussinger, D., Kerr, I.M., Heinrich, P.C., Graeve, L., 1998. Activation of the Janus kinase/signal transducer and activator of transcription pathway by osmotic shock. J. Biol. Chem. 273, 22962–22968. https://doi.org/10.1074/jbc.273.36.22962

Gibbons, R.D., Hur, K., Bhaumik, D.K., Mann, J.J., 2005. The Relationship Between Antidepressant Medication Use and Rate of Suicide. Arch. Gen. Psychiatry 62, 165. https://doi.org/10.1001/archpsyc.62.2.165

Giebułtowicz, J., Nałecz-Jawecki, G., 2014. Occurrence of antidepressant residues in the sewage-impacted Vistula and Utrata rivers and in tap water in Warsaw (Poland). Ecotoxicol. Environ. Saf. 104, 103–109. https://doi.org/10.1016/j.ecoenv.2014.02.020

Gillman, P.K., 2007. Tricyclic antidepressant pharmacology and therapeutic drug interactions updated. Br. J. Pharmacol. 151, 737–748. https://doi.org/10.1038/sj.bjp.0707253

Go, E.J., Lee, J.Y., Kim, Y.H., Park, C.K., 2024. Site-Specific Transient Receptor Potential Channel Mechanisms and Their Characteristics for Targeted Chronic Itch Treatment. Biomolecules 14, 1–16. https://doi.org/10.3390/biom14010107

Goel, S., Wang, Q., Watt, A.C., Tolaney, S.M., Dillon, D.A., Li, W., Ramm, S., Palmer, A.C., Yuzugullu, H., Varadan, V., Tuck, D., Harris, L.N., Wong, K.K., Liu, X.S., Sicinski, P., Winer, E.P., Krop, I.E., Zhao, J.J., 2016. Overcoming Therapeutic Resistance in HER2-Positive Breast Cancers with CDK4/6 Inhibitors. Cancer Cell 29, 255–269.

https://doi.org/10.1016/j.ccell.2016.02.006

Golder, S., Medaglio, D., O'Connor, K., Hennessy, S., Gross, R., Gonzalez Hernandez, G., 2023. Reasons for Discontinuation or Change of Selective Serotonin Reuptake Inhibitors in Online Drug Reviews. JAMA Netw. open 6, e2323746. https://doi.org/10.1001/jamanetworkopen.2023.23746

González Alonso, S., Catalá, M., Maroto, R.R., Gil, J.L.R., de Miguel, Á.G., Valcárcel, Y., 2010. Pollution by psychoactive pharmaceuticals in the Rivers of Madrid metropolitan area (Spain). Environ. Int. 36, 195–201. https://doi.org/10.1016/j.envint.2009.11.004

Goodwin, Z., Oh, I., Mathyer, M., Quiggle, A., de Guzman Strong, C., 2017. 461 Recent evolution for an involucrin/sperm mitochondria haplotype associated with epidermal function in modern humans. J. Invest. Dermatol. 137, S79. https://doi.org/10.1016/j.jid.2017.02.480

Gosmann, N.P., De Abreu Costa, M., De Barros Jaeger, M., Motta, L.S., Frozi, J., Spanemberg, L., Manfro, G.G., Cuijpers, P., Pine, D.S., Salum, G.A., 2021. Selective serotonin reuptake inhibitors, and serotonin and norepinephrine reuptake inhibitors for anxiety, obsessive-compulsive, and stress disorders: A 3-level network metaanalysis. PLoS Med. 18, 1–20. https://doi.org/10.1371/journal.pmed.1003664

Guler, Y., Ford, A.T., 2010. Anti-depressants make amphipods see the light. Aquat. Toxicol. 99, 397–404. https://doi.org/10.1016/j.aquatox.2010.05.019

Guo, Z., Kanjanapangka, J., Liu, N., Liu, S., Liu, C., Wu, Z., Wang, Y., Loh, T., Kowolik, C., Jamsen, J., Zhou, M., Truong, K., Chen, Y., Zheng, L., Shen, B., 2012. Sequential Posttranslational Modifications Program FEN1 Degradation during Cell-Cycle Progression. Mol. Cell 47, 444–456. https://doi.org/10.1016/j.molcel.2012.05.042

Gupta, A., 2018. Augmenting Wound Healing with Photobiomodulation Therapy, in: Low-Level Light Therapy: Photobiomodulation. SPIE, pp. 135–147. https://doi.org/10.1117/3.2295638.ch10

Han, D., Huang, M., Wang, T., Li, Z., Chen, Y., Liu, C., Lei, Z., Chu, X., 2019. Lysine methylation of transcription factors in cancer. Cell Death Dis. 10. https://doi.org/10.1038/s41419-019-1524-2

Han, J., Jing, Y., Han, F., Sun, P., 2021. Comprehensive analysis of expression, prognosis and immune infiltration for TIMPs in glioblastoma. BMC Neurol. 21, 447. https://doi.org/10.1186/s12883-021-02477-1

Hanahan, D., Weinberg, R.A., 2011. Hallmarks of cancer: The next generation. Cell 144, 646–674. https://doi.org/10.1016/j.cell.2011.02.013

Heald, A., Stedman, M., Farman, S., Ruzhdi, N., Davies, M., Taylor, D., 2021. Seasonal Variation in Antidepressant Prescribing. Prim. Care Companion CNS Disord. 23. https://doi.org/10.4088/PCC.20m02790

Hedna, K., Fastbom, J., Erlangsen, A., Waern, M., 2021. Antidepressant Use and Suicide Rates in Adults Aged 75 and Above: A Swedish Nationwide Cohort Study. Front. Public Heal. 9, 1–9. https://doi.org/10.3389/fpubh.2021.611559

Henry, T.B., Kwon, J.W., Armbrust, K.L., Black, M.C., 2004. Acute and chronic toxicity of five selective serotonin reuptake inhibitors in Ceriodaphnia dubia. Environ. Toxicol. Chem. 23, 2229–2233. https://doi.org/10.1897/03-278

Hiebert, P., Werner, S., 2019. Regulation of wound healing by the nrf2 transcription factor—more than cytoprotection. Int. J. Mol. Sci. 20. https://doi.org/10.3390/ijms20163856

Hillhouse, T.M., Porter, J.H., 2015. A brief history of the development of antidepressant drugs: From monoamines to glutamate. Exp. Clin. Psychopharmacol. 23, 1–21. https://doi.org/10.1037/a0038550

Hjorth, O., Frick, A., Gingnell, M., Engman, J., Björkstrand, J., Faria, V., Alaie, I., Carlbring, P., Andersson, G., Jonasson, M., Lubberink, M., Antoni, G., Reis, M., Wahlstedt, K., Fredrikson, M., Furmark, T., 2022. Serotonin and dopamine transporter availability in social anxiety disorder after combined treatment with escitalopram and cognitive-behavioral therapy. Transl. Psychiatry 12, 1–10. https://doi.org/10.1038/s41398-022-02187-3

Holbert, C.E., Dunworth, M., Foley, J.R., Dunston, T.T., Stewart, T.M., Casero, R.A., 2020. Autophagy induction by exogenous polyamines is an artifact of bovine serum amine oxidase activity in culture serum. J. Biol. Chem. 295, 9061–9068. https://doi.org/10.1074/jbc.ra120.013867

Horowitz, H.I., Spielvogel, A.R., 1971. Hemostasis, in: Thrombosis and Bleeding Disorders. Elsevier, pp. 412–456. https://doi.org/10.1016/B978-0-12-077750-1.50013-1

Hosgood, G., 1993. Wound Healing: The Role of Platelet-Derived Growth Factor and Transforming Growth Factor Beta. Vet. Surg. 22, 490–495. https://doi.org/10.1111/j.1532-950X.1993.tb00426.x

Hosseini, M., Brown, J., Khosrotehrani, K., Bayat, A., Shafiee, A., 2022. Skin biomechanics: a potential therapeutic intervention target to reduce scarring. Burn. Trauma 10. https://doi.org/10.1093/burnst/tkac036

Hsiung, S.C., Tamir, H., Franke, T.F., Liu, K.P., 2005. Roles of extracellular signal-regulated kinase and Akt signaling in coordinating nuclear transcription factor-κB-dependent cell

survival after serotonin 1A receptor activation. J. Neurochem. 95, 1653–1666. https://doi.org/10.1111/j.1471-4159.2005.03496.x

Hu, M.S.-M., Rennert, R.C., McArdle, A., Chung, M.T., Walmsley, G.G., Longaker, M.T., Lorenz, H.P., 2014. The Role of Stem Cells During Scarless Skin Wound Healing. Adv. Wound Care 3, 304–314. https://doi.org/10.1089/wound.2013.0471

Hughes, S.R., Kay, P., Brown, L.E., 2013. Global synthesis and critical evaluation of pharmaceutical data sets collected from river systems. Environ. Sci. Technol. 47, 661–677. https://doi.org/10.1021/es3030148

Hui, J., Zhang, J., Kim, H., Tong, C., Ying, Q., Li, Z., Mao, X., Shi, G., Yan, J., Zhang, Z., Xi, G., 2015. Fluoxetine regulates neurogenesis in vitro through modulation of gsk-3b/b-catenin signaling. Int. J. Neuropsychopharmacol. 18, 1–12. https://doi.org/10.1093/ijnp/pyu099

Hustoft, H.K., Malerod, H., Wilson, S.R., 2012. A Critical Review of Trypsin Digestion for LC-MS Based Proteomics. https://doi.org/10.13140/2.1.2226.7846

Ido-Kitamura, Y., Sasaki, T., Kobayashi, M., Kim, H.J., Lee, Y.S., Kikuchi, O., Yokota-Hashimoto, H., Iizuka, K., Accili, D., Kitamura, T., 2012. Hepatic FoxO1 Integrates Glucose Utilization and Lipid Synthesis through Regulation of Chrebp O-Glycosylation. PLoS One 7. https://doi.org/10.1371/journal.pone.0047231

Imoto, Y., Kira, T., Sukeno, M., Nishitani, N., Nagayasu, K., Nakagawa, T., Kaneko, S., Kobayashi, K., Segi-Nishida, E., 2015. Role of the 5-HT4 receptor in chronic fluoxetine treatment-induced neurogenic activity and granule cell dematuration in the dentate gyrus. Mol. Brain 8, 1–12. https://doi.org/10.1186/s13041-015-0120-3

Jampel, H.D., 1992. Effect of Brief Exposure to Mitomycin C on Viability and Proliferation of Cultured Human Tenon's Capsule Fibroblasts. Ophthalmology 99, 1471–1476. https://doi.org/10.1016/S0161-6420(92)31781-6

Jing, E., Straw-Wilson, K., 2016. Sexual dysfunction in selective serotonin reuptake inhibitors (SSRIs) and potential solutions: A narrative literature review. Ment. Heal. Clin. 6, 191–196. https://doi.org/10.9740/mhc.2016.07.191

Juan, W.C., Hong, W., 2016. Targeting the Hippo signaling pathway for tissue regeneration and cancer therapy. Genes (Basel). 7, 1–25. https://doi.org/10.3390/genes7090055

Jung, A.C., Staiger, T., Sullivan, M., 1997. The efficacy of selective serotonin reuptake inhibitors for the management of chronic pain. J. Gen. Intern. Med. 12, 384–389. https://doi.org/10.1007/s11606-006-5088-3

Jung, S.H., Yun, J.L., Ho, J.H., 2006. EGF stimulates proliferation of mouse embryonic stem

cells: Involvement of Ca2+ influx and p44/42 MAPKs. Am. J. Physiol. - Cell Physiol. 290, 123–133. https://doi.org/10.1152/ajpcell.00142.2005

Kaihola, H., Olivier, J., Poromaa, I.S., Åkerud, H., 2015. The effect of antenatal depression and selective serotonin reuptake inhibitor treatment on nerve growth factor signaling in human placenta. PLoS One 10, 1–15. https://doi.org/10.1371/journal.pone.0116459

Kang, L.J., Nguyen, K.V.A., Eom, S., Choi, Y.J., Nguyen, C.N., Lee, J., Kim, C., Lee, S., Lee, S.G., Lee, J.H., 2019. Stimulating DDX3 expression by serotonin 5-HT receptor 7 through phosphorylation of p53 via the AC-PKA-ERK signaling pathway. J. Cell. Biochem. 120, 18193–18208. https://doi.org/10.1002/jcb.29125

Kang, S.U., Kim, H.J., Ma, S., Oh, D.Y., Jang, J.Y., Seo, C., Lee, Y.S., Kim, C.H., 2024. Liquid plasma promotes angiogenesis through upregulation of endothelial nitric oxide synthase-induced extracellular matrix metabolism: potential applications of liquid plasma for vascular injuries. Cell Commun. Signal. 22, 1–18. https://doi.org/10.1186/s12964-023-01412-w

Kato, M., 2017. Acetylation-mediated protein complex dissociation as a key step for active transcription of human disease-related genes. Integr. Mol. Med. 4, 1–3. https://doi.org/10.15761/imm.1000312

Katolik, A., Oswald, A.J., 2017. Antidepressants for Economists and Business-School Researchers: An Introduction and Review. Die Unternehmung 71, 448–463. https://doi.org/10.5771/0042-059x-2017-4-448

Kawabe, H., Brose, N., 2011. The role of ubiquitylation in nerve cell development. Nat. Rev. Neurosci. 12, 251–268. https://doi.org/10.1038/nrn3009

Kendall, I., Slotten, H.A., Codony, X., Burgueño, J., Pauwels, P.J., Vela, J.M., Fone, K.C.F., 2011. E-6801, a 5-HT6 receptor agonist, improves recognition memory by combined modulation of cholinergic and glutamatergic neurotransmission in the rat. Psychopharmacology (Berl). 213, 413–430. https://doi.org/10.1007/s00213-010-1854-3

Khan, M.Z., Khan, A., Xiao, J., Ma, Y., Ma, J., Gao, J., Cao, Z., 2020. Role of the jak-stat pathway in bovine mastitis and milk production. Animals 10, 1–16. https://doi.org/10.3390/ani10112107

Kim, H.E., Cho, H., Ishihara, A., Kim, B., Kim, O., 2018. Cell proliferation and migration mechanism of caffeoylserotonin and serotonin via serotonin 2B receptor in human keratinocyte HaCaT cells. BMB Rep. 51, 188–193. https://doi.org/10.5483/BMBRep.2018.51.4.209

Kim, M., Kim, J., Shin, Y.K., Kim, K.Y., 2020. Gentisic acid stimulates keratinocyte

proliferation through erk1/2 phosphorylation. Int. J. Med. Sci. 17, 626–631. https://doi.org/10.7150/ijms.36484

Kim, M., Kim, K.Y., 2023. Wound healing effects of Asparagus lucidus Lindl extract through the phosphorylation of ERK1/2. BMC Complement. Med. Ther. 23, 1–8. https://doi.org/10.1186/s12906-023-04066-w

Kimura, H., Okubo, N., Chosa, N., Kyakumoto, S., Kamo, M., Miura, H., Ishisaki, A., 2013. EGF positively regulates the proliferation and migration, and negatively regulates the myofibroblast differentiation of periodontal ligament-derived endothelial progenitor cells through MEK/ERK-and JNK-dependent signals. Cell. Physiol. Biochem. 32, 899–914. https://doi.org/10.1159/000354493

Kirkton, C., McIntyre, I.M., 2006. Therapeutic and toxic concentrations of mirtazapine. J. Anal. Toxicol. 30, 687–691. https://doi.org/10.1093/jat/30.9.687

Kitagishi, Y., Nakanishi, A., Ogura, Y., Matsuda, S., 2014. Dietary regulation of PI3K/AKT/GSK-3β pathway in Alzheimer's disease. Alzheimer's Res. Ther. 6, 1–7. https://doi.org/10.1186/alzrt265

Kleywegt, S., Payne, M., Ng, F., Fletcher, T., 2019. Environmental loadings of Active Pharmaceutical Ingredients from manufacturing facilities in Canada. Sci. Total Environ. 646, 257–264. https://doi.org/10.1016/j.scitotenv.2018.07.240

Kominato, H., Takeda, K., Mizutani, K., Mikami, R., Kido, D., Buranasin, P., Saito, N., Takemura, S., Nakagawa, K., Nagasawa, T., Iwata, T., 2022. Metformin accelerates wound healing by Akt phosphorylation of gingival fibroblasts in insulin-resistant prediabetes mice. J. Periodontol. 93, 258–270. https://doi.org/10.1002/JPER.21-0362

Kreke, N., Dietrich, D.R., 2008. Physiological endpoints for potential SSRI interactions in fish. Crit. Rev. Toxicol. 38, 215–247. https://doi.org/10.1080/10408440801891057

Kubera, M., Simbirtsev, A., Mathison, R., Maes, M., 2000. Effects of repeated fluoxetine and citalopram administration on cytokine release in C57BL r 6 mice. Psychiatry Res. 255–266.

Kurashiki, T., Horikoshi, Y., Kamizaki, K., Sunaguchi, T., Hara, K., Morimoto, M., Kitagawa, Y., Nakaso, K., Otsuki, A., Matsura, T., 2022. Molecular mechanisms underlying the promotion of wound repair by coenzyme Q10: PI3K/Akt signal activation via alterations to cell membrane domains. J. Clin. Biochem. Nutr. 70, 21–141. https://doi.org/10.3164/jcbn.21-141

Kwon, S.-H., Ju, S.-A., Kang, J.-H., Kim, C.-S., Yoo, H.-M., Yu, R., 2008. Chemokine Lkn-1/CCL15 enhances matrix metalloproteinase-9 release from human macrophages and

macrophage-derived foam cells. Nutr. Res. Pract. 2, 134. https://doi.org/10.4162/nrp.2008.2.2.134

Laberge, S., Cruikshank, W.W., Beer, J., Center, D.M., 1996. Secretion of IL-16 (lymphocyte chemoattractant factor) from serotonin- stimulated CD8+ T cells in vitro. □. J. iImunology 310–315.

Lachowski, D., Cortes, E., Rice, A., Pinato, D., Rombouts, K., del Rio Hernandez, A., 2019. Matrix stiffness modulates the activity of MMP-9 and TIMP-1 in hepatic stellate cells to perpetuate fibrosis. Sci. Rep. 9, 7299. https://doi.org/10.1038/s41598-019-43759-6

Lajeunesse, A., Smyth, S.A., Barclay, K., Sauvé, S., Gagnon, C., 2012. Distribution of antidepressant residues in wastewater and biosolids following different treatment processes by municipal wastewater treatment plants in Canada. Water Res. 46, 5600–5612. https://doi.org/10.1016/j.watres.2012.07.042

Lalani, E., Menon, R., Mufti, M.A., Kumfa, C., Raji, M., 2023. Mirtazapine: A One-Stop Strategy for Treatment of Opioid Withdrawal Symptoms. Cureus 15. https://doi.org/10.7759/cureus.43821

Lamber, E.P., Beuron, F., Morris, E.P., Svergun, D.I., Mittnacht, S., 2013. Structural Insights into the Mechanism of Phosphoregulation of the Retinoblastoma Protein. PLoS One 8. https://doi.org/10.1371/journal.pone.0058463

Lang, U.E., Kocabayoglu, P., Cheng, G.Z., Ghiassi-Nejad, Z., Muñoz, U., Vetter, D., Eckstein, D.A., Hannivoort, R.A., Walsh, M.J., Friedman, S.L., 2013. GSK3β phosphorylation of the KLF6 tumor suppressor promotes its transactivation of p21. Oncogene 32, 4557–4564. https://doi.org/10.1038/onc.2012.457

Lattimore, K.A., Donn, S.M., Kaciroti, N., Kemper, A.R., Neal, C.R., Vazquez, D.M., 2005. Selective serotonin reuptake inhibitor (SSRI) use during pregnancy and effects on the fetus and newborn: A meta-analysis. J. Perinatol. 25, 595–604. https://doi.org/10.1038/sj.jp.7211352

Lee, H.J., Park, M.K., Kim, S.Y., Park Choo, H.Y., Lee, A.Y., Lee, C.H., 2011. Serotonin induces melanogenesis via serotonin receptor 2A. Br. J. Dermatol. 165, 1344–1348. https://doi.org/10.1111/j.1365-2133.2011.10490.x

Lei, L., Luo, Y., Kang, D., Yang, F., Meng, D., Wang, J.Z., Liu, R., Wang, X., Li, H.L., 2023. Gypenoside IX restores Akt/GSK-3β pathway and alleviates Alzheimer's disease-like neuropathology and cognitive deficits. Aging (Albany. NY). 15, 14172–14191. https://doi.org/10.18632/aging.205295

Leivonen, S.-K., Lazaridis, K., Decock, J., Chantry, A., Edwards, D.R., Kähäri, V.-M., 2013.

TGF-β-Elicited Induction of Tissue Inhibitor of Metalloproteinases (TIMP)-3 Expression in Fibroblasts Involves Complex Interplay between Smad3, p38α, and ERK1/2. PLoS One 8, e57474. https://doi.org/10.1371/journal.pone.0057474

Li, B., Jia, S., Yue, T., Yang, L., Huang, C., Verkhratsky, A., Peng, L., 2017. Biphasic regulation of caveolin-1 gene expression by fluoxetine in astrocytes: Opposite effects of PI3K/AKT and MAPK/ERK signaling pathways on c-fos. Front. Cell. Neurosci. 11, 1–11. https://doi.org/10.3389/fncel.2017.00335

Li, K., Zhou, G., Xiao, Y., Gu, J., Chen, Q., Xie, S., Wu, J., 2022. Risk of Suicidal Behaviors and Antidepressant Exposure Among Children and Adolescents: A Meta-Analysis of Observational Studies. Front. Psychiatry 13, 1–10. https://doi.org/10.3389/fpsyt.2022.880496

Li, Yue, Liu, Y., Huang, X., Ren, J., 2022. Analysis of protein phosphorylation combining capillary electrophoresis with ATP analog labeling technique. Electrophoresis 43, 548–558. https://doi.org/10.1002/elps.202100251

Li, Yang, Yang, M., Zhang, L., Mao, Z., Lin, Y., Xu, S., Fang, Z., Che, L., Feng, B., Li, J., Zhuo, Y., Wu, D., 2022. Dietary Fiber Supplementation in Gestating Sow Diet Improved Fetal Growth and Placental Development and Function Through Serotonin Signaling Pathway. Front. Vet. Sci. 9, 1–13. https://doi.org/10.3389/fvets.2022.831703

Lih, T.M., Clark, D.J., Zhang, H., 2019. Omic-Sig: Utilizing Omics Data to Explore and Visualize Kinase-Substrate Interactions. https://doi.org/10.1101/746123

Lu, L., Finegold, M.J., Johnson, R.L., 2018. Hippo pathway coactivators yap and taz are required to coordinate mammalian liver regeneration. Exp. Mol. Med. 50. https://doi.org/10.1038/emm.2017.205

Lundeberg, L., El-Nour, H., Mohabbati, S., Morales, M., Azmitia, E., Nordlind, K., 2002. Expression of serotonin receptors in allergic contact eczematous human skin. Arch. Dermatol. Res. 294, 393–398. https://doi.org/10.1007/s00403-002-0350-y

Ma, C., Zeng, C., Jin, L., Yang, Y., Li, P., Chen, L., Wang, J., 2015. GSK3β mediates the carcinogenic effect of HPV16 in cervical cancer. Sci. Rep. 5, 2–10. https://doi.org/10.1038/srep16555

Macrì, F., Castiglione, S., Faggiano, S., Vigorito, I., Casaburo, M., Fanotti, N., Piacentini, L., Vigetti, D., Vinci, M.C., Raucci, A., 2024. High phosphate-induced JAK-STAT signalling sustains Vascular Smooth Muscle Cells inflammation and limits calcification. Vascul. Pharmacol. 155, 107328. https://doi.org/10.1016/j.vph.2024.107328

Maingrette, F., Dussault, S., Dhahri, W., Desjarlais, M., Mathieu, R., Turgeon, J., Haddad, P.,

Groleau, J., Perez, G., Rivard, A., 2015. Psychological stress impairs ischemia-induced neovascularization: Protective effect of fluoxetine. Atherosclerosis 241, 569–578. https://doi.org/10.1016/j.atherosclerosis.2015.06.010

Malemud, C.J., 2017. Negative regulators of JAK/STAT signaling in rheumatoid arthritis and osteoarthritis. Int. J. Mol. Sci. 18. https://doi.org/10.3390/ijms18030484

Malinin, A., Oshrine, B., Serebruany, V., 2004. Treatment with selective serotonin reuptake inhibitors for enhancing wound healing 103–109. https://doi.org/10.1016/j.mehy.2003.10.021

Man, X.-Y., Finnson, K.W., Baron, M., Philip, A., 2012. CD109, a TGF-β co-receptor, attenuates extracellular matrix production in scleroderma skin fibroblasts. Arthritis Res. Ther. 14, R144. https://doi.org/10.1186/ar3877

Marchocki, Z., Russell, N.E., Donoghue, K.O., 2013. Selective serotonin reuptake inhibitors and pregnancy: A review of maternal, fetal and neonatal risks and benefits. Obstet. Med. 6, 155–158. https://doi.org/10.1177/1753495X13495194

Martins, A.M., Ascenso, A., Ribeiro, H.M., Marto, J., 2020. The Brain-Skin Connection and the Pathogenesis of Psoriasis: A Review with a Focus on the Serotonergic System. Cells 9. https://doi.org/10.3390/cells9040796

Mayo-Wilson, E., Dias, S., Mavranezouli, I., Kew, K., Clark, D.M., Ades, A.E., Pilling, S., 2014. Psychological and pharmacological interventions for social anxiety disorder in adults: A systematic review and network meta-analysis. The Lancet Psychiatry 1, 368–376. https://doi.org/10.1016/S2215-0366(14)70329-3

Meigui, Z., Li, J., Xi, J., Xi, L., Ma, R., Zhou, R., Zhang, B., Li, Y., Bai, Z., 2022. (2E)-1-(2,4,6-trimethoxyphenyl)-3-(3-nitrophenyl)-2-propen-1-one Promotes Apoptosis By Regulating ERK/MAPK Pathway In Hepatocellular Carcinoma Cells. https://doi.org/10.21203/rs.3.rs-2058947/v1

Meyer, S.C., Levine, R.L., 2014. Molecular pathways: Molecular basis for sensitivity and resistance to JAK kinase inhibitors. Clin. Cancer Res. 20, 2051–2059. https://doi.org/10.1158/1078-0432.CCR-13-0279

Mia, M.M., Singh, M.K., 2022. New Insights into Hippo/YAP Signaling in Fibrotic Diseases. Cells 11, 1–22. https://doi.org/10.3390/cells11132065

Misra, J.R., Irvine, K.D., 2018. The hippo signaling network and its biological functions. Annu. Rev. Genet. 52, 65–87. https://doi.org/10.1146/annurev-genet-120417-031621

Mohr, A., Chatain, N., Domoszlai, T., Rinis, N., Sommerauer, M., Vogt, M., Müller-Newen, G., 2012. Dynamics and non-canonical aspects of JAK/STAT signalling. Eur. J. Cell Biol.

91, 524–532. https://doi.org/10.1016/j.ejcb.2011.09.005

Mole, R.A., Brooks, B.W., 2019. Global scanning of selective serotonin reuptake inhibitors: occurrence, wastewater treatment and hazards in aquatic systems. Environ. Pollut. 250, 1019–1031. https://doi.org/10.1016/j.envpol.2019.04.118

Molz, S., Dal-Cim, T., Budni, J., Martín-de-Saavedra, M.D., Egea, J., Romero, A., del Barrio, L., Rodrigues, A.L.S., López, M.G., Tasca, C.I., 2011. Neuroprotective effect of guanosine against glutamate-induced cell death in rat hippocampal slices is mediated by the phosphatidylinositol-3 kinase/Akt/ glycogen synthase kinase 3β pathway activation and inducible nitric oxide synthase inhibition. J. Neurosci. Res. 89, 1400–1408. https://doi.org/10.1002/jnr.22681

Montilla, A.M., Gómez-García, F., Gómez-Arias, P.J., Gay-Mimbrera, J., Hernández-Parada, J., Isla-Tejera, B., Ruano, J., 2019. Scoping Review on the Use of Drugs Targeting JAK/STAT Pathway in Atopic Dermatitis, Vitiligo, and Alopecia Areata. Dermatol. Ther. (Heidelb). 9, 655–683. https://doi.org/10.1007/s13555-019-00329-y

Moon, S.Y., Kim, K.D., Yoo, J., Lee, J.H., Hwangbo, C., 2021. Phytochemicals targeting JAK–STAT pathways in inflammatory bowel disease: Insights from animal models. Molecules 26. https://doi.org/10.3390/molecules26092824

Moore, K.E., Gozani, O., 2014. An unexpected journey: Lysine methylation across the proteome. Biochim. Biophys. Acta - Gene Regul. Mech. 1839, 1395–1403. https://doi.org/10.1016/j.bbagrm.2014.02.008

Morales, J.K., Falanga, Y.T., Depcrynski, A., Fernando, J., Ryan, J.J., 2010. Mast cell homeostasis and the JAK–STAT pathway. Genes Immun. 11, 599–608. https://doi.org/10.1038/gene.2010.35

Mössner, R., Daniel, S., Schmitt, A., Albert, D., Lesch, K.P., 2001. Modulation of serotonin transporter function by interleukin-4. Life Sci. 68, 873–880. https://doi.org/10.1016/S0024-3205(00)00992-9

Mössner, R., Lesch, K.P., 1998. Role of serotonin in the immune system and in neuroimmune interactions. Brain. Behav. Immun. 12, 249–271. https://doi.org/10.1006/brbi.1998.0532

Moutal, A., Villa, L.S., Yeon, S.K., Householder, K.T., Park, K.D., Sirianni, R.W., Khanna, R., 2018. CRMP2 Phosphorylation Drives Glioblastoma Cell Proliferation. Mol. Neurobiol. 55, 4403–4416. https://doi.org/10.1007/s12035-017-0653-9

Nakajima, W., Sharma, K., Lee, J.Y., Maxim, N.T., Hicks, M.A., Vu, T.T., Luu, A., Yeudall, W.A., Tanaka, N., Harada, H., 2016. DNA damaging agent-induced apoptosis is regulated by MCL-1 phosphorylation and degradation mediated by the Noxa/MCL-1/CDK2

complex. Oncotarget 7, 36353–36365. https://doi.org/10.18632/oncotarget.9217

Nambu, M., Ishihara, M., Nakamura, S., Mizuno, H., Yanagibayashi, S., Kanatani, Y., Hattori, H., Takase, B., Ishizuka, T., Kishimoto, S., Amano, Y., Yamamoto, N., Azuma, R., Kiyosawa, T., 2007. Enhanced healing of mitomycin C-treated wounds in rats using inbred adipose tissue-derived stromal cells within an atelocollagen matrix. Wound Repair Regen. 15, 505–510. https://doi.org/10.1111/j.1524-475X.2007.00258.x

Nebigil, C.G., Etienne, N., Messaddeq, N., Maroteaux, L., 2003. Serotonin is a novel survival factor of cardiomyocytes: mitochondria as a target of 5-HT2B receptor signaling. FASEB J. 17, 1373–1375. https://doi.org/10.1096/fj.02-1122fje

Nguyen, C.M., Tartar, D.M., Bagood, M.D., So, M., Nguyen, A.V., Gallegos, A., Fregoso, D., Serrano, J., Nguyen, D., Degovics, D., Adams, A., Harouni, B., Fuentes, J.J., Gareau, M.G., Crawford, R.W., Soulika, A.M., Isseroff, R.R., 2019. Topical fluoxetine as a novel therapeutic that improves wound healing in diabetic mice. Diabetes 68, 1499–1507. https://doi.org/10.2337/db18-1146

Ni, Y.G., Miledi, R., 1997. Blockage of 5HT2C serotonin receptors by fluoxetine (Prozac). Proc. Natl. Acad. Sci. U. S. A. 94, 2036–2040. https://doi.org/10.1073/pnas.94.5.2036

Nishi, H., Hashimoto, K., Panchenko, A.R., 2011. Phosphorylation in protein-protein binding: Effect on stability and function. Structure 19, 1807–1815. https://doi.org/10.1016/j.str.2011.09.021

Nishi, H., Shaytan, A., Panchenko, A.R., 2014. Physicochemical mechanisms of protein regulation by phosphorylation. Front. Genet. 5, 1–10. https://doi.org/10.3389/fgene.2014.00270

Nishimoto, T., Kihara, T., Akaike, A., Niidome, T., Sugimoto, H., 2008. A-Amino-3-Hydroxy-5-Methyl-4-Isoxazole Propionate Attenuates Glutamate-Induced Caspase-3 Cleavage Via Regulation of Glycogen Synthase Kinase 3B. J. Neurosci. Res. 86, 1096–1105. https://doi.org/10.1002/jnr.21567

Nordlind, K., Azmitia, E.C., Slominski, A., 2008. The skin as a mirror of the soul: Exploring the possible roles of serotonin. Exp. Dermatol. 17, 301–311. https://doi.org/10.1111/j.1600-0625.2007.00670.x

Oakes, K.D., Coors, A., Escher, B.I., Fenner, K., Garric, J., Gust, M., Knacker, T., Küster, A., Kussatz, C., Metcalfe, C.D., Monteiro, S., Moon, T.W., Mennigen, J.A., Parrott, J., Péry, A.R.R., Ramil, M., Roennefahrt, I., Tarazona, J. V., Sánchez-Argüello, P., Ternes, T.A., Trudeau, V.L., Boucard, T., Van Der Kraak, G.J., Servos, M.R., 2010. Environmental risk assessment for the serotonin re uptake inhibitor fluoxetine: Case study using the european

risk assessment framework. Integr. Environ. Assess. Manag. 6, 524–539. https://doi.org/10.1002/ieam.77

Önal, H.T., Yetkin, D., Ayaz, F., 2023. Immunostimulatory activity of fluoxetine in macrophages via regulation of the PI3K and P38 signaling pathways. Immunol. Res. 71, 413–421. https://doi.org/10.1007/s12026-022-09350-4

Ozgok Kangal, M.K., Regan, J.-P., 2022. Wound Healing. Treasure Island (FL).

Pan, D., 2007. Hippo signaling in organ size control. Genes Dev. 21, 886–897. https://doi.org/10.1101/gad.1536007

Pan, S.M., Zhou, Y.F., Zuo, N., Jiao, R.Q., Kong, L.D., Pan, Y., 2022. Fluoxetine increases astrocytic glucose uptake and glycolysis in corticosterone-induced depression through restricting GR-TXNIP-GLUT1 Pathway. Front. Pharmacol. 13, 1–17. https://doi.org/10.3389/fphar.2022.872375

Pandian, J., Panneerpandian, P., Devanandan, H.J., Sekar, B.T., Balakrishnan, K., Selvarasu, K., Muthupandi, K., Ganesan, K., 2020. Identification of the targeted therapeutic potential of doxycycline for a subset of gastric cancer patients. Ann. N. Y. Acad. Sci. 1467, 94–111. https://doi.org/10.1111/nyas.14288

Parrish, J.C., Nichols, D.E., 2006. Serotonin 5-HT2A receptor activation induces 2-arachidonoylglycerol release through a phospholipase c-dependent mechanism. J. Neurochem. 99, 1164–1175. https://doi.org/10.1111/j.1471-4159.2006.04173.x

Passaro, M.L., Matarazzo, F., Abbadessa, G., Pezone, A., Porcellini, A., Tranfa, F., Rinaldi, M., Costagliola, C., 2023. Glaucoma as a Tauopathy—Is It the Missing Piece in the Glaucoma Puzzle? J. Clin. Med. 12. https://doi.org/10.3390/jcm12216900

Pekmez, M., Milat, N.S., 2020. Evaluation of in Vitro Wound Healing Activity of Thymoquinone. Eur. J. Biol. 79, 151–156. https://doi.org/10.26650/EurJBiol.2020.0044

Pellicoro, A., Aucott, R.L., Ramachandran, P., Robson, A.J., Fallowfield, J.A., Snowdon, V.K., Hartland, S.N., Vernon, M., Duffield, J.S., Benyon, C.R., Forbes, S.J., Iredale, J.P., 2012. Elastin accumulation is regulated at the level of degradation by macrophage metalloelastase (MMP-12) during experimental liver fibrosis. Hepatology 55, 1965–1975. https://doi.org/10.1002/hep.25567

Peng, L., Gu, L., Li, B., Hertz, L., 2014. Fluoxetine and all other SSRIs are 5-HT_{2B} Agonists - Importance for their Therapeutic Effects. Curr. Neuropharmacol. 12, 365–379. https://doi.org/10.2174/1570159x12666140828221720

Penkova, N.I., Nikolova, J.G., 2017. Serotonin and its Functions as Gastrointestinal Hormone. J. Gastrointest. Dig. Syst. 07. https://doi.org/10.4172/2161-069x.1000537

Peretti, S., Judge, R., Hindmarch, I., 2000. Safety and tolerability considerations: tricyclic antidepressants vs. selective serotonin reuptake inhibitors. Acta Psychiatr. Scand. 101, 17–25. https://doi.org/10.1111/j.1600-0447.2000.tb10944.x

Periayah MH, Halim AS, Saad AZM, 2017. Mechanism action of platelets and crucial blood coagulation pathways in Hemostasis. Int. J. Hematol. Stem Cell Res. 11, 319–327.

Perrot-Minnot, M.J., Kaldonski, N., Cézilly, F., 2007. Increased susceptibility to predation and altered anti-predator behaviour in an acanthocephalan-infected amphipod. Int. J. Parasitol. 37, 645–651. https://doi.org/10.1016/j.ijpara.2006.12.005

Pho, H., Amorim, M.R., Qiu, Q., Shin, M.K., Kim, L.J., Anokye-Danso, F., Jun, J.J., Ahima, R.S., Branco, L.G.S., Kuhn, D.M., Mateika, J.H., Polotsky, V.Y., 2022. The effect of brain serotonin deficiency on breathing is magnified by age. Physiol. Rep. 10, 1–11. https://doi.org/10.14814/phy2.15245

Poggini, S., Golia, M.T., Alboni, S., Milior, G., Sciarria, L.P., Viglione, A., Bon, G.M., Brunello, N., Puglisi-Allegra, S., Limatola, C., Maggi, L., Branchi, I., 2019. Combined fluoxetine and metformin treatment potentiates antidepressant efficacy increasing IGF2 expression in the dorsal hippocampus. Neural Plast. 2019. https://doi.org/10.1155/2019/4651031

Polter, A.M., Yang, S., Jope, R.S., Li, X., 2012. Functional significance of glycogen synthase kinase-3 regulation by serotonin. Cell. Signal. 24, 265–271. https://doi.org/10.1016/j.cellsig.2011.09.009

Quatresooz, P., Kharfi, M., Paquet, P., Vroome, V., Cauwenbergh, G., Piérard, G.E., 2006. Healing effect of ketanserin on chronic leg ulcers in patients with diabetes. J. Eur. Acad. Dermatology Venereol. 20, 277–281. https://doi.org/10.1111/j.1468-3083.2006.01422.x

Reinke, J.M., Sorg, H., 2012. Wound repair and regeneration. Eur. Surg. Res. 49, 35–43. https://doi.org/10.1159/000339613

Reyes, D., Ballaré, C., Castellano, G., Soronellas, D., Bagó, J.R., Blanco, J., Beato, M., 2014. Activation of mitogen-and stress-activated kinase 1 is required for proliferation of breast cancer cells in response to estrogens or progestins. Oncogene 33, 1570–1580. https://doi.org/10.1038/onc.2013.95

Riahi, R., Yang, Y., Zhang, D.D., Wong, P.K., 2012. Advances in wound-healing assays for probing collective cell migration. J. Lab. Autom. 17, 59–65. https://doi.org/10.1177/2211068211426550

Rochat, B., Baumann, P., Audus, K.L., 1999. Transport mechanisms for the antidepressant citalopram in brain microvessel endothelium. Brain Res. 831, 229–236.

https://doi.org/10.1016/S0006-8993(99)01461-4

Rodriguez-Barucg, Q., Garcia, A.A., Garcia-merino, B., Akinmola, T., Okotie-eboh, T., Francis, T., Bringas, E., Ortiz, I., Wade, M.A., Dowle, A., Joyce, D.A., Hardman, M.J., Wilkinson, H.N., Beltran-alvarez, P., 2024. Environmental fluoxetine promotes skin cell proliferation and wound healing ☆. Environ. Pollut. 362, 124952. https://doi.org/10.1016/j.envpol.2024.124952

Roose, S.P., Rutherford, B.R., 2016. Selective Serotonin Reuptake Inhibitors and Operative Bleeding Risk. J. Clin. Psychopharmacol. 36, 704–709. https://doi.org/10.1097/JCP.0000000000000575

Rosengren, S., Corr, M., Boyle, D.L., 2010. Platelet-derived growth factor and transforming growth factor beta synergistically potentiate inflammatory mediator synthesis by fibroblast-like synoviocytes. Arthritis Res. Ther. 12, R65. https://doi.org/10.1186/ar2981

Rothgiesser, K.M., Fey, M., Hottiger, M.O., 2010. Acetylation of p65 at lysine 314 is important for late NF-κB-dependent gene expression. BMC Genomics 11. https://doi.org/10.1186/1471-2164-11-22

Sadiq, A., Shah, A., Jeschke, M.G., Belo, C., Hayat, M.Q., Murad, S., Amini-Nik, S., 2018. The role of serotonin during skin healing in post-thermal injury. Int. J. Mol. Sci. 19, 1–20. https://doi.org/10.3390/ijms19041034

Sahu, A., Gopalakrishnan, L., Gaur, N., Chatterjee, O., Mol, P., Modi, P.K., Dagamajalu, S., Advani, J., Jain, S., Keshava Prasad, T.S., 2018. The 5-Hydroxytryptamine signaling map: an overview of serotonin-serotonin receptor mediated signaling network. J. Cell Commun. Signal. 12, 731–735. https://doi.org/10.1007/s12079-018-0482-2

Sahu, B., Pihlajamaa, P., Zhang, K., Palin, K., Ahonen, S., Cervera, A., Ristimäki, A., Aaltonen, L.A., Hautaniemi, S., Taipale, J., 2021. Human cell transformation by combined lineage conversion and oncogene expression. Oncogene 40, 5533–5547. https://doi.org/10.1038/s41388-021-01940-0

Salgado, R., Marques, R., Noronha, J.P., Mexia, J.T., Carvalho, G., Oehmen, A., Reis, M.A.M., 2011. Assessing the diurnal variability of pharmaceutical and personal care products in a full-scale activated sludge plant. Environ. Pollut. 159, 2359–2367. https://doi.org/10.1016/j.envpol.2011.07.004

Samarajeewa, A., Goldemann, L., Vasefi, M.S., Ahmed, N., Gondora, N., Khanderia, C., Mielke, J.G., Beazely, M.A., 2014. 5-HT7 receptor activation promotes an increase in TrkB receptor expression and phosphorylation. Front. Behav. Neurosci. 8, 1–9.

https://doi.org/10.3389/fnbeh.2014.00391

Sanchez, C., Reines, E.H., Montgomery, S.A., 2014. A comparative review of escitalopram, paroxetine, and sertraline: Are they all alike? Int. Clin. Psychopharmacol. 29, 185–196. https://doi.org/10.1097/YIC.0000000000000023

Savill, J.S., Wyllie, A.H., Henson, J.E., Walport, M.J., Henson, P.M., Haslett, C., 1989. Macrophage phagocytosis of aging neutrophils in inflammation. Programmed cell death in the neutrophil leads to its recognition by macrophages. J. Clin. Invest. 83, 865–875. https://doi.org/10.1172/JCI113970

Sawicka, A., Hartl, D., Goiser, M., Pusch, O., Stocsits, R.R., Tamir, I.M., Mechtler, K., Seiser, C., 2014. H3S28 phosphorylation is a hallmark of the transcriptional response to cellular stress. Genome Res. 24, 1808–1820. https://doi.org/10.1101/gr.176255.114

Schallreuter, K.U., Salem, M.A.E.L., Gibbons, N.C.J., Martinez, A., Slominski, R., Lüdemann, J., Rokos, H., 2012. Blunted epidermal L-tryptophan metabolism in vitiligo affects immune response and ROS scavenging by Fenton chemistry, part 1: epidermal H 2 O 2 /ONOO – -mediated stress abrogates tryptophan hydroxylase and dopa decarboxylase activities, leading to low se. FASEB J. 26, 2457–2470. https://doi.org/10.1096/fj.11-197137

Schlüsener, M.P., Hardenbicker, P., Nilson, E., Schulz, M., Viergutz, C., Ternes, T.A., 2015. Occurrence of venlafaxine, other antidepressants and selected metabolites in the Rhine catchment in the face of climate change. Environ. Pollut. 196, 247–256. https://doi.org/10.1016/j.envpol.2014.09.019

Schneider, C.A., Rasband, W.S., Eliceiri, K.W., 2012. NIH Image to ImageJ: 25 years of image analysis. Nat. Methods 9, 671–675. https://doi.org/10.1038/nmeth.2089

Schultz, G., Chin, G., Moldawer, L., 2011. Principles of Wound Healing, in: Mechanisms of Vascular Disease: A Reference Book for Vascular Specialists. p. 23.

Schultz, M.M., Furlong, E.T., Kolpin, D.W., Werner, S.L., Schoenfuss, H.L., Barber, L.B., Blazer, V.S., Norris, D.O., Vajda, A.M., 2010. Antidepressant pharmaceuticals in two U.S. effluent-impacted streams: Occurrence and fate in water and sediment and selective uptake in fish neural tissue. Environ. Sci. Technol. 44, 1918–1925. https://doi.org/10.1021/es9022706

Schultz, M.M., Painter, M.M., Bartell, S.E., Logue, A., Furlong, E.T., Werner, S.L., Schoenfuss, H.L., 2011. Selective uptake and biological consequences of environmentally relevant antidepressant pharmaceutical exposures on male fathead minnows. Aquat. Toxicol. 104, 38–47. https://doi.org/10.1016/j.aquatox.2011.03.011

Seuwen, K., Magnaldo, I., Pouysségur, J., 1988. Serotonin stimulates DNA synthesis in fibroblasts acting through 5-HT1B receptors coupled to a Gi-protein. Nature 335, 254–256. https://doi.org/10.1038/335254a0

Shao, S., Zhuang, X., Zhang, L., Qiao, T., 2022. Antidepressants Fluoxetine Mediates Endoplasmic Reticulum Stress and Autophagy of Non–Small Cell Lung Cancer Cells Through the ATF4-AKT-mTOR Signaling Pathway. Front. Pharmacol. 13, 1–15. https://doi.org/10.3389/fphar.2022.904701

Shi, Y., Sun, H., 2020. Down-regulation of lncrna linc00152 suppresses gastric cancer cell migration and invasion through inhibition of the ERK/MAPK signaling pathway. Onco. Targets. Ther. 13, 2115–2124. https://doi.org/10.2147/OTT.S217452

Shishido, S.N., Nguyen, T.A., 2016. Induction of apoptosis by PQ1, a gap junction enhancer that upregulates connexin 43 and activates the MAPK signaling pathway in mammary carcinoma cells. Int. J. Mol. Sci. 17, 1–19. https://doi.org/10.3390/ijms17020178

Shraim, A., Diab, A., Alsuhaimi, A., Niazy, E., Metwally, M., Amad, M., Sioud, S., Dawoud, A., 2017. Analysis of some pharmaceuticals in municipal wastewater of Almadinah Almunawarah. Arab. J. Chem. 10, S719–S729. https://doi.org/10.1016/j.arabjc.2012.11.014

Silva, L.J.G., Lino, C.M., Meisel, L.M., Pena, A., 2012. Selective serotonin re-uptake inhibitors (SSRIs) in the aquatic environment: An ecopharmacovigilance approach. Sci. Total Environ. 437, 185–195. https://doi.org/10.1016/j.scitotenv.2012.08.021

Simpson, D.M., Ross, R., 1972. The neutrophilic leukocyte in wound repair. J. Clin. Invest. 51, 2009–2023. https://doi.org/10.1172/JCI107007

Singh, E.K., Nazarova, L.A., Lapera, S.A., Alexander, L.D., McAlpine, S.R., 2010. Histone deacetylase inhibitors: Synthesis of cyclic tetrapeptides and their triazole analogs. Tetrahedron Lett. 51, 4357–4360. https://doi.org/10.1016/j.tetlet.2010.06.050

Skapinakis, P., Bakola, E., Salanti, G., Lewis, G., Kyritsis, A.P., Mavreas, V., 2010. Efficacy and acceptability of selective serotonin reuptake inhibitors for the treatment of depression in Parkinson's disease: A systematic review and meta-analysis of randomized controlled trials. BMC Neurol. 10. https://doi.org/10.1186/1471-2377-10-49

Slominski, A., Pisarchik, A., Semak, I., Sweatman, T., Wortsman, J., Szczesniewski, A., Slugocki, G., McNulty, J., Kauser, S., Tobin, D.J., Jing, C., Johansson, O., 2002. Serotoninergic and melatoninergic systems are fully expressed in human skin. FASEB J. 16, 896–898. https://doi.org/10.1096/fj.01-0952fje

Slominski, A., Pisarchik, A., Zbytek, B., Tobin, D.J., Kauser, S., Wortsman, J., 2003.

Functional activity of serotoninergic and melatoninergic systems expressed in the skin. J. Cell. Physiol. 196, 144–153. https://doi.org/10.1002/jcp.10287

Slominski, R.M., Chen, J.Y., Raman, C., Slominski, A.T., 2024. Photo-neuro-immuno-endocrinology: How the ultraviolet radiation regulates the body, brain, and immune system. Proc. Natl. Acad. Sci. U. S. A. 121, 1–8. https://doi.org/10.1073/pnas.2308374121

Smith, E.M., Chu, S., Paterson, G., Metcalfe, C.D., Wilson, J.Y., 2010. Chemosphere Cross-species comparison of fluoxetine metabolism with fish liver microsomes. Chemosphere 79, 26–32. https://doi.org/10.1016/j.chemosphere.2010.01.058

Sommi, R.W., Crismon, M.L., Bowden, C.L., 1987. Fluoxetine: A Serotonin-specific, Second-generation Antidepressant. Pharmacother. J. Hum. Pharmacol. Drug Ther. 7, 1–14. https://doi.org/10.1002/j.1875-9114.1987.tb03496.x

Sorg, H., Tilkorn, D.J., Hager, S., Hauser, J., Mirastschijski, U., 2017. Skin Wound Healing: An Update on the Current Knowledge and Concepts. Eur. Surg. Res. 58, 81–94. https://doi.org/10.1159/000454919

Sousa-Ferreira, L., Aveleira, C., Botelho, M., Álvaro, A.R., Pereira De Almeida, L., Cavadas, C., 2014. Fluoxetine induces proliferation and inhibits differentiation of hypothalamic neuroprogenitor cells in vitro. PLoS One 9. https://doi.org/10.1371/journal.pone.0088917

Stapel, B., Melzer, C., von der Ohe, J., Hillemanns, P., Bleich, S., Kahl, K.G., Hass, R., 2021. Effect of SSRI exposure on the proliferation rate and glucose uptake in breast and ovary cancer cell lines. Sci. Rep. 11, 1–14. https://doi.org/10.1038/s41598-020-80850-9

Stark, G.R., Wang, Y., Lu, T., 2011. Lysine methylation of promoter-bound transcription factors and relevance to cancer. Cell Res. 21, 375–380. https://doi.org/10.1038/cr.2010.174

Stojadinovic, O., Lee, B., Vouthounis, C., Vukelic, S., Pastar, I., Blumenberg, M., Brem, H., Tomic-Canic, M., 2007. Novel genomic effects of glucocorticoids in epidermal keratinocytes: Inhibition of apoptosis, interferon-γ pathway, and wound healing along with promotion of terminal differentiation. J. Biol. Chem. 282, 4021–4034. https://doi.org/10.1074/jbc.M606262200

Strawn, J.R., Welge, J.A., Wehry, A.M., Keeshin, B., Rynn, M.A., 2015. EFFICACY AND TOLERABILITY OF ANTIDEPRESSANTS IN PEDIATRIC ANXIETY DISORDERS: A SYSTEMATIC REVIEW AND META-ANALYSIS. Depress. Anxiety 32, 149–157. https://doi.org/10.1002/da.22329

Sumpter, J.P., Donnachie, R.L., Johnson, A.C., 2014. The apparently very variable potency of

the anti-depressant fluoxetine. Aquat. Toxicol. 151, 57–60. https://doi.org/10.1016/j.aquatox.2013.12.010

Tai, C., Tzeng, C., 2014. Adenosine Triphosphate Activates Mitogen-Activated 142, 1554–1560.

Taraboletti, G., D'Ascenzo, S., Borsotti, P., Giavazzi, R., Pavan, A., Dolo, V., 2002. Shedding of the Matrix Metalloproteinases MMP-2, MMP-9, and MT1-MMP as Membrane Vesicle-Associated Components by Endothelial Cells. Am. J. Pathol. 160, 673–680. https://doi.org/10.1016/S0002-9440(10)64887-0

Tate, K., Kirk, B., Tseng, A., Ulffers, A., Litwa, K., 2021. Effects of the selective serotonin reuptake inhibitor fluoxetine on developing neural circuits in a model of the human fetal cortex. Int. J. Mol. Sci. 22. https://doi.org/10.3390/ijms221910457

Tian, X.Q., Guo, F.F., Sun, D.F., Wang, Y.C., Yang, L., Chen, S.L., Hong, J., Fang, J.Y., 2017. Downregulation of ZNF278 arrests the cell cycle and decreases the proliferation of colorectal cancer cells via inhibition of the ERK/MAPK pathway. Oncol. Rep. 38, 3685–3692. https://doi.org/10.3892/or.2017.6031

Tijani, A.O., Nunez, E., Singh, K., Khanna, G., Puri, A., 2021. Transdermal Route: A Viable Option for Systemic Delivery of Antidepressants. J. Pharm. Sci. 110, 3129–3149. https://doi.org/10.1016/j.xphs.2021.05.015

Timmer, C.J., Sitsen, J.M.A., Delbressine, L.P., 2000. of Mirtazapine 38, 461–474.

Ukil, A., Kar, S., Srivastav, S., Ghosh, K., Das, P.K., 2011. Curative effect of 18β-glycyrrhetinic acid in experimental visceral leishmaniasis depends on phosphatase-dependent modulation of cellular MAP kinases. PLoS One 6. https://doi.org/10.1371/journal.pone.0029062

Vadaq, N., Zhang, Y., Meeder, E., Van de Wijer, L., Gasem, M.H., Joosten, L.A.B., Netea, M.G., de Mast, Q., Matzaraki, V., Schellekens, A., Fu, J., van der Ven, A.J.A.M., 2022. Microbiome-Related Indole and Serotonin Metabolites are Linked to Inflammation and Psychiatric Symptoms in People Living with HIV. Int. J. Tryptophan Res. 15. https://doi.org/10.1177/11786469221126888

Vaiana, C.A., Leonard, M.K., Drummy, L.F., Singh, K.M., Bubulya, A., Vaia, R.A., Naik, R.R., Kadakia, M.P., 2011. Epidermal growth factor: Layered silicate nanocomposites for tissue regeneration. Biomacromolecules 12, 3139–3146. https://doi.org/10.1021/bm200616v

van Harten, J., 1993. Clinical Pharmacokinetics of Selective Serotonin Reuptake Inhibitors. Clin. Pharmacokinet. 24, 203–220. https://doi.org/10.2165/00003088-199324030-00003

van Westrhenen, R., Aitchison, K.J., Ingelman-Sundberg, M., Jukić, M.M., 2020. Pharmacogenomics of Antidepressant and Antipsychotic Treatment: How Far Have We Got and Where Are We Going? Front. Psychiatry 11, 1–11. https://doi.org/10.3389/fpsyt.2020.00094

Vaswani, M., Linda, F.K., Ramesh, S., 2003. Role of selective serotonin reuptake inhibitors in psychiatric disorders: A comprehensive review. Prog. Neuro-Psychopharmacology Biol. Psychiatry 27, 85–102. https://doi.org/10.1016/S0278-5846(02)00338-X

Veves, A., Giurini, J.M., LoGerfo, F.W., 2012. The diabetic foot: Medical and surgical management: Third edition. Diabet. Foot Med. Surg. Manag. Third Ed. 1–554. https://doi.org/10.1007/978-1-61779-791-0

Viji, R.I., Sameer Kumar, V.B., Kiran, M.S., Sudhakaran, P.R., 2009. Modulation of endothelial nitric oxide synthase by fibronectin. Mol. Cell. Biochem. 323, 91–100. https://doi.org/10.1007/s11010-008-9967-2

Vleugels, R., Verlinden, H., Broeck, J. Vanden, 2015. Serotonin, serotonin receptors and their actions in insects. Neurotransmitter. https://doi.org/10.14800/nt.314

Von Wolff, A., Hölzel, L.P., Westphal, A., Härter, M., Kriston, L., 2013. Selective serotonin reuptake inhibitors and tricyclic antidepressants in the acute treatment of chronic depression and dysthymia: A systematic review and meta-analysis. J. Affect. Disord. 144, 7–15. https://doi.org/10.1016/j.jad.2012.06.007

Wahl, S.M., Wong, H., McCartney-Francis, N., 1989. Role of growth factors in inflammation and repair. J. Cell. Biochem. 40, 193–199. https://doi.org/10.1002/jcb.240400208

Wang, C.C., Man, G.C.W., Chu, C.Y., Borchert, A., Ugun-Klusek, A., Billett, E.E., Kühn, H., Ufer, C., 2014. Serotonin receptor 6 mediates defective brain development in monoamine oxidase A-deficient mouse embryos. J. Biol. Chem. 289, 8252–8263. https://doi.org/10.1074/jbc.M113.522094

Wang, R., Song, Y., Liu, X., Wang, Q., Wang, Y., Li, L., Kang, C., Zhang, Q., 2017. UBE2C induces EMT through Wnt/β-catenin and PI3K/Akt signaling pathways by regulating phosphorylation levels of Aurora-A. Int. J. Oncol. 50, 1116–1126. https://doi.org/10.3892/ijo.2017.3880

Wang, Y.W., Ren, J.H., Xia, K., Wang, S.H., Yin, T.F., Xie, D.H., Li, L.H., 2012. Effect of mitomycin on normal dermal fibroblast and HaCat cell: An in vitro study. J. Zhejiang Univ. Sci. B 13, 997–1005. https://doi.org/10.1631/jzus.B1200055

Wang, Y.X., Zhang, X.R., Zhang, Z.J., Li, L., Xi, G.J., Wu, D., Wang, Y.J., 2014. Protein kinase Mζ is involved in the modulatory effect of fluoxetine on hippocampal neurogenesis

in vitro. Int. J. Neuropsychopharmacol. 29, 1429–1441. https://doi.org/10.1017/S1461145714000364

Watanabe, N., Omori, I.M., Nakagawa, A., Cipriani, A., Barbui, C., Churchill, R., Furukawa, T.A., 2011. Mirtazapine versus other antidepressive agents for depression. Cochrane Database Syst. Rev. https://doi.org/10.1002/14651858.cd006528.pub2

Wei, Y., Yang, W.J., Wang, Q.J., Lin, P.C., Zhao, J.Y., Xu, W., Zhao, S.M., He, X. Di, 2019. Cell-Wide Survey of Amide-Bonded Lysine Modifications by Using Deacetylase CobB. Biol. Proced. Online 21, 1–12. https://doi.org/10.1186/s12575-019-0109-x

Weinberger, J., Klaper, R., 2014. Environmental concentrations of the selective serotonin reuptake inhibitor fluoxetine impact specific behaviors involved in reproduction, feeding and predator avoidance in the fish Pimephales promelas (fathead minnow). Aquat. Toxicol. 151, 77–83. https://doi.org/10.1016/j.aquatox.2013.10.012

Welsh, D.J., Harnett, M., MacLean, M., Peacock, A.J., 2004. Proliferation and Signaling in Fibroblasts. Am. J. Respir. Crit. Care Med. 170, 252–259. https://doi.org/10.1164/rccm.200302-264oc

Wilkinson, H.N., Hardman, M.J., 2020a. Wound healing: cellular mechanisms and pathological outcomes. Open Biol. 10. https://doi.org/10.1098/rsob.200223

Wilkinson, H.N., Hardman, M.J., 2020b. Senescence in Wound Repair: Emerging Strategies to Target Chronic Healing Wounds. Front. Cell Dev. Biol. 8, 1–13. https://doi.org/10.3389/fcell.2020.00773

Wilkinson, H.N., Kidd, A.S., Roberts, E.R., Hardman, M.J., 2021. Human ex vivo wound model and whole-mount staining approach to accurately evaluate skin repair. J. Vis. Exp. 2021, 1–18. https://doi.org/10.3791/62326

Wilson, K., Mottram, P., 2004. A comparison of side effects of selective serotonin reuptake inhibitors and tricyclic antidepressants in older depressed patients: A meta-analysis. Int. J. Geriatr. Psychiatry 19, 754–762. https://doi.org/10.1002/gps.1156

Wood, K.M., Hashemi, P., 2013. Fast-Scan Cyclic Voltammetry Analysis of Dynamic Serotonin Reponses to Acute Escitalopram. ACS Chem. Neurosci. 4, 715–720. https://doi.org/10.1021/cn4000378

Woodman, S.G., Steinkey, D., Dew, W.A., Burket, S.R., Brooks, B.W., Pyle, G.G., 2016. Effects of sertraline on behavioral indices of crayfish Orconectes virilis. Ecotoxicol. Environ. Saf. 134, 31–37. https://doi.org/10.1016/j.ecoenv.2016.08.011

Woods, S., Clarke, N.N., Layfield, R., Fone, K.C.F., 2012. 5-HT6 receptor agonists and antagonists enhance learning and memory in a conditioned emotion response paradigm

by modulation of cholinergic and glutamatergic mechanisms. Br. J. Pharmacol. 167, 436–449. https://doi.org/10.1111/j.1476-5381.2012.02022.x

Writer, J.H., Ferrer, I., Barber, L.B., Thurman, E.M., 2013. Widespread occurrence of neuro-active pharmaceuticals and metabolites in 24 Minnesota rivers and wastewaters. Sci. Total Environ. 461–462, 519–527. https://doi.org/10.1016/j.scitotenv.2013.04.099

Wu, F., Song, L., Gong, Y., Wang, Y., Li, H., Zhang, S., 2023. Antimicrobial Peptide Pt5-1c Promotes Keratinocyte Migration and Proliferation via EGFR-mediated Akt/MAPK/STAT3 pathways. ChemistrySelect 8. https://doi.org/10.1002/slct.202203707

Wu, H.L., Pang, S.L., Liu, Q.Z., Wang, Q., Cai, M.X., Shang, J., 2014. 5-HT1A/1B receptors as targets for optimizing pigmentary responses in C57BL/6 mouse skin to stress. PLoS One 9. https://doi.org/10.1371/journal.pone.0089663

Xiao, H.H., Sham, T.T., Chan, C.O., Li, M.H., Chen, X., Wu, Q.C., Mok, D.K.W., Yao, X.S., Wong, M.S., 2018. A metabolomics study on the bone protective effects of a lignan-rich fraction from Sambucus Williamsii Ramulus in aged rats. Front. Pharmacol. 9. https://doi.org/10.3389/fphar.2018.00932

Yamazaki, Y., Matsubara, T., Takahashi, T., Kurashige, T., Dohi, E., Hiji, M., Nagano, Y., Yamawaki, T., Matsumoto, M., 2011. Granulovacuolar degenerations appear in relation to hippocampal phosphorylated tau accumulation in various neurodegenerative disorders. PLoS One 6. https://doi.org/10.1371/journal.pone.0026996

Yang, H., Cao, Q., Xiong, X., Zhao, P., Shen, D., Zhang, Y., Zhang, N., 2020. Fluoxetine regulates glucose and lipid metabolism via the PI3K-AKT signaling pathway in diabetic rats. Mol. Med. Rep. 22, 3073–3080. https://doi.org/10.3892/mmr.2020.11416

Yao, K., Qiu, S., Tian, L., Snider, W.D., Flannery, J.G., Schaffer, D. V., Chen, B., 2016. Wnt Regulates Proliferation and Neurogenic Potential of Müller Glial Cells via a Lin28/let-7 miRNA-Dependent Pathway in Adult Mammalian Retinas. Cell Rep. 17, 165–178. https://doi.org/10.1016/j.celrep.2016.08.078

Ye, H., Li, L., Guo, H., Yin, Y., 2012. MYBL2 is a substrate of GSK3-like kinase BIN2 and acts as a corepressor of BES1 in brassinosteroid signaling pathway in Arabidopsis. Proc. Natl. Acad. Sci. U. S. A. 109, 20142–20147. https://doi.org/10.1073/pnas.1205232109

Yoon, D.J., Nguyen, C., Bagood, M.D., Fregoso, D.R., Yang, H. ya, Medina Lopez, A.I., Crawford, R.W., Tran, J., Isseroff, R.R., 2021. Topical Fluoxetine as a Potential Nonantibiotic Adjunctive Therapy for Infected Wounds. J. Invest. Dermatol. 141, 1608-1612.e3. https://doi.org/10.1016/j.jid.2020.11.016

You, L., Nie, J., Sun, W.J., Zheng, Z.Q., Yang, X.J., 2012. Lysine acetylation: Enzymes, bromodomains and links to different diseases. Essays Biochem. 52, 1–12. https://doi.org/10.1042/BSE0520001

Yu, F.X., Zhao, B., Guan, K.L., 2015. Hippo Pathway in Organ Size Control, Tissue Homeostasis, and Cancer. Cell 163, 811–828. https://doi.org/10.1016/j.cell.2015.10.044

Yuksel, E.P., Ilkaya, F., Yildiz, L., Aydin, F., Senturk, N., Denizli, H., Canturk, T., Turanli, A.Y., 2014. Effects of paroxetine on cutaneous wound healing in healthy and diabetic rats. Adv. Ski. Wound Care 27, 216–221. https://doi.org/10.1097/01.ASW.0000445920.14039.64

Zahra, T., Voloshyna, D., Bseiso, A., Shaik, T.A., Ferman, H.G., Sathish, M., Al Barznji, S., Saleem, F., Ghaffari, M.A.Z., 2022. Bupropion-Induced Dystonia: A Case Report. Cureus. https://doi.org/10.7759/cureus.29857

Zeng, J., Liu, D., Qiu, Z., Huang, Y., Chen, B., Wang, L., Xu, H., Huang, N., Liu, L., Li, W., 2014. GSK3β overexpression indicates poor prognosis and its inhibition reduces cell proliferation and survival of non-small cell lung cancer cells. PLoS One 9, 1–11. https://doi.org/10.1371/journal.pone.0091231

Zhang, W., Tan, X., Lin, S., Gou, Y., Han, C., Zhang, C., Ning, W., Wang, C., Xue, Y., 2022. CPLM 4.0: An updated database with rich annotations for protein lysine modifications. Nucleic Acids Res. 50, D451–D459. https://doi.org/10.1093/nar/gkab849

Zhang, W., Wu, Y., 2020. Mitogen- and stress-activated protein kinase-1 activation is involved in melanocortin-induced BDNF expression in Neuro2a neuronal cells. Neuroreport 31, 1007–1014. https://doi.org/10.1097/WNR.0000000000001508

Zhang, X., Zheng, M., Dill, D., Shi, X., Qiao, Y., 2010. The Role of Interleukin-1 in Wound Biology. Part II: In Vivo and Human Translational Studies 111, 1534–1542. https://doi.org/10.1213/ANE.0b013e3181f691eb

Zhang, Y.Q., Gao, X., Ji, G.C., Huang, Y.L., Wu, G.C., 2001. Expression of 5-HT2A receptor mRNA in rat nucleus raphe magnus neurons after peripheral inflammation. Acta Pharmacol. Sin. 22, 923–928.

Zhang, Z.Y., 2017. Drugging the undruggable: Therapeutic potential of targeting protein tyrosine phosphatases. Acc. Chem. Res. 50, 122–129. https://doi.org/10.1021/acs.accounts.6b00537

Zhao, B., Tumaneng, K., Guan, K.L., 2011. The Hippo pathway in organ size control, tissue regeneration and stem cell self-renewal. Nat. Cell Biol. 13, 877–883. https://doi.org/10.1038/ncb2303

Zhao, Y.W., Pan, Y.Q., Tang, M.M., Lin, W.J., 2018. Blocking p38 signaling reduces the activation of pro-inflammatory cytokines and the phosphorylation of p38 in the habenula and reverses depressive-like behaviors induced by neuroinflammation. Front. Pharmacol. 9, 1–14. https://doi.org/10.3389/fphar.2018.00511

Zheng, K., Yarmarkovich, M., Bantog, C., Bayer, R., Patapoff, T.W., 2014. Influence of glycosylation pattern on the molecular properties of monoclonal antibodies. MAbs 6, 649–658. https://doi.org/10.4161/mabs.28588

Zheng, Y., Zhang, W., Pendleton, E., Leng, S., Wu, J., Chen, R., Sun, X.J., 2009. Improved insulin sensitivity by calorie restriction is associated with reduction of ERK and p70S6K activities in the liver of obese Zucker rats. J. Endocrinol. 203, 337–347. https://doi.org/10.1677/JOE-09-0181

Zhu, B., He, Q., Xiang, J., Qi, F., Cai, H., Mao, J., Zhang, C., Zhang, Q., Li, H., Lu, L., Wang, T., Yu, W., 2017. Quantitative Phosphoproteomic Analysis Reveals Key Mechanisms of Cellular Proliferation in Liver Cancer Cells. Sci. Rep. 7, 1–12. https://doi.org/10.1038/s41598-017-10716-0

Zhu, W., Stevens, A.P., Dettmer, K., Gottfried, E., Hoves, S., Kreutz, M., Holler, E., Canelas, A.B., Kema, I., Oefner, P.J., 2011. Quantitative profiling of tryptophan metabolites in serum, urine, and cell culture supernatants by liquid chromatography-tandem mass spectrometry. Anal. Bioanal. Chem. 401, 3249–3261. https://doi.org/10.1007/s00216-011-5436-y

Zmijewski, M.A., Slominski, A.T., 2011. Neuroendocrinology of the skin: An overview and selective analysis. Dermatoendocrinol. 3, 3–10. https://doi.org/10.4161/derm.3.1.14617